

Utah State University

DigitalCommons@USU

All Graduate Theses and Dissertations

Graduate Studies

8-2022

Defining Areas of Interest Using Voronoi and Modified Voronoi Tesselations to Analyze Eye-Tracking Data

Joanna D. Coltrin
Utah State University

Follow this and additional works at: <https://digitalcommons.usu.edu/etd>



Part of the [Mathematics Commons](#), and the [Statistics and Probability Commons](#)

Recommended Citation

Coltrin, Joanna D., "Defining Areas of Interest Using Voronoi and Modified Voronoi Tesselations to Analyze Eye-Tracking Data" (2022). *All Graduate Theses and Dissertations*. 8508.

<https://digitalcommons.usu.edu/etd/8508>

This Thesis is brought to you for free and open access by the Graduate Studies at DigitalCommons@USU. It has been accepted for inclusion in All Graduate Theses and Dissertations by an authorized administrator of DigitalCommons@USU. For more information, please contact digitalcommons@usu.edu.



DEFINING AREAS OF INTEREST USING VORONOI AND MODIFIED VORONOI
TESSELATIONS TO ANALYZE EYE-TRACKING DATA

by

Joanna D. Coltrin

A thesis submitted in partial fulfillment
of the requirements for the degree

of

MASTER OF SCIENCE

in

Statistics

Approved:

Jürgen Symanzik, Ph.D.
Major Professor

Adele Cutler, Ph.D.
Committee Member

Sarah Schwartz, Ph.D.
Committee Member

Breanna Studenka, Ph.D.
Committee Member

D. Richard Cutler, Ph.D.
Vice Provost for Graduate Studies

UTAH STATE UNIVERSITY
Logan, Utah

2022

Copyright © Joanna D. Coltrin 2022

All Rights Reserved

ABSTRACT

Defining Areas of Interest Using Voronoi and Modified Voronoi Tessellations to Analyze
Eye-Tracking Data

by

Joanna D. Coltrin, Master of Science

Utah State University, 2022

Major Professor: Jürgen Symanzik, Ph.D.

Department: Mathematics and Statistics

A variety of methods have been used to analyze eye-tracking data. One method involves defining areas of interest (AOIs). These are predefined areas of an image used to determine characteristics of eye-tracking data. While most AOIs are defined by hand, the Voronoi Tessellation (VT) Method and Limited-Radius Voronoi Tessellation (LRVT) Method define AOIs with hand-selected centers and tessellations separating each center at the exact mid-lines. The LRVT method includes adjustable radius parameters for roughly circular AOIs. The LRVT Method is an adaptable systematic approach that is ideal where the AOIs are not separated images but are parts of one continuous image. In this thesis, we demonstrate using the VT and LRVT methods to define AOIs and analyze eye-tracking data. Specifically, our study tries to determine where people are looking when ranking the stability of an actor holding certain postures. Participants with recent experience practicing yoga (Treatment group) were compared to others without such recent experiences (Control group). The eye-tracking treatment and control data was compared between and within AOIs to determine if the images were studied differently based on which group each participant belonged to and where those differences occurred.

PUBLIC ABSTRACT

Defining Areas of Interest Using Voronoi and Modified Voronoi Tesselations to Analyze
Eye-Tracking Data

Joanna D. Coltrin

Eye tracking is a technology used to track where someone is looking. Eye-tracking technology is often used to study what people focus on when looking at a photo of another person. The eye-tracking technology records points on a photo that a person is looking at. When the photo being looked at shows a person, the points can be categorized by body part such as head, right hand, left hand, and torso. This thesis presents the use of partially circular areas to define the body parts of the person in the photo and therefore categorize the points collected by the eye-tracker. The participants for this study consisted of 20 people who practiced yoga and 20 people who did not practice yoga. These participants were asked to look at 22 pictures of a person standing in different postures. In this thesis, we analyze differences in how those who practice yoga look at the pictures compared to those who do not practice yoga using the partially circular areas to define where the points belong.

ACKNOWLEDGMENTS

I would like to thank my advisor, Dr. Jürgen Symanzik for his time, knowledge, and guided direction with regards to this research and with my professional growth in the field of Statistics. I am grateful beyond words for his unique ability to address my questions with great attentiveness that helped me learn how to find my answers. I appreciate his genuine support and encouragement of my progress and I will forever be grateful for the mentorship he has provided to me. I truly value his example and all of the ways he inspired me to grow and use that growth to help others.

I would like to thank my committee members. First, I would like to thank Dr. Sarah Schwartz for her expertise in multilevel modelling and her guidance and support in helping apply the broad concepts to this data. I would also like to thank Dr. Breanna Studenka who possesses the talent and enthusiasm that served as a springboard for this research. I appreciate the conversations we shared that helped me direct the research with her unique expertise. I would like to thank Dr. Adele Cutler for the time and talents she lent to this research. I appreciate the time she has spent encouraging me and guiding my efforts. Additionally, I would like to thank my colleague Eric McKinney for the time he devoted to preparing this data, discussing theoretical and computational challenges, and offering suggestions and support along the way.

I would like to thank my family for their continual encouragement. Finally, I would like to thank my husband for the constant support he provided at great personal sacrifice. Without him, I would not have the confidence or drive needed to complete this part of my education.

Joanna Coltrin

CONTENTS

	Page
ABSTRACT	iii
PUBLIC ABSTRACT	v
ACKNOWLEDGMENTS	vi
LIST OF TABLES	ix
LIST OF FIGURES	xii
1 Introduction	1
1.1 Eye-Tracking Analyses	1
1.1.1 Eye-Tracking Variables	1
1.1.2 Eye-Tracking Stimuli	2
1.2 Areas of Interest	3
1.2.1 Methods to Define AOIs	3
1.2.2 Visualizations	5
1.3 USU Posture Study	5
1.3.1 Participants	7
1.3.2 Postures	7
1.3.3 Tasks	9
1.3.4 Research Hypothesis	12
1.4 Thesis Overview	13
2 Methods	15
2.1 Data Transformation	15
2.1.1 Calibration Motivation	15
2.1.2 Affine Transformations	18
2.1.3 Transformation Application	20
2.1.4 Multivariate Median Calculation Exception	22
2.2 Defining Areas of Interest	23
2.2.1 Defining Round 1 AOI Centers	24
2.2.2 Defining Round 2 AOI Centers	25
2.2.3 Voronoi Tessellation AOIs	28
2.2.4 Limited Radius Voronoi Tessellation AOIs	30
2.3 Statistical Methods	31
2.3.1 Preliminary Analyses	31
2.3.2 Primary Analyses Overview	35
2.3.3 Generalized Linear Mixed Effect Models for Count Data	37
2.3.4 Adjustments for Multiple Comparisons	62
2.3.5 Supporting Software	62

3	Results	64
3.1	General Observations from Gaze-Point Data	64
3.2	Generalized Linear Mixed Effects Analyses	71
3.2.1	Multilevel Analysis Structure	73
3.2.2	General Results for all GLMMs	74
3.2.3	Zero-Inflated Negative Binomial Results	75
3.2.4	Pairwise Comparison Results	86
4	Discussion	95
4.1	Conclusions	96
4.1.1	Defining AOIs	96
4.1.2	Statistical Method Selection	97
4.2	Outlook	98
	APPENDICES	103
A	Visualizations for AOI Centers	104
B	Visualizations of Round 1 VT, Round 1 LRVT, Round 2 VT, and Round 2 LRVT AOIs	111
C	Contour Plots of Gaze-Point Data for All Participants	123
D	Extensive Tables of p-values for Statistical Analyses	127
E	Estimates Tables for Multilevel Analyses	140
F	Gaze-Point Visualizations by Posture ID	151
	REFERENCES	195

LIST OF TABLES

Table	Page
1.1 Commonly measured variables in eye-tracking analyses.	2
1.2 USU Posture Study terms.	12
2.1 Round 1 VT Posture ID 1 contingency table showing number of gaze points contributed to each AOI (14) from each Group (2)	36
2.2 Mixed Effect Model general notation.	40
2.3 Mixed Effect Model estimable parameter specification and notation.	41
2.4 AOI notation definitions for Posture IDs $j = 1, \dots, 5$	45
2.5 Display of $n = 25$ unique AOIs and how AOI number $l(j)$ (numbered inside the table) depends on the Posture ID j for Round 1 Voronoi Tessellations. . .	46
2.6 Regression model comparison	57
3.1 Model comparisons for each AOI iteration	73
3.2 Posture IDs associated with View Number 2	75
3.3 Frequency of the Round 1 AOI labels among the 22 Posture IDs	76
3.4 Frequency of the Round 2 AOI labels among the 22 Posture IDs	77
3.5 Comparison of ZINB models with and without interactions for each AOI iteration	78
3.6 Wald Chi-Square statistics, degrees of freedom, and p-values for multilevel models	79
3.7 Zero-Inflated Negative Binomial multilevel regression estimates for Round 1 VT AOI iteration	82
3.8 Zero-Inflated Negative Binomial multilevel regression estimates for Round 1 LRVT AOI iteration	83
3.9 Zero-Inflated Negative Binomial multilevel regression estimates for Round 2 VT AOI iteration	84

3.10	Zero-Inflated Negative Binomial multilevel regression estimates for Round 2 LRVT AOI iteration	85
3.11	Zero-Inflated Negative Binomial Multilevel Regression Estimated Gaze-Point Counts for each AOI by Group for Round 1 VT Iteration	87
3.12	Zero-Inflated Negative Binomial Multilevel regression estimated marginal mean gaze-point counts for each AOI by Group for Round 1 LRVT iteration	89
3.13	Zero-Inflated Negative Binomial Multilevel regression estimated marginal mean gaze-point counts for each AOI by Group for Round 2 VT iteration	91
3.14	Zero-Inflated Negative Binomial Multilevel regression estimated marginal mean gaze-point counts for each AOI by Group for Round 2 LRVT iteration	93
D.1	EMM rate ratio for Poisson GLMM showing raw p-values, Bonferroni adjusted p-values, and BH q-values for Round 1 VT data iteration (alternative = “two- sided”).	128
D.2	EMM rate ratio for Poisson GLMM showing raw p-values, Bonferroni adjusted p-values, and BH q-values for Round 1 LRVT data iteration (alternative = “two-sided”).	129
D.3	EMM rate ratio for Poisson GLMM showing raw p-values, Bonferroni adjusted p-values, and BH q-values for Round 2 VT data iteration (alternative = “two- sided”).	130
D.4	EMM rate ratio for Poisson GLMM showing raw p-values, Bonferroni adjusted p-values, and BH q-values for Round 2 LRVT data iteration (alternative = “two-sided”).	131
D.5	EMM rate ratio for ZIP GLMM showing raw p-values, Bonferroni adjusted p-values, and BH q-values for Round 1 VT data iteration (alternative = “two- sided”).	132
D.6	EMM rate ratio for ZIP GLMM showing raw p-values, Bonferroni adjusted p-values, and BH q-values for Round 1 LRVT data iteration (alternative = “two-sided”).	133
D.7	EMM rate ratio for ZIP GLMM showing raw p-values, Bonferroni adjusted p-values, and BH q-values for Round 2 VT data iteration (alternative = “two- sided”).	134
D.8	EMM rate ratio for ZIP GLMM showing raw p-values, Bonferroni adjusted p-values, and BH q-values for Round 2 LRVT data iteration (alternative = “two-sided”).	135

D.9	EMM rate ratio for ZINB GLMM showing raw p-values, Bonferroni adjusted p-values, and BH q-values for Round 1 VT data iteration (alternative = “two-sided”).	136
D.10	EMM rate ratio for ZINB GLMM showing raw p-values, Bonferroni adjusted p-values, and BH q-values for Round 1 LRVT data iteration (alternative = “two-sided”).	137
D.11	EMM rate ratio for ZINB GLMM showing raw p-values, Bonferroni adjusted p-values, and BH q-values for Round 2 VT data iteration (alternative = “two-sided”).	138
D.12	EMM rate ratio for ZINB GLMM showing raw p-values, Bonferroni adjusted p-values, and BH q-values for Round 2 LRVT data iteration (alternative = “two-sided”).	139
E.1	Poisson multilevel regression estimates for Round 1 VT AOI iteration	142
E.2	Poisson multilevel regression estimates for Round 1 LRVT AOI iteration . . .	143
E.3	Poisson multilevel regression estimates for Round 2 VT AOI iteration	144
E.4	Poisson multilevel regression estimates for Round 2 LRVT AOI iteration . . .	145
E.5	Zero Inflated Poisson multilevel regression estimates for Round 1 VT AOI iteration	147
E.6	Zero-Inflated Poisson multilevel regression estimates for Round 1 LRVT AOI iteration	148
E.7	Zero-Inflated Poisson multilevel regression estimates for Round 2 VT AOI iteration	149
E.8	Zero-Inflated Poisson multilevel regression estimates for Round 2 LRVT AOI iteration	150

LIST OF FIGURES

Figure	Page
1.1 Methods to define AOIs from left to right: hand-drawn, grid, Voronoi Tessellation, Limited Radius Voronoi Tessellation.	4
1.2 Scatterplot (top left), heatmap (top right), scanpath map (bottom left), and contour plot (bottom right) visualizations for eye-tracking data. The eye-tracking data used comes from all Control participants viewing Posture ID 1.	6
1.3 Posture IDs 1-22 (from left to right: first row 1-6; second row 7-12; third row 13-18; fourth row 19-22) used in the USU Posture Study.	8
1.4 Time bar displayed at the bottom of each posture image.	9
1.5 Researcher wearing the eye-tracker (left) and researcher standing on the force plate wearing the eye-tracker while analyzing a posture (right).	10
1.6 Viewing Order of Posture IDs.	11
2.1 Calibration photo referred to as Posture ID 0 and Posture ID 23.	16
2.2 Gaze points for Control participant C7 (top) and Treatment participant T18 (bottom) for Posture ID 0 (left) and Posture ID 23 (right).	17
2.3 Representation of categorization of calibration gaze points to a corner or outlying area using gaze points from participant C7 for Posture ID 0 and Posture ID 23 combined.	18
2.4 Four types of transformations that, combined, make up an affine transformation.	19
2.5 Gaze points from participant C7 for the calibration photo Posture ID 0 and Posture ID 23 before (left) and after (right) the affine transformation.	21
2.6 Contour plots of gaze points from all participants from Posture IDs 0 and 23 before (left) and after (right) transformation.	21
2.7 Gaze points from participant C7 for Posture IDs 5 (top), 15 (middle), and 20 (bottom) before (left) and after (right) affine transformation.	22
2.8 Original gaze points from participant C3 for Posture ID 0 (left) and Posture ID 23 (right).	23

2.9	Round 1 AOI centers for Posture IDs 1 (far left), 5 (left), 7 (right), and 8 (far right).	24
2.10	Variation of gaze points around calibration dots using percentile radii.	25
2.11	Contour plots of all participant gaze-point concentration for Posture IDs 1 (far left), 5 (left), 7 (right), and 8 (far right).	26
2.12	Scatterplots (top) and contour plots (bottom) for all participants in red (far left), Treatment group in brown (left), Control group in green (right), and differentiated groups (far right) for Posture ID 7.	27
2.13	Round 2 AOI centers for Posture IDs 1 (far left), 5 (left), 7 (right), and 8 (far right).	27
2.14	Round 1 VT AOIs for Posture IDs 1 (far left), 5 (left), 7 (right), and 8 (far right).	28
2.15	Round 2 VT AOIs for Posture IDs 1 (far left), 5 (left), 7 (right), and 8 (far right).	29
2.16	Round 1 LRVT AOIs for Posture IDs 1 (far left), 5 (left), 7 (right), and 8 (far right).	30
2.17	Round 2 LRVT AOIs for Posture IDs 1 (far left), 5 (left), 7 (right), and 8 (far right).	30
2.18	Posture ID 7 Round 1 AOIs (top) and Round 2 AOIs (bottom) defined by the VT method (left) and LRVT method (right).	32
2.19	Multilevel structure of eye-tracking data.	39
3.1	Box plots with dot plots overlaid where each red dot represents the number of gaze points for one of the 40 participants for each Posture ID. Large red dots represent gaze-point counts when the participant viewed the Posture ID as View Number 2, the first Posture ID viewed after the calibration posture.	65
3.2	Box plots with dot plots overlaid where each brown dot represents the number of gaze points for one of the 20 Treatment participants and each green triangle represents the number of gaze points for one of the 20 Control participants for each Posture ID. Large brown dots and large green triangles represent gaze-point counts when the participant viewed the Posture ID as View Number 2, the first Posture ID viewed after the calibration posture.	66
3.3	Box plots with dot plots overlaid where each red dot represents the number of gaze points for one of the 40 participants for each posture given by View Number. The large red dots represent gaze-point counts for View Number 2.	68

3.4	Box plots with dot plots overlaid where each brown dot represents the number of gaze points for one of the 20 Treatment participants and each green triangle represents the number of gaze points for one of the 20 Control participants for each posture given by View Number. The large brown dots and large green triangles represent gaze-point counts for View Number 2.	69
3.5	Posture ID 7 bar chart (left) and scatterplot (right) of gaze points for Round 1 VT AOIs.	72
3.6	Visual for EMM rate ratio pairwise comparison of predicted mean number of gaze points including 95% confidence intervals for Round 1 VT AOIs across all postures.	88
3.7	Visual for EMM rate ratio pairwise comparison of predicted mean number of gaze points including 95% confidence intervals for Round 1 LRVT AOIs. . . .	90
3.8	Visual for EMM rate ratio pairwise comparison of predicted mean number of gaze points including 95% confidence intervals for Round 2 VT AOIs.	92
3.9	Visual for EMM rate ratio pairwise comparison of predicted mean number of gaze points including 95% confidence intervals for Round 2 LRVT AOIs. . . .	94
A.1	Round 1 AOI labels.	107
A.2	Round 2 AOI labels.	110
B.1	Round 1 VT AOIs.	113
B.2	Round 1 LRVT AOIs.	116
B.3	Round 2 VT AOIs.	119
B.4	Round 2 LRVT AOIs.	122
C.1	Contours of gaze-point data from all participants	126
F.1	Posture ID 1 gaze-point bar chart (left) and scatterplot (right) for Round 1 VT (top) and Round 1 LRVT (bottom) AOIs.	152
F.2	Posture ID 1 gaze-point bar chart (left) and scatterplot (right) for Round 2 VT (top) and Round 2 LRVT (bottom) AOIs.	153
F.3	Posture ID 2 gaze-point bar chart (left) and scatterplot (right) for Round 1 VT (top) and Round 1 LRVT (bottom) AOIs.	154
F.4	Posture ID 2 gaze-point bar chart (left) and scatterplot (right) for Round 2 VT (top) and Round 2 LRVT (bottom) AOIs.	155

F.5	Posture ID 3 gaze-point bar chart (left) and scatterplot (right) for Round 1 VT (top) and Round 1 LRV T (bottom) AOIs.	156
F.6	Posture ID 3 gaze-point bar chart (left) and scatterplot (right) for Round 2 VT (top) and Round 2 LRV T (bottom) AOIs.	157
F.7	Posture ID 4 gaze-point bar chart (left) and scatterplot (right) for Round 1 VT (top) and Round 1 LRV T (bottom) AOIs.	158
F.8	Posture ID 4 gaze-point bar chart (left) and scatterplot (right) for Round 2 VT (top) and Round 2 LRV T (bottom) AOIs.	159
F.9	Posture ID 5 gaze-point bar chart (left) and scatterplot (right) for Round 1 VT (top) and Round 1 LRV T (bottom) AOIs.	160
F.10	Posture ID 5 gaze-point bar chart (left) and scatterplot (right) for Round 2 VT (top) and Round 2 LRV T (bottom) AOIs.	161
F.11	Posture ID 6 gaze-point bar chart (left) and scatterplot (right) for Round 1 VT (top) and Round 1 LRV T (bottom) AOIs.	162
F.12	Posture ID 6 gaze-point bar chart (left) and scatterplot (right) for Round 2 VT (top) and Round 2 LRV T (bottom) AOIs.	163
F.13	Posture ID 7 gaze-point bar chart (left) and scatterplot (right) for Round 1 VT (top) and Round 1 LRV T (bottom) AOIs.	164
F.14	Posture ID 7 gaze-point bar chart (left) and scatterplot (right) for Round 2 VT (top) and Round 2 LRV T (bottom) AOIs.	165
F.15	Posture ID 8 gaze-point bar chart (left) and scatterplot (right) for Round 1 VT (top) and Round 1 LRV T (bottom) AOIs.	166
F.16	Posture ID 8 gaze-point bar chart (left) and scatterplot (right) for Round 2 VT (top) and Round 2 LRV T (bottom) AOIs.	167
F.17	Posture ID 9 gaze-point bar chart (left) and scatterplot (right) for Round 1 VT (top) and Round 1 LRV T (bottom) AOIs.	168
F.18	Posture ID 9 gaze-point bar chart (left) and scatterplot (right) for Round 2 VT (top) and Round 2 LRV T (bottom) AOIs.	169
F.19	Posture ID 10 gaze-point bar chart (left) and scatterplot (right) for Round 1 VT (top) and Round 1 LRV T (bottom) AOIs.	170
F.20	Posture ID 10 gaze-point bar chart (left) and scatterplot (right) for Round 2 VT (top) and Round 2 LRV T (bottom) AOIs.	171

F.21 Posture ID 11 gaze-point bar chart (left) and scatterplot (right) for Round 1 VT (top) and Round 1 LRV T (bottom) AOIs.	172
F.22 Posture ID 11 gaze-point bar chart (left) and scatterplot (right) for Round 2 VT (top) and Round 2 LRV T (bottom) AOIs.	173
F.23 Posture ID 12 gaze-point bar chart (left) and scatterplot (right) for Round 1 VT (top) and Round 1 LRV T (bottom) AOIs.	174
F.24 Posture ID 12 gaze-point bar chart (left) and scatterplot (right) for Round 2 VT (top) and Round 2 LRV T (bottom) AOIs.	175
F.25 Posture ID 13 gaze-point bar chart (left) and scatterplot (right) for Round 1 VT (top) and Round 1 LRV T (bottom) AOIs.	176
F.26 Posture ID 13 gaze-point bar chart (left) and scatterplot (right) for Round 2 VT (top) and Round 2 LRV T (bottom) AOIs.	177
F.27 Posture ID 14 gaze-point bar chart (left) and scatterplot (right) for Round 1 VT (top) and Round 1 LRV T (bottom) AOIs.	178
F.28 Posture ID 14 gaze-point bar chart (left) and scatterplot (right) for Round 2 VT (top) and Round 2 LRV T (bottom) AOIs.	179
F.29 Posture ID 15 gaze-point bar chart (left) and scatterplot (right) for Round 1 VT (top) and Round 1 LRV T (bottom) AOIs.	180
F.30 Posture ID 15 gaze-point bar chart (left) and scatterplot (right) for Round 2 VT (top) and Round 2 LRV T (bottom) AOIs.	181
F.31 Posture ID 16 gaze-point bar chart (left) and scatterplot (right) for Round 1 VT (top) and Round 1 LRV T (bottom) AOIs.	182
F.32 Posture ID 16 gaze-point bar chart (left) and scatterplot (right) for Round 2 VT (top) and Round 2 LRV T (bottom) AOIs.	183
F.33 Posture ID 17 gaze-point bar chart (left) and scatterplot (right) for Round 1 VT (top) and Round 1 LRV T (bottom) AOIs.	184
F.34 Posture ID 17 gaze-point bar chart (left) and scatterplot (right) for Round 2 VT (top) and Round 2 LRV T (bottom) AOIs.	185
F.35 Posture ID 18 gaze-point bar chart (left) and scatterplot (right) for Round 1 VT (top) and Round 1 LRV T (bottom) AOIs.	186
F.36 Posture ID 18 gaze-point bar chart (left) and scatterplot (right) for Round 2 VT (top) and Round 2 LRV T (bottom) AOIs.	187

F.37 Posture ID 19 gaze-point bar chart (left) and scatterplot (right) for Round 1 VT (top) and Round 1 LRVT (bottom) AOIs.	188
F.38 Posture ID 19 gaze-point bar chart (left) and scatterplot (right) for Round 2 VT (top) and Round 2 LRVT (bottom) AOIs.	189
F.39 Posture ID 20 gaze-point bar chart (left) and scatterplot (right) for Round 1 VT (top) and Round 1 LRVT (bottom) AOIs.	190
F.40 Posture ID 20 gaze-point bar chart (left) and scatterplot (right) for Round 2 VT (top) and Round 2 LRVT (bottom) AOIs.	191
F.41 Posture ID 21 gaze-point bar chart (left) and scatterplot (right) for Round 1 VT (top) and Round 1 LRVT (bottom) AOIs.	192
F.42 Posture ID 21 gaze-point bar chart (left) and scatterplot (right) for Round 2 VT (top) and Round 2 LRVT (bottom) AOIs.	193
F.43 Posture ID 22 gaze-point bar chart (left) and scatterplot (right) for Round 1 VT (top) and Round 1 LRVT (bottom) AOIs.	194
F.44 Posture ID 22 gaze-point bar chart (left) and scatterplot (right) for Round 2 VT (top) and Round 2 LRVT (bottom) AOIs.	195

CHAPTER 1

Introduction

1.1 Eye-Tracking Analyses

Eye tracking is a technology used to track where a participant is looking. Eye tracking is used primarily to find what participants give their attention to (Holmqvist et al., 2011). To collect this information, an eye-tracking device records video of a participant's eye to estimate where this participant is looking. Although eye tracking has been practiced since the late 1800s with rudimentary technology (Delabarre, 1898; Huey, 1898), current eye-tracking devices record a participant's eye movements and produce a series of coordinates that describe the location of the participant's gaze. The raw data the eye-tracking device produces are called gaze points (Krafka et al., 2016). However, most raw data collected with eye-tracking devices contain noise caused by two sources: the eye-tracking device and the participant. Specifically, variation in the eye-tracking algorithm calculations cause a random scattering of gaze points (raw data provided by the eye tracker) around the true fixation point of the eye (Van der Lans et al., 2011). Additionally, excessive noise within the data can arise when the participant blinks (Hershman et al., 2018).

1.1.1 Eye-Tracking Variables

While this research focuses on the raw gaze points collected by the eye-tracking device, most eye-tracking studies use fixation points calculated from the gaze points. Calculating fixation points is the most common way to address excess noise in the data. Two techniques for calculating fixation points involve (1) averaging gaze points into fixation points (also called position-variance techniques by Duchowski (2007) and dispersion-based fixations by Holmqvist et al. (2011)), or (2) separating gaze points using thresholds on saccade¹ velocities (also called saccade velocity techniques) (Duchowski, 2007; Holmqvist et al., 2011).

¹Saccades are rapid eye movements between fixation points.

Table 1.1: Commonly measured variables in eye-tracking analyses.

Variable
Gaze points (raw x and y coordinates)
Fixation locations
Fixation durations
Fixation rate (per participant or across participants)
Fixation duration mean (per participant or across participants)
Number of fixations (per participant or across participants)
Scanpath (typically fixation sequence)

Eye-tracking studies include the analysis of common eye-tracking variables including gaze points or fixation points. Duchowski (2007) pointed out that statistical analyses generally consist of analysis of variance (ANOVA) on the dependent variables collected during the eye-tracking experiment, e.g., fixation durations, fixation counts, etc., depending on the experimental design and its hypotheses. While not comprehensive, Table 1.1 shows a list of commonly measured variables in eye-tracking analyses.

1.1.2 Eye-Tracking Stimuli

In eye-tracking analyses, participants are asked to study an object in a given area. The area where gaze points are recorded is referred to as the observation area. The object within the observation area that a researcher introduces to participants is called the stimulus.

There are two main categories of stimuli: static and dynamic. Static stimuli include still images that are either separated or continuous. A separated static stimulus is an image that is spread across one observation area such as a food label (Ares et al., 2013) or a research poster (Li, 2017) where content of the stimulus is separated by white space. A static stimulus is considered continuous if it cannot be separated and spread over the observation area. One example of a continuous static stimulus that is common in eye-tracking research is the human face (Almourad et al., 2018; Figueiredo et al., 2018).

An observation area with a dynamic stimulus would include a recording of a moving object or objects. Eye-tracking was used to research what participants focus on when watching footage of soccer players (Vaeyens et al., 2007), recorded surgeries (Fichtel et al., 2019), and

simulated pediatric trauma footage (Damji et al., 2019). Vaeyens et al. (2007) also included an interactive component to their eye-tracking analysis which added a measure tracking participants’ reaction to the soccer footage.

1.2 Areas of Interest

While the calculation of fixation points is the most common way to reduce noise in the data, an increasingly popular alternative is to analyze the raw gaze-point data in predefined sub-regions of the observation area called areas of interest (AOIs) (Hessels et al., 2016). In addition to reducing noise, these AOIs are often defined to address the level of interest in specific regional areas.

1.2.1 Methods to Define AOIs

A variety of techniques are being used to define AOIs for stimuli in the current literature. The most common method for defining AOIs is to draw these areas by hand (Cantoni et al., 2012; Hessels et al., 2016). The task of drawing AOIs by hand often falls on experts in the content area being studied (Fichtel et al., 2019). This method is most commonly implemented on separated static stimuli (Ares et al., 2013). However, as the stimuli used for eye-tracking studies have become more complex, this elementary technique is still being implemented (Hessels et al., 2016). Because it is entirely subjective, this method is far from ideal.

The systematic approach to defining AOIs that is most frequently applied involves using regular grids across the observation area (Wästlund et al., 2018). This method is useful since these AOIs are content independent, and consequently, easily generated. However, inferential statistics have shown to be dependent on the granularity of the grid (Duchowski, 2007; McKinney and Symanzik, 2019).

Another approach to defining AOIs systematically is called the Voronoi Tessellation (VT) method adapted from Voronoi (1909). This method requires the center of each AOI to be defined. Lines that separate each AOI center at the exact midpoint are drawn and

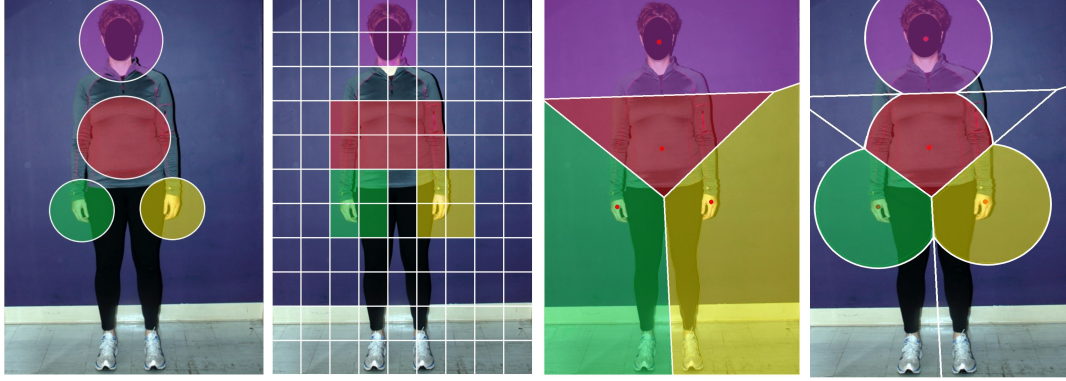


Fig. 1.1: Methods to define AOIs from left to right: hand-drawn, grid, Voronoi Tessellation, Limited Radius Voronoi Tessellation.

form tessellations.² Each tessellation becomes an AOI for the observation area. Thus, each gaze point belongs to the AOI where the distance from that point to the AOI center is the shortest. This approach gives the advantage of being systematic while not being restricted to the shape or size of grid cells. This method has only one element of subjectivity to the AOI definitions: the researcher has the freedom to select AOI centers. This method also ensures that every gaze point belongs to an AOI. One drawback to the VT method is that the outermost AOIs extend to the edges of the observation area which often gives an inaccurate categorization to the outermost gaze points, especially if the stimulus is small in relation to the observation area.

The final approach discussed by Hessels et al. (2016) is called the Limited-Radius Voronoi Tessellation (LRVT) method. This method uses the same underlying idea as the original Voronoi Tessellation method in creating the AOIs. However, the LRVT method adds a maximum radius to each AOI that applies to the centers and limits the extent of each AOI. The LRVT method provides the same advantages as the VT method and adds the benefit of a user-defined limit. Researchers can be more confident when classifying eye-tracking data found in these AOIs because outlying gaze points are excluded. This approach is now being used with dynamic stimuli as well as with static stimuli (Hessels et al., 2018).

²Tessellations are generally shapes of repeating patterns that cover the surface of a plane. However, tessellations can be any combination of shapes that cover a plane with no overlapping areas or gaps (e.g., jigsaw puzzles).

Hessels et al. (2016) compared the methods described above and noted their respective pros and cons. A depiction of these four approaches to defining AOIs can be seen in Figure 1.1. Goldberg and Helfman (2010) suggested that the size of the AOI should depend on three factors: the importance of capturing every gaze point, the amount of white space surrounding the stimulus, and the expected variance in gaze-point positions across participants. Holmqvist et al. (2011) also pointed out that the precision and accuracy of the recorded data should be considered when determining AOI size.

It is important to use a systematic method to define AOIs that creates meaningful breaks between each AOI when using static continuous stimuli. The VT method provides the advantage of being systematic without depending on an arbitrary grid cell size or the restrictive grid shape. The LRVT method extends those advantages to include the ability to reduce the chances of misclassification of the outermost gaze points.

1.2.2 Visualizations

Blascheck et al. (2017) suggested that visual analytics are well-suited for exploratory data analysis with eye-tracking data. In a comparison of a variety of eye-tracking analysis visualizations, Blascheck et al. (2017) indicated that variations of scatterplots, scanpath maps, and heatmaps are among the most commonly used. While the first two methods are often used to visualize eye-tracking data, if there is a large amount of data, these visualizations run the risk of overplotting. Hence, gaze points that are overlapping are impossible to detect. When plotting a large amount of data, a heatmap gives the most accurate depiction of gaze-point concentration. Another visualization of eye-tracking data that is rarely used is the contour plot. Contour plots provide the same advantages as heatmaps while using only contour lines and not coloring the entire observation area. A depiction of scatterplot, heatmap, scanpath map, and contour plot visualizations for eye-tracking data are provided in Figure 1.2.

1.3 USU Posture Study

The Utah State University (USU) Posture Study attempts to answer, among other

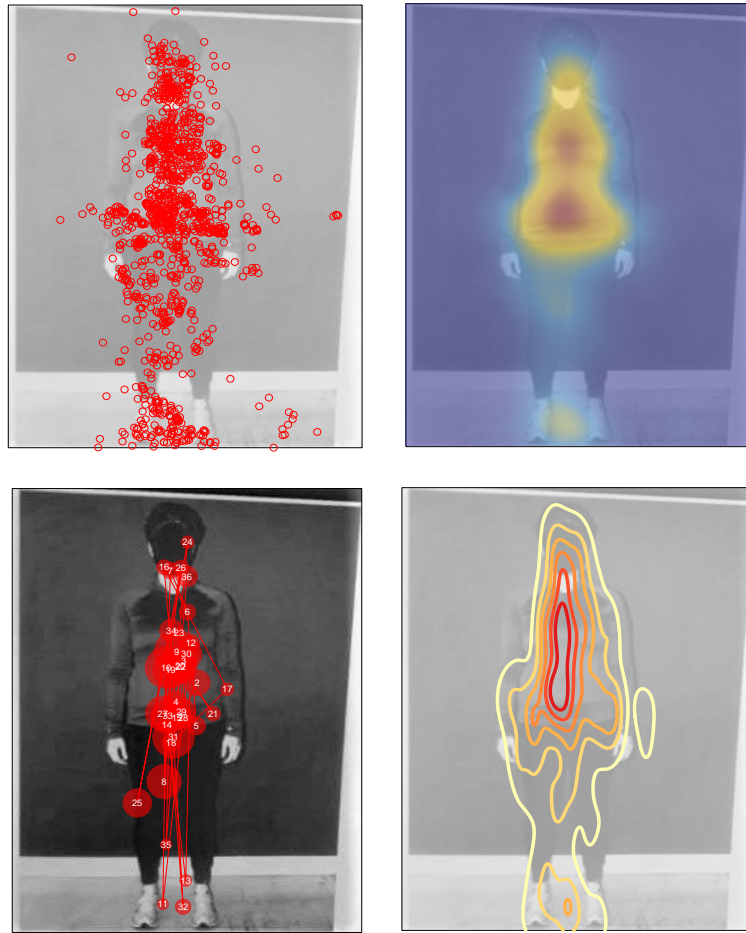


Fig. 1.2: Scatterplot (top left), heatmap (top right), scanpath map (bottom left), and contour plot (bottom right) visualizations for eye-tracking data. The eye-tracking data used comes from all Control participants viewing Posture ID 1.

hypotheses, the following: Does a person’s judgment of action capabilities of another person depend on personal knowledge and experience with human movement? (Symanzik et al., 2018). Specifically, “When participants look at an image to judge the stability of a posture, are there differences between participants with and without recent yoga experience? If so, where do those differences occur?” (Coltrin et al., 2020).

Literature that is focused on action capabilities asks participants to estimate the ability of another person to perform certain tasks (Rochat, 1995). Yet any visual information gathered to answer action capability research questions has been limited to making a participant

identify in what direction another person might be looking or what they might be looking at (Michelon and Zacks, 2006). Damacharla et al. (2018) used eye tracking to study the prediction of human error in given tasks as a means of understanding team dynamics. However, we are unaware of any study using eye tracking to determine what particular visual information might be used for judgments about action capabilities. Therefore, no literature exists to describe how one might set up and conduct such a human posture study, in particular when incorporating mobile eye-tracking equipment as a major component of the data recording, data processing, and data analysis. Numerous preliminary test participants helped evaluate and refine the setup of the study. Data and results from these preliminary tests appear in Symanzik et al. (2017), Symanzik et al. (2018), McKinney and Symanzik (2019), and Coltrin et al. (2020).

1.3.1 Participants

Two groups of participants were used in the USU Posture Study. The first group consisted of 20 volunteer students from USU’s psychology pool that had not practiced yoga at least twice a week for the past three months. The second group consisted of another 20 volunteer students that reported practicing yoga at least twice a week for the past three months. These participant groups will be referred to as the Control group (those without recent yoga experience) and the Treatment group (those with recent yoga experience).

1.3.2 Postures

There are 22 observation stimuli used for this study. Each observation area includes a stimulus subject holding a unique posture. These observation areas are hereafter referred to as postures. Each of the 40 participants were asked to look at a series of these 22 postures. Symanzik et al. (2018) explained that these postures were derived by systematically developing one posture per axis of rotation and within each axis of rotation, choosing three postures of increasing difficulty. Three postures were chosen for sagittal, frontal, and transverse plane rotation. Three postures were chosen for the sagittal and frontal, sagittal and

transverse, frontal and transverse, and all three planes of rotation combinations.³ Thus, with the addition of a posture with no rotation, 22 postures are used. The difficulty of the three postures within each rotation was arbitrarily determined by the experimenter. Each posture is given an identification number referred to as the Posture ID. Figure 1.3 shows each of the 22 postures viewed by the participants.

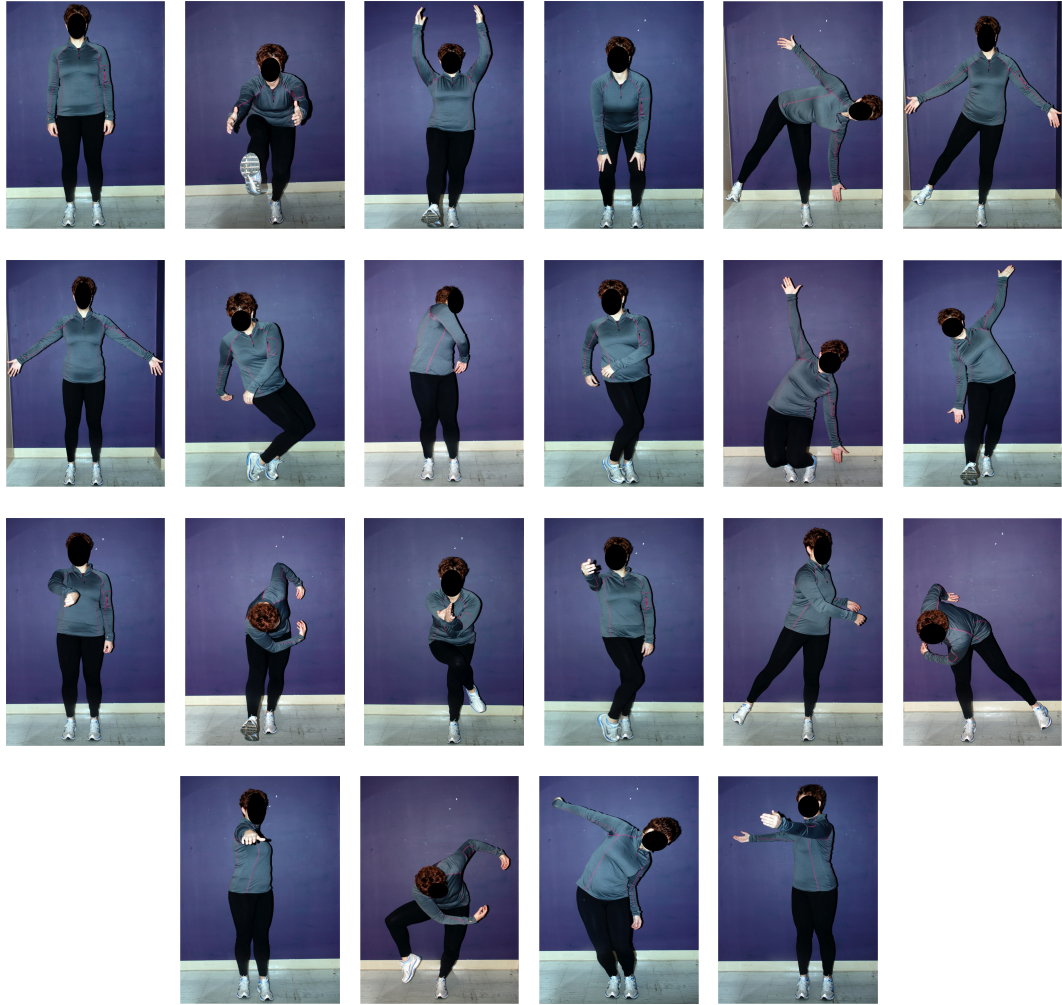


Fig. 1.3: Posture IDs 1-22 (from left to right: first row 1-6; second row 7-12; third row 13-18; fourth row 19-22) used in the USU Posture Study.

³The sagittal plane divides the human body into left and right halves, the frontal plane into front and back halves, and the transverse plane into superior and inferior halves (upper and lower halves separated at the hips).

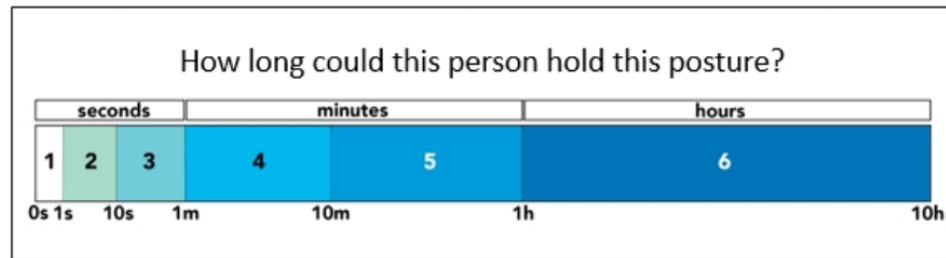


Fig. 1.4: Time bar displayed at the bottom of each posture image.

1.3.3 Tasks

Participants were fitted with the ETMOBILE eye-tracking device manufactured by Applied Science Laboratories (ASL) and instructed to stand on a COBALT force plate manufactured by Bertec to measure the participants' balancing abilities. The data collected from the force plate will be analyzed in the future and is not included for the purpose of the present analysis. Participants were shown a calibration posture and asked to look at a series of dots appearing one at a time for four seconds a piece in each corner of the calibration posture. After completing the initial calibration, participants were shown a randomized series of the 22 postures. For each posture, the participant was asked "How long do you think this person could hold this posture?" The participants were shown a time bar at the bottom of each posture as depicted in Figure 1.4 and were required to respond with a number between 1 and 6 that represented a time interval in which the participant judged the stimulus subject could hold the posture. Once the participant responded with the number, the experimenter displayed the next posture for them to judge. Thus, the amount of time each participant took to make the judgment varied. The participant time interval responses (a number between 1 and 6) will be analyzed in the future. After completing this task for all 22 postures, the eye-tracking calibration was reassessed to ensure valid data was collected during the entire trial. Figure 1.5 demonstrates how the data was recorded. The eye tracker recorded the raw x and y coordinates 30 times per second in 30 Hz video output. This data was extracted for each participant and Posture ID individually.

The order in which a participant viewed the Posture IDs was randomized to reduce bias



Fig. 1.5: Researcher wearing the eye-tracker (left) and researcher standing on the force plate wearing the eye-tracker while analyzing a posture (right).

in the eye-tracking data. It was assumed that postures shown first would take the participants a longer amount of time to make the judgment while they familiarized themselves with the time bar and the task. It was also assumed that some participants might get tired of the task and the time taken to make the judgment might change near the end of the sequence. Longer response times result in more eye-tracking data being collected and could bias results for a given Posture ID if the images were not randomized. Twenty randomized orders of Posture IDs were used. Two participants (one from each participant group) were assigned to each randomized order. Each participant was assigned an ID referred to as the Subject ID that indicate the participant group and the assigned viewing order that the participant was assigned to. Participants T1, T2, and T20 were Treatment participants assigned to viewing orders 1, 2, and 20, respectively. Participants C1, C2, and C20 were Control participants assigned to the same viewing order as their Treatment counterparts. Thus T10 and C10 were each assigned viewing order 10. The structure of the viewing orders is depicted in Figure 1.6. Additionally, a list of common terms and definitions as they apply to the USU Posture Study are included in Table 1.2

During the data collection process, it was necessary to replace several participant's data with a new participant's data for a variety of reasons. Some of the reasons were because of

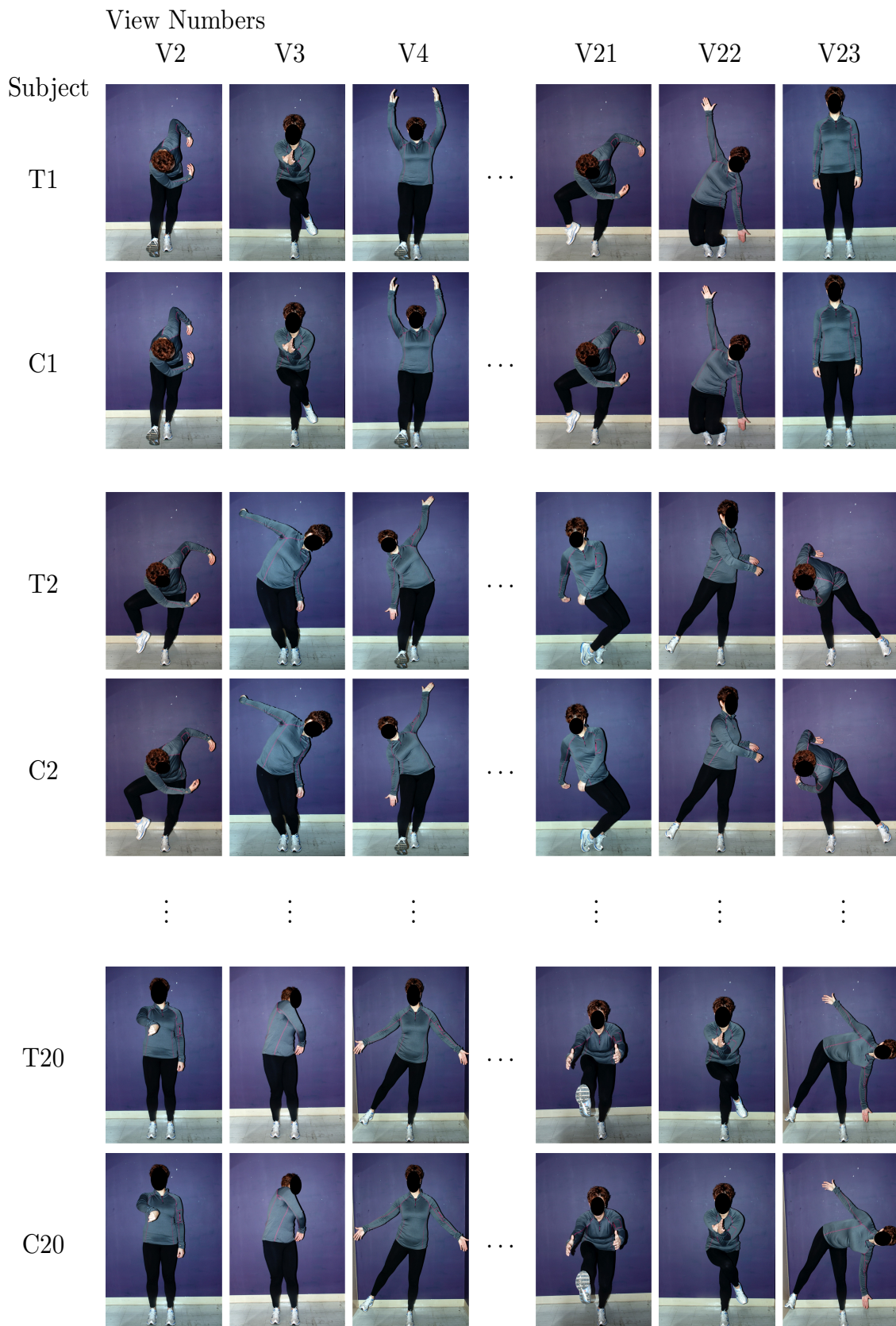


Fig. 1.6: Viewing Order of Posture IDs.

Table 1.2: USU Posture Study terms.

Term	Description
Posture	General term used to describe an observation area
Posture ID	A number (1-22) that describes a particular posture
View Number	A number (1-22) that describes when a particular posture was viewed by a participant
View Order	A randomized sequence of Posture IDs (20 random sequences used)
Subject ID	A unique ID for each participant describing their participant group (T/C) and View Order (1-20). T1, T2, ..., T20, C1, C2, ..., C20
Stimulus subject	An image of a subject holding a posture that participants were asked to judge (22 subject stimuli for this study)

technical problems and others were due to confounding factors arising during the recording of the data. Overall, ten Treatment and six Control participants gave eye-tracking data that had to be replaced. Most often, if a participant's initial or final calibration data was not properly recorded, a new participant was recruited and provided with the same slide ordering (and Subject ID) as the previous participant. Two Treatment participants did not complete the experiment due to feeling dizzy. Other reasons for replacing participant's data include the following: participants unconsciously manipulating the eye-tracking equipment during the experiment, data corruption during removal of the eye-tracking device, and miscommunication between participants and the data recorder. In the end, only participants who followed the experiment instructions, provided congruent initial and final calibration data, and whose eye-tracker recordings demonstrated a clean capture of the participant's eye movements throughout the experiment were kept. Otherwise, they were replaced by a new participant. Replacement participants adopted the original Subject ID that represented their group and View Order.

1.3.4 Research Hypothesis

We anticipate that the visual information used to judge stability will differ between Treatment and Control participants. Therefore, we expect the gaze-point distributions will differ within areas of interest between Treatment and Control groups for the 22 postures.

1.4 Thesis Overview

In Chapter 2 of this thesis, we discuss how the VT and LRVT areas of interest are implemented for the USU Posture Study. Specifically, Section 2.1 discusses how and why the gaze points were transformed. Section 2.2 details how the AOI centers were defined in two different ways referred to as Round 1 and Round 2. For each round, AOIs were created using the VT and LRVT methods. This led to four AOI iterations that were used to classify gaze points: Round 1 VT, Round 1 LRVT, Round 2 VT, and Round 2 LRVT. Section 2.3 explains the approach and statistical analyses used to analyze differences between participant groups' gaze-point distributions among AOIs for all 22 postures and for the four AOI iterations. The Wald Chi-Square test is explained, as is the Generalized Linear Mixed Effects Model (GLMMs) fit to the gaze-point data that the Wald Chi-Square test evaluates. Finally, the Estimated Marginal Means test is used to evaluate which AOIs show differences from GLMMs with significant Wald test statistics.

In Chapter 3, results from these analyses are presented. Section 3.1 describes general observations about participants' gaze points for each Posture ID and each View Number. In Section 3.2, the Wald Chi-Square test results are presented for all GLMMs that were able to converge. The Zero-Inflated Negative Binomial (ZINB) model proves to be the best fit for the data and shows an insignificant relationship between participant group and AOI for gaze points in all AOI iterations except for the Round 2 LRVT iteration. The follow-up Estimated Marginal Means (EMM) tests show no significant differences between groups in any specific AOIs for the Round 2 ZINB model.

In Chapter 4, the results are explained, implications are discussed, and suggestions for future work with systematic AOIs are provided. In Section 4.1, we discuss how all analyses agree that there is a significant difference in the gaze-point distributions between AOIs. However, we cannot confidently conclude that there are statistically significant differences within each AOI between Treatment and Control gaze-point distributions. The Wald Chi-Square test on the Zero-Inflated Negative Binomial Mixed Effects Model gives insignificant results for the interaction between Group and AOI for all data iterations except Round 2

LRVT. The significant finding does not translate into any significant pairwise comparisons of the gaze-point counts for the groups in any of the AOIs for this iteration. However, the model with the best fit finds highly significant results when comparing the AOIs not accounting for Group differences. In Section 4.2, future work is suggested for analyzing gaze-point data with the LRVT method; namely that multiple radii are chosen and compared to understand the affect the radius selection may have on analyses and conclusions. All of the analyses were conducted with the R statistical computing platform (R Core Team, 2020).

CHAPTER 2

Methods

The Methods section consists of three parts: transforming the data, defining the areas of interest, and describing the statistical analyses used. We had to first transform the gaze points to accurately reflect where participants were looking. We then defined the AOI centers and implemented Voronoi Tessellations and Limited-Radius Voronoi Tessellations to each Posture ID. Finally, we describe analyses used to compare Treatment and Control gaze points between AOIs for each of the 22 postures.

2.1 Data Transformation

We determined that the gaze points the eye tracker collected were slightly inaccurate based on data collected from the calibration postures. Before grouping gaze points in their proper AOIs and running analyses, we had to first implement a proper data transformation to most accurately represent the location of each gaze point.

2.1.1 Calibration Motivation

Each participant was required to view a calibration image before and after viewing the 22 postures. The calibration image displayed four dots, one in each corner of the image. These dots appeared separately for four seconds each. The calibration image that appeared at the beginning of the session is labeled Posture ID 0 and this same image that appeared at the end of the session is labeled Posture ID 23. The calibration image as described appears as Figure 2.1. The eye-tracking device recorded gaze points at a frequency of 30 Hz. Hence, the output produced approximately 30 gaze points per second. The gaze points for Posture ID 0 were compared to those for Posture ID 23 for each participant separately. The comparisons showed that each participant experienced a bias in the multivariate median of gaze points that was similar for Posture ID 0 and Posture ID 23, but differed from participant



Fig. 2.1: Calibration photo referred to as Posture ID 0 and Posture ID 23.

to participant as shown in Figure 2.2.

In an effort to eliminate this bias and make sure the gaze points more accurately represented the true gaze locations, an affine transformation matrix A was calculated for each of the 40 participants separately as defined in Section 2.1.2. However, in order to calculate an affine transformation matrix for each participant (using their calibration data), two sets of points are required: a set of biased coordinates and their associated “true” locations. The raw gaze-point medians for each corner served as the set of biased coordinates, while the coordinates of the black dots in the calibration postures that the participants were instructed to look at served as the set of “true” locations.

To define the multivariate median gaze point for each of the corners, gaze points for the first and last calibration postures were combined for each participant individually. Gaze points were then divided into five categories: top left corner (TL), top right corner (TR), bottom left corner (BL), bottom right corner (BR) and the outlying area. Originally, since participants were asked to look at each corner for four seconds and each second recorded 30 gaze points, we considered categorizing the first 120 gaze points as TL points, the next 120 gaze points as TR points and so forth. However, individual variation in delay from participants switching their gaze to the next calibration dot and inclusion of gaze points in

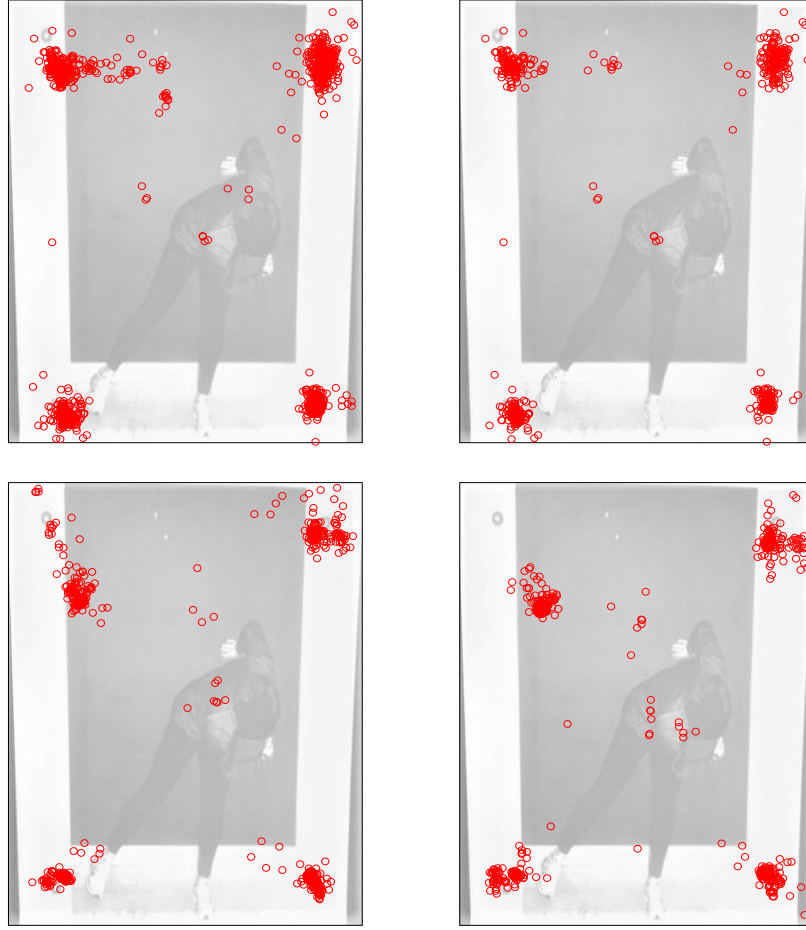


Fig. 2.2: Gaze points for Control participant C7 (top) and Treatment participant T18 (bottom) for Posture ID 0 (left) and Posture ID 23 (right).

the center of the observation area compromise the accuracy of this classification method. Instead, gaze points in a circular area around the calibration dot were classified as belonging to that corner. Specifically, the radii for circular areas for each corner were found by identifying the shortest Euclidean distance between the four calibration dot centers (letters X in Figure 2.3) and dividing that distance by two. Using this distance for the radii allowed for the largest circular areas for each corner without any overlap. Figure 2.3 provides a visual representation of this classification. All gaze points that have a Euclidean distance from a calibration dot less than the radius were considered belonging to that corner or category. Visually, gaze points plotted inside a circular area belong to the associated calibration cor-

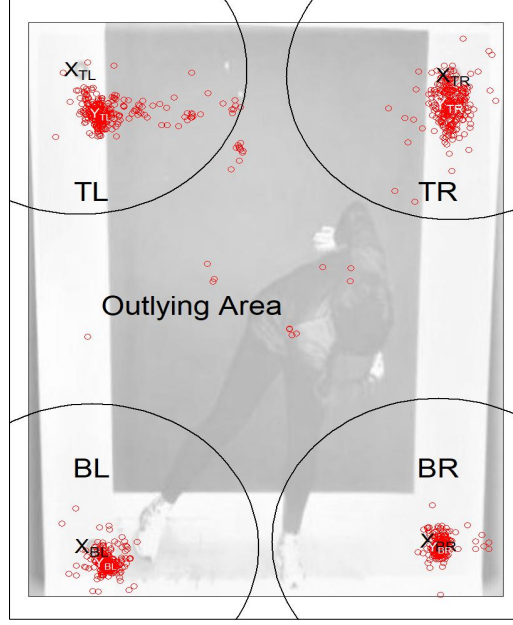


Fig. 2.3: Representation of categorization of calibration gaze points to a corner or outlying area using gaze points from participant C7 for Posture ID 0 and Posture ID 23 combined.

ner. The multivariate medians were calculated for all gaze points belonging to each corner separately. Thus, each participant had a unique set of four median coordinates that served as that participant's biased coordinates (letters Y in Figure 2.3). The x and y coordinates for the top left corner are indicated by X_{TL} and Y_{TL} from the X and Y matrices. This notation follows for all corners as depicted in Figure 2.3.

2.1.2 Affine Transformations

Affine transformations consist of any combination of the following transformations: scale, rotational, shear, and translational. These transformations are visually depicted in Figure 2.4. Let Y be a 4×2 matrix of the multivariate medians of the raw x and y coordinates for the gaze points for each of the four corner calibration dots. While scale, rotational, and shear transformations can be accomplished by multiplying a 2×2 matrix to the coordinates needing to be transformed (Y), translational transformations require an additional dimension in order to be accomplished in a single matrix multiplication (Li et al.,

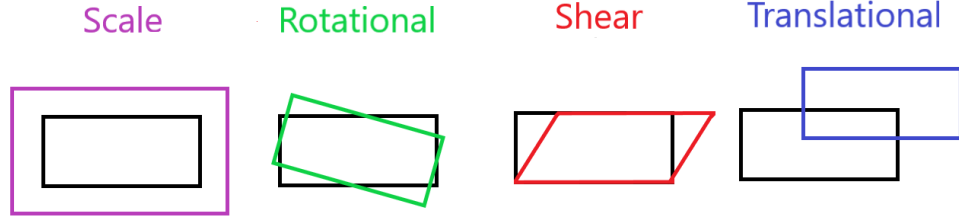


Fig. 2.4: Four types of transformations that, combined, make up an affine transformation.

2009). Hence, let X be a 4×2 matrix of the x and y coordinates that define the centers of each of the four calibration dots in the calibration images. The X and Y defined coordinates for participant C7 are plotted in Figure 2.3. Define

$$X' = [X | \vec{1}] \quad (2.1)$$

and

$$Y' = [Y | \vec{1}], \quad (2.2)$$

where X' and Y' are equivalent to X and Y with an additional column of 1s.

X and Y are related to each other via the transformation matrix A according to the formula

$$Y'A = X'. \quad (2.3)$$

Since Y' and X' are known, the transformation matrix can be derived by multiplying $(Y')^g$, a generalized left inverse of Y' , to the left-hand side of both sides of the Equation 2.3 in order to isolate A . This generalized inverse is defined as

$$(Y')^g = [(Y')^T(Y')]^{-1}(Y')^T. \quad (2.4)$$

Thus,

$$\begin{aligned}
Y'A &= X' \\
\Leftrightarrow [(Y')^T(Y')]^{-1}(Y')^TY'A &= [(Y')^T(Y')]^{-1}(Y')^TX' \\
\Leftrightarrow (Y')^gY'A &= (Y')^gX' \\
\Leftrightarrow IA &= (Y')^gX' \\
\Leftrightarrow A &= (Y')^gX'.
\end{aligned} \tag{2.5}$$

Once we have obtained the affine transformation matrix A for one participant, that participant's remaining gaze points can be corrected. If the multivariate median coordinates for participant P_1 are defined in the matrix Y_{P_1} , and the affine transformation matrix for that participant is defined as A_{P_1} , then all the coordinates X_{P_1} for this participant across all posture IDs are computed according to the formula:

$$X'_{P_1} = Y'_{P_1} A_{P_1}. \tag{2.6}$$

The transformed coordinates X_{P_1} are obtained by simply removing the last column of 1s from X'_{P_1} .

2.1.3 Transformation Application

The affine transformations for each participant were defined using the **Morpho** R package (Schlager, 2017). After computing the transformation using the multivariate medians, each participant's gaze points across all postures in the study were transformed using Formula 2.6. Figure 2.5 demonstrates how the calibration gaze points for one participant are influenced by that participant's affine transformation. Additionally, Figure 2.6 shows how the gaze-point concentration shifts after all the transformations on Posture ID 0 and 23 gaze points for each participant separately have been applied. These same transformations were applied to gaze points for all postures as depicted in Figure 2.7. After these transformations were applied, some of the gaze points that were originally near the edge of the posture were plotted outside the observation area as portrayed in Figure 2.5. Because the stimulus subject in the postures throughout the study were located centrally in the observation areas, we omitted

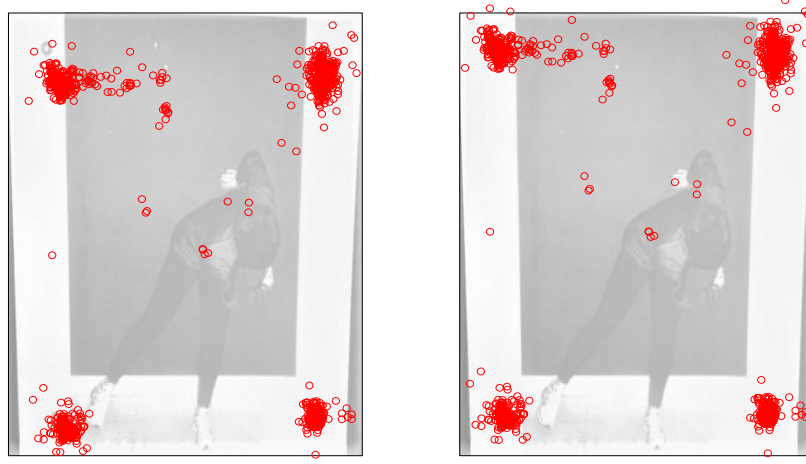


Fig. 2.5: Gaze points from participant C7 for the calibration photo Posture ID 0 and Posture ID 23 before (left) and after (right) the affine transformation.

these outlying transformed points as they likely represent gaze points recorded when the participants were not looking at the stimulus.

Using an affine transformation will not always produce an exact or perfect match because of the variability in the gaze-point data and the complexity of the transformation, but it will produce an optimized transformation matrix. In other words, the matrix computed

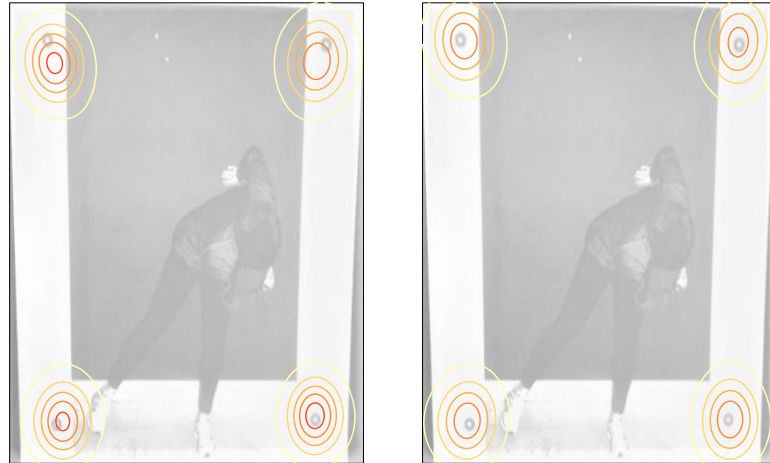


Fig. 2.6: Contour plots of gaze points from all participants from Posture IDs 0 and 23 before (left) and after (right) transformation.

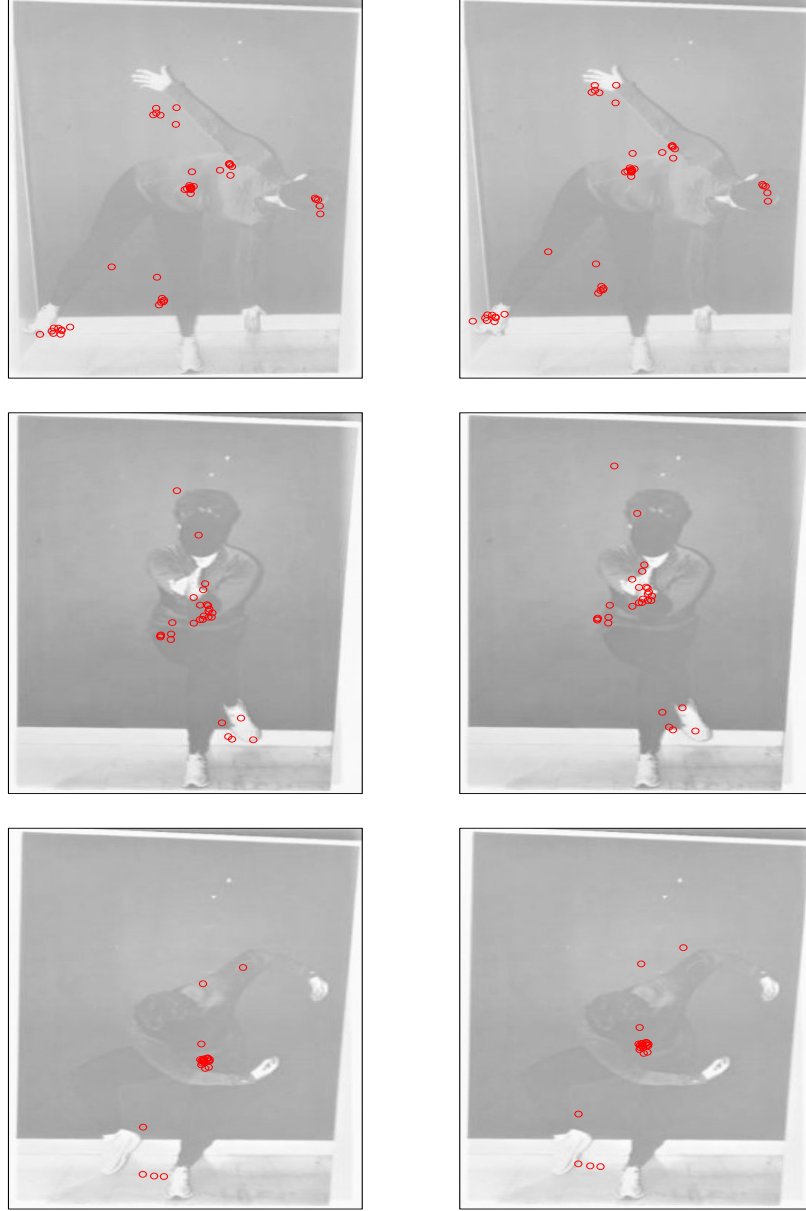


Fig. 2.7: Gaze points from participant C7 for Posture IDs 5 (top), 15 (middle), and 20 (bottom) before (left) and after (right) affine transformation.

is best suited to match the transformed coordinates with the true centers.

2.1.4 Multivariate Median Calculation Exception

The method for computing the multivariate medians was used for all participants with

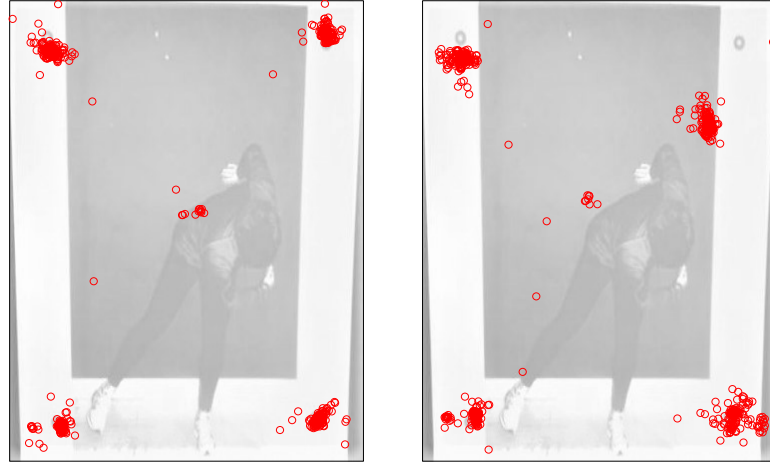


Fig. 2.8: Original gaze points from participant C3 for Posture ID 0 (left) and Posture ID 23 (right).

one exception. Likely, a recording error occurred for one Control participant, C3, in the recording of gaze points for the top right calibration corner for the Posture ID 23. These gaze-point coordinates appear much closer to the center of the observation area for Posture ID 23 than the calibration gaze points in the top right corner of Posture ID 0, as shown in Figure 2.8. The data from this participant was not ideal and this participant was therefore considered for replacement. However, there were not enough resources to replace this participant's data. After reviewing this participant's video recording, it appeared that this error in the recording of gaze points for the final calibration was isolated. None of the gaze points for Posture IDs 1 to 22 appeared to be affected. Thus, when calculating the median for the top right calibration corner for participant C3, only the gaze points from Posture ID 0 were used.

2.2 Defining Areas of Interest

The aim of the study is to identify whether or not there are differences in the gaze-point locations between Treatment and Control groups using areas of interest and comparing gaze-point proportions within these AOIs for each participant group. We used both the Voronoi Tessellation and Limited-Radius Voronoi Tessellation methods to create the AOIs. Both of

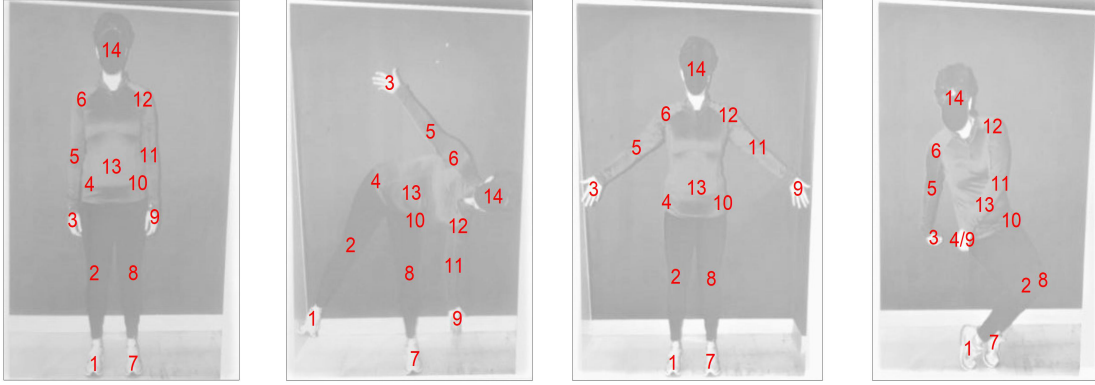


Fig. 2.9: Round 1 AOI centers for Posture IDs 1 (far left), 5 (left), 7 (right), and 8 (far right).

these methods require user-identified AOI centers.

2.2.1 Defining Round 1 AOI Centers

A kinesiology expert was given the series of postures and asked to identify centers of meaningful areas of the stimulus subject for each Posture ID. Figure 2.9 shows the centers that were chosen for a sample of the postures. These centers are referred to as our Round 1 AOI centers, a comprehensive list of which can be found in Appendix A as Figure A.1. Each center was labeled with a number identified by the expert to indicate a particular body part, most often a joint. Specifically, the areas and their associated labels are as follows: Right Foot (1), Right Knee (2), Right Hand (3), Right Hip (4), Right Elbow (5), Right Shoulder (6), Left Foot (7), Left Knee (8), Left Hand (9), Left Hip (10), Left Elbow (11), Left Shoulder (12), the Center of Mass: Torso (13), Head (14). These labels are shortened in the proceeding tables and graphs where the words Right and Left are abbreviated to Rt and Lt. The Center of Mass: Torso (13) is shortened to Torso (13). If any of these pre-defined body parts overlapped in a particular Posture ID, the area center was labeled with both numbers. For example, Posture ID 8 shows an image of a person with the left hand over the right hip. The far right image in Figure 2.9 shows this part of the stimulus subject with a single AOI labeled “4/9”. If a particular body part was not visible in a posture,

the associated number was not used. Posture ID 9 shows the stimulus subject leaning to their left where the left hand, elbow, and shoulder are occluded. Thus the ninth image of Figure A.1 does not include AOIs labeled 9, 11, or 12. Therefore, the highest AOI label number does not necessarily indicate the total number of AOIs on any given Posture ID.

2.2.2 Defining Round 2 AOI Centers

The AOI centers were first chosen to represent major joints, the torso, and the head. It became apparent that the Round 1 AOI centers on these Posture IDs were close together and would result in many small AOIs. Knowing that the variation in gaze-point positions should be taken into account when defining AOI size, we redefined AOI centers after analyzing the gaze-point data. This round of center definitions referred to as Round 2 AOI centers is data-driven.

First, we gathered the transformed data from the calibration images and used the circular areas represented in Figure 2.3 to categorize gaze points. Second, the Euclidean

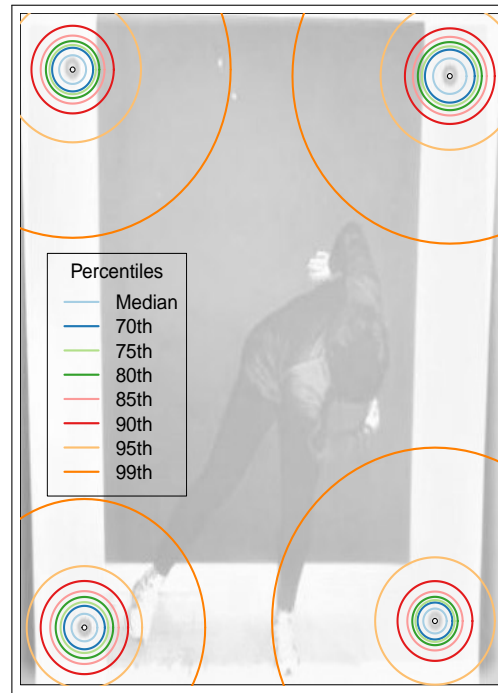


Fig. 2.10: Variation of gaze points around calibration dots using percentile radii.

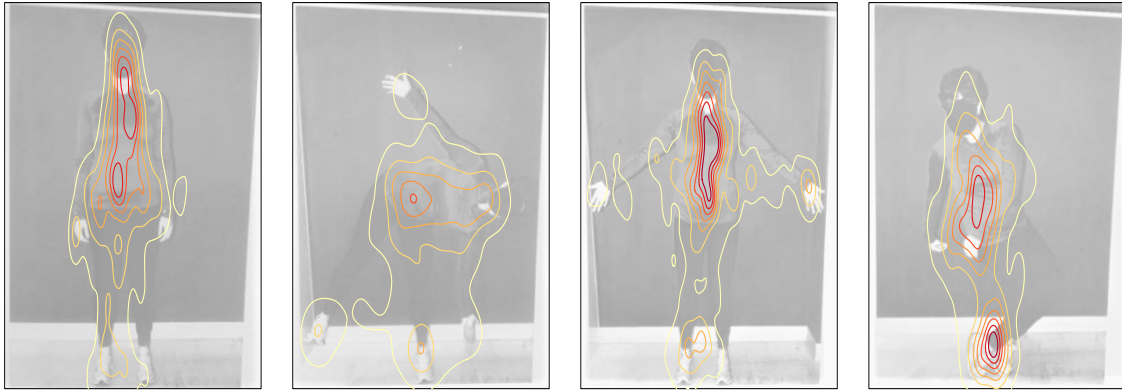


Fig. 2.11: Contour plots of all participant gaze-point concentration for Posture IDs 1 (far left), 5 (left), 7 (right), and 8 (far right).

distances from the transformed gaze points to the associated calibration dots were measured in each corner separately. Finally, the median Euclidean distance and several other percentile distances were applied as radii to circles drawn in Figure 2.10 with the calibration dots as the center of these circles. The 90th percentile radii, for example, show that 90% of the gaze points for those corners fall within that circular area.

The calibration data in the bottom right hand corner most accurately described the variation of gaze points around a given point because the pre-transformation and post-transformation gaze points were closest to the BR calibration dot as shown by the contours in Figure 2.6 and as depicted by the percentiles (median through 90th percentile) in Figure 2.10.

After gathering this information, the expert was asked to define another set of AOI centers for each Posture ID. In addition to the variation information given in Figure 2.10, this expert was given contour plots depicting the distribution of all gaze points on each Posture ID, a sample of which can be seen in Figure 2.11. A comprehensive list of contour plots for all Posture IDs is provided in Appendix C as Figure C.1. Additionally, Figure 2.12 shows how individual gaze points and contour plots are visualized and differentiated between Treatment and Control groups.

While each of these figures provides insight on how gaze points were distributed on the postures, Figure 2.10 and the postures in Figure C.1 were those provided specifically to help

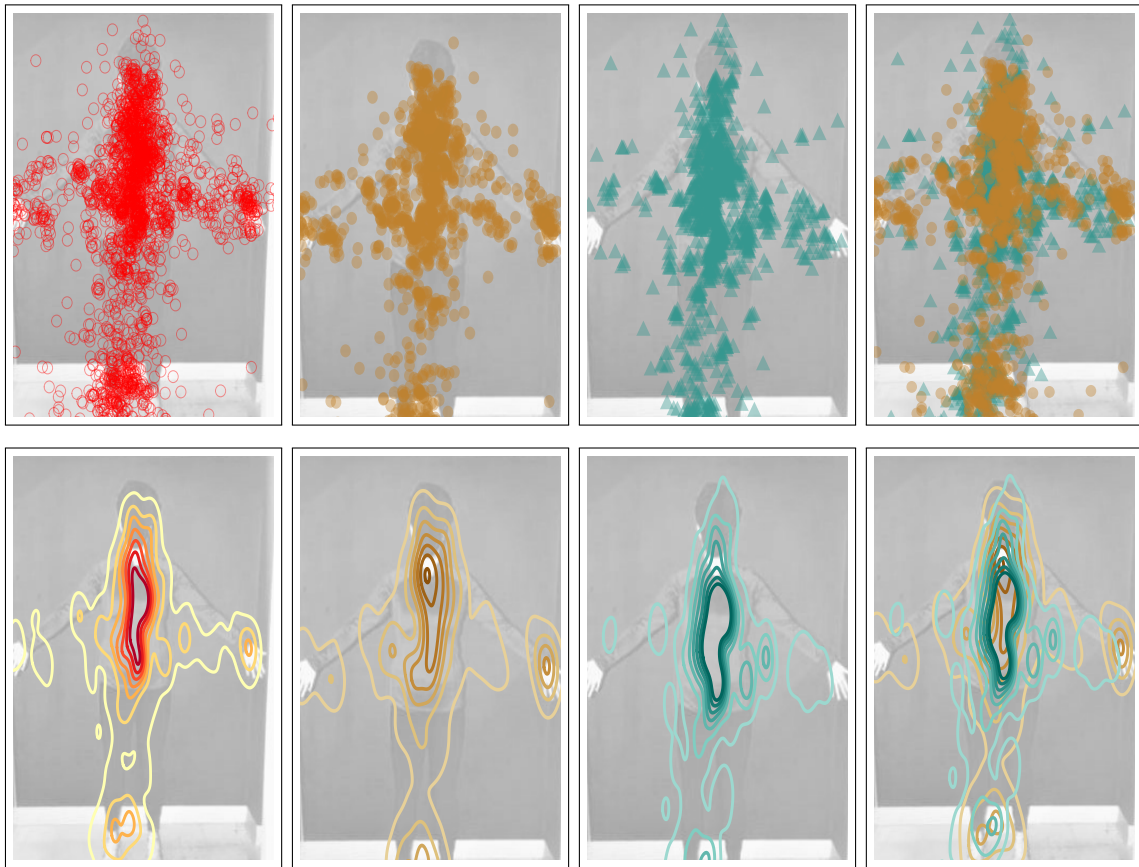


Fig. 2.12: Scatterplots (top) and contour plots (bottom) for all participants in red (far left), Treatment group in brown (left), Control group in green (right), and differentiated groups (far right) for Posture ID 7.

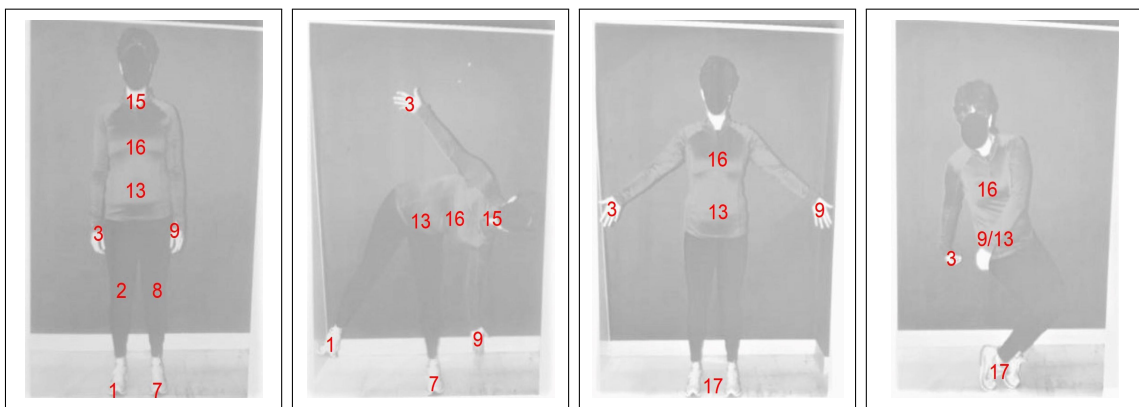


Fig. 2.13: Round 2 AOI centers for Posture IDs 1 (far left), 5 (left), 7 (right), and 8 (far right).

the expert define Round 2 AOI centers. A sample of these data-driven AOI center definitions are provided in Figure 2.13 and a comprehensive list of figures showing Round 2 AOIs for each Posture ID are provided in Appendix A as Figure A.2. The same naming construct used for Round 1 AOIs was also used for Round 2 AOIs with the addition of three new labels: Neck or Center of Shoulders (15), Sternum (16), and Middle of Feet/Base of Support (17). The first new label is shortened to Neck (15) and the third one to Middle of Feet (17) for brevity in the following tables and graphics. Unlike Round 1, Round 2 omits more of the defined areas than just those that are occluded. The only areas that are included were ones the expert felt were areas of focus from the contour plots in Figure C.1. This leads to far fewer AOIs per Posture ID in Round 2 as compared to the number of AOIs in Round 1. Where Round 1 has between 9 and 14 AOIs on any given posture, Round 2 postures only contain between 2 and 9 AOIs each.

2.2.3 Voronoi Tessellation AOIs

The first kind of AOIs defined for both Round 1 and Round 2 centers are known as Voronoi Tessellation AOIs. These are created using the `ggvoronoi` package in R (Garrett et al., 2019). The lines that are drawn are lines that separate each AOI center at the exact midpoint. The tessellations that are formed show the systematic AOIs and give the visual representation that any gaze point that falls within an area belongs to the associated AOI

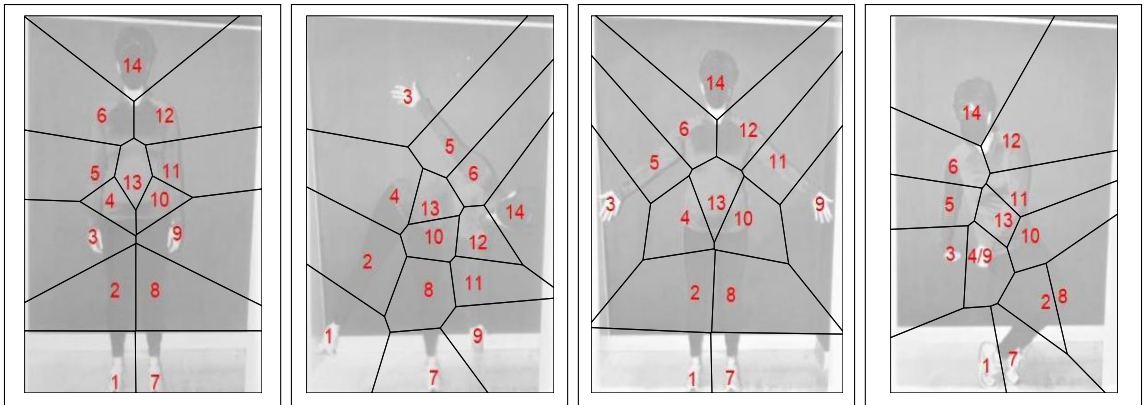


Fig. 2.14: Round 1 VT AOIs for Posture IDs 1 (far left), 5 (left), 7 (right), and 8 (far right).

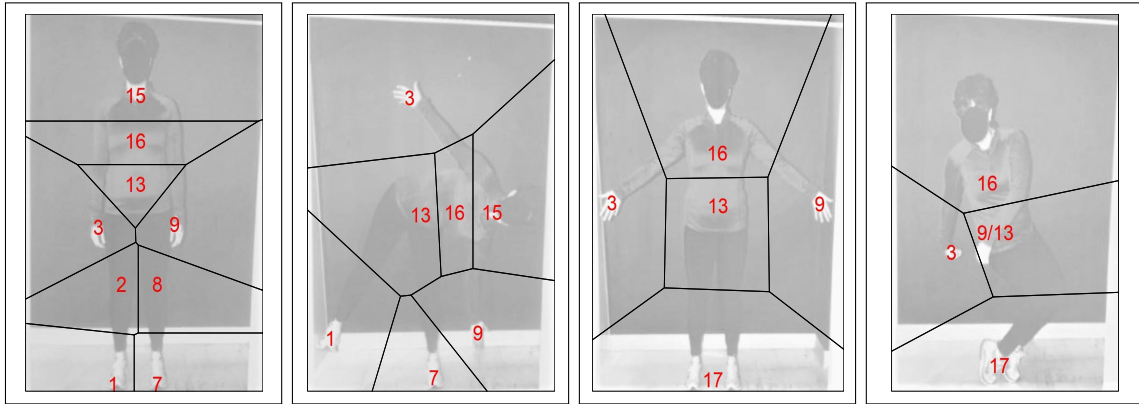


Fig. 2.15: Round 2 VT AOIs for Posture IDs 1 (far left), 5 (left), 7 (right), and 8 (far right).

because the gaze point has the shortest Euclidean distance to that AOI center. A sample of the tessellations for Round 1 is given in Figure 2.14 and the tessellations for Round 1 AOI centers for all Posture IDs can be seen in Appendix B as Figure B.1. To categorize the gaze points into the proper AOIs, the `point.in.polygon` function from the `sp` R package was used. This function returns a "True" for any coordinate that falls within a defined polygon or a "False" otherwise.

A sample of the tessellations for Round 2 is given in Figure 2.15 and the tessellations for Round 2 AOI centers for all Posture IDs can be seen in Appendix B as Figure B.3. Most AOIs in Round 2 are fairly large. Because Round 2 postures occluded many visible defined AOI labels, Round 2 postures have fewer AOI centers than do Round 1 postures. Therefore, Round 2 VT AOIs are much larger than most Round 1 VT AOIs. However, the outermost AOIs from VT Round 1 are usually large as this method defines every part of the observation area in the combined AOIs. The danger in using this method is that gaze points on the outer edges of the observation area are still categorized by the nearest AOI center. Take Posture ID 8 in Round 2 from Figure 2.15 for instance. The AOI with label 16 indicates this Area of Interest is the sternum. However, this area is so large that gaze points along the top of the observation area are categorized as sternum gaze points. The participant could easily be looking at the head or shoulders of the stimulus subject, yet these gaze points are broadly categorized due to the inclusive nature of the Voronoi Tessellation AOI method.

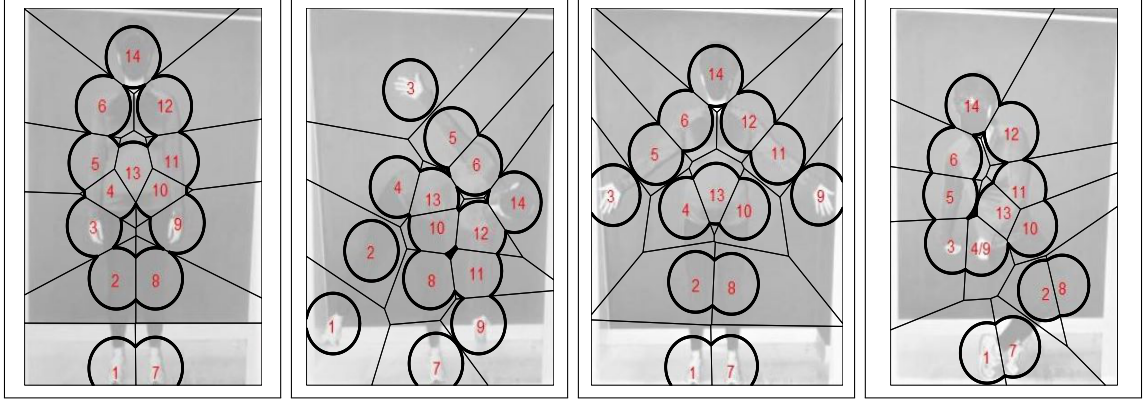


Fig. 2.16: Round 1 LRVT AOIs for Posture IDs 1 (far left), 5 (left), 7 (right), and 8 (far right).

The Limited-Radius Voronoi Tessellation method accounts for this categorization flaw, while still maintaining a systematic approach.

2.2.4 Limited Radius Voronoi Tessellation AOIs

After Voronoi Tessellations were used to create AOIs for Rounds 1 and 2, we applied the Limited-Radius Voronoi Tessellation method to these postures by defining a maximum radius applied to all AOI centers. Each gaze point is defined as belonging to an AOI if the gaze point falls inside the original AOI tessellation *and* the Euclidean distance from the gaze

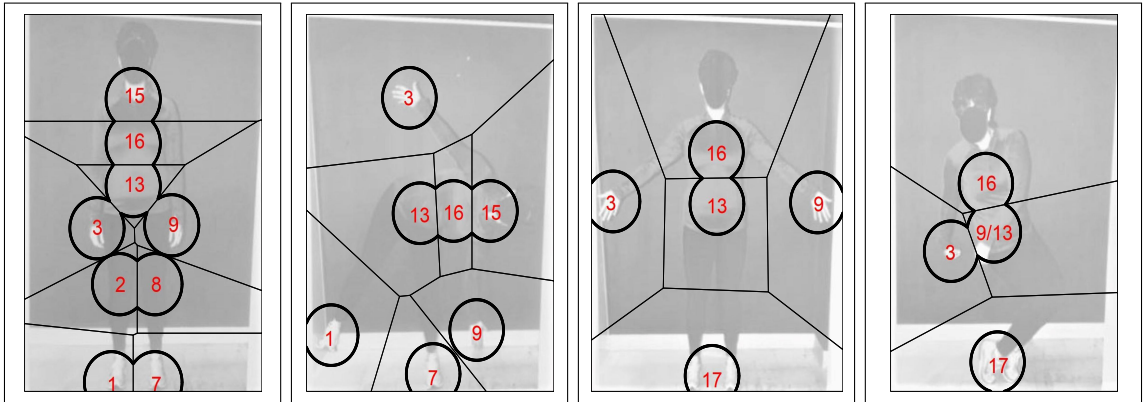


Fig. 2.17: Round 2 LRVT AOIs for Posture IDs 1 (far left), 5 (left), 7 (right), and 8 (far right).

point to the AOI center is less than the defined maximum radius. The restriction this method requires for each AOI addresses the inclusive categorization disadvantage with the Voronoi Tessellation method. The LRVT method gives flexibility in defining the maximum radius. For this study, we used the radius value of the 90th percentile for the bottom right-hand corner gaze points from the calibration data shown in Figure 2.10. A sample of the LRVT AOIs is shown in Figure 2.16 for Round 1 and Figure 2.17 for Round 2. A comprehensive list of postures with LRVT AOIs for Round 1 and Round 2 is provided in Appendix B as Figures B.2 and B.4 respectively. Any gaze points that did not fall within the LRVT AOIs were categorized in one additional area labeled “Outside Area”.

A comparison of how the different AOI iterations appear for one Posture ID (7) is given in Figure 2.18. These AOI iterations are hereafter referred to as Round 1 VT, Round 1 LRVT, Round 2 VT, and Round 2 LRVT. Each gaze point is classified into an AOI four different times; one classification for each AOI iteration. Each of the four classifications of gaze-point data will hereafter be referred to as data iterations and will be labelled the same as the AOI iterations.

2.3 Statistical Methods

Several statistical analyses are used to understand gaze-point distributions for these Posture IDs. Preliminary analyses are used to determine if the number of gaze points contributed to Posture IDs varied or if the number of gaze points varied depending on when the participants viewed the postures. Primary analyses are conducted to answer the research questions. These analyses are discussed at length throughout this section.

2.3.1 Preliminary Analyses

Before analyzing the data to answer the primary research question, preliminary analyses were performed on the gaze-point data to determine if a particular Posture ID proves to be more difficult for participants indicated by a significantly higher number of gaze points. We also analyze whether the order in which participants looked at a posture affects the number of gaze points contributed. The same data are analyzed after classifying gaze points as

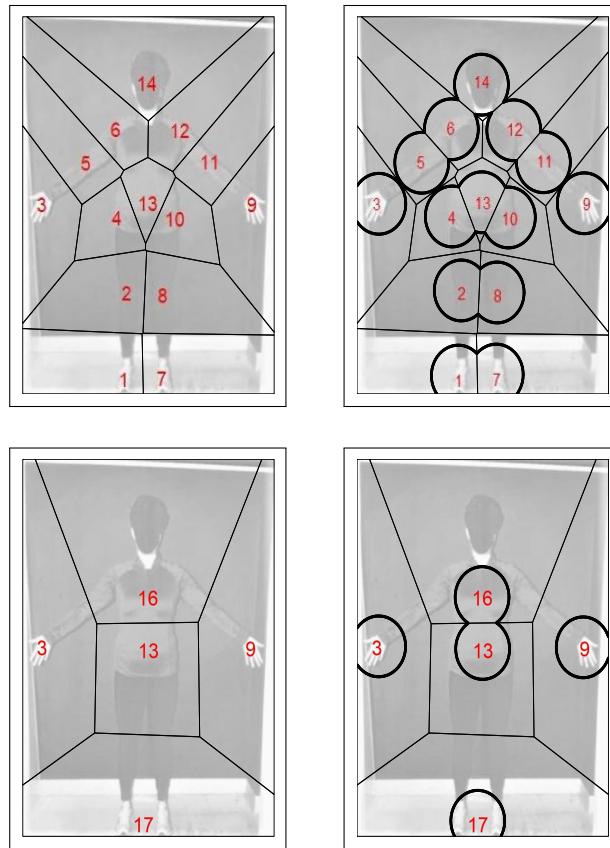


Fig. 2.18: Posture ID 7 Round 1 AOIs (top) and Round 2 AOIs (bottom) defined by the VT method (left) and LRV method (right).

belonging to the Treatment group or Control group.

Kruskal-Wallis Test

Because there are 22 Posture IDs of varying difficulty, meaning some of the postures would be more difficult for a person to hold, Some of these Posture IDs could be more difficult for participants to judge. This difficulty in judging could be seen by the number of gaze points contributed by each participant to the Posture ID. If a Posture ID is more difficult to judge, we expect to see higher numbers of gaze points contributed to that Posture ID. The Kruskal-Wallis test was used to assess whether there is a discrepancy in the number of gaze points contributed by participants to these Posture IDs.

The Kruskal-Wallis test is a non-parametric method to test whether a group of samples come from the same distribution (Breslow, 1970). It is apparent that a non-parametric method is needed because the distribution of gaze-point sums for participants would give skewed distributions.

The Kruskal-Wallis test statistic is calculated with the formula:

$$H = (N - 1) \frac{\sum_{i=1}^g n_i (\bar{r}_i - \bar{r})^2}{\sum_{i=1}^g \sum_{j=1}^{n_i} (r_{ij} - \bar{r})^2}. \quad (2.7)$$

Here, N is the total number of observations across all groups, g is the number of groups, n_i is the number of observations in group i , r_{ij} is the rank (among all observations) of observation j from group i , \bar{r}_i is the rank of all observations in group i , and \bar{r} is the average of all the r_{ij} (Dunn, 1964). Specific calculations for \bar{r}_i and \bar{r} are given as

$$\bar{r}_i = \frac{\sum_{j=1}^{n_i} r_{ij}}{n_i}, \quad (2.8)$$

and

$$\bar{r} = \frac{1}{2}(N + 1). \quad (2.9)$$

The hypotheses tested using the Kruskal-Wallis test are: H_O : The distribution of the gaze-point sums contributed to each Posture ID by each participant are the same for each Posture ID; and H_A : at least one distribution of gaze-point sums for a Posture ID differs from the distribution of sums for another Posture ID.

We used this same test to analyze whether the order in which a participant looked at any posture affected the number of gaze points contributed. We hypothesized that participants may need to familiarize themselves with the task leading to higher gaze-point sums to postures viewed at the beginning of the study. We also considered that if participants grew tired from the task, they may take longer to analyze each posture. To test to see if viewing order affected the sum values of gaze points, we used the Kruskal-Wallis test with the hypotheses: H_O : The distribution of the gaze-point sums contributed to each View Number by each participant are the same for each View Number; and H_A : at least one distribution of gaze-point sums for a View Number differs from the distribution of sums for another View Number.

Wilcoxon Signed Rank Test

We extended the preliminary analyses by including the differences in gaze-point contribution from Treatment participants and Control participants within each Posture ID and View Number. The Wilcoxon Signed Rank test is a non-parametric method to test whether paired samples come from the same population (Woolson, 2007). We organized participants into 20 matched pairs ($n = 20$), because each Treatment participant had one Control participant that viewed the Posture IDs in the same order. Because there were 20 pairs, we were able to use the normal approximation ($n > 20$). Calculating this test statistic requires ranking the gaze-point differences from each matched pair in each Posture ID. Differences are given as D_i and the ranks from 1 to n for smallest to largest $|D_i|$ are given as R_i . These ranks are summed separately for the ranks where D_i values are positive (W^+) and where D_i values are negative (W^-). The normal approximation of the Wilcoxon Signed Rank test statistic is given as:

$$z = \frac{W - \mu_W}{\sigma_W}. \quad (2.10)$$

Here, $W = \max(W^+, W^-)$, $\mu_W = \frac{n(n+1)}{4}$, and $\sigma_W = \sqrt{\frac{n(n+1)(2n+1)}{24}}$ (Cureton, 1967; Wilcoxon, 1992). This statistical method tests whether there are differences between the median of the gaze-point counts for each of the Treatment participants (M_T) and the median of the gaze-point counts for each of the Control participants (M_C). The hypotheses are given as: $H_O : M_T = M_C$; and $H_A : M_T \neq M_C$ for each Posture ID separately.

This test analyzes group differences for postures by View Order with the hypotheses: $H_O : M_T = M_C$; and $H_A : M_T \neq M_C$ for each View Number separately.

Results from these preliminary analyses determine what biases might be seen in the primary analyses and help researchers adjust accordingly.

2.3.2 Primary Analyses Overview

Our primary research questions asks: “When participants look at an image to judge the stability of a posture, are there differences between participants with and without recent yoga experience? If so, where do those differences occur?” To answer these questions, we decided to analyze the differences in Treatment and Control gaze-point distributions among the AOIs.

We considered several approaches to analyzing this data with the goal of answering these research questions. Initially, we considered aggregating the data at the group (Treatment and Control) level and analyze the data for each posture separately using Chi-Square or Fisher’s Exact tests. However, such tests are inappropriate because there are only 40 subjects but the aggregate counts make it appear as though there are many more. For instance, Table 2.1 shows that there are 2343 gaze points for Posture ID 1 alone. Treating these gaze points as independent observations instead of being clustered by participant and posture is referred to as pseudo replication (Lazic, 2010), and the results of such analyses would be meaningless.

The alternative analysis more appropriate for this data uses Generalized Linear Mixed Effect Models (GLMMs) which analyze the main interaction of gaze-point distribution by

Table 2.1: Round 1 VT Posture ID 1 contingency table showing number of gaze points contributed to each AOI (14) from each Group (2)

Area of Interest	Group		Row Totals
	Treatment	Control	
Rt Foot (1)	84	87	171
Rt Knee (2)	75	83	158
Rt Hand (3)	84	44	128
Rt Hip (4)	112	142	254
Rt Elbow (5)	17	16	33
Rt Shoulder (6)	41	97	138
Lt Foot (7)	9	60	69
Lt Knee (8)	21	43	64
Lt Hand (9)	26	53	79
Lt Hip (10)	64	134	198
Lt Elbow (11)	26	40	66
Lt Shoulder (12)	161	118	279
Torso (13)	191	223	414
Head (14)	157	135	292
Column Totals	1068	1275	2343

group within AOI while accounting for the Posture ID and participant random effects. Specifically, we fit Poisson Regression, Negative Binomial Regression, Zero-Inflated Poisson Regression (ZIP), and Zero-Inflated Negative Binomial Regression (ZINB). The zero-inflated models were chosen because a given participant could contribute no gaze points for several AOIs across the 22 Posture IDs and that those zero counts may influence the gaze-point distributions. Thus, our hypotheses for the multilevel analyses are as follows: H_O : There are no differences in gaze-point distributions within AOIs between the Treatment and the Control groups across all 22 postures combined. H_A : There are differences in gaze-point distributions within AOIs between the Treatment and the Control groups across all 22 postures combined.

Each of these models were tested for each of the four iterations of data at the 5% significance level. We corrected for multiple adjustments using the Benjamini Hochberg Adjustment on the multilevel models when analyzing pairwise interactions for all AOIs for the specific AOI round. There are 25 AOIs in the combined 22 postures for Round 1 VT data and 26 AOIs for Round 1 LRV data (adding the outside area). There are 17 AOIs in

the combined 22 postures for Round 2 VT data and 18 AOIs for Round 2 LRVT data.

2.3.3 Generalized Linear Mixed Effect Models for Count Data

In order to run analyses on multilevel data without aggregating the data, a more sophisticated (less general) multilevel model should be used. Multilevel models analyze the interaction researchers are interested in while taking into account the structure of the data. A common example of hierarchical data is when test scores are collected from students that are nested in classes which are nested in schools. This is an example of a three-level model. Tests like the Chi-Square test and Fisher’s Exact test are less sophisticated because they do not account for the nested data structure. Hox et al. (2017) provided a detailed explanation of such models. While we could make assumptions about our data and thus assume which model will be the best fit, running a collection of models that could be appropriate and comparing these models is the best way to ensure that the proper model is used. Xie et al. (2013) demonstrated this technique and Darbro (2020) provided a tutorial on running some of the basic multilevel models.

Multilevel models are also called Mixed Effects Models because they are made up of both fixed effects and random effects. Fixed effects are effects that are assumed to have a fixed or constant relationship with the response variable across all observations. Group, AOI, and the interaction are predictor variables that are assumed to be fixed and have fixed effects on the response variable. The random effects added to the model account for variation found at different levels of the model. For our data, accounted for participant-to-participant differences and Posture ID-to-Posture ID differences.

Mixed Effects Models are flexible enough to allow for differences in exposure time (resulting in a varying number of total gaze points per posture) from participant to participant. This is a critical component of these models as the participants took as much time as they needed to come to a conclusion about how long the subject could hold the posture and this resulted in a varying number of total gaze points per Posture ID. This led to data that were unbalanced from one participant to another because these gaze-point counts are weighted differently depending on the number of total gaze points contributed to any given Posture

ID. Therefore, a model that is capable of handling the unbalanced data is required.

It is important to note that the gaze-point count that serves as the response variable is collected at the AOI level and not at the Posture ID level. Thus, we are not suggesting that the response variable leads to unbalanced data. This variation is at the Posture ID level and means that the gaze-point count from a given AOI cannot be directly compared from one participant to the other because these participants contributed a different number of gaze points to the Posture ID as a whole.

A single-level regression equation with two predictors is given as follows:

$$\tilde{Y}_i = \beta_0 + \beta_1 \tilde{X}_{1_i} + \beta_2 \tilde{X}_{2_i} + \epsilon_i. \quad (2.11)$$

In this model: \tilde{Y}_i represents the outcome variable (also called response or dependent variable), β_0 represents a fixed intercept; β_1 and β_2 represent fixed estimates for predictor 1 (\tilde{X}_{1_i}) and predictor 2 (\tilde{X}_{2_i}); and ϵ_i represents random residuals. The subscript i is the index that notes the level of the model. Since this is a single-level model, i represents the only level of this model.

For this study, the outcome variable we want to predict is the gaze-point count. The variables we want to use for the prediction of the gaze-point count are referred to as the predictor variables or explanatory variables. There are two predictor variables being Group (Treatment or Control) and location which is categorized by AOI. Group is a predictor variable that can be found at the Participant (macrounit) level. While we only have two predictor variables, the multilevel analysis for this dataset has three levels. The highest level, also referred to as the macrounit or level 3, is the participant. Each participant looks at a series of the twenty-two Posture IDs, thus Posture ID is the mesounit or level 2. Each Posture ID is divided into areas of interest which makes AOI the lowest level, also called the microunit or level 1. The dependent variable, gaze-point count, is measured at the lowest level. A depiction of this multilevel structure is shown in Figure 2.19 and all notation is organized in Table 2.2 and Table 2.3.

A multilevel model equation with three levels that has one predictor at the microunit

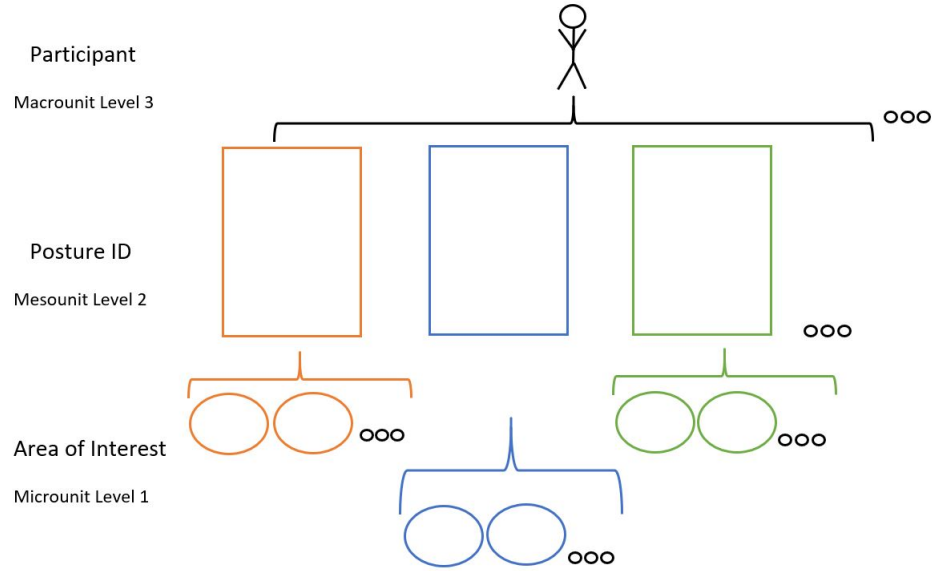


Fig. 2.19: Multilevel structure of eye-tracking data.

level (1) and one predictor at the macrounit level (3) is needed for this data set. The index i represents units at the macrounit level; Participant. The index j represents units at the mesounit level (2); Posture ID. The index $k(j, l(j))$ represents units at the microunit level; AOI. The max value of $k(j, l(j))$ for a given posture j represents the total number of AOIs on a given posture, not the particular AOI. Table 2.4 shows that the value of $k(j, l(j))$ indicates a different location depending on the Posture ID. When $k(j, l(j)) = 10$ on Posture IDs 1, 2, 3, and 5, this relates to AOI location 10. When $k(j, l(j)) = 10$ on Posture ID 4, this relates to AOI location 18. Table 2.5 provides a complete connection between $k(j, l(j))$ and AOI location n for every Posture ID.

The variable \tilde{Y}_{ijk} represents the observed dependent variable, gaze-point count. The predictor (AOI) at the microunit level is represented by W_{ijk} and the predictor (Group) at the macrounit level is given as V_i . A more detailed list of notations is provided in Table 2.2.

Recall, in ordinary Multiple Linear Regression with a single level, the expected value of the Dependent Variable (\tilde{Y}_i) is a linear combination of the predictor variables X_1 and X_2 given as $\eta_i = \beta_0 + \beta_1 X_{1i} + \beta_2 X_{2i}$ where the residuals ϵ_i follow the normal distribution as seen in Equation 2.12:

Table 2.2: Mixed Effect Model general notation.

Notation	Type	Description
<i>Experimental Specifications</i>		
$q = 40$	Sample Size	Number of Participants
$p = 22$	Sample Size	Number of Posture IDs
$i = 1, \dots, q$	Index	Macrounits, units within level 1 (Participant)
$j = 1, \dots, p$	Index	Mesounits, units within level 2 (Posture ID)
$l(j)$	22 Sample Sizes	Number of AOIs, different for each Posture ID j (see Table 2.5)
$k = k(j, l(j))$	Index	Microunits, units within level 3 (AOI)
$m = 2$	Constant	Number of Groups (Treatment and Control)
$n = 25$	Constant	Number of unique AOIs (see rows of Table 2.5)
$\xi = 1$	Degrees of Freedom	Predictor variable Group ($m - 1$)
$\zeta = 24$	Degrees of Freedom	Predictor variable AOI ($n - 1$)
$\psi = 24$	Degrees of Freedom	Interaction between predictors ($(m - 1)(n - 1)$)
<i>Model Variables</i>		
\tilde{Y}_{ijk}	Dependent	Count of gaze points
V_i	Fixed Predictor	Group indicator: for the i^{th} Participant, 1 = Treatment, 0 = Control
W_{ijk}	Fixed Predictors	24 AOI indicators: for the i^{th} Participant on j^{th} Posture ID, 1 = k^{th} AOI, else 0
$V_i W_{ijk}$	Fixed Predictors	24 Interaction indicators: for the i^{th} Participant and j^{th} Posture ID, 1 = k^{th} AOI and Treatment, else 0
S_i	Random Predictors	40 Participant indicators: 1 = i^{th} Participant, else 0
T_{ij}	Random Predictors	880 Participant \times Posture ID combination indicators: 1 = i^{th} Participant and j^{th} Posture ID, else 0

Note: All notation that includes the subscript k such as \tilde{Y}_{ijk} , W_{ijk} , and $V_i W_{ijk}$ are shortened from $k(j, l(j))$ for brevity and clarity of which level the estimates are measured from. All fixed and random effects are on the log count of the Dependent Variable, \tilde{Y}_{ijk} when Poisson Regression with the log link is used.

Table 2.3: Mixed Effect Model estimable parameter specification and notation.

Notation	Type	Description
<i>Intermediate Marginal Effects: across Participants, specific to each AOI, within Posture ID</i>		
β_{0jk}	Fixed Intercept	Marginal Mean for the Control Group
β_{1jk}	Fixed Slopes	Marginal Main Effect of Group, Treatment vs. Control
<i>Intermediate Marginal Effects: across Participants, specific to each Posture ID</i>		
γ_{00k}	Fixed Intercept	Global Marginal Mean for the Control Group: $\bar{\beta}_{0jk}$
γ_{10k}	Fixed Slopes	Marginal Main Effect of Group, Treatment vs. Control, constrained to be equivalent across Posture IDs β_{1jk}
<i>Overall Marginal Effects: across all Participants and Posture IDs</i>		
δ_{000}	Fixed Intercept	Global Marginal Mean for the Control group on the reference AOI, $\bar{\beta}_{0jk} = \bar{\gamma}_{00k}$
δ_{100}	Fixed Slope	Marginal Main Effect of Group, the difference in the Marginal Mean for the Treatment Group compared to the Control Group
δ_{00k}	Fixed Slopes	Marginal Main Effects of each unique AOI compared to the reference AOI
δ_{10k}	Fixed Slopes	Marginal Interactions between Group and AOI
u_{i0}	Random Intercepts	Macrounit Uniquenesses in intercept for Participant i
u_{0j}	Random Intercepts	Mesounit Uniquenesses in intercept for Posture ID j
ϵ_{ijk}	Residuals	Microunit Uniqueness in intercept for the i^{th} Participant for the j^{th} Posture ID for the k^{th} AOI

Note: All notation that includes the subscript k such as δ_{00k} , β_{0jk} , and ϵ_{ijk} are shortened from $k(j, l(j))$ for brevity and clarity of which level the estimates are measured from.

The reference category for AOI is specified as the last or 25th unique AOI.

$\bar{\beta}_{0jk}$ refers to the mean β_{0jk} across all jk and $\bar{\gamma}_{00k}$ refers to the mean γ_{00k} across all k .

$$\begin{aligned}
\tilde{Y}_i &= E(\tilde{Y}_i | X_{1i}, X_{2i}) + \epsilon_i \\
&= \eta_i + \epsilon_i \\
&= \beta_0 + \beta_1 X_{1i} + \beta_2 X_{2i} + \epsilon_i.
\end{aligned} \tag{2.12}$$

Conversely, Generalized Linear Models allow the Dependent Variable to have an arbitrary distribution (rather than simple normal distribution) for an arbitrary function of the Dependent Variable (the link function, $g(\tilde{Y}_i)$) to vary linearly with the predictors (X_{1i}, X_{2i}). This single-level Generalized Linear Model is given in Equation 2.13:

$$\begin{aligned}
\tilde{Y}_i &= E(\tilde{Y}_i | X_{1i}, X_{2i}) + \epsilon_i \\
&= g^{-1}(\eta_i | X_{1i}, X_{2i}) + \epsilon_i \\
&= g^{-1}(\beta_0 + \beta_1 X_{1i} + \beta_2 X_{2i}) + \epsilon_i.
\end{aligned} \tag{2.13}$$

The multilevel model generalization follows in Equation 2.14:

$$\begin{aligned}
\tilde{Y}_{ijk} &= E(\tilde{Y}_{ijk} | V_i, W_{ijk}) + \epsilon_{ijk} \\
&= g^{-1}(\eta_{ijk} | V_i, W_{ijk}) + \epsilon_{ijk}.
\end{aligned} \tag{2.14}$$

It should be noted that the number of unique AOI locations varies between the four AOI iterations. The number of unique AOIs is given as follows: Round 1 VT = 25 (given as n in Table 2.2 because these tables are based on the Round 1 VT AOI iteration), Round 1 LRVT = 26, Round 2 VT = 17, Round 2 LRVT = 18. For this explanation, we focus on the Round 1 VT iteration exclusively. To simplify some of the notation, we use $k = k(j, l(j))$. At the microunit level (AOI within Posture ID), the linear prediction is dependent only upon the microunit level predictor AOI (W_{ijk}). As shown in Equation 2.15, β_{0jk} refers to the intercept and β_{1jk} refers to the Treatment Main Effect for a specific AOI (k) and Posture ID (j):

$$\eta_{ijk} = \beta_{0jk} + \beta_{1jk} W_{ijk}. \tag{2.15}$$

At the mesounit level (Posture ID), we specify that the intercepts (β_{0jk}) may differ

for various combinations of Participant and Posture ID (T_{ij}), however the Treatment Effect (β_{1jk}) is constant. Thus, the intercept is partitioned into the mean across Posture ID (γ_{00k}) and the uniqueness of each Posture ID (u_{0j}) as seen in Equation 2.16 and 2.17:

$$\beta_{0jk} = \gamma_{00k} + u_{0j}T_{ij}, \quad (2.16)$$

$$\beta_{1jk} = \gamma_{10k}. \quad (2.17)$$

Similarly, at the macrounit level (Participant), we specify that the intercept (γ_{00k}) may differ by the macrounit level predictor Group, Treatment vs. Control (V_i), and Participant uniqueness (S_i). As in Equation 2.17, the slopes are held constant. This is shown in Equations 2.18 and 2.19:

$$\gamma_{00k} = \delta_{000} + \delta_{100}V_i + u_{i0}S_i, \quad (2.18)$$

$$\gamma_{10k} = \delta_{00k} + \delta_{10k}V_i. \quad (2.19)$$

The multilevel form for our generalized multilevel model with three levels, one predictor at the microunit level, and one predictor at the macrounit level, is found with back-substitution given in Equation 2.20 as follows:

$$\begin{aligned} \eta_{ijk} &= \beta_{0jk} + \beta_{1jk}W_{ijk} \\ &= (\gamma_{00k} + u_{0j}T_{ij}) + (\gamma_{10k}) \cdot W_{ijk} \\ &= (\delta_{000} + \delta_{100}V_i + u_{i0}S_i + u_{0j}T_{ij}) + (\delta_{00k} + \delta_{10k}V_i) \cdot W_{ijk} \\ &= \delta_{000} + \delta_{100}V_i + u_{i0}S_i + u_{0j}T_{ij} + \delta_{00k}W_{ijk} + \delta_{10k}V_iW_{ijk} \\ &= \delta_{000} + \delta_{100}V_i + \delta_{00k}W_{ijk} + \delta_{10k}V_iW_{ijk} + u_{0j}T_{ij} + u_{i0}S_i \\ &= \delta_{000} + V_i\delta_{100} + W_{ijk}\delta_{00k} + V_iW_{ijk}\delta_{10k} + T_{ij}u_{0j} + S_iu_{i0}. \end{aligned} \quad (2.20)$$

Further substitution of Equation 2.20 into Equation 2.14 yields the combined form of Equation 2.21,

$$E(\tilde{Y}_{ijk}|V_i, W_{ijk}) = g^{-1}(\delta_{000} + V_i\delta_{100} + W_{ijk}\delta_{00k} + V_iW_{ijk}\delta_{10k} + T_{ij}u_{0j} + S_iu_{i0}). \quad (2.21)$$

This is related to the basic form of a Mixed Effects Model in matrix notation given in Equation 2.22 as:

$$\tilde{Y}_{ijk} = g^{-1}(\mathbf{X}\delta + \mathbf{Z}u) + \epsilon_{ijk}. \quad (2.22)$$

In this matrix notation of the final equation, \tilde{Y}_{ijk} is the response variable of gaze-point count collected at the microunit level. \mathbf{X} is a matrix of 0s and 1s where 1s indicate the fixed effect being evaluated and δ is a vector of the fixed effect estimates. \mathbf{Z} represents a matrix of the random effects with u as the vector of random effect estimates. Together, $\mathbf{X}\delta$ indicate the fixed effects and $\mathbf{Z}u$ indicate the random effects of the model. The ϵ vector for this multilevel model represents the variance of the residuals.

More specifically, \mathbf{X} from Equation 2.22 represents a matrix of the fixed effects V_i , W_{ijk} , and V_iW_{ijk} where each fixed effect contributes a number of columns equal to one less than the number of categories for the variable (see Matrix \mathbf{X} from Equation 2.24). This occurs because these effects are categorical and the final category is treated as the reference category. Each column consists of 1s where the category is present and 0 elsewhere. The matrix \mathbf{Z} from Equation 2.22 is a matrix of the random effects T_{ij} and S_i . Each of the random effects contributes a number of columns to the \mathbf{Z} matrix equal to the number of levels for that effect.

The structure of the vectors and matrices that make up Equation 2.22 are included separately where \tilde{Y}_{ijk} is given in Equation 2.23, $\mathbf{X}\delta$ is given in Equation 2.24, and $\mathbf{Z}u + \epsilon$ is given in Equation 2.25. Lee et al. (2006), Moghimbeigi et al. (2008), and Hur et al. (2002) described that the random effects are normally distributed. Lee et al. (2006) indicated that complex correlation structures can be specified for the random components to accommodate

Table 2.4: AOI notation definitions for Posture IDs $j = 1, \dots, 5$.

Posture ID j	AOI Number $l(j)$	AOI Location n	$k(j, l(j))$
1	1	1	$k(1, 1)$
1	2	2	$k(1, 2)$
\vdots	\vdots	\vdots	\vdots
1	14	14	$k(1, 14)$
2	1	1	$k(2, 1)$
2	2	2	$k(2, 2)$
\vdots	\vdots	\vdots	\vdots
2	14	14	$k(2, 14)$
3	1	1	$k(3, 1)$
3	2	2	$k(3, 2)$
\vdots	\vdots	\vdots	\vdots
3	14	14	$k(3, 14)$
4	1	1	$k(4, 1)$
4	2	6	$k(4, 2)$
4	3	7	$k(4, 3)$
4	4	12	$k(4, 4)$
4	5	13	$k(4, 5)$
4	6	14	$k(4, 6)$
4	7	15	$k(4, 7)$
4	8	16	$k(4, 8)$
4	9	17	$k(4, 9)$
4	10	18	$k(4, 10)$
5	1	1	$k(5, 1)$
5	2	2	$k(5, 2)$
\vdots	\vdots	\vdots	\vdots
5	14	14	$k(5, 14)$

clustering depending on the context of the study. The matrix structure of this model was verified using the `getME` function from the `lme4` R package (Bates et al., 2015) to obtain the \mathbf{X} and \mathbf{Z} matrices.

Table 2.5: Display of $n = 25$ unique AOIs and how AOI number $l(j)$ (numbered inside the table) depends on the Posture ID j for Round 1 Voronoi Tessellations.

		Posture ID (j)																					
n	AOI Label	1	2	3	4	5	6	7	8	9	10	11	12	13	14	15	16	17	18	19	20	21	22
1	Rt Foot (1)	1	1	1	1	1	1	1	1	1	1	1	1	1	1	1	1	1	1	1	1	1	1
2	Rt Knee (2)	2	2	2		2	2	2	2	2		2	2	2	2	2		2	2	2	2	2	2
3	Rt Hand (3)	3	3	3		3	3	3	3	3	2	3	3	3	3		2	3	3		3	3	3
4	Rt Hip (4)	4	4	4		4	4	4		4		4	4	4		3	3	4		3		4	4
5	Rt Elbow (5)	5	5	5		5	5	5	4	5	3	5	5	5	4		4	5	4		4	5	5
6	Rt Shoulder (6)	6	6	6	2	6	6	6	5	6	4	6	6	6		4	5	6	5		5	6	
7	Lt Foot (7)	7	7	7	3	7	7	7	6	7	5	7	7	7	5	5	6	7	6	4	6	7	6
8	Lt Knee (8)	8	8	8		8	8	8	7	8		8	8	8	6	6		8	7	5	7	8	7
9	Lt Hand (9)	9	9	9		9	9	9				9	9	9	7		7	9	8		8	9	8
10	Lt Hip (10)	10	10	10		10	10	10	8	9	6	10	10	10	8	7	8	10	9	6	9	10	9
11	Lt Elbow (11)	11	11	11		11	11	11	9		7	11	11	11	9		9		10		10	11	10
12	Lt Shoulder (12)	12	12	12	4	12	12	12	10		8	12	12	12	10	8	10	11			11	12	11
13	Torso (13)	13	13	13	5	13	13	13	11	10	9	13	13	13	11		11	12		7	12	13	12
14	Head (14)	14	14	14	6	14	14	14	12	11	10	14	14	14	12	9	12	13	11	8	13	14	13
15	Rt Knee (2) Rt Hand (3)				7																		
16	Rt Hip (4) Rt Elbow (5)				8																		
17	Lt Knee (8) Lt Hand (9)				9																		
18	Lt Hip (10) Lt Elbow (11)				10																		
19	Rt Hip (4) Lt Hand (9)								13		11												
20	Rt Knee (2) Lt Knee (8)										12						13						
21	Rt Hip (4) Rt Shoulder (6)														13								
22	Rt Hand (3) Lt Hand (9)															10							
23	Rt Elbow (5) Lt Elbow (11) Torso (13)															11							
24	Rt Hip (4) Lt Shoulder (12) Torso (13)																		12				
25	Rt Hand (3) Rt Elbow (5) Rt Shoulder (6)																			9			

Note: Rt = Right; Lt = Left.

\tilde{Y}_{ijk} Vector:

$$\begin{bmatrix}
 y_{1,1,k(1,1)} \\
 y_{1,1,k(1,2)} \\
 \vdots \\
 y_{1,1,k(1,14)} \\
 y_{1,2,k(2,1)} \\
 y_{1,2,k(2,2)} \\
 \vdots \\
 y_{1,2,k(2,14)} \\
 \vdots \\
 y_{1,22,k(22,13)} \\
 \vdots \\
 y_{20,1,k(1,1)} \\
 y_{20,1,k(1,2)} \\
 \vdots \\
 y_{20,1,k(1,14)} \\
 y_{20,2,k(2,1)} \\
 y_{20,2,k(2,2)} \\
 \vdots \\
 y_{20,2,k(2,14)} \\
 \vdots \\
 y_{20,22,k(22,13)} \\
 y_{21,1,k(1,1)} \\
 y_{21,1,k(1,2)} \\
 \vdots \\
 y_{21,1,k(1,14)} \\
 y_{21,2,k(2,1)} \\
 y_{21,2,k(2,2)} \\
 \vdots \\
 y_{21,2,k(2,14)} \\
 \vdots \\
 y_{21,22,k(22,13)} \\
 \vdots \\
 y_{i,j,k(j,l(j))} \\
 \vdots \\
 y_{40,1,k(1,1)} \\
 y_{40,1,k(1,2)} \\
 \vdots \\
 y_{40,1,k(1,14)} \\
 y_{40,2,k(2,1)} \\
 y_{40,2,k(2,2)} \\
 \vdots \\
 y_{40,2,k(2,14)} \\
 \vdots \\
 y_{40,22,k(22,13)}
 \end{bmatrix}$$

(2.23)

X Matrix and δ Vector:

1	$V_{1,1}$	$W_{1,1,k(1,1),1}$	\cdots	$W_{1,1,k(1,1),24}$	$V_1 W_{1,1,k(1,1),1}$	\cdots	$V_1 W_{1,1,k(1,1),24}$
1	$V_{1,1}$	$W_{1,1,k(1,2),1}$	\cdots	$W_{1,1,k(1,2),24}$	$V_1 W_{1,1,k(1,2),1}$	\cdots	$V_1 W_{1,1,k(1,2),24}$
\vdots	\vdots	\vdots	\vdots	\vdots	\vdots	\vdots	\vdots
1	$V_{1,1}$	$W_{1,1,k(1,14),1}$	\cdots	$W_{1,1,k(1,14),24}$	$V_1 W_{1,1,k(1,14),1}$	\cdots	$V_1 W_{1,1,k(1,14),24}$
1	$V_{1,1}$	$W_{1,2,k(2,1),1}$	\cdots	$W_{1,2,k(2,1),24}$	$V_1 W_{1,2,k(2,1),1}$	\cdots	$V_1 W_{1,2,k(2,1),24}$
1	$V_{1,1}$	$W_{1,2,k(2,2),1}$	\cdots	$W_{1,2,k(2,2),24}$	$V_1 W_{1,2,k(2,2),1}$	\cdots	$V_1 W_{1,2,k(2,2),24}$
\vdots	\vdots	\vdots	\vdots	\vdots	\vdots	\vdots	\vdots
1	$V_{1,1}$	$W_{1,2,k(2,14),1}$	\cdots	$W_{1,2,k(2,14),24}$	$V_1 W_{1,2,k(2,14),1}$	\cdots	$V_1 W_{1,2,k(2,14),24}$
\vdots	\vdots	\vdots	\vdots	\vdots	\vdots	\vdots	\vdots
1	$V_{1,1}$	$W_{1,22,k(22,13),1}$	\cdots	$W_{1,22,k(22,13),24}$	$V_1 W_{1,22,k(22,13),1}$	\cdots	$V_1 W_{1,22,k(22,13),24}$
\vdots	\vdots	\vdots	\vdots	\vdots	\vdots	\vdots	\vdots
1	$V_{20,1}$	$W_{20,1,k(1,1),1}$	\cdots	$W_{20,1,k(1,1),24}$	$V_{20} W_{20,1,k(1,1),1}$	\cdots	$V_{20} W_{20,1,k(1,1),24}$
1	$V_{20,1}$	$W_{20,1,k(1,2),1}$	\cdots	$W_{20,1,k(1,2),24}$	$V_{20} W_{20,1,k(1,2),1}$	\cdots	$V_{20} W_{20,1,k(1,2),24}$
\vdots	\vdots	\vdots	\vdots	\vdots	\vdots	\vdots	\vdots
1	$V_{20,1}$	$W_{20,1,k(1,14),1}$	\cdots	$W_{20,1,k(1,14),24}$	$V_{20} W_{20,1,k(1,14),1}$	\cdots	$V_{20} W_{20,1,k(1,14),24}$
1	$V_{20,1}$	$W_{20,2,k(2,1),1}$	\cdots	$W_{20,2,k(2,1),24}$	$V_{20} W_{20,2,k(2,1),1}$	\cdots	$V_{20} W_{20,2,k(2,1),24}$
1	$V_{20,1}$	$W_{20,2,k(2,2),1}$	\cdots	$W_{20,2,k(2,2),24}$	$V_{20} W_{20,2,k(2,2),1}$	\cdots	$V_{20} W_{20,2,k(2,2),24}$
\vdots	\vdots	\vdots	\vdots	\vdots	\vdots	\vdots	\vdots
1	$V_{20,1}$	$W_{20,2,k(2,14),1}$	\cdots	$W_{20,2,k(2,14),24}$	$V_{20} W_{20,2,k(2,14),1}$	\cdots	$V_{20} W_{20,2,k(2,14),24}$
\vdots	\vdots	\vdots	\vdots	\vdots	\vdots	\vdots	\vdots
1	$V_{20,1}$	$W_{20,22,k(22,13),1}$	\cdots	$W_{20,22,k(22,13),24}$	$V_{20} W_{20,22,k(22,13),1}$	\cdots	$V_{20} W_{20,22,k(22,13),24}$
1	$V_{21,1}$	$W_{21,1,k(1,1),1}$	\cdots	$W_{21,1,k(1,1),24}$	$V_{21} W_{21,1,k(1,1),1}$	\cdots	$V_{21} W_{21,1,k(1,1),24}$
1	$V_{21,1}$	$W_{21,1,k(1,2),1}$	\cdots	$W_{21,1,k(1,2),24}$	$V_{21} W_{21,1,k(1,2),1}$	\cdots	$V_{21} W_{21,1,k(1,2),24}$
\vdots	\vdots	\vdots	\vdots	\vdots	\vdots	\vdots	\vdots
1	$V_{21,1}$	$W_{21,1,k(1,14),1}$	\cdots	$W_{21,1,k(1,14),24}$	$V_{21} W_{21,1,k(1,14),1}$	\cdots	$V_{21} W_{21,1,k(1,14),24}$
1	$V_{21,1}$	$W_{21,2,k(2,1),1}$	\cdots	$W_{21,2,k(2,1),24}$	$V_{21} W_{21,2,k(2,1),1}$	\cdots	$V_{21} W_{21,2,k(2,1),24}$
1	$V_{21,1}$	$W_{21,2,k(2,2),1}$	\cdots	$W_{21,2,k(2,2),24}$	$V_{21} W_{21,2,k(2,2),1}$	\cdots	$V_{21} W_{21,2,k(2,2),24}$
\vdots	\vdots	\vdots	\vdots	\vdots	\vdots	\vdots	\vdots
1	$V_{21,1}$	$W_{21,2,k(2,14),1}$	\cdots	$W_{21,2,k(2,14),24}$	$V_{21} W_{21,2,k(2,14),1}$	\cdots	$V_{21} W_{21,2,k(2,14),24}$
\vdots	\vdots	\vdots	\vdots	\vdots	\vdots	\vdots	\vdots
1	$V_{21,1}$	$W_{21,22,k(22,13),1}$	\cdots	$W_{21,22,k(22,13),24}$	$V_{21} W_{21,22,k(22,13),1}$	\cdots	$V_{21} W_{21,22,k(22,13),24}$
\vdots	\vdots	\vdots	\vdots	\vdots	\vdots	\vdots	\vdots
1	$V_{i,\xi}$	$W_{i,j,k(j,l(j)),1}$	\cdots	$W_{i,j,k(j,l(j)),\zeta}$	$V_i W_{i,j,k(j,l(j)),1}$	\cdots	$V_i W_{i,j,k(j,l(j)),\psi}$
\vdots	\vdots	\vdots	\vdots	\vdots	\vdots	\vdots	\vdots
1	$V_{40,1}$	$W_{40,1,k(1,1),1}$	\cdots	$W_{40,1,k(1,1),24}$	$V_{40} W_{40,1,k(1,1),1}$	\cdots	$V_{40} W_{40,1,k(1,1),24}$
1	$V_{40,1}$	$W_{40,1,k(1,2),1}$	\cdots	$W_{40,1,k(1,2),24}$	$V_{40} W_{40,1,k(1,2),1}$	\cdots	$V_{40} W_{40,1,k(1,2),24}$
\vdots	\vdots	\vdots	\vdots	\vdots	\vdots	\vdots	\vdots
1	$V_{40,1}$	$W_{40,1,k(1,14),1}$	\cdots	$W_{40,1,k(1,14),24}$	$V_{40} W_{40,1,k(1,14),1}$	\cdots	$V_{40} W_{40,1,k(1,14),24}$
1	$V_{40,1}$	$W_{40,2,k(2,1),1}$	\cdots	$W_{40,2,k(2,1),24}$	$V_{40} W_{40,2,k(2,1),1}$	\cdots	$V_{40} W_{40,2,k(2,1),24}$
1	$V_{40,1}$	$W_{40,2,k(2,2),1}$	\cdots	$W_{40,2,k(2,2),24}$	$V_{40} W_{40,2,k(2,2),1}$	\cdots	$V_{40} W_{40,2,k(2,2),24}$
\vdots	\vdots	\vdots	\vdots	\vdots	\vdots	\vdots	\vdots
1	$V_{40,1}$	$W_{40,2,k(2,14),1}$	\cdots	$W_{40,2,k(2,14),24}$	$V_{40} W_{40,2,k(2,14),1}$	\cdots	$V_{40} W_{40,2,k(2,14),24}$
\vdots	\vdots	\vdots	\vdots	\vdots	\vdots	\vdots	\vdots
1	$V_{40,1}$	$W_{40,22,k(22,13),1}$	\cdots	$W_{40,22,k(22,13),24}$	$V_{40} W_{40,22,k(22,13),1}$	\cdots	$V_{40} W_{40,22,k(22,13),24}$

$\left[\begin{array}{c} \delta_{0,0,0} \\ \delta_{1,0,0} \\ \delta_{0,0,1} \\ \vdots \\ \delta_{0,0,24} \\ \delta_{1,0,1} \\ \vdots \\ \delta_{1,0,24} \end{array} \right] \quad (2.24)$

¹An additional index was added to V_i , W_{ijk} , and $V_i W_{ijk}$ (ξ , ζ , and ψ respectively) that indicates the number of columns used for the predictor variable.

Z Matrix, **u** Vector, and ϵ Vector:

$$\begin{bmatrix}
 T_{1,1,1} & \cdots & T_{1,1,22} & S_{1,1} & \cdots & S_{1,40} \\
 T_{1,1,1} & \cdots & T_{1,1,22} & S_{1,1} & \cdots & S_{1,40} \\
 \vdots & & \vdots & \vdots & & \vdots \\
 T_{1,1,1} & \cdots & T_{1,1,22} & S_{1,1} & \cdots & S_{1,40} \\
 T_{1,2,1} & \cdots & T_{1,2,22} & S_{1,1} & \cdots & S_{1,40} \\
 T_{1,2,1} & \cdots & T_{1,2,22} & S_{1,1} & \cdots & S_{1,40} \\
 \vdots & & \vdots & \vdots & & \vdots \\
 T_{1,2,1} & \cdots & T_{1,2,22} & S_{1,1} & \cdots & S_{1,40} \\
 \vdots & & \vdots & \vdots & & \vdots \\
 T_{1,22,1} & \cdots & T_{1,22,22} & S_{1,1} & \cdots & S_{1,40} \\
 \vdots & & \vdots & \vdots & & \vdots \\
 T_{20,1,1} & \cdots & T_{20,1,22} & S_{20,1} & \cdots & S_{20,40} \\
 T_{20,1,1} & \cdots & T_{20,1,22} & S_{20,1} & \cdots & S_{20,40} \\
 \vdots & & \vdots & \vdots & & \vdots \\
 T_{20,1,1} & \cdots & T_{20,1,22} & S_{20,1} & \cdots & S_{20,40} \\
 T_{20,2,1} & \cdots & T_{20,2,22} & S_{20,1} & \cdots & S_{20,40} \\
 T_{20,2,1} & \cdots & T_{20,2,22} & S_{20,1} & \cdots & S_{20,40} \\
 \vdots & & \vdots & \vdots & & \vdots \\
 T_{20,2,1} & \cdots & T_{20,2,22} & S_{20,1} & \cdots & S_{20,40} \\
 \vdots & & \vdots & \vdots & & \vdots \\
 T_{20,22,1} & \cdots & T_{20,22,22} & S_{20,1} & \cdots & S_{20,40} \\
 T_{21,1,1} & \cdots & T_{21,1,22} & S_{21,1} & \cdots & S_{21,40} \\
 T_{21,1,1} & \cdots & T_{21,1,22} & S_{21,1} & \cdots & S_{21,40} \\
 \vdots & & \vdots & \vdots & & \vdots \\
 T_{21,1,1} & \cdots & T_{21,1,22} & S_{21,1} & \cdots & S_{21,40} \\
 T_{21,2,1} & \cdots & T_{21,2,22} & S_{21,1} & \cdots & S_{21,40} \\
 T_{21,2,1} & \cdots & T_{21,2,22} & S_{21,1} & \cdots & S_{21,40} \\
 \vdots & & \vdots & \vdots & & \vdots \\
 T_{21,2,1} & \cdots & T_{21,2,22} & S_{21,1} & \cdots & S_{21,40} \\
 \vdots & & \vdots & \vdots & & \vdots \\
 T_{21,22,1} & \cdots & T_{21,22,22} & S_{21,1} & \cdots & S_{21,40} \\
 \vdots & & \vdots & \vdots & & \vdots \\
 T_{i,j,1} & \cdots & T_{i,j,p} & S_{i,1} & \cdots & S_{i,q} \\
 \vdots & & \vdots & \vdots & & \vdots \\
 T_{40,1,1} & \cdots & T_{40,1,22} & S_{40,1} & \cdots & S_{40,40} \\
 T_{40,1,1} & \cdots & T_{40,1,22} & S_{40,1} & \cdots & S_{40,40} \\
 \vdots & & \vdots & \vdots & & \vdots \\
 T_{40,1,1} & \cdots & T_{40,1,22} & S_{40,1} & \cdots & S_{40,40} \\
 T_{40,2,1} & \cdots & T_{40,2,22} & S_{40,1} & \cdots & S_{40,40} \\
 T_{40,2,1} & \cdots & T_{40,2,22} & S_{40,1} & \cdots & S_{40,40} \\
 \vdots & & \vdots & \vdots & & \vdots \\
 T_{40,2,1} & \cdots & T_{40,2,22} & S_{40,1} & \cdots & S_{40,40} \\
 \vdots & & \vdots & \vdots & & \vdots \\
 T_{40,22,1} & \cdots & T_{40,22,22} & S_{40,1} & \cdots & S_{40,40}
 \end{bmatrix}
 +
 \begin{bmatrix}
 u_{0,1} \\
 \vdots \\
 u_{0,22} \\
 u_{1,0} \\
 \vdots \\
 u_{40,0}
 \end{bmatrix}
 +
 \begin{bmatrix}
 \epsilon_{1,1,k(1,1)} \\
 \epsilon_{1,1,k(1,2)} \\
 \vdots \\
 \epsilon_{1,1,k(1,14)} \\
 \epsilon_{1,2,k(2,1)} \\
 \epsilon_{1,2,k(2,2)} \\
 \vdots \\
 \epsilon_{1,2,k(2,14)} \\
 \vdots \\
 \epsilon_{1,22,k(22,13)} \\
 \vdots \\
 \epsilon_{20,1,k(1,1)} \\
 \epsilon_{20,1,k(1,2)} \\
 \vdots \\
 \epsilon_{20,1,k(1,14)} \\
 \epsilon_{20,2,k(2,1)} \\
 \epsilon_{20,2,k(2,2)} \\
 \vdots \\
 \epsilon_{20,2,k(2,14)} \\
 \vdots \\
 \epsilon_{20,22,k(22,13)} \\
 \epsilon_{21,1,k(1,1)} \\
 \epsilon_{21,1,k(1,2)} \\
 \vdots \\
 \epsilon_{21,1,k(1,14)} \\
 \epsilon_{21,2,k(2,1)} \\
 \epsilon_{21,2,k(2,2)} \\
 \vdots \\
 \epsilon_{21,2,k(2,14)} \\
 \vdots \\
 \epsilon_{21,22,k(22,13)} \\
 \vdots \\
 \epsilon_{i,j,k(j,l(j))} \\
 \vdots \\
 \epsilon_{40,1,k(1,1)} \\
 \epsilon_{40,1,k(1,2)} \\
 \vdots \\
 \epsilon_{40,1,k(1,14)} \\
 \epsilon_{40,2,k(2,1)} \\
 \epsilon_{40,2,k(2,2)} \\
 \vdots \\
 \epsilon_{40,2,k(2,14)} \\
 \vdots \\
 \epsilon_{40,22,k(22,13)}
 \end{bmatrix}
 \quad (2.25)$$

²An additional index was added to T_{ij} and S_i (p and q respectively) that indicates the number of columns used for the random effect.

The matrices and vectors shown in Equations 2.23 - 2.25 are accurate yet difficult to understand with the proper notation structure. A simplified example is provided to show how these matrices work in an easier to understand setting. This example includes four participants ($q = 4$), two from the Treatment group (the first two participants) and two from the Control group. Three postures ($p = 3$) are used and there are $n = 5$ unique AOI locations for the AOIs which are indicated by letters a through e . Posture 1 has three AOIs: a , b , and c . Posture 2 has two AOIs: a and d . Posture 3 has three AOIs: a , c , and e .

Equation 2.26 shows the matrix notation for this simplified example with the proper 0 and 1 structure of the \mathbf{X} and \mathbf{Z} matrices. The color coding differentiates the three postures. As previously mentioned, the use of categorical effects leads to the final category serving as a reference category. This is why the δ vector does not include $\delta_{0,0,5}$ or $\delta_{1,0,5}$. The fifth AOI (AOI e) serves as the reference AOI.

\tilde{Y}_{ijk} vector, \mathbf{X} Matrix, δ Vector, \mathbf{Z} Matrix, \mathbf{u} Vector, and ϵ Vector for the simplified example:

$$\begin{aligned}
& \left[\begin{array}{c} y_{1,1,a} \\ y_{1,1,b} \\ y_{1,1,c} \\ y_{1,2,a} \\ y_{1,2,d} \\ y_{1,3,a} \\ y_{1,3,c} \\ y_{1,3,e} \\ y_{2,1,a} \\ y_{2,1,b} \\ y_{2,1,c} \\ y_{2,2,a} \\ y_{2,2,d} \\ y_{2,3,a} \\ y_{2,3,c} \\ y_{2,3,e} \\ y_{3,1,a} \\ y_{3,1,b} \\ y_{3,1,c} \\ y_{3,2,a} \\ y_{3,2,d} \\ y_{3,3,a} \\ y_{3,3,c} \\ y_{3,3,e} \\ y_{4,1,a} \\ y_{4,1,b} \\ y_{4,1,c} \\ y_{4,2,a} \\ y_{4,2,d} \\ y_{4,3,a} \\ y_{4,3,c} \\ y_{4,3,e} \end{array} \right] = \left[\begin{array}{ccccccc} 1 & 1 & 1 & 0 & 0 & 0 & 1 & 0 & 0 & 0 \\ 1 & 1 & 0 & 1 & 0 & 0 & 0 & 1 & 0 & 0 \\ 1 & 1 & 0 & 0 & 1 & 0 & 0 & 0 & 1 & 0 \\ 1 & 1 & 1 & 0 & 0 & 0 & 1 & 0 & 0 & 0 \\ 1 & 1 & 0 & 0 & 0 & 1 & 0 & 0 & 0 & 1 \\ 1 & 1 & 1 & 0 & 0 & 0 & 1 & 0 & 0 & 0 \\ 1 & 1 & 0 & 0 & 1 & 0 & 0 & 0 & 1 & 0 \\ 1 & 1 & 0 & 0 & 0 & 0 & 0 & 0 & 0 & 0 \\ 1 & 1 & 1 & 0 & 0 & 0 & 1 & 0 & 0 & 0 \\ 1 & 1 & 0 & 1 & 0 & 0 & 0 & 1 & 0 & 0 \\ 1 & 1 & 0 & 0 & 1 & 0 & 0 & 0 & 1 & 0 \\ 1 & 1 & 0 & 0 & 0 & 0 & 0 & 0 & 0 & 0 \\ 1 & 0 & 1 & 0 & 0 & 0 & 0 & 0 & 0 & 0 \\ 1 & 0 & 0 & 1 & 0 & 0 & 0 & 0 & 0 & 0 \\ 1 & 0 & 0 & 0 & 1 & 0 & 0 & 0 & 0 & 0 \\ 1 & 0 & 1 & 0 & 0 & 0 & 0 & 0 & 0 & 0 \\ 1 & 0 & 0 & 0 & 1 & 0 & 0 & 0 & 0 & 0 \\ 1 & 0 & 0 & 0 & 0 & 0 & 0 & 0 & 0 & 0 \\ 1 & 0 & 1 & 0 & 0 & 0 & 0 & 0 & 0 & 0 \\ 1 & 0 & 0 & 1 & 0 & 0 & 0 & 0 & 0 & 0 \\ 1 & 0 & 0 & 0 & 1 & 0 & 0 & 0 & 0 & 0 \\ 1 & 0 & 1 & 0 & 0 & 0 & 0 & 0 & 0 & 0 \\ 1 & 0 & 0 & 0 & 1 & 0 & 0 & 0 & 0 & 0 \\ 1 & 0 & 0 & 0 & 0 & 0 & 0 & 0 & 0 & 0 \end{array} \right] + \left[\begin{array}{c} \delta_{0,0,0} \\ \delta_{1,0,0} \\ \delta_{0,0,1} \\ \delta_{0,0,2} \\ \delta_{0,0,3} \\ \delta_{0,0,4} \\ \delta_{1,0,1} \\ \delta_{1,0,2} \\ \delta_{1,0,3} \\ \delta_{1,0,4} \end{array} \right] + \left[\begin{array}{c} u_{0,1} \\ u_{0,2} \\ u_{0,3} \\ u_{1,0} \\ u_{2,0} \\ u_{3,0} \\ u_{4,0} \end{array} \right] + \left[\begin{array}{c} \epsilon_{1,1,a} \\ \epsilon_{1,1,b} \\ \epsilon_{1,1,c} \\ \epsilon_{1,2,a} \\ \epsilon_{1,2,d} \\ \epsilon_{1,3,a} \\ \epsilon_{1,3,c} \\ \epsilon_{1,3,e} \\ \epsilon_{2,1,a} \\ \epsilon_{2,1,b} \\ \epsilon_{2,1,c} \\ \epsilon_{2,2,a} \\ \epsilon_{2,2,d} \\ \epsilon_{2,3,a} \\ \epsilon_{2,3,c} \\ \epsilon_{2,3,e} \\ \epsilon_{3,1,a} \\ \epsilon_{3,1,b} \\ \epsilon_{3,1,c} \\ \epsilon_{3,2,a} \\ \epsilon_{3,2,d} \\ \epsilon_{3,3,a} \\ \epsilon_{3,3,c} \\ \epsilon_{3,3,e} \\ \epsilon_{4,1,a} \\ \epsilon_{4,1,b} \\ \epsilon_{4,1,c} \\ \epsilon_{4,2,a} \\ \epsilon_{4,2,d} \\ \epsilon_{4,3,a} \\ \epsilon_{4,3,c} \\ \epsilon_{4,3,e} \end{array} \right] \quad (2.26)
\end{aligned}$$

Generalized Linear Mixed Effect Models are created by fitting many models using dummy variables for all but one parameter, which allows the model to estimate this parameter. Once these parameters are fitted, they are included in the more complex model. For this study, we are interested in how the interaction of participant group (Group) and location (AOI) affect the gaze-point counts. Our fixed effects for this model are Group, AOI, and the interaction between Group and AOI. The random effects that must be controlled for are Posture ID (level 2) and participant (level 3). Accounting for these random effects allows the model to test the main interaction without requiring balanced data. In other words, the total number of gaze points one participant contributes to a Posture ID can be much higher or lower than contributed by another participant. GLMMs account for this unbalanced data. Analysis on the gaze-point counts (as opposed to gaze-point proportions) is appropriate because the counts in an AOI for an individual are analyzed in the context of all counts for the Posture ID.

Application of GLMMs with Probability Density Functions

While many GLMMs are used for continuous response variables, there exist GLMMs for categorical and count response variables. Since the dependent variable for our data is the gaze-point count within each AOI for each Posture ID for each participant, models capable of handling count data are necessary. Poisson Regression and Negative Binomial Regression are the most common models used for count data. Zero-inflated variations of both the Poisson and Negative Binomial models also exist.

Mixed Effects Models produce statistics that can be compared to assess which of the models is the best fit for the data. The models are compared with Akaike Information Criterion (AIC) and Bayesian Information Criterion (BIC) statistics. The AIC and BIC values are penalized model selection criteria (Burnham and Anderson, 2004). As such, these values are often used in conjunction to compare models and identify models with the lowest false negative rates (low AIC value) and lowest false positive rates (low BIC value). Log-likelihood values are similarly used to compare models in that choosing the model with a log-likelihood estimate that has the smallest absolute value maximizes the probability of choosing the most accurate model (Baldi et al., 2000).

After the GLMMs with different regression models are compared, the model with the

best fit should be tested to see if the interaction term is significant. This is done by running the analysis without the interaction term and using the AIC, BIC, and log-likelihood values to determine which model is a better fit and running the Chi-Square test to determine if the difference between the analyses is significant. Here, the hypotheses are: H_O : the GLMM with the interaction term = the GLMM without the interaction term; and H_A : the GLMM with the interaction term \neq the GLMM without the interaction term. If the results of this test are not significant (meaning there is no significant difference in the models if the interaction term is used or not) the model without the interaction should be used. This is because adding an interaction term makes calculating the estimates more complex and if there is no significance with the interaction term, the model excluding the interaction should be the one used when collecting and interpreting results. Since there is no interaction term, these models produce p-values for each of the main effects to test to see if there are significant differences within the levels of that main effect. If the interaction is found to be significant, the model with the interaction should be used for collecting and interpreting results.

Poisson Regression

One of the most common models used for count data is Poisson Regression. The underlying Poisson distribution can be used when the outcome variable takes on a fixed value $[0, \infty)$ that represents the number of occurrences of an event (Coxe et al., 2009). The Poisson distribution is a right-skewed distribution with a lower bound at 0 which has one parameter λ that represents the value of both the mean and the variance. Thus, $\lambda = \mu = \sigma^2$ (Coxe et al., 2009). Poisson Regression is a type of log-linear model because the relationship between the log-transformed count outcome and the covariates is linear (Fitzmaurice et al., 2012). Hox et al. (2017) provided a thorough explanation of how Poisson Regression is implemented in the multilevel framework. The probability density function of the Poisson model is defined as

$$P(\tilde{Y} = y) = \frac{e^{-\lambda} \lambda^y}{y!}, y \in \mathbb{N}_0; \quad (2.27)$$

where \mathbb{N}_0 indicates positive integers including 0, λ is the mean number of event occurrences and y is the number of event occurrences (Xie et al., 2013). The canonical link function

(logarithm) is given as

$$\eta = \ln(\lambda) \Leftrightarrow \lambda = e^\eta. \quad (2.28)$$

The final model for the Poisson Regression GLMM described by Hox et al. (2017) is

$$\eta_{ijk} = \delta_{000} + V_i \delta_{100} + W_{ijk} \delta_{00k} + V_i W_{ijk} \delta_{10k} + T_{ij} u_{0j} + S_i u_{i0}. \quad (2.29)$$

Note that there is no error term in this model. This happens because Poisson Regression assumes $\mu = \sigma_e^2$ where σ_e^2 is the residual variance. Poisson Regression is appropriate to use only when the number of events (gaze-point counts) are statistically independent. Knowing the skewed nature of the Poisson distribution and the constraint that μ and σ^2 are equivalent, this approach is best used when the observed counts are relatively small. If the counts are high, it is likely that $\mu < \sigma^2$ which means the model has overdispersion that the Poisson distribution cannot account for. Overdispersion occurs when the variance is higher than the mean.

Arundina et al. (2017) used a Poisson Regression model on multilevel dengue fever data to study the number of cases per village where collections of villages make up sub regions. Liao et al. (2016) used a three-level Poisson Regression model to study disease count by week, year, and province in China.

While Poisson Regression is simple (using only one parameter) and suitable in many instances, it does not account for overdispersion. A Negative Binomial model is much better in this case, and since it is not always possible to identify if data are overdispersed, typically both models are fit and then compared.

Negative Binomial Regression

Poisson Regression having only one parameter makes it a relatively simple model to run for count data. However, the requirement that this one parameter describes both the mean and the variance also makes this model quite restrictive (Land et al., 1996). Poisson Regression gives no allowance for the possibility of overdispersion or a higher variance than the mean. Negative Binomial Regression makes up for these deficiencies by accounting

for overdispersion. The underlying probability density function for the Negative Binomial Regression model is defined as

$$P(\tilde{Y} = y) = (1 - \pi) \frac{\Gamma(y + \frac{1}{\alpha})}{y! \Gamma(\frac{1}{\alpha})} \left(\frac{1}{1 + \alpha\lambda} \right)^{\frac{1}{\alpha}} \left(\frac{\lambda}{\frac{1}{\alpha} + \lambda} \right)^y, y \in \mathbb{N}_0, \quad (2.30)$$

where λ is the mean number of event occurrences, y is the number of event occurrences, and α is an ancillary parameter indicating the degree of overdispersion (Cheung, 2002). The canonical link function for the Negative Binomial model adds an error ϵ as follows:

$$\eta + \epsilon = \ln(\lambda) \Leftrightarrow \lambda = e^{\eta + \epsilon} = e^{\eta} e^{\epsilon}. \quad (2.31)$$

Adding the error term ϵ to this model allows for a higher level of variation than what is possible in the Poisson Regression framework (Hox et al., 2017). The Negative Binomial model is more general which can be preferable if the data being described do not fit the restrictions of the Poisson model (Xie et al., 2013).

Zero-Inflated Models

While the Poisson and Negative Binomial models are common models used for count data, neither of these models are capable of providing a good fit for data that have a high amount of zero counts. Both the Poisson and Negative Binomial models have variants that handle zero-inflated data. It is assumed that zero-inflated data have two types of zero counts. The zero-inflated models assume that some zeros would presumably always be zeros (extra zeros) while others would follow the Poisson or Negative Binomial distribution (sample zeros) (Hox et al., 2017).

Understanding that zero counts have two classifications in the zero-inflated models, Zero-Inflated Poisson Regression (ZIP) gives a different probability for the occurrence of an event if the count is expected to be zero than if the count is expected to be greater than zero.

$$P(\tilde{Y} = y) = \begin{cases} \pi + (1 - \pi)e^{-\lambda}, & \text{if } y = 0 \\ (1 - \pi) \frac{e^{-\lambda} \lambda^y}{y!}, & \text{if } y \in \mathbb{N} \end{cases} \quad (2.32)$$

Here, \mathbb{N} indicates positive integers and π is the probability of being an extra zero (Cheung, 2002). When N is the sample mean and s^2 is the sample variance of the response variable calculated at the microunit level, π is estimated as $\pi = \frac{s^2 - N^2}{s^2 + N^2 - N}$ (Lambert, 1992). Lee et al. (2006) explained the Zero-Inflated Poisson GLMM at length using three-level data related to breastfeeding mothers in Australia as a motivating example.

The probability of the occurrence of an event under the Zero-Inflated Negative Binomial model (ZINB) is given as

$$P(\tilde{Y} = y) = \begin{cases} \pi + (1 - \pi)(1 + \alpha\lambda^c)^{-\frac{\lambda^{1-c}}{\alpha}}, & \text{if } y = 0 \\ (1 - \pi) \frac{\Gamma(y + \frac{\lambda^{1-c}}{\alpha})}{y! \Gamma(\frac{\lambda^{1-c}}{\alpha})} (1 + \alpha\lambda^c)^{-\frac{\lambda^{1-c}}{\alpha}} \left(1 + \frac{\lambda^{-c}}{\alpha}\right)^{-y}, & \text{if } y \in \mathbb{N} \end{cases} \quad (2.33)$$

where α is an ancillary parameter indicating the degree of overdispersion just as is true for the α parameter given in Equation 2.30. The index c identifies the particular form of the Negative Binomial distribution (Saha and Dong, 1997). When $c = 0$, the Negative Binomial distribution variance is $(1 + \alpha)\lambda$ and when $c = 1$, the variance is $\lambda + \alpha\lambda^2$ (Ridout et al., 2001). When $c = 1$, the lower equation is equivalent to Equation 2.30.

Zandkarimi et al. (2019) described the multilevel Zero-Inflated Negative Binomial model and the variables and equations used for a three-level GLMM. Moghimbeigi et al. (2008) discussed the multilevel Zero-Inflated Negative Binomial analysis at length and applied it to data related to counts of teeth requiring additional attention by a dentist.

Essentially, the zero-inflated models account for the inflation of zero counts by categorizing the zero counts as sample zeros or extra zeros. After accounting for inflation, the data with sample zero counts match the original distributions more closely. Thus, the zero-inflated models fit zero-inflated data by accounting for the excess zeros.

Comparison of Poisson, Negative Binomial, and Zero-Inflated Models

Table 2.6 is provided to clarify the similarities and differences among the Poisson Regression, Negative Binomial Regression, Zero-Inflated Poisson Regression, and Zero-Inflated Negative Binomial Regression models. Table 2.6 shows that the Poisson and Zero-Inflated Poisson models have one parameter and as such are more restrictive models while the Neg-

Table 2.6: Regression model comparison

Model Attributes	Poisson	Negative Binomial	ZIP	ZINB
One parameter ($\mu = \sigma_e^2$)	✓		✓	
More restrictive	✓		✓	
Accounts for overdispersion ($\mu < \sigma_e^2$)		✓		✓
More general		✓		✓
Accounts for high zero count			✓	✓

ative Binomial and Zero-Inflated Negative Binomial models account for overdispersion and are more general in nature. This table also shows that the zero-inflated models account for high zero counts.

It should be noted that if any of these models fails to converge, there are optimizations that can be used and sometimes these optimizers will allow a model to converge. However, an optimizer does not guarantee that a model will be able to converge. The Nelder Mead optimizer directly compares functions in multidimensional space and the BOBYQA optimizer uses a derivative-free bound-constrained approach to allow these GLMMs to converge (Bates et al., 2015).

Wald Chi-Square Test

GLMMs require a specified distribution to fit. After the model is fit, this fit is assessed using the Wald Chi-Square test. There is another test called the Wald z-test for parameter estimates that runs a separate test for each estimate. The Wald Chi-Square test should not be confused with this test because the Wald Chi-Square test is an omnibus test that tests for the significance of several parameters in a model at once. often called the Wald test for simplicity. This test compares the model to the same model without the fixed effects to see if the fixed effects significantly improve the prediction of the response variable. The Wald test uses a Wald test statistic to determine if the models with fixed effects are significantly better at predicting the counts (Kodde and Palm, 1986). The Wald test evaluates Fisher information at the Maximum Likelihood Estimate (MLE) (Agresti, 1990). The Wald test gives broad applicability and flexibility with complex models such as the ones described. GLMMs are most commonly assessed with the Wald test due to the complex nature of these models and the broad applicability and flexibility of the Wald test. The Wald formula is

given by Fox (1997).

It should be noted that the Wald test calculates degrees of freedom by taking the number of categories from both interaction variables, subtracting each by one, and multiplying these numbers together in the formula $df = (r - 1)(c - 1)$ where r represents the number of rows and c represents the number of columns. This is the same calculation used for single-level models. This general and possibly overly simplified method for defining degrees of freedom means results from the Wald test statistics should be validated by pairwise comparisons.

The null hypothesis specific to a Wald test is $H_O : \delta_{100}, \delta_{00k}$ and $\delta_{10k} = 0$ simultaneously. This indicates that the fixed effects of Group, AOI, and the cross-level interaction between Group and AOI do not significantly improve the ability to predict \tilde{Y}_{ijk} (see Tables 2.2 and 2.3). The alternative hypothesis is H_A : at least one of the $\delta_{100}, \delta_{00k}$ or $\delta_{10k} \neq 0$ indicating that these fixed parameters are significant when predicting \tilde{Y}_{ijk} . The Wald test can be used for the GLMMs with the four specified distributions of Poisson, Negative Binomial, ZIP, and ZINB.

When the GLMM model being tested has an interaction term, the model should be run with and without the interaction term.

Pairwise Comparisons Using Estimated Marginal Mean Rate Ratios

While we can see if there is overall significance for each AOI iteration through the use of the Wald test on GLMMs, the best way to understand where any differences between groups in gaze-point counts occur is by using Estimated Marginal Means (EMMs). EMMs are used as a post hoc test to understand results of GLMM analyses. Literature uses terms like Least Square means (LS-means) or Population Marginal means (Searle et al., 1980), however, we use the term Estimated Marginal Means for consistency with the terms used in the related programming code. Estimated Marginal Means estimate the averages that we would expect to see with balanced data (Goodnight and Harvey, 1978). Cai (2014) described that EMMs provide an estimate for certain linear combinations of population parameters.

Because i, j, k are the terms used consistently across the field to indicate the macrounit, mesounit, and microunit, we speak of k again (see Table 2.2) rather than $k(j, l(j))$ to indicate the microunit of unique AOI location. Searle et al. (1980) described the structure of EMMs using a framework of a two-way crossed (rows-by-columns) classification having a rows and

b columns. Searle et al. (1980) stated that y_{ijk} refers to the k th observation in row i and column j with the expected value

$$E(y_{ijk}) = \mu_{ij} \quad (2.34)$$

where $i = 1, \dots, a$ and $j = 1, \dots, b$, and $k = 1, \dots, n_{ij}$ when the cell in row i and column j has n_{ij} observations in it. The model that includes an interaction term is given as:

$$E(y_{ijk}) = \mu_{ij} = \mu + \alpha_i + \beta_j + \gamma_{ij} \quad (2.35)$$

where μ is a general mean, α_i and β_j are effects due to row i and column j , respectively, and γ_{ij} is the interaction term corresponding to row i and column j . To relate this model equation to the data and notation given for the GLMM, we see the system of equations represented as

$$E(\tilde{Y}_{i0k}) = \mu_{i0k} = \delta_{000} + \delta_{i00} + \delta_{00k} + \delta_{i0k}. \quad (2.36)$$

Here, level j is reduced to 0 because this post hoc test is looking specifically at the Treatment and Control groups (i) and how they relate to the unique AOIs (k) regardless of the Posture ID (j).

To give an example using the simplified data structure introduced in Equation 2.26, we will use the five unique AOIs indicated with $k = 1, 2, 3, 4, 5$ which are indicated in Equation 2.26 as $k = a, b, c, d, e$. The means we want to estimate and compare are the gaze-point means from each Group ($i = 1, 2$) within each AOI ($k = 1, 2, 3, 4, 5$). This combination of Group and AOI values is different from what is used for the matrix example 2.26 because the use of less unique AOIs in this example makes these example matrices easier to read. An \mathbf{L} matrix is constructed to compute Estimated Marginal Means. The population marginal

mean is computed as $\tilde{L}\hat{\omega}$ where \tilde{L} is the coefficient matrix associated with the marginal mean and $\hat{\omega}$ is the estimate of the fixed-effects parameter vector. We can express the population marginal means as a linear combination of the population parameters $\mathbf{L}\omega$. Our population parameters can be estimated using $\tilde{L}\hat{\omega}$ where

$$\hat{\omega} = \left[\widehat{\tilde{\delta}_{000}} \widehat{\tilde{\delta}_{100}} \widehat{\tilde{\delta}_{200}} \widehat{\tilde{\delta}_{001}} \widehat{\tilde{\delta}_{002}} \widehat{\tilde{\delta}_{003}} \widehat{\tilde{\delta}_{004}} \widehat{\tilde{\delta}_{005}} \widehat{\tilde{\delta}_{101}} \widehat{\tilde{\delta}_{102}} \widehat{\tilde{\delta}_{103}} \widehat{\tilde{\delta}_{104}} \widehat{\tilde{\delta}_{105}} \widehat{\tilde{\delta}_{201}} \widehat{\tilde{\delta}_{202}} \widehat{\tilde{\delta}_{203}} \widehat{\tilde{\delta}_{204}} \widehat{\tilde{\delta}_{205}} \right].$$

These are the same estimates obtained in our original GLMM model. The matrix \tilde{L} for our EMMs $E(\tilde{Y}_{i0k})$ is given as

$$\tilde{L} = \begin{bmatrix} 1 & 1 & 0 & 1 & 0 & 0 & 0 & 0 & 1 & 0 & 0 & 0 & 0 & 0 & 0 & 0 & 0 \\ 1 & 1 & 0 & 0 & 1 & 0 & 0 & 0 & 0 & 1 & 0 & 0 & 0 & 0 & 0 & 0 & 0 \\ 1 & 1 & 0 & 0 & 0 & 1 & 0 & 0 & 0 & 0 & 1 & 0 & 0 & 0 & 0 & 0 & 0 \\ 1 & 1 & 0 & 0 & 0 & 0 & 1 & 0 & 0 & 0 & 0 & 1 & 0 & 0 & 0 & 0 & 0 \\ 1 & 1 & 0 & 0 & 0 & 0 & 0 & 1 & 0 & 0 & 0 & 0 & 1 & 0 & 0 & 0 & 0 \\ 1 & 0 & 1 & 1 & 0 & 0 & 0 & 0 & 0 & 0 & 0 & 0 & 0 & 1 & 0 & 0 & 0 \\ 1 & 0 & 1 & 0 & 1 & 0 & 0 & 0 & 0 & 0 & 0 & 0 & 0 & 0 & 1 & 0 & 0 \\ 1 & 0 & 1 & 0 & 0 & 1 & 0 & 0 & 0 & 0 & 0 & 0 & 0 & 0 & 0 & 1 & 0 \\ 1 & 0 & 1 & 0 & 0 & 0 & 1 & 0 & 0 & 0 & 0 & 0 & 0 & 0 & 0 & 0 & 1 \\ 1 & 0 & 1 & 0 & 0 & 0 & 0 & 1 & 0 & 0 & 0 & 0 & 0 & 0 & 0 & 0 & 1 \end{bmatrix}. \quad (2.37)$$

In this matrix, each row relates to a specific combination. The first row relates to where $i = 1$ and $k = 1$, the second row relates to where $i = 1$ and $k = 2$, the third row relates to where $i = 1$ and $k = 3$, the fourth row relates to where $i = 1$ and $k = 4$, and the fifth row relates to the $i = 1, k = 5$ combination. The final five rows are identical except here, $i = 2$.

The \tilde{L} matrix and $\hat{\omega}$ vector described above are used when a Gaussian GLMM is computed. Thus, the elements of $\hat{\omega}$ are not directly correlated to the δ vector in Equation 2.24 because the reference categories are not included in the latter.

When Poisson, Negative Binomial, or their zero-inflated variants are used in the GLMM framework, the mean rate ratio is calculated instead of the mean difference. This is because

these regression models use a log link and are therefore on the exponential scale. To obtain the mean rate ratios where $i = 1, 2$ and $k = 1, 2, 3, 4, 5$, the estimates used are given as

$$\widehat{\omega} = \left[\widehat{\delta_{000}} \widehat{\delta_{100}} \widehat{\delta_{001}} \widehat{\delta_{002}} \widehat{\delta_{003}} \widehat{\delta_{004}} \widehat{\delta_{101}} \widehat{\delta_{102}} \widehat{\delta_{103}} \widehat{\delta_{104}} \right].$$

Here, $i = 2$ and $k = 5$ serve as reference categories. The \mathbf{L} matrix is given as

$$\mathbf{L} = \begin{bmatrix} 0 & 1 & 0 & 0 & 0 & 0 & 1 & 0 & 0 & 0 \\ 0 & 1 & 0 & 0 & 0 & 0 & 0 & 1 & 0 & 0 \\ 0 & 1 & 0 & 0 & 0 & 0 & 0 & 0 & 1 & 0 \\ 0 & 1 & 0 & 0 & 0 & 0 & 0 & 0 & 0 & 1 \\ 0 & 1 & 0 & 0 & 0 & 0 & 0 & 0 & 0 & 0 \end{bmatrix}. \quad (2.38)$$

When multiplying the matrices, the result is as follows.

$$\mathbf{L}\widehat{\omega} = \begin{bmatrix} \widehat{\delta_{100}} + \widehat{\delta_{101}} \\ \widehat{\delta_{100}} + \widehat{\delta_{102}} \\ \widehat{\delta_{100}} + \widehat{\delta_{103}} \\ \widehat{\delta_{100}} + \widehat{\delta_{104}} \\ \widehat{\delta_{100}} \end{bmatrix}. \quad (2.39)$$

The mean rate ratios are obtained by exponentiating the vector $\mathbf{L}\widehat{\omega}$ ($e^{\mathbf{L}\widehat{\omega}}$). The z-values are obtained by taking the estimated values $\mathbf{L}\widehat{\omega}$ found in Equation 2.39 and dividing these values by their standard errors SE . Because the dataset is so large, a normal approximation is suitable, hence the z-values are used in place of the t-values. The EMM rate ratios are evaluated for each interaction where the standard error SE is given as

$$SE = \frac{s}{\sqrt{n_{ij}}}.$$

Here, s is the standard deviation and n_{ij} indicates the number of observations used to calculate the EMM rate ratio (Harvey, 1960). Therefore, each row of the matrix \mathbf{L} is related

to a unique AOI and helps provide a contrast between the treatment and control groups within that AOI. Thus the hypotheses for each AOI separately are H_O : the EMM rate ratio = 1, meaning that the gaze-point counts for the Treatment and the Control groups are equivalent for each AOI and H_A : the EMM rate ratio $\neq 1$, meaning that there is a difference in gaze-point count for the Treatment and Control groups.

2.3.4 Adjustments for Multiple Comparisons

When any analysis is run multiple times on different iterations of data, the p-values must be adjusted to reduce inflated levels of significance. The Bonferroni adjustment (Napierala, 2012) can be used as a conservative approach to correct for multiple comparisons. The Bonferroni adjustment limits the family-wise Type I error rate by multiplying each p-value by the number of tests conducted (Napierala, 2012).

The Benjamini-Hochberg correction is another adjustment for multiple comparisons that is used to control for the false discovery rate. While the Benjamini-Hochberg correction is not as conservative of an adjustment as the Bonferroni adjustment, it is a more powerful generalization to the context of multiplicity of the conventional test of significance (Thissen et al., 2002). When p-values are adjusted using the Benjamini-Hochberg correction, the results are q-values. These values are obtained by applying the following formula:

$$q_o = p_o \left(\frac{v}{o} \right). \quad (2.40)$$

Here, q_o represents the o th q-value, p_o represents the o th p-value, and v represents the total number of p-values being adjusted when ranked from 1 to o (Benjamini and Hochberg, 1995; Gao, 2011). These q-values are the number of false discoveries in an experiment divided by the total number of discoveries.

The Benjamini-Hochberg correction is best used for exploratory analyses whereas the Bonferroni adjustment is a preferable adjustment for confirmatory analyses.

2.3.5 Supporting Software

The following are a list of package and functions in R that are used to run the analyses previously described. The `lme4` package in R (Bates et al., 2015) can be used to fit the

Poisson Regression and Negative Binomial Regression models and the `glmmTMB` package in R (Brooks et al., 2017) can be used to fit the Zero-Inflated Poisson and Zero-Inflated Negative Binomial Regression models. Both the `lme4` and `glmmTMB` packages give options to run the Nelder Mead and BOBYQA optimizers.

The Wald test statistics for `lme4` objects (Poisson and Negative Binomial models) is computed with the `Anova` function in the `car` package (Fox and Weisberg, 2019). For `glmmTMB` objects (Zero-Inflated models), the `Anova.glmmTMB` function in the `glmmTMB` package provides the Wald test statistic. While the F-test is used and sometimes preferred as a less-general assessment of the model fit, the `Anova.glmmTMB` function gives the option to compute an F-statistic, but the function has not yet been programmed to run the F-test.

The `emmeans` function from the `emmeans` R package can be used to run the joint tests of LS-means comparing the group counts within each AOI between groups (Lenth, 2021). The `emmip` function from the `emmeans` R package can be used to provide the visual comparisons.

CHAPTER 3

Results

The statistical approach used for our multilevel data is the Generalized Linear Mixed Effects Model (GLMM) which analyzes the gaze-point data as a whole for all 22 Posture IDs shown in Figure 1.3. The four iterations of data are differentiated in Section 2.2 and depicted in Figure 2.18.

In the GLMM approach, the overall interaction between Treatment and Control gaze-point counts within AOIs are analyzed across all 22 Posture IDs. Four generalizations were investigated: Poisson, Negative Binomial, Zero-Inflated Poisson, and Zero-Inflated Negative Binomial Regression (see Section 2.3.3). These alternatives are compared to find the model with the best fit and the effectiveness of the models is assessed using the Wald Chi-Square test. Estimated Marginal Mean rate ratios are used when the Wald Chi-Square test gives significance to find which AOIs show meaningful differences in gaze-point counts. All of these tests are described in depth in Section 2.3.3.

Results are considered statistically significant at the 0.05 level and statistical significance is divided into three tiers: $*p < 0.05$ is significant, $**p < 0.01$ is highly significant, and $***p < 0.001$ is very highly statistically significant. The tables in Appendix D report all of the raw p-values from the original tests, the Bonferroni adjusted p-values, and the Benjamini-Hochberg (BH) adjusted p-values as described at the end of Section 2.3.4. There are some Bonferroni adjusted p-values that are not significant while the BH values showed significance. Because the BH adjustment is best used for exploratory analyses, p-values adjusted by the BH correction are emphasized. For each of the analyses, two-sided tests are conducted as we gauge whether or not the Treatment group looked at the postures differently than the Control group and we did not have prior experience to suggest how these groups might look at these postures differently.

3.1 General Observations from Gaze-Point Data

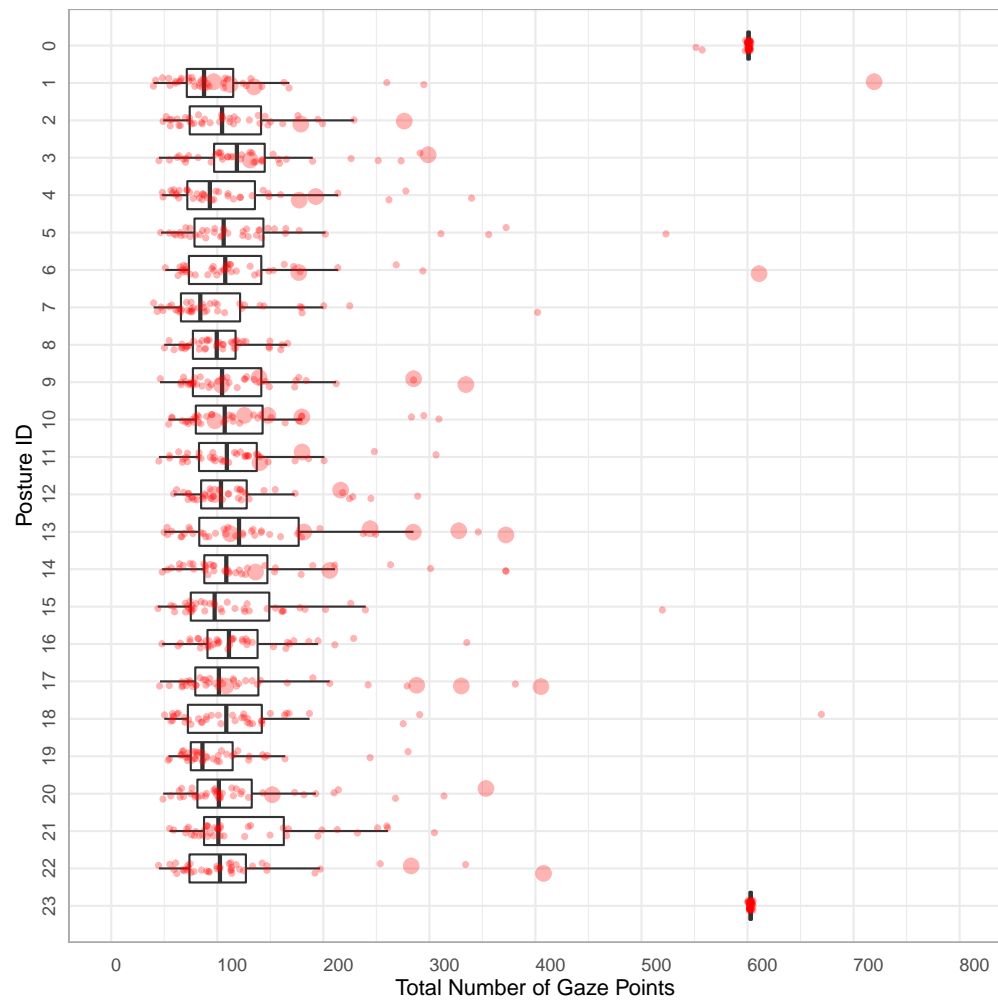


Fig. 3.1: Box plots with dot plots overlaid where each red dot represents the number of gaze points for one of the 40 participants for each Posture ID. Large red dots represent gaze-point counts when the participant viewed the Posture ID as View Number 2, the first Posture ID viewed after the calibration posture.

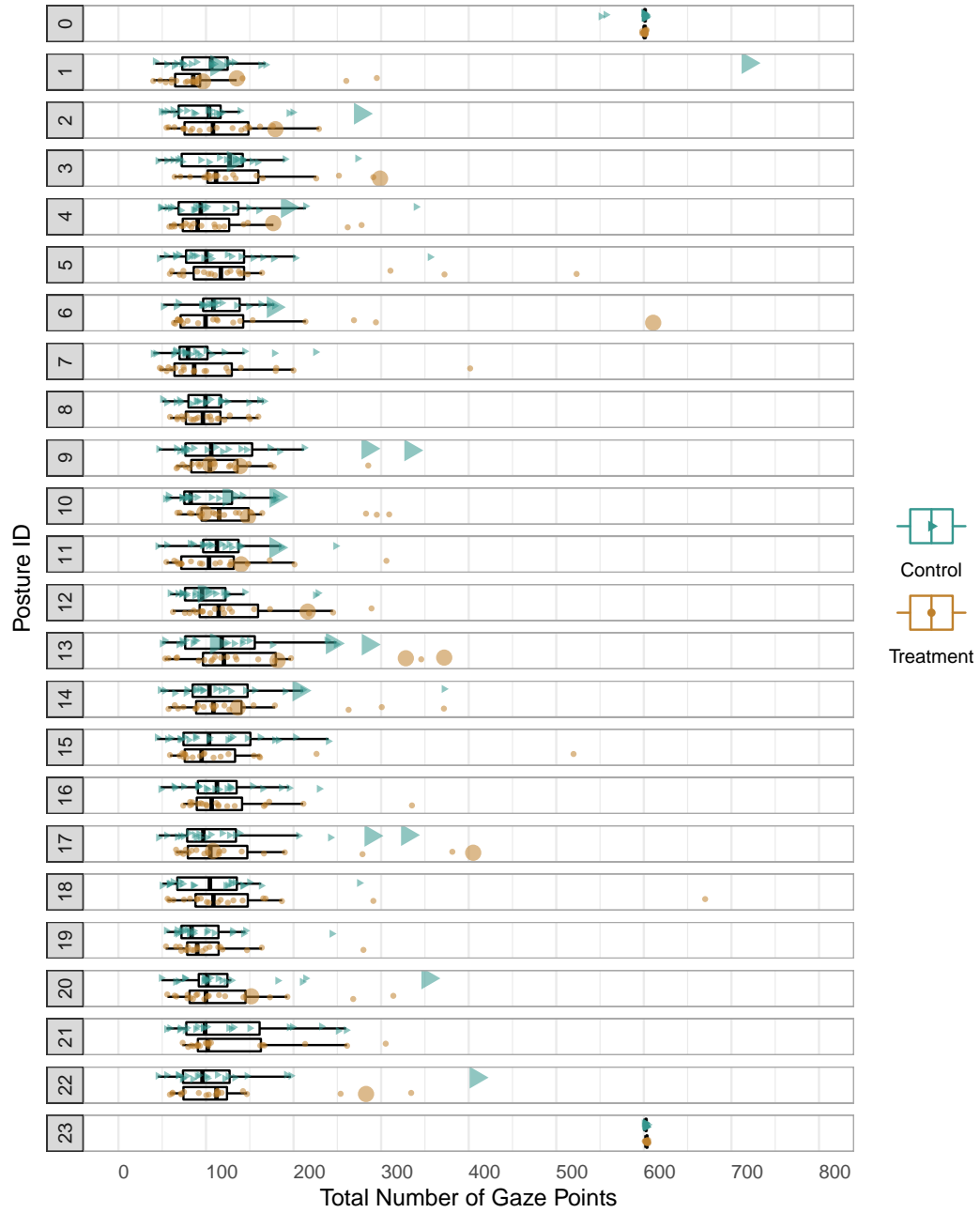


Fig. 3.2: Box plots with dot plots overlaid where each brown dot represents the number of gaze points for one of the 20 Treatment participants and each green triangle represents the number of gaze points for one of the 20 Control participants for each Posture ID. Large brown dots and large green triangles represent gaze-point counts when the participant viewed the Posture ID as View Number 2, the first Posture ID viewed after the calibration posture.

Before running the statistical tests, general observations were made about the gaze-point data as a whole. The Kruskal-Wallis test described in Section 2.3.1 assessed Posture IDs 1-22 omitting Posture IDs 0 and 23 because the calibration postures were timed, leading to a specific number of gaze points for these postures. The calibration postures contains four control points and each participant was given 5 seconds for each point. The eye-tracking software collected 30 gaze points per second. Thus, 4 points \times 5 seconds \times 30 points per second gives about 600 gaze points for each participant for each calibration posture. The hypotheses for this test are: H_O : The distribution of the gaze-point sums contributed to each View Number by each participant are the same for each View Number; and H_A : At least one distribution of gaze-point sums for a View Number differs from the distribution of sums for another View Number. The Kruskal-Wallis test gives a test statistic of 26.037 and p-value of 0.205 suggesting that there are no significant differences in total number of gaze points contributed by participants between Posture IDs. The distribution of the total number of gaze points each participant contributed to each Posture ID can be see in Figure 3.1. This graph supports the results from the hypothesis test.

These data are further categorized by Treatment group and Control group within each Posture ID and analyzed using the Wilcoxon Signed Rank test (also summarized in Section 2.3.1) to see if there are group differences for any Posture IDs. The hypotheses for the Wilcoxon Signed Rank test are: H_O : $M_T = M_C$; and H_A : $M_T \neq M_C$ for each Posture ID separately with M_T representing the median gaze-point count for the Treatment group and M_C representing the median gaze-point count for the Control group. Raw p-values for each Posture ID are all non-significant with the lowest p-value being 0.0678. There is not enough evidence to suggest that Treatment participants have different median gaze-point counts for each of the 22 postures when compared to the Control participants. The distribution of the number of gaze points for each participant categorized by group for each Posture ID can be see in Figure 3.2. This graph supports the results from the hypothesis test.

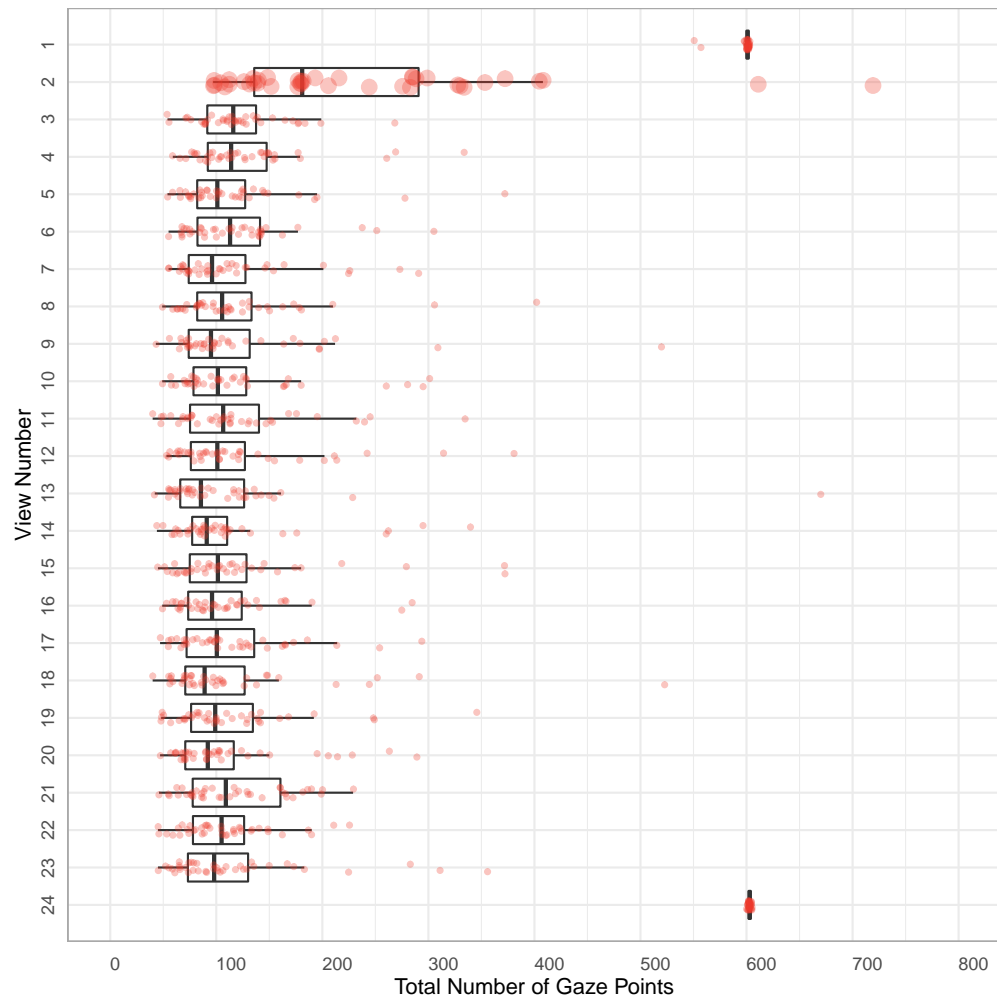


Fig. 3.3: Box plots with dot plots overlaid where each red dot represents the number of gaze points for one of the 40 participants for each posture given by View Number. The large red dots represent gaze-point counts for View Number 2.

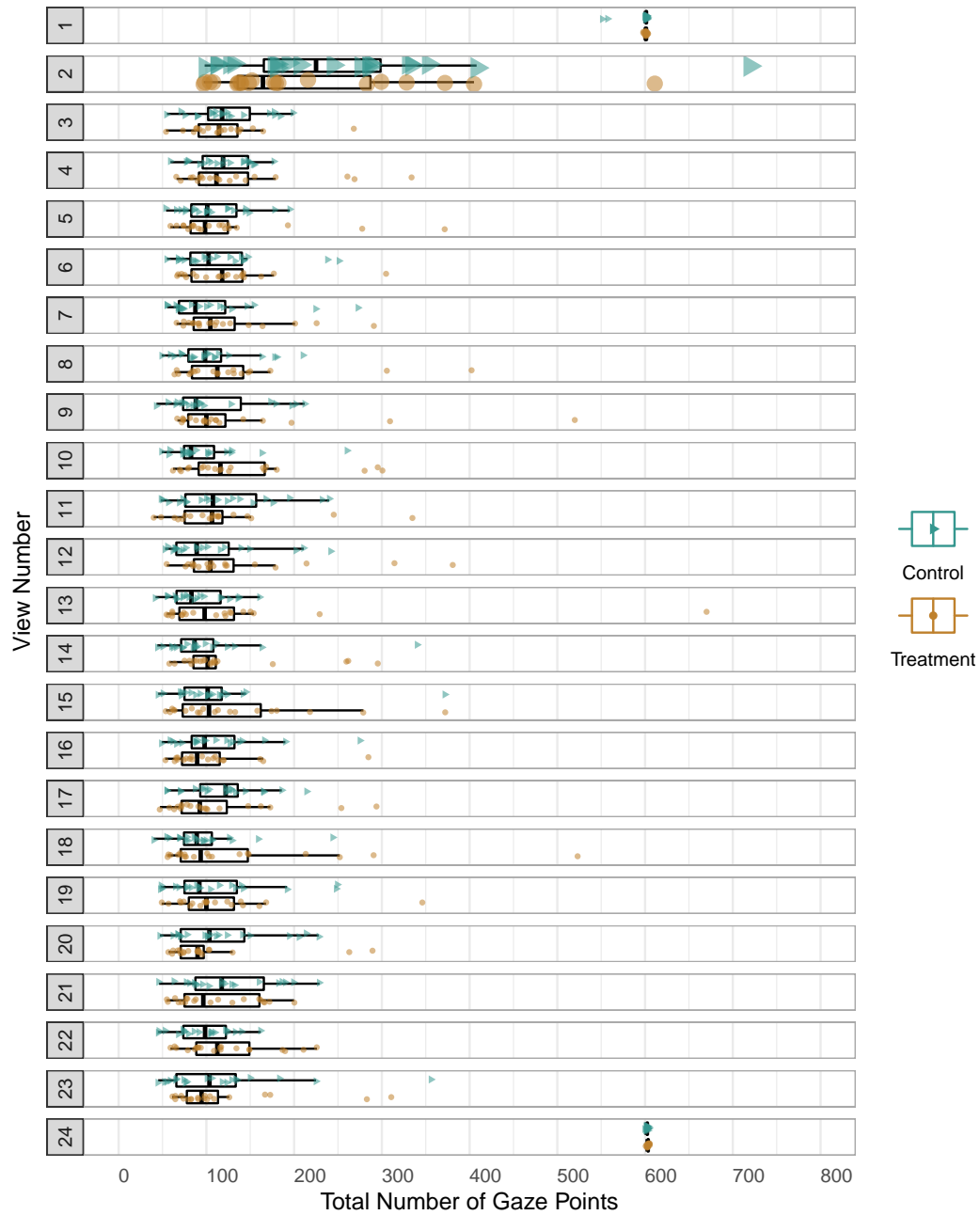


Fig. 3.4: Box plots with dot plots overlaid where each brown dot represents the number of gaze points for one of the 20 Treatment participants and each green triangle represents the number of gaze points for one of the 20 Control participants for each posture given by View Number. The large brown dots and large green triangles represent gaze-point counts for View Number 2.

Because the order of the Posture IDs were randomized, we wanted to see if the order in which participants saw a posture had an effect on the median gaze-point counts, regardless of the particular Posture ID. Remembering that gaze-point counts are collected at the rate of 30 gaze points per second, the gaze-point count for these postures is related to the time it took to make a judgment about a posture. The Kruskal-Wallis test yields a test statistic of 71.88 and a p-value of $1.75e^{-07}$ when comparing View Numbers 2-23. View Numbers 1 and 24 are excluded from these analyses because they represent the initial and final calibration postures for all participants. To understand this significant result, we looked at the box plots of the total gaze points for each View Number as seen in Figure 3.3. Visually, View Number 2 shows a higher median number of total gaze points than View Numbers 3-23. View Number 2 also shows an extended right tail. To visualize the contribution View Number 2 counts have on each posture, the dot plot points for this View Number are enlarged in Figures 3.1 and 3.2. This is replicated in Figures 3.3 and 3.4 for clarity and consistency.

To see if View Number 2 exclusively contributed to this significance, we ran the same analysis on View Numbers 3-23 and obtained a test statistic of 19.51 and p-value of 0.4889. Thus, View Number 2 gaze-point counts are significantly higher than the gaze-point counts of the postures for the other View Numbers. We assume that the inflated gaze-point counts seen in View Number 2 are related to the extra time which equates to higher median gaze-point counts; each participant needed to familiarize themselves with the task and the timebar described in Section 1.3 and displayed in Figure 1.4.

These data are categorized by Treatment group and Control group within each Posture ID and analyzed using the Wilcoxon Signed Rank test to see if there are group differences in median number of gaze points for any View Numbers. The raw p-value for View Number 10 is significant (0.0424) but when this p-value is corrected by the Benjamini-Hochberg adjustment, the resulting q-value is insignificant (0.6678) and all other raw and adjusted p-values are non-significant. The distribution of number of gaze points for each participant categorized by group for each View Number can be seen in Figure 3.4. This graph provides visual evidence to support the conclusion that there are no significant differences between Treatment and Control group total number of gaze points for any particular View Numbers.

Although the viewing order for Posture IDs was randomized, the following statistical models were run without View Number 2 gaze-point counts. Recall that View Number 2

data were omitted before any further analyses were run because the gaze-point counts were abnormally high, likely due to the time it took participants to familiarize themselves with the task. Because the Posture IDs were viewed in a random order (see Figure 1.6 for a visual description), we realized that including View Number 2 would bias the data. View Number 2 was therefore removed from analyses on all data iterations before collecting the results presented in the remainder of this chapter.

The effect of removing View Number 2 from the model can be demonstrated using the example from Equation 2.26. View Number 1 is the calibration slide for all four participants. We assume that for View Number 2 for participants 1 and 3 is Posture ID 3. View Number 3 for these participants is Posture ID 1, View Number 4 for these participants is Posture ID 2, and View Number 5 for these participants is another calibration slide. In other words, the first and third participants view Posture IDs 1, 2, and 3 in the order (View Numbers) 3, 4, 2 after the calibration View Number 1 and before the calibration View Number 5. Rows 6-8 and rows 22-24 of the Y_{ijk} vector, \mathbf{X} matrix, \mathbf{Z} matrix, and ϵ vector shown in Equation 2.26 are omitted.

Similarly, we assume that View Number 2 for participants 2 and 4 is Posture ID 2, View Number 3 for these participants is Posture ID 3, View Number 4 for these participants is Posture ID 1, and View Number 5 for these participants is another calibration slide. In other words, the second and fourth participants view Posture IDs 1, 2, and 3 in the order (View Numbers) 4, 2, 3 after the calibration View Number 1 and before the calibration View Number 5. Here, rows 12-13 and rows 28-29 of the Y_{ijk} vector, \mathbf{X} matrix, \mathbf{Z} matrix, and ϵ vector shown in Equation 2.26 therefore would be omitted. Since the order of the postures is randomized, none of the δ or u variables are dropped completely from the model.

Visualizations for the results for Posture IDs 1-22 are provided in Appendix F as Figures F.1-F.44. For illustration, Posture ID 7 is shown in Figure 3.5.

3.2 Generalized Linear Mixed Effects Analyses

We ran Generalized Linear Mixed Effects Models using four specified models, namely Poisson, Negative Binomial, Zero-Inflated Poisson, and Zero-Inflated Negative Binomial described in Section 2.3.3. We chose to fit a Poisson Regression model because while we anticipated a high number of occurrences (gaze points), we also expected to see a high amount

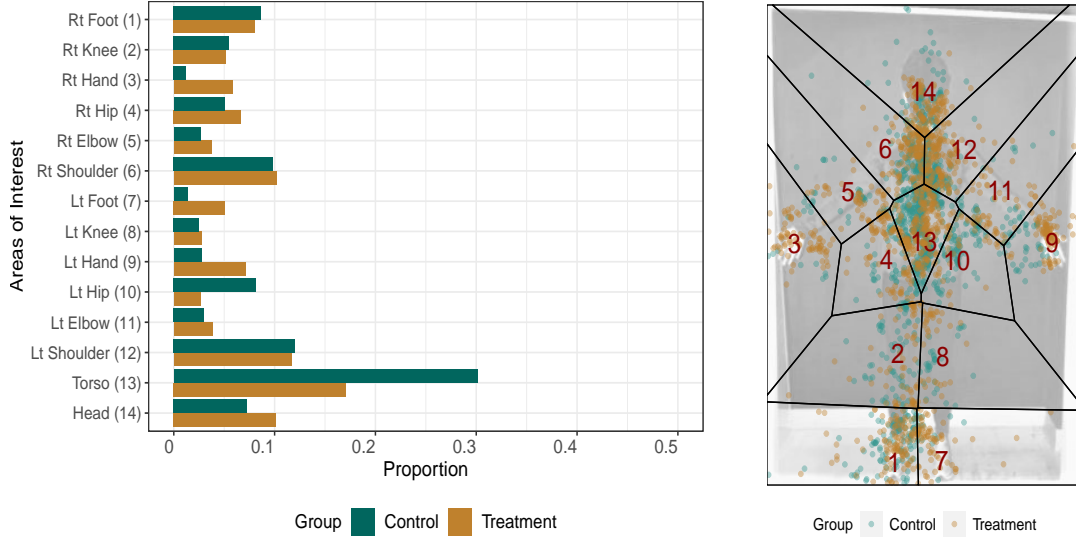


Fig. 3.5: Posture ID 7 bar chart (left) and scatterplot (right) of gaze points for Round 1 VT AOIs.

of variability. This model was fit understanding that the Poisson model may appropriately fit our data if the mean and variance of the gaze points were comparable in size.

Recognizing that the Poisson model may not be the best fit for our data, we also used a Negative Binomial Regression model described in Section 2.3.3. We ran this model to see if accounting for overdispersion would provide a more accurate fit for our data.

While it seems possible that either Poisson or Negative Binomial models could provide a good fit for our data, we could anticipate additional zero counts in AOIs from individual participants that could not easily be explained by the Poisson and Negative Binomial models. This is of particular concern for the AOIs whose centers were defined in Round 1 because there are a much higher number of AOIs per Posture ID (9-14) as compared to the Round 2 AOIs (2-9). It seemed unlikely that each participant would have gaze points for all Posture IDs that would fall into each of the AOIs as they were defined. The zero-inflated models operate by classifying the zero counts as either a sample (true) zero or an extra zero. In the context of this study, it is presumed that if we had each participant look at each posture longer, there would be some gaze points that fall into AOIs with a zero count and that there would still be some AOIs with zero counts. Data with a high number of zero counts lead to models that do not follow either the Poisson or Negative Binomial models well. We ran

Table 3.1: Model comparisons for each AOI iteration

AOI Iteration	Model	AIC	BIC	Log-Likelihood
Round 1 VT	Poisson	105181	105560	-52539
	ZIP	77876	78262	-38885
	ZINB ⁺	53850	54243	-26871
Round 1 LRV	Poisson	106178	106575	-53035
	ZIP	78407	78811	-39148
	ZINB ⁺	55434	55846	-27661
Round 2 VT	Poisson	53770	53997	-26849
	ZIP	43992	44225	-24228
	ZINB ⁺	27666	27906	-13795
Round 2 LRV	Poisson	59114	59361	-29519
	ZIP	46647	46901	-23285
	ZINB ⁺	30912	31172	-15416

⁺ Indicates model that is the best fit for the AOI iteration

Zero-Inflated Poisson and Zero-Inflated Negative Binomial model fits and compared these zero-inflated variants to the original model fits.

When we ran the model fits, we obtained results for Poisson, Zero-Inflated Poisson, and Zero-Inflated Negative Binomial models directly. However, the Negative Binomial Regression analysis would not converge when run on any of the iterations of the data. Though both the Nelder Mead and BOBYQA optimizers were applied to the Negative Binomial model for all four AOI iterations as described in the *Comparison of Poisson, Negative Binomial, and Zero-Inflated Models* part of Section 2.3.3, convergence was not achieved. Table 3.1 shows how the Poisson, ZIP, and ZINB models compare based on each model's AIC, BIC, and Log-Likelihood values as introduced in Section 2.3.3.

Understanding the selection criteria described in Section 2.3.3, Table 3.1 indicates that Zero-Inflated Negative Binomial Regression is the best fit for the gaze-point data and will provide the most accurate analysis for each iteration of the data according to all three criteria. For ZINB, the AIC and BIC statistics and the absolute log-likelihood values are smallest, compared with those for the two other models.

3.2.1 Multilevel Analysis Structure

As we present pairwise results for AOIs defined in all Posture IDs for a given round, it is important to understand that because these AOIs appear with different frequencies across

the Posture IDs, a different weight should be given to significant results for AOIs that appear less frequently. It is also important to remember that the gaze points from View Number 2 were removed from this analysis. Table 3.2 shows which Posture IDs were used as View Number 2 for each pair of participants.

Because the multilevel models analyze the data as a whole rather than looking at each individual posture, pairwise results are given for each defined AOI that appeared in that iteration or round of data analyzed. The Round 1 defined centers typically included all 14 of the main regions the expert was interested in. However, there are some Posture IDs where a particular AOI is occluded naturally by the stance of the stimulus subject in the image. In other Posture IDs, some of these regions overlap and the resulting AOI is labeled as a mixture of the two regions. For example, the AOI “Rt Hand (3)” and AOI “Lt Hand (9)” appeared in nearly all of the Posture IDs. However, Posture ID 15 has one AOI labeled “Rt Hand (3)/ Lt Hand (9)”. While all AOIs are included in the multilevel analyses, it is important to understand that these AOIs do not appear proportionally within the Posture IDs across the study. Table 3.3 shows how often each AOI appears for Round 1 in the 22 Posture IDs taking into account the AOIs that did not appear because they are included in View Number 2 postures.

Round 2 AOIs appear a lot less systematically than the Round 1 AOIs as explained in Section 2.2.2. A comprehensive list of the AOIs used in Round 2 and the number of Posture IDs each AOI appears in are displayed in Table 3.4.

Because the AOIs appear in the Posture IDs disproportionately, the pairwise levels of significance should be interpreted cautiously. Significance may not be achieved as easily in an AOI that rarely occurs in the 22 postures as the confidence bands for these AOIs are wider to account for the higher amount of variability in gaze-point counts for AOIs occurring in one posture as compared to AOIs that appear in most postures.

3.2.2 General Results for all GLMMs

Though the four models were compared prior to running the Wald tests explained in the *Wald Chi-Square* part of Section 2.3.3, and one model was selected as the best fit for each of the data iterations, the Wald test is performed on each of the models to see how the significance of the models compare. The hypotheses used for the Wald test are: $H_O : \delta_{100}$,

Table 3.2: Posture IDs associated with View Number 2

Participants	Posture ID
C1 & T1	14
C2 & T2	20
C3 & T3	3
C4 & T4	12
C5 & T5	1
C6 & T6	6
C7 & T7	13
C8 & T8	1
C9 & T9	9
C10 & T10	10
C11 & T11	4
C12 & T12	17
C13 & T13	13
C14 & T14	17
C15 & T15	9
C16 & T16	22
C17 & T17	2
C18 & T18	11
C19 & T19	10
C20 & T20	13

δ_{00k} and $\delta_{10k} = 0$ simultaneously; and H_A : at least one of the δ_{100} , δ_{00k} or $\delta_{10k} \neq 0$ (refer to Table 2.3 for notation clarification). The null hypothesis indicates that the fixed parameters are not significant when predicting $\tilde{Y}_{ijk(j,l(j))}$. Table 3.6 shows a high level of significance for the Poisson and ZIP models for each iteration of the data with p-values each being less than $2e^{-16}$. However, the ZINB model shows significance for only one iteration of the data being Round 2 LRVT with a p-value of 0.0026.

3.2.3 Zero-Inflated Negative Binomial Results

The Zero-Inflated Negative Binomial models, as described in the *Zero-Inflated Models* part of Section 2.3.3, are deemed to be the best fit for the data. These models are further analyzed within each round comparing these models with and without the interaction term to determine if the interaction was significant. These results are provided in Table 3.5 where it is shown that the interaction is only significant for the Round 2 LRVT iteration. Table 3.6 provides the test statistics and p-values for the Poisson, ZIP, and ZINB Regression models

Table 3.3: Frequency of the Round 1 AOI labels among the 22 Posture IDs

Round 1 AOI Label	Frequency	Max Occurrences	Actual Occurrences
Rt Foot (1)	22	880	840
Rt Knee (2)	19	760	726
Rt Hand (3)	19	760	722
Rt Hip (4)	16	640	610
Rt Elbow (5)	19	760	722
Rt Shoulder (6)	19	760	726
Lt Foot (7)	22	880	840
Lt Knee (8)	19	760	726
Lt Hand (9)	16	640	610
Lt Hip (10)	21	840	802
Lt Elbow (11)	17	680	650
Lt Shoulder (12)	19	760	724
Torso (13)	20	800	760
Head (14)	22	880	840
Rt Knee (2)/ Rt Hand (3)	1	40	38
Rt Hip (4)/ Rt Elbow (5)	1	40	38
Lt Knee (8)/ Lt Hand (9)	1	40	38
Lt Hip (10)/ Lt Elbow (11)	1	40	38
Rt Hip (4)/ Lt Hand (9)	2	80	76
Rt Knee (2)/ Lt Knee (8)	2	80	76
Rt Hip (4)/ Rt Shoulder (6)	1	40	38
Rt Hand (3)/ Lt Hand (9)	1	40	38
Rt Elbow (5)/ Lt Elbow (11)/ Torso (13)	1	40	40
Rt Hip (4)/ Lt Shoulder (12)/ Torso (13)	1	40	40
Rt Hand (3)/ Rt Elbow (5)/ Rt Shoulder (6)	1	40	40
Outside Area ⁺	22	880	880

+ Indicates the AOI for LRVT defined AOIs for all gaze points that fall outside all other AOIs

for each AOI iteration including the interaction term. The ZINB results are divided into the model including the interaction and the model without the interaction with statistics for the Group and AOI main effects separately and models with the best fit are differentiated. The p-values for the Group main effect are all non-significant, meaning that these models did not find significant differences between the Treatment and Control gaze-point counts across the 22 postures. However, the p-values for the AOI main effect are all highly statistically significant meaning that these models show that there is evidence to suggest that the gaze-point counts differ for at least one AOI or that there are differences between gaze-point counts across the AOIs.

Table 3.4: Frequency of the Round 2 AOI labels among the 22 Posture IDs

Round 2 AOI Label	Frequency	Max Occurrences	Actual Occurrences
Rt Foot (1)	11	440	414
Rt Knee (2)	1	40	36
Rt Hand (3)	14	560	542
Lt Foot (7)	8	320	306
Lt Knee (8)	2	80	76
Lt Hand (9)	15	600	570
Torso (13)	14	560	536
Head (14)	3	120	112
Neck (15)	12	480	456
Sternum (16)	9	360	348
Middle of Feet (17)	11	440	420
Lt Hand (9)/ Torso (13)	1	40	40
Rt Shoulder (6)/ Neck (15)	1	40	36
Rt Hand (3)/ Lt Hand (9)/ Sternum (16)	1	40	40
Rt Elbow (5)/ Torso (13)	1	40	36
Lt Shoulder (12)/ Torso (13)	1	40	40
Rt Hand (3)/ Neck (15)	1	40	40
Outside Area ⁺	22	880	880

+ Indicates the AOI for LRV T defined AOIs for all gaze points that fall outside all other AOIs

Tables with the results of the microunit-level estimates (δ s) are provided here as Tables 3.7 - 3.10. These tables relate to the Round 1 VT (Table 3.7), Round 1 LRV T (Table 3.8), Round 2 VT (Table 3.9), and Round 2 LRV T (Table 3.10) AOI iterations. In all these tables, we provide the estimates for ZINB models with and without the interaction. The estimates for models without the interaction (on the right-hand side) should be referenced for interpretation of Tables 3.7 - 3.9 and the estimates for the model with the interaction (on the left-hand side) should be referenced for interpretation of Table 3.10. Appendix E includes tables with estimates for Poisson and Zero-Inflated Poisson interaction models as Tables E.1 - E.8.

To understand how these δ s are to be interpreted, we begin by using Table 3.7 and since the model comparisons with and without interaction do not show significance (from Table 3.5), we will interpret the $\hat{\delta}_{1,0,0}$ that is 0.02 on the right-hand side of this table for the model not including the interaction. Here, the standard error (SE) is 0.12, the rate ratio (RR) is 1.02, and the z-value is 0.18. The ratio is calculated by exponentiating the

Table 3.5: Comparison of ZINB models with and without interactions for each AOI iteration

AOI Iteration	Interaction	AIC	BIC	Log-Likelihood	χ^2 (df)	p-value
Round 1 VT	Yes	53850	54243	-26871	33.17 (24)	0.101
	No ⁺	53835	54053	-26888		
Round 1 LRVT	Yes	55434	55846	-27661	32.02 (25)	0.158
	No ⁺	55416	55644	-27677		
Round 2 VT	Yes	27666	27906	-13795	15.88 (16)	0.461
	No ⁺	27650	27789	-13803		
Round 2 LRVT	Yes ⁺	30912	31172	-15416	37.32 (17)	0.003**
	No	30916	31065	-15435		

*** $p < 0.001$; ** $p < 0.01$; * $p < 0.05$ + indicates the model with the best fit

estimate, i.e., $e^{\hat{\delta}_{1,0,0}}$. Thus $e^{0.02} \approx 1.02$. The z-value is calculated by dividing the estimate by the standard error, thus $\frac{0.02}{0.12} \approx 0.18$. The reason some of these values do not give the exact same values as seen in the table is because the table only shows two decimal places for clarity where the rate ratios and z-values were calculated using the exact (not rounded) values. Where $\delta_{1,0,0}$ represents the difference in the marginal mean for the Treatment group compared to the Control group, the rate ratio of 1.02 means that the Treatment group has overall 2% more gaze points than the Control group. The z-value and resulting p-value 0.855 show that this difference (2% more gaze points from the Treatment group) is not a significant difference at the 0.05 significance level.

Continuing to look at Table 3.7, we see that $\hat{\delta}_{0,0,1} = -0.43$ with a standard error of 0.07, a rate ratio of 0.65, and z-value of -6.38 . The rate ratio of 0.65 shows that gaze points for AOI Rt Foot (1) occur 35% less often than in the reference category for AOI being Torso (13). This is a significant difference (p-value < 0.001).

With this understanding of the interpretation of the rate ratios, Table 3.7 rate ratios being most commonly less than 1 and 19 of the 24 p-values being statistically significant suggests that most of the AOIs have a significantly lower mean gaze-point counts compared to the AOI reference category Torso (13). The interpretation of the rate ratios in Table 3.8 is similar to what is seen from the Round 1 VT results. The rate ratios in this table are nearly all less than 1 and most procure statistically significant p-values. The notable exception here is for the AOI Rt Hand (3)/ Lt Hand (9) which gives a rate ratio of 3.08 and a p-value < 0.001 meaning that this AOI has overall 208% more gaze points than the reference

Table 3.6: Wald Chi-Square statistics, degrees of freedom, and p-values for multilevel models

AOI Iteration	Model	Wald Statistic	df	p-value
R1VT	Poisson Int.	531.18	24	$< 2e^{-16***}$
	ZIP Int.	393.89	24	$< 2e^{-16***}$
	ZINB Int.	33.46	24	0.0948
	ZINB No Int. Group ⁺	0.03	1	0.9050
	ZINB No Int. AOI ⁺	744.73	24	$< 2e^{-16***}$
R1LRVT	Poisson Int.	462.71	25	$< 2e^{-16***}$
	ZIP Int.	334.38	25	$< 2e^{-16***}$
	ZINB Int.	32.23	25	0.1513
	ZINB No Int. Group ⁺	0.01	1	0.8549
	ZINB No Int. AOI ⁺	920.20	25	$< 2e^{-16***}$
R2VT	Poisson Int.	330.38	16	$< 2e^{-16***}$
	ZIP Int.	336.69	16	$< 2e^{-16***}$
	ZINB Int.	15.99	16	0.4535
	ZINB No Int. Group ⁺	0.01	1	0.9400
	ZINB No Int. AOI ⁺	791.99	16	$< 2e^{-16***}$
R2LRVT	Poisson Int.	641.01	17	$< 2e^{-16***}$
	ZIP Int.	616.09	17	$< 2e^{-16***}$
	ZINB Int. ⁺	37.79	17	0.0026**
	ZINB No Int. Group	0.01	1	0.9049
	ZINB No Int. AOI	935.86	17	$< 2e^{-16***}$

*** $p < 0.001$; ** $p < 0.01$; * $p < 0.05$. ⁺ Indicates the model with the best fit.

AOI Torso (13) and this finding is statistically significant. Table 3.9 rate ratios have a less consistent interpretation where 7 AOIs show less gaze points than AOI 13 at a significant level, but 6 AOIs show more gaze points which are significant at the 0.05 level.

Because Table 3.10 gives results for Round 2 LRVT, the estimates for the model including the interaction should be interpreted. We are able to interpret the interaction δ_{10k} estimates here because the model including interaction shows a significant difference from the model without interaction as given in Table 3.5 with a p-value of 0.003. However, these values should be interpreted cautiously because the interpretation of a δ related to AOI is dependent on the reference category of the Group main effect and interpretation of a δ related to Group is dependent on the reference category of the AOI main effect.

For example, in Table 3.10, we see that the interaction $\hat{\delta}_{1,0,0} = -0.18$ with a standard error of 0.14, a rate ratio of 0.84, and z-value of -1.26 . The rate ratio of 0.84 means that the Treatment group has overall 16% less gaze points than the Control group in the

reference category for AOI: Torso (13). The z-value and resulting p-value 0.207 shows that this difference (16% less gaze points from the Treatment group in AOI 13) is not a significant difference.

Continuing to look at Table 3.10, we see that $\hat{\delta}_{0,0,1} = -0.41$ with a standard error of 0.10, a rate ratio of 0.66, and z-value of -4.36 . The rate ratio of 0.66 shows that gaze points for AOI Rt Foot (1) occur 34% less than in AOI Torso (13) *in* the reference category for Group: Control. This is a significant difference (p-value < 0.001) at the 0.05 significance level. Again, these values should be interpreted cautiously because these interpretations are dependent on the reference category of the other main effect. For example, the interpretation of the rate ratio and p-value for AOI Rt Foot (1) $\hat{\delta}_{0,0,1}$ only applies for the reference category of the main effect for Group being Control.

We are also able to interpret how much variability there is within the random effects using the variances at the bottom of Table 3.10. We find the no interaction random effect variance of 0.13 for participant and the no interaction random effect variance of 0.02 for Posture ID. The comparison of these random effect variances suggest that there is much more participant-to-participant variability than there is Posture ID-to-Posture ID variability. Although these values are interesting, we have no pre-specified hypotheses regarding the relative sizes of these two variance components. Rather than focusing on the variance components themselves, our research questions are about the fixed effects after accounting for the various sources of variability indicative of the nested nature of the data.

Interpreting the results for the interaction effects ($\hat{\delta}_{10k}$) is even more difficult. Looking at Table 3.10, we see that $\hat{\delta}_{1,0,1} = 0.24$ with a standard error of 0.13, rate ratio of 1.27, and z-value of 1.83. The rate ratio comparing Rt Foot (1) with Torso (13) is computed by taking the product of the exponentiated $\hat{\delta}_{0,0,1}$ and the exponentiated $\hat{\delta}_{1,0,1}$. Here, $e^{-0.41} \times e^{0.24} = 0.66 \times 1.27 \approx 0.84$. This suggests that in the Treatment group, the gaze points in the AOI Rt Foot (1) occur 16% less than the Treatment gaze points in the AOI Torso (13).

If we interpret findings from the largest AOI main effect rate ratio ($\hat{\delta}_{0,0,13}$) being 2.77, this shows that AOI Rt Hand (3)/ Lt Hand (9)/ Sternum (16) (AOI 3/9/16) gets 177% or 277 times as many gaze points as AOI Torso (13), but only for participants in the Control group. To understand how the Treatment group affects AOI 3/9/16, we find 2.77×0.81 (where 0.81 is the rate ratio for $\hat{\delta}_{1,0,13}$) which gives 2.25 meaning there are 2.25 times as

many gaze points for AOI 3/9/16 than AOI 13 in the Treatment group, but this finding is not significant because the p-value of the interaction $\hat{\delta}_{1,0,13}$ is not significant where p-value = 0.443. This means that the gaze-point counts for AOI 3/9/16 are significant for participants in the Control group but not significant for participants in the Treatment group.

Looking at the interaction AOIs that are significant, we find that the AOI Lt Hand (9) ($\hat{\delta}_{1,0,6}$) gives an interaction p-value of 0.026. Comparing the AOI Lt Hand (9) to AOI Torso (13) in the Control group shows there are 56% less gaze points in AOI 9 (rate ratio = 0.44, p-value < 0.001). In the Treatment group, the gaze-point contribution is 40% less in the AOI Lt Hand (9) than in the AOI Torso (13) because the rate ratio is found as $0.44 \times 1.36 \approx 0.60$. This difference is significant with a p-value of 0.026.

Interpretation of these rate ratios for the Round 2 LRVT model including the interaction is not intuitive, however, doing pairwise comparisons using Estimated Marginal Mean rate ratios provides clarity and shows how each group compares within each AOI. Typically, the EMM rate ratios would only be calculated for the iteration where the interaction is shown to be significant (Round 2 LRVT) to see if this significance translates into pairwise differences. However, we provide EMM results for all ZINB models in Section 3.2.4 to serve as an exhaustive comparison.

Table 3.7: Zero-Inflated Negative Binomial multilevel regression estimates for Round 1 VT AOI iteration

	Model Including Interaction					Model Not Including Interaction			
	$\hat{\delta}$ label	$\hat{\delta}$ (SE)	RR	z-value	p-value	$\hat{\delta}$ (SE)	RR	z-value	p-value
FIXED EFFECTS									
Intercept	$\hat{\delta}_{0,0,0}$	2.40 (0.11)	11.03	22.38	< 0.001***	2.33 (0.10)	10.27	23.59	< 0.001***
Group, Treatment vs Control	$\hat{\delta}_{1,0,0}$	-0.13 (0.15)	0.88	-0.86	0.387	0.02 (0.12)	1.02	0.18	0.855
AOI (Round 1)									
Rt Foot (1)	$\hat{\delta}_{0,0,1}$	-0.51 (0.09)	0.60	-5.45	< 0.001***	-0.43 (0.07)	0.65	-6.38	< 0.001***
Rt Knee (2)	$\hat{\delta}_{0,0,2}$	-1.18 (0.10)	0.31	-11.55	< 0.001***	-1.01 (0.07)	0.36	-13.82	< 0.001***
Rt Hand (3)	$\hat{\delta}_{0,0,3}$	-0.61 (0.11)	0.54	-5.51	< 0.001***	-0.63 (0.08)	0.53	-7.86	< 0.001***
Rt Hip (4)	$\hat{\delta}_{0,0,4}$	-0.74 (0.10)	0.48	-7.10	< 0.001***	-0.68 (0.07)	0.51	-9.06	< 0.001***
Rt Elbow (5)	$\hat{\delta}_{0,0,5}$	-0.96 (0.10)	0.38	-9.43	< 0.001***	-0.83 (0.07)	0.44	-11.18	< 0.001***
Rt Shoulder (6)	$\hat{\delta}_{0,0,6}$	-0.21 (0.10)	0.81	-2.18	0.029*	-0.21 (0.07)	0.81	-3.01	0.003**
Lt Foot (7)	$\hat{\delta}_{0,0,7}$	-1.06 (0.10)	0.35	-10.41	< 0.001***	-0.97 (0.08)	0.38	-12.82	< 0.001***
Lt Knee (8)	$\hat{\delta}_{0,0,8}$	-1.25 (0.11)	0.29	-11.34	< 0.001***	-1.20 (0.08)	0.30	-14.83	< 0.001***
Lt Hand (9)	$\hat{\delta}_{0,0,9}$	-1.22 (0.12)	0.30	-10.35	< 0.001***	-1.10 (0.09)	0.33	-12.82	< 0.001***
Lt Hip (10)	$\hat{\delta}_{0,0,10}$	-0.89 (0.10)	0.41	-8.60	< 0.001***	-0.92 (0.08)	0.40	-12.19	< 0.001***
Lt Elbow (11)	$\hat{\delta}_{0,0,11}$	-1.12 (0.11)	0.33	-9.91	< 0.001***	-1.12 (0.08)	0.33	-13.63	< 0.001***
Lt Shoulder (12)	$\hat{\delta}_{0,0,12}$	-0.77 (0.10)	0.46	-7.53	< 0.001***	-0.61 (0.07)	0.54	-8.37	< 0.001***
Head (14)	$\hat{\delta}_{0,0,13}$	-0.35 (0.10)	0.71	-3.62	< 0.001***	-0.15 (0.07)	0.86	-2.26	0.024*
Rt Knee (2)/ Rt Hand (3)	$\hat{\delta}_{0,0,14}$	0.16 (0.29)	1.18	0.56	0.578	0.18 (0.21)	1.19	0.83	0.407
Rt Hip (4)/ Rt Elbow (5)	$\hat{\delta}_{0,0,15}$	-1.54 (0.37)	0.21	-4.12	< 0.001***	-1.16 (0.26)	0.31	-4.38	< 0.001***
Lt Knee (8)/ Lt Hand (9)	$\hat{\delta}_{0,0,16}$	-0.38 (0.33)	0.69	-1.12	0.261	-0.38 (0.25)	0.69	-1.52	0.129
Lt Hip (10)/ Lt Elbow (11)	$\hat{\delta}_{0,0,17}$	-1.72 (0.39)	0.18	-4.46	< 0.001***	-1.56 (0.27)	0.21	-5.73	< 0.001***
Rt Hip (4)/ Lt Hand (9)	$\hat{\delta}_{0,0,18}$	0.17 (0.22)	1.18	0.77	0.441	0.12 (0.16)	1.12	0.74	0.459
Rt Knee (2)/ Lt Knee (8)	$\hat{\delta}_{0,0,19}$	-1.10 (0.24)	0.33	-4.58	< 0.001***	-0.79 (0.17)	0.45	-4.60	< 0.001***
Rt Hip (4)/ Rt Shoulder (6)	$\hat{\delta}_{0,0,20}$	-0.83 (0.31)	0.43	-2.66	0.008**	-0.84 (0.23)	0.43	-3.60	< 0.001***
Rt Hand (3)/ Lt Hand (9)	$\hat{\delta}_{0,0,21}$	1.09 (0.29)	2.96	3.71	< 0.001***	1.03 (0.21)	2.79	4.85	< 0.001***
Rt Elbow (5)/ Lt Elbow (11)/ Torso (13)	$\hat{\delta}_{0,0,22}$	-0.04 (0.30)	0.96	-0.14	0.887	-0.25 (0.22)	0.78	-1.13	0.259
Rt Hip (4)/ Lt Shoulder (12)/ Torso (13)	$\hat{\delta}_{0,0,23}$	-0.17 (0.29)	0.84	-0.59	0.558	-0.11 (0.21)	0.89	-0.52	0.604
Rt Hand (3)/ Rt Elbow (5)/ Rt Shoulder (6)	$\hat{\delta}_{0,0,24}$	1.00 (0.28)	2.72	3.56	< 0.001***	0.90 (0.21)	2.46	4.33	< 0.001***
Interaction: Group (Treatment) \times AOI			χ^2 (24) = 33.17			0.101			
Rt Foot (1)	$\hat{\delta}_{1,0,1}$	0.17 (0.13)	1.19	1.27	0.203				
Rt Knee (2)	$\hat{\delta}_{1,0,2}$	0.34 (0.14)	1.40	2.35	0.019*				
Rt Hand (3)	$\hat{\delta}_{1,0,3}$	-0.02 (0.15)	0.98	-0.13	0.897				
Rt Hip (4)	$\hat{\delta}_{1,0,4}$	0.12 (0.15)	1.13	0.85	0.395				
Rt Elbow (5)	$\hat{\delta}_{1,0,5}$	0.28 (0.14)	1.33	1.97	0.049*				
Rt Shoulder (6)	$\hat{\delta}_{1,0,6}$	0.01 (0.14)	1.01	0.05	0.963				
Lt Foot (7)	$\hat{\delta}_{1,0,7}$	0.19 (0.14)	1.21	1.35	0.176				
Lt Knee (8)	$\hat{\delta}_{1,0,8}$	0.12 (0.15)	1.13	0.79	0.431				
Lt Hand (9)	$\hat{\delta}_{1,0,9}$	0.25 (0.16)	1.28	1.55	0.122				
Lt Hip (10)	$\hat{\delta}_{1,0,10}$	-0.05 (0.14)	0.96	-0.32	0.749				
Lt Elbow (11)	$\hat{\delta}_{1,0,11}$	0.02 (0.15)	1.02	0.13	0.896				
Lt Shoulder (12)	$\hat{\delta}_{1,0,12}$	0.31 (0.14)	1.37	2.20	0.028*				
Head (14)	$\hat{\delta}_{1,0,13}$	0.38 (0.13)	1.46	2.82	0.005**				
Rt Knee (2)/ Rt Hand (3)	$\hat{\delta}_{1,0,14}$	0.04 (0.40)	1.04	0.10	0.920				
Rt Hip (4)/ Rt Elbow (5)	$\hat{\delta}_{1,0,15}$	0.70 (0.51)	2.02	1.39	0.164				
Lt Knee (8)/ Lt Hand (9)	$\hat{\delta}_{1,0,16}$	0.02 (0.47)	1.02	0.04	0.966				
Lt Hip (10)/ Lt Elbow (11)	$\hat{\delta}_{1,0,17}$	0.33 (0.52)	1.40	0.64	0.522				
Rt Hip (4)/ Lt Hand (9)	$\hat{\delta}_{1,0,18}$	-0.11 (0.30)	0.90	-0.36	0.717				
Rt Knee (2)/ Lt Knee (8)	$\hat{\delta}_{1,0,19}$	0.59 (0.33)	1.80	1.77	0.077				
Rt Hip (4)/ Rt Shoulder (6)	$\hat{\delta}_{1,0,20}$	-0.03 (0.45)	0.97	-0.07	0.944				
Rt Hand (3)/ Lt Hand (9)	$\hat{\delta}_{1,0,21}$	-0.13 (0.39)	0.88	-0.32	0.751				
Rt Elbow (5)/ Lt Elbow (11)/ Torso (13)	$\hat{\delta}_{1,0,22}$	-0.56 (0.42)	0.57	-1.32	0.187				
Rt Hip (4)/ Lt Shoulder (12)/ Torso (13)	$\hat{\delta}_{1,0,23}$	0.12 (0.41)	1.12	0.29	0.773				
Rt Hand (3)/ Rt Elbow (5)/ Rt Shoulder (6)	$\hat{\delta}_{1,0,24}$	-0.21 (0.39)	0.81	-0.54	0.590				
RANDOM EFFECTS									
Participant Intercepts	Notation	Var.	SD						
	u_{i0}	0.13	0.36						
Posture Intercepts	u_{0j}	0.02	0.14						

RR = Rate Ratio; Reference AOI category: Torso (13); *** $p < 0.001$; ** $p < 0.01$; * $p < 0.05$

Zero-inflation parameter: with interaction = -1.50; without interaction = -1.50;

Overdispersion parameter: with interaction = 0.74; without interaction = 0.73

Table 3.8: Zero-Inflated Negative Binomial multilevel regression estimates for Round 1 LRVT AOI iteration

	Model Including Interaction					Model Not Including Interaction			
	$\hat{\delta}$ label	$\hat{\delta}$ (SE)	RR	z-value	p-value	$\hat{\delta}$ (SE)	RR	z-value	p-value
FIXED EFFECTS									
Intercept	$\hat{\delta}_{0,0,0}$	2.27 (0.11)	9.66	20.53	< 0.001***	2.21 (0.10)	9.12	21.88	< 0.001***
Group, Treatment vs Control	$\hat{\delta}_{1,0,0}$	-0.10 (0.15)	0.91	-0.64	0.519	0.01 (0.12)	1.01	0.12	0.905
AOI (Round 1)									
Rt Foot (1)	$\hat{\delta}_{0,0,1}$	-0.56 (0.10)	0.57	-5.56	< 0.001***	-0.52 (0.07)	0.59	-7.07	< 0.001***
Rt Knee (2)	$\hat{\delta}_{0,0,2}$	-1.35 (0.11)	0.26	-12.24	< 0.001***	-1.17 (0.08)	0.31	-14.74	< 0.001***
Rt Hand (3)	$\hat{\delta}_{0,0,3}$	-0.56 (0.12)	0.57	-4.77	< 0.001***	-0.62 (0.09)	0.54	-7.19	< 0.001***
Rt Hip (4)	$\hat{\delta}_{0,0,4}$	-0.81 (0.11)	0.44	-7.39	< 0.001***	-0.77 (0.08)	0.46	-9.67	< 0.001***
Rt Elbow (5)	$\hat{\delta}_{0,0,5}$	-0.92 (0.11)	0.40	-8.49	< 0.001***	-0.85 (0.08)	0.43	-10.86	< 0.001***
Rt Shoulder (6)	$\hat{\delta}_{0,0,6}$	-0.27 (0.10)	0.76	-2.68	0.007**	-0.28 (0.07)	0.76	-3.79	< 0.001***
Lt Foot (7)	$\hat{\delta}_{0,0,7}$	-1.14 (0.11)	0.32	-10.47	< 0.001***	-1.07 (0.08)	0.34	-13.12	< 0.001***
Lt Knee (8)	$\hat{\delta}_{0,0,8}$	-1.30 (0.12)	0.27	-11.08	< 0.001***	-1.30 (0.09)	0.27	-14.91	< 0.001***
Lt Hand (9)	$\hat{\delta}_{0,0,9}$	-1.22 (0.12)	0.29	-9.87	< 0.001***	-1.14 (0.09)	0.32	-12.54	< 0.001***
Lt Hip (10)	$\hat{\delta}_{0,0,10}$	-0.93 (0.11)	0.40	-8.50	< 0.001***	-0.97 (0.08)	0.38	-12.10	< 0.001***
Lt Elbow (11)	$\hat{\delta}_{0,0,11}$	-1.15 (0.12)	0.32	-9.50	< 0.001***	-1.15 (0.09)	0.32	-13.16	< 0.001***
Lt Shoulder (12)	$\hat{\delta}_{0,0,12}$	-0.92 (0.11)	0.40	-8.47	< 0.001***	-0.76 (0.08)	0.47	-9.72	< 0.001***
Head (14)	$\hat{\delta}_{0,0,13}$	-0.30 (0.10)	0.74	-3.00	0.003**	-0.14 (0.07)	0.87	-1.96	0.050
Rt Knee (2)/ Rt Hand (3)	$\hat{\delta}_{0,0,14}$	0.16 (0.30)	1.17	0.52	0.605	0.18 (0.23)	1.19	0.78	0.437
Rt Hip (4)/ Rt Elbow (5)	$\hat{\delta}_{0,0,15}$	-1.47 (0.39)	0.23	-3.79	< 0.001***	-1.10 (0.27)	0.33	-4.02	< 0.001***
Lt Knee (8)/ Lt Hand (9)	$\hat{\delta}_{0,0,16}$	-0.63 (0.35)	0.53	-1.79	0.073	-0.52 (0.27)	0.59	-1.96	0.052
Lt Hip (10)/ Lt Elbow (11)	$\hat{\delta}_{0,0,17}$	-1.66 (0.41)	0.19	-4.04	< 0.001***	-1.72 (0.29)	0.18	-5.90	< 0.001***
Rt Hip (4)/ Lt Hand (9)	$\hat{\delta}_{0,0,18}$	0.19 (0.23)	1.21	0.85	0.397	0.16 (0.17)	1.17	0.94	0.346
Rt Knee (2)/ Lt Knee (8)	$\hat{\delta}_{0,0,19}$	-1.83 (0.28)	0.16	-6.50	< 0.001***	-1.40 (0.20)	0.25	-7.14	< 0.001***
Rt Hip (4)/ Rt Shoulder (6)	$\hat{\delta}_{0,0,20}$	-0.77 (0.34)	0.46	-2.28	0.023*	-0.80 (0.25)	0.45	-3.23	0.001**
Rt Hand (3)/ Lt Hand (9)	$\hat{\delta}_{0,0,21}$	1.20 (0.30)	3.31	3.93	< 0.001***	1.12 (0.22)	3.08	5.15	< 0.001***
Rt Elbow (5)/ Lt Elbow (11)/ Torso (13)	$\hat{\delta}_{0,0,22}$	0.08 (0.31)	1.08	0.24	0.807	-0.15 (0.23)	0.86	-0.66	0.511
Rt Hip (4)/ Lt Shoulder (12)/ Torso (13)	$\hat{\delta}_{0,0,23}$	-0.10 (0.31)	0.90	-0.34	0.734	-0.06 (0.22)	0.94	-0.27	0.790
Rt Hand (3)/ Rt Elbow (5)/ Rt Shoulder (6)	$\hat{\delta}_{0,0,24}$	1.03 (0.29)	2.80	3.51	< 0.001***	0.92 (0.22)	2.51	4.27	< 0.001***
Outside Area	$\hat{\delta}_{0,0,25}$	0.07 (0.09)	1.07	0.77	0.443	0.16 (0.07)	1.17	2.41	0.016*
Interaction: Group (Treatment) \times AOI			χ^2 (25) = 32.02		0.158				
Rt Foot (1)	$\hat{\delta}_{1,0,1}$	0.10 (0.14)	1.11	0.71	0.475				
Rt Knee (2)	$\hat{\delta}_{1,0,2}$	0.35 (0.15)	1.42	2.28	0.022*				
Rt Hand (3)	$\hat{\delta}_{1,0,3}$	-0.11 (0.16)	0.90	-0.68	0.496				
Rt Hip (4)	$\hat{\delta}_{1,0,4}$	0.09 (0.16)	1.09	0.57	0.569				
Rt Elbow (5)	$\hat{\delta}_{1,0,5}$	0.14 (0.15)	1.15	0.95	0.345				
Rt Shoulder (6)	$\hat{\delta}_{1,0,6}$	-0.01 (0.14)	0.99	-0.04	0.966				
Lt Foot (7)	$\hat{\delta}_{1,0,7}$	0.16 (0.15)	1.17	1.03	0.305				
Lt Knee (8)	$\hat{\delta}_{1,0,8}$	0.01 (0.16)	1.01	0.08	0.933				
Lt Hand (9)	$\hat{\delta}_{1,0,9}$	0.18 (0.17)	1.20	1.07	0.285				
Lt Hip (10)	$\hat{\delta}_{1,0,10}$	-0.09 (0.15)	0.92	-0.58	0.560				
Lt Elbow (11)	$\hat{\delta}_{1,0,11}$	0.00 (0.16)	1.00	-0.03	0.977				
Lt Shoulder (12)	$\hat{\delta}_{1,0,12}$	0.32 (0.15)	1.38	2.13	0.033*				
Head (14)	$\hat{\delta}_{1,0,13}$	0.32 (0.14)	1.38	2.26	0.024*				
Rt Knee (2)/ Rt Hand (3)	$\hat{\delta}_{1,0,14}$	0.04 (0.43)	1.04	0.09	0.925				
Rt Hip (4)/ Rt Elbow (5)	$\hat{\delta}_{1,0,15}$	0.67 (0.53)	1.95	1.26	0.208				
Lt Knee (8)/ Lt Hand (9)	$\hat{\delta}_{1,0,16}$	0.26 (0.51)	1.30	0.51	0.613				
Lt Hip (10)/ Lt Elbow (11)	$\hat{\delta}_{1,0,17}$	-0.09 (0.56)	0.91	-0.16	0.870				
Rt Hip (4)/ Lt Hand (9)	$\hat{\delta}_{1,0,18}$	-0.08 (0.32)	0.92	-0.25	0.801				
Rt Knee (2)/ Lt Knee (8)	$\hat{\delta}_{1,0,19}$	0.78 (0.38)	2.18	2.04	0.042*				
Rt Hip (4)/ Rt Shoulder (6)	$\hat{\delta}_{1,0,20}$	-0.06 (0.48)	0.94	-0.12	0.903				
Rt Hand (3)/ Lt Hand (9)	$\hat{\delta}_{1,0,21}$	-0.15 (0.41)	0.86	-0.35	0.723				
Rt Elbow (5)/ Lt Elbow (11)/ Torso (13)	$\hat{\delta}_{1,0,22}$	-0.59 (0.44)	0.55	-1.36	0.174				
Rt Hip (4)/ Lt Shoulder (12)/ Torso (13)	$\hat{\delta}_{1,0,23}$	0.08 (0.43)	1.09	0.19	0.847				
Rt Hand (3)/ Rt Elbow (5)/ Rt Shoulder (6)	$\hat{\delta}_{1,0,24}$	-0.22 (0.40)	0.80	-0.56	0.577				
Outside Area	$\hat{\delta}_{1,0,25}$	0.18 (0.13)	1.20	1.38	0.168				
RANDOM EFFECTS									
Participant Intercepts	Notation	Var.	SD	Var. SD					
	\bar{u}_{i0}	0.13	0.36	0.13 0.37					
Posture Intercepts	\bar{u}_{0j}	0.02	0.14	0.02 0.14					

RR = Rate Ratio; Reference AOI category: Torso (13); *** $p < 0.001$; ** $p < 0.01$; * $p < 0.05$

Zero-inflation parameter: with interaction = -1.47; without interaction = -1.47;

Overdispersion parameter: with interaction = 0.68; without interaction = 0.67

Table 3.9: Zero-Inflated Negative Binomial multilevel regression estimates for Round 2 VT AOI iteration

	Model Including Interaction					Model Not Including Interaction			
	$\widehat{\delta}$ label	$\widehat{\delta}$ (SE)	RR	z-value	p-value	$\widehat{\delta}$ (SE)	RR	z-value	p-value
FIXED EFFECTS									
Intercept	$\widehat{\delta}_{0,0,0}$	2.94 (0.12)	18.94	25.17	< 0.001***	2.89 (0.11)	18.05	25.66	< 0.001***
Group, Treatment vs Control	$\widehat{\delta}_{1,0,0}$	-0.09 (0.14)	0.91	-0.68	0.497	0.01 (0.12)	1.01	0.08	0.940
AOI (Round 2)									
Rt Foot (1)	$\widehat{\delta}_{0,0,1}$	-0.48 (0.09)	0.62	-5.56	< 0.001***	-0.38 (0.07)	0.68	-5.78	< 0.001***
Rt Knee (2)	$\widehat{\delta}_{0,0,2}$	-0.80 (0.26)	0.45	-3.09	0.002**	-0.77 (0.19)	0.46	-4.11	< 0.001***
Rt Hand (3)	$\widehat{\delta}_{0,0,3}$	-0.44 (0.09)	0.64	-5.06	< 0.001***	-0.45 (0.07)	0.64	-6.94	< 0.001***
Lt Foot (7)	$\widehat{\delta}_{0,0,4}$	-0.96 (0.11)	0.38	-8.74	< 0.001***	-0.86 (0.09)	0.42	-10.01	< 0.001***
Lt Knee (8)	$\widehat{\delta}_{0,0,5}$	-0.65 (0.19)	0.52	-3.33	< 0.001***	-0.61 (0.15)	0.54	-4.06	< 0.001***
Lt Hand (9)	$\widehat{\delta}_{0,0,6}$	-0.91 (0.09)	0.40	-10.53	< 0.001***	-0.81 (0.06)	0.44	-12.60	< 0.001***
Head (14)	$\widehat{\delta}_{0,0,7}$	0.47 (0.13)	1.60	3.58	< 0.001***	0.48 (0.10)	1.62	4.68	< 0.001***
Neck (15)	$\widehat{\delta}_{0,0,8}$	-0.01 (0.08)	0.99	-0.07	0.941	0.11 (0.06)	1.11	1.84	0.065
Sternum (16)	$\widehat{\delta}_{0,0,9}$	0.19 (0.09)	1.22	2.21	0.027*	0.17 (0.07)	1.19	2.60	0.009**
Middle of Feet (17)	$\widehat{\delta}_{0,0,10}$	-0.81 (0.09)	0.44	-9.41	< 0.001***	-0.75 (0.06)	0.47	-11.62	< 0.001***
Lt Hand (9)/ Torso (13)	$\widehat{\delta}_{0,0,11}$	-0.36 (0.21)	0.70	-1.70	0.089	-0.30 (0.16)	0.74	-1.85	0.065
Rt Shoulder (6)/ Neck (15)	$\widehat{\delta}_{0,0,12}$	-0.10 (0.22)	0.90	-0.46	0.645	0.08 (0.17)	1.08	0.45	0.653
Rt Hand (3)/ Lt Hand (9)/ Sternum (16)	$\widehat{\delta}_{0,0,13}$	0.90 (0.21)	2.47	4.32	< 0.001***	0.78 (0.16)	2.17	4.72	< 0.001***
Rt Elbow (5)/ Torso (13)	$\widehat{\delta}_{0,0,14}$	0.89 (0.22)	2.43	3.96	< 0.001***	0.94 (0.18)	2.55	5.23	< 0.001***
Lt Shoulder (12)/ Torso (13)	$\widehat{\delta}_{0,0,15}$	0.64 (0.22)	1.90	2.96	0.003**	0.72 (0.17)	2.05	4.15	< 0.001***
Rt Hand (3)/ Neck (15)	$\widehat{\delta}_{0,0,16}$	0.80 (0.21)	2.24	3.87	< 0.001***	0.83 (0.16)	2.28	5.11	< 0.001***
Interaction: Group (Treatment) \times AOI			χ^2 (16) = 15.88		0.461				
Rt Foot (1)	$\widehat{\delta}_{1,0,1}$	0.21 (0.11)	1.23	1.81	0.070				
Rt Knee (2)	$\widehat{\delta}_{1,0,2}$	0.07 (0.35)	1.08	0.21	0.836				
Rt Hand (3)	$\widehat{\delta}_{1,0,3}$	0.00 (0.11)	1.00	-0.03	0.978				
Lt Foot (7)	$\widehat{\delta}_{1,0,4}$	0.22 (0.15)	1.24	1.47	0.141				
Lt Knee (8)	$\widehat{\delta}_{1,0,5}$	0.08 (0.25)	1.08	0.31	0.755				
Lt Hand (9)	$\widehat{\delta}_{1,0,6}$	0.22 (0.12)	1.24	1.89	0.059				
Head (14)	$\widehat{\delta}_{1,0,7}$	0.02 (0.16)	1.02	0.16	0.876				
Neck (15)	$\widehat{\delta}_{1,0,8}$	0.23 (0.11)	1.26	2.10	0.035*				
Sternum (16)	$\widehat{\delta}_{1,0,9}$	-0.05 (0.12)	0.95	-0.42	0.673				
Middle of Feet (17)	$\widehat{\delta}_{1,0,10}$	0.12 (0.12)	1.13	1.03	0.303				
Lt Hand (9)/ Torso (13)	$\widehat{\delta}_{1,0,11}$	0.13 (0.27)	1.14	0.49	0.625				
Rt Shoulder (6)/ Neck (15)	$\widehat{\delta}_{1,0,12}$	0.34 (0.28)	1.41	1.22	0.223				
Rt Hand (3)/ Lt Hand (9)/ Sternum (16)	$\widehat{\delta}_{1,0,13}$	-0.29 (0.26)	0.75	-1.11	0.266				
Rt Elbow (5)/ Torso (13)	$\widehat{\delta}_{1,0,14}$	0.11 (0.27)	1.12	0.42	0.677				
Lt Shoulder (12)/ Torso (13)	$\widehat{\delta}_{1,0,15}$	0.17 (0.26)	1.19	0.67	0.505				
Rt Hand (3)/ Neck (15)	$\widehat{\delta}_{1,0,16}$	0.05 (0.26)	1.05	0.17	0.864				
RANDOM EFFECTS						Var.	SD		
Participant Intercepts	\bar{u}_{i0}	0.13	0.37						
Posture Intercepts	\bar{u}_{0j}	0.09	0.30						

RR = Rate Ratio; Reference AOI category: Torso (13); *** $p < 0.001$; ** $p < 0.01$; * $p < 0.05$

Zero-inflation parameter: with interaction = -1.84; without interaction = -1.84;

Overdispersion parameter: with interaction = 1.66; without interaction = 1.64

Table 3.10: Zero-Inflated Negative Binomial multilevel regression estimates for Round 2 LRV T AOI iteration

	Model Including Interaction					Model Not Including Interaction			
	$\hat{\delta}$ label	$\hat{\delta}$ (SE)	RR	z-value	p-value	$\hat{\delta}$ (SE)	RR	z-value	p-value
FIXED EFFECTS									
Intercept	$\hat{\delta}_{0,0,0}$	2.56 (0.11)	12.98	22.69	< 0.001***	2.49 (0.11)	12.02	23.01	< 0.001***
Group, Treatment vs Control	$\hat{\delta}_{1,0,0}$	-0.18 (0.14)	0.84	-1.26	0.207	-0.01 (0.12)	0.99	-0.12	0.905
AOI (Round 2)									
Rt Foot (1)	$\hat{\delta}_{0,0,1}$	-0.41 (0.10)	0.66	-4.36	< 0.001***	-0.30 (0.07)	0.74	-4.25	< 0.001***
Rt Knee (2)	$\hat{\delta}_{0,0,2}$	-0.73 (0.30)	0.48	-2.43	0.015*	-0.64 (0.21)	0.53	-3.06	0.002**
Rt Hand (3)	$\hat{\delta}_{0,0,3}$	-0.16 (0.10)	0.85	-1.61	0.107	-0.22 (0.08)	0.80	-2.90	0.004**
Lt Foot (7)	$\hat{\delta}_{0,0,4}$	-0.98 (0.13)	0.37	-7.80	< 0.001***	-0.86 (0.10)	0.42	-9.00	< 0.001***
Lt Knee (8)	$\hat{\delta}_{0,0,5}$	-0.57 (0.21)	0.57	-2.69	0.007**	-0.49 (0.16)	0.61	-3.14	0.002**
Lt Hand (9)	$\hat{\delta}_{0,0,6}$	-0.82 (0.10)	0.44	-7.92	< 0.001***	-0.68 (0.08)	0.51	-8.81	< 0.001***
Head (14)	$\hat{\delta}_{0,0,7}$	0.44 (0.13)	1.55	3.38	< 0.001***	0.45 (0.10)	1.57	4.56	< 0.001***
Neck (15)	$\hat{\delta}_{0,0,8}$	0.02 (0.08)	1.02	0.23	0.822	0.12 (0.06)	1.13	2.00	0.045*
Sternum (16)	$\hat{\delta}_{0,0,9}$	0.21 (0.09)	1.24	2.28	0.023*	0.17 (0.07)	1.19	2.48	0.013*
Middle of Feet (17)	$\hat{\delta}_{0,0,10}$	-0.69 (0.10)	0.50	-6.97	< 0.001***	-0.60 (0.08)	0.55	-8.00	< 0.001***
Lt Hand (9)/ Torso (13)	$\hat{\delta}_{0,0,11}$	-0.16 (0.22)	0.85	-0.71	0.476	0.04 (0.16)	1.05	0.27	0.785
Rt Shoulder (6)/ Neck (15)	$\hat{\delta}_{0,0,12}$	0.24 (0.23)	1.27	1.06	0.290	0.26 (0.17)	1.29	1.52	0.130
Rt Hand (3)/ Lt Hand (9)/ Sternum (16)	$\hat{\delta}_{0,0,13}$	1.02 (0.21)	2.77	4.95	< 0.001***	0.93 (0.16)	2.54	5.85	< 0.001***
Rt Elbow (5)/ Torso (13)	$\hat{\delta}_{0,0,14}$	-0.07 (0.22)	0.94	-0.30	0.765	-0.04 (0.17)	0.96	-0.23	0.819
Lt Shoulder (12)/ Torso (13)	$\hat{\delta}_{0,0,15}$	-0.24 (0.21)	0.79	-1.11	0.265	-0.13 (0.17)	0.88	-0.79	0.431
Rt Hand (3)/ Neck (15)	$\hat{\delta}_{0,0,16}$	0.94 (0.21)	2.55	4.51	< 0.001***	0.82 (0.16)	2.28	5.11	< 0.001***
Outside Area	$\hat{\delta}_{0,0,17}$	0.54 (0.07)	1.72	7.73	< 0.001***	0.72 (0.05)	2.05	13.82	< 0.001***
Interaction: Group (Treatment) \times AOI			χ^2 (17) = 37.32		0.003**				
Rt Foot (1)	$\hat{\delta}_{1,0,1}$	0.24 (0.13)	1.27	1.83	0.067				
Rt Knee (2)	$\hat{\delta}_{1,0,2}$	0.18 (0.40)	1.19	0.44	0.659				
Rt Hand (3)	$\hat{\delta}_{1,0,3}$	-0.11 (0.13)	0.90	-0.82	0.413				
Lt Foot (7)	$\hat{\delta}_{1,0,4}$	0.27 (0.17)	1.31	1.56	0.119				
Lt Knee (8)	$\hat{\delta}_{1,0,5}$	0.16 (0.28)	1.18	0.58	0.560				
Lt Hand (9)	$\hat{\delta}_{1,0,6}$	0.31 (0.14)	1.36	2.22	0.026*				
Head (14)	$\hat{\delta}_{1,0,7}$	0.03 (0.17)	1.03	0.20	0.841				
Neck (15)	$\hat{\delta}_{1,0,8}$	0.22 (0.12)	1.25	1.90	0.057				
Sternum (16)	$\hat{\delta}_{1,0,9}$	-0.10 (0.13)	0.91	-0.77	0.441				
Middle of Feet (17)	$\hat{\delta}_{1,0,10}$	0.20 (0.13)	1.22	1.50	0.134				
Lt Hand (9)/ Torso (13)	$\hat{\delta}_{1,0,11}$	0.38 (0.29)	1.47	1.35	0.178				
Rt Shoulder (6)/ Neck (15)	$\hat{\delta}_{1,0,12}$	0.04 (0.30)	1.04	0.12	0.902				
Rt Hand (3)/ Lt Hand (9)/ Sternum (16)	$\hat{\delta}_{1,0,13}$	-0.21 (0.27)	0.81	-0.77	0.443				
Rt Elbow (5)/ Torso (13)	$\hat{\delta}_{1,0,14}$	0.06 (0.29)	1.06	0.20	0.838				
Lt Shoulder (12)/ Torso (13)	$\hat{\delta}_{1,0,15}$	0.23 (0.28)	1.26	0.83	0.404				
Rt Hand (3)/ Neck (15)	$\hat{\delta}_{1,0,16}$	-0.25 (0.27)	0.78	-0.91	0.365				
Outside Area	$\hat{\delta}_{1,0,17}$	0.35 (0.10)	1.41	3.53	< 0.001***				
RANDOM EFFECTS						Var.	SD		
Participant Intercepts	\bar{u}_{i0}	0.13	0.36						
Posture Intercepts	\bar{u}_{0j}	0.06	0.25						

RR = Rate Ratio; Reference AOI category: Torso (13); *** $p < 0.001$; ** $p < 0.01$; * $p < 0.05$

Zero-inflation parameter: with interaction = -1.36; without interaction = -1.36;

Overdispersion parameter: with interaction = 1.63; without interaction = 1.59

3.2.4 Pairwise Comparison Results

The findings from the Wald test for ZINB models are supported by pairwise EMM rate ratios described in the *Pairwise Comparison Using Estimated Marginal Mean Rate Ratios* part of Section 2.3.3. The hypotheses for EMM rate ratio tests are: H_O : the EMM rate ratio = 1 meaning that the gaze-point counts for the Treatment and the Control groups are equivalent for each AOI; and H_A : the EMM rate ratio $\neq 1$, meaning that there is a difference in gaze-point count for the Treatment and Control groups for each AOI separately. These ratio tests are conducted for each AOI separately.

Table 3.11 shows the rate ratios for Treatment vs. Control and the associated raw p-values for each AOI along with the mean gaze-point counts and their 95% confidence intervals for each Group and each AOI for Round 1 VT. Figure 3.6 shows a visual comparison of the means and confidence intervals from Round 1 VT that are provided in Table 3.11. Similarly, Table 3.12 and Figure 3.7 provide this information and visuals for Round 1 LRVT, Table 3.13 and Figure 3.8 give Round 2 VT results, and Table 3.14 and Figure 3.9 give the information and visuals for Round 2 LRVT.

Table 3.11: Zero-Inflated Negative Binomial Multilevel Regression Estimated Gaze-Point Counts for each AOI by Group for Round 1 VT Iteration

AOI Labels (Round 1)	Treatment (Trt)			Control (Ctl)			Trt vs. Ctl	
	Counts	CI (95%)		Counts	CI (95%)		RR	p-value
Rt Foot (1)	6.90	5.57,	8.54]	6.60	5.33,	8.18]	1.04	0.767
Rt Knee (2)	4.19	3.35,	5.25]	3.40	2.71,	4.27]	1.23	0.179
Rt Hand (3)	5.20	4.11,	6.56]	6.01	4.72,	7.65]	0.86	0.364
Rt Hip (4)	5.28	4.19,	6.65]	5.29	4.20,	6.65]	0.10	0.992
Rt Elbow (5)	4.92	3.92,	6.18]	4.21	3.35,	5.28]	1.17	0.317
Rt Shoulder (6)	7.94	6.39,	9.86]	8.95	7.21,	11.11]	0.89	0.423
Lt Foot (7)	4.09	3.24,	5.16]	3.82	3.05,	4.80]	1.07	0.667
Lt Knee (8)	3.15	2.48,	4.01]	3.17	2.49,	4.03]	0.99	0.968
Lt Hand (9)	3.68	2.86,	4.74]	3.26	2.53,	4.21]	1.13	0.481
Lt Hip (10)	3.82	3.04,	4.81]	4.54	3.60,	5.72]	0.84	0.271
Lt Elbow (11)	3.23	2.53,	4.12]	3.59	2.80,	4.60]	0.90	0.526
Lt Shoulder (12)	6.18	4.93,	7.75]	5.12	4.08,	6.43]	1.21	0.228
Torso (13)	9.72	7.86,	12.03]	11.03	8.94,	13.61]	0.88	0.387
Head (14)	10.02	8.10,	12.40]	7.79	6.27,	9.68]	1.29	0.088
Rt Knee (2)/ Rt Hand (3)	11.90	6.64,	21.33]	12.97	7.25,	23.20]	0.92	0.831
Rt Hip (4)/ Rt Elbow (5)	4.20	2.07,	8.54]	2.36	1.12,	4.96]	1.78	0.257
Lt Knee (8)/ Lt Hand (9)	6.82	3.42,	13.57]	7.58	3.90,	14.73]	0.90	0.823
Lt Hip (10)/ Lt Elbow (11)	2.43	1.17,	5.04]	1.97	0.92,	4.24]	1.23	0.692
Rt Hip (4)/ Lt Hand (9)	10.30	6.68,	15.88]	13.02	8.42,	20.15]	0.79	0.441
Rt Knee (2)/ Lt Knee (8)	5.84	3.62,	9.40]	3.68	2.27,	5.96]	1.59	0.172
Rt Hip (4)/ Rt Shoulder (6)	4.09	2.10,	7.97]	4.79	2.57,	8.93]	0.85	0.729
Rt Hand (3)/ Lt Hand (9)	25.41	14.48,	44.6]	32.68	18.25,	58.52]	0.78	0.528
Rt Elbow (5)/ Lt Elbow (11)/ Torso (13)	5.34	2.86,	9.98]	10.57	5.84,	19.14]	0.51	0.109
Rt Hip (4)/ Lt Shoulder (12)/ Torso (13)	9.20	5.12,	16.52]	9.28	5.17,	16.67]	0.99	0.982
Rt Hand (3)/ Rt Elbow (5)/ Rt Shoulder (6)	21.48	12.20,	37.82]	30.01	17.10,	52.69]	0.72	0.392

RR = Rate Ratio; *** $p < 0.001$; ** $p < 0.01$; * $p < 0.05$

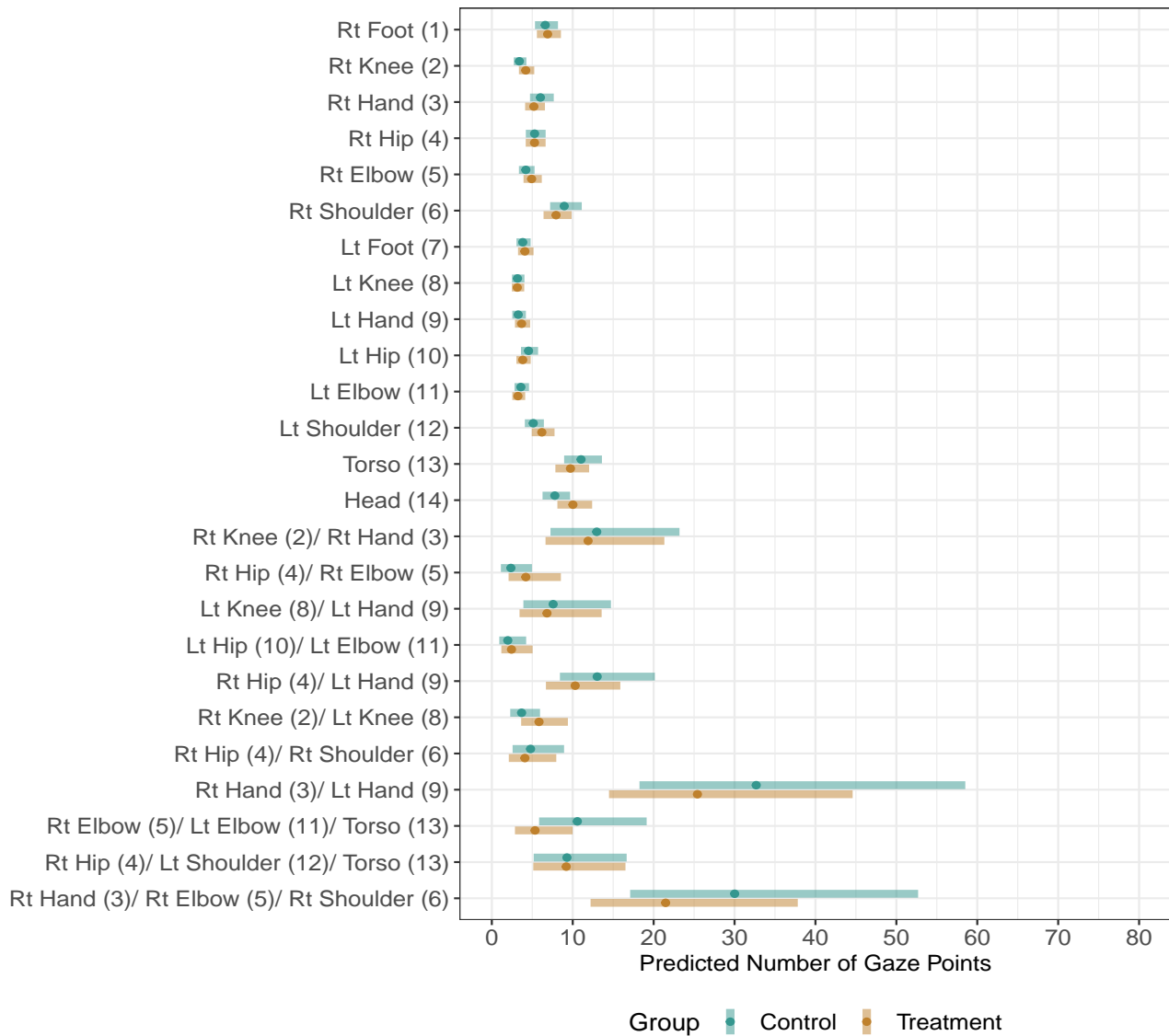


Fig. 3.6: Visual for EMM rate ratio pairwise comparison of predicted mean number of gaze points including 95% confidence intervals for Round 1 VT AOIs across all postures.

Table 3.12: Zero-Inflated Negative Binomial Multilevel regression estimated marginal mean gaze-point counts for each AOI by Group for Round 1 LRVT iteration

AOI Labels (Round 1)	Treatment (Trt)			Control (Ctl)			Trt vs. Ctl	
	Counts	CI (95%)		Counts	CI (95%)		RR	p-value
Rt Foot (1)	5.52	[4.40,	6.91]	5.49	[4.38,	6.88]	1.01	0.976
Rt Knee (2)	3.24	[2.55,	4.11]	2.51	[1.98,	3.20]	1.29	0.125
Rt Hand (3)	4.50	[3.52,	5.76]	5.51	[4.27,	7.12]	0.82	0.223
Rt Hip (4)	4.26	[3.34,	5.43]	4.30	[3.38,	5.46]	0.99	0.958
Rt Elbow (5)	4.03	[3.18,	5.11]	3.85	[3.03,	4.88]	1.05	0.780
Rt Shoulder (6)	6.64	[5.30,	8.32]	7.36	[5.88,	9.22]	0.90	0.505
Lt Foot (7)	3.27	[2.56,	4.18]	3.09	[2.43,	3.92]	1.06	0.721
Lt Knee (8)	2.42	[1.87,	3.12]	2.63	[2.04,	3.39]	0.92	0.628
Lt Hand (9)	3.08	[2.37,	4.01]	2.84	[2.18,	3.70]	1.09	0.646
Lt Hip (10)	3.18	[2.50,	4.05]	3.83	[3.01,	4.87]	0.83	0.255
Lt Elbow (11)	2.77	[2.15,	3.58]	3.07	[2.37,	3.98]	0.90	0.558
Lt Shoulder (12)	4.81	[3.80,	6.09]	3.84	[3.03,	4.88]	1.25	0.167
Torso (13)	8.77	[7.04,	10.92]	9.66	[7.78,	12.00]	0.91	0.519
Head (14)	8.90	[7.14,	11.08]	7.13	[5.69,	8.93]	1.25	0.148
Rt Knee (2)/ Rt Hand (3)	10.68	[5.63,	20.25]	11.30	[6.18,	20.68]	0.95	0.896
Rt Hip (4)/ Rt Elbow (5)	3.94	[1.87,	8.28]	2.23	[1.04,	4.80]	1.77	0.285
Lt Knee (8)/ Lt Hand (9)	6.04	[2.81,	12.99]	5.14	[2.55,	10.34]	1.18	0.754
Lt Hip (10)/ Lt Elbow (11)	1.52	[0.69,	3.34]	1.83	[0.81,	4.14]	0.83	0.738
Rt Hip (4)/ Lt Hand (9)	9.80	[6.16,	15.59]	11.71	[7.41,	18.49]	0.84	0.583
Rt Knee (2)/ Lt Knee (8)	3.05	[1.79,	5.19]	1.54	[0.88,	2.71]	1.98	0.078
Rt Hip (4)/ Rt Shoulder (6)	3.82	[1.92,	7.61]	4.46	[2.28,	8.74]	0.86	0.747
Rt Hand (3)/ Lt Hand (9)	25.06	[13.99,	44.90]	31.94	[17.46,	58.42]	0.79	0.559
Rt Elbow (5)/ Lt Elbow (11)/ Torso (13)	5.21	[2.73,	9.95]	10.42	[5.64,	19.25]	0.50	0.117
Rt Hip (4)/ Lt Shoulder (12)/ Torso (13)	8.58	[4.62,	15.91]	8.71	[4.74,	15.99]	0.99	0.972
Rt Hand (3)/ Rt Elbow (5)/ Rt Shoulder (6)	19.59	[10.88,	35.26]	27.03	[15.07,	48.51]	0.73	0.429
Outside Area	11.29	[9.16,	13.92]	10.37	[8.41,	12.80]	1.09	0.560

RR = Rate Ratio; *** $p < 0.001$; ** $p < 0.01$; * $p < 0.05$

It should be noted that these p-values are the raw p-values, however, none of them are significant so an adjustment for multiple comparisons is not necessary. More result tables are provided in Appendix D that provide raw and adjusted p-values for all converging models (Poisson, Zero-Inflated Poisson, and Zero-Inflated Negative Binomial for all AOI iterations) as Tables D.1 - D.12.

The EMM rate ratios for Round 1 VT for the ZINB model are not significant as shown in Table 3.11. This result is predicted by the lack of a significant overall interaction (p-value 0.101 shown in Table 3.7) and supported by Figure 3.6. This is consistent with the lack of overall significance from the Wald test results for the model as a whole (p-value = 0.0948 from Table 3.6). Similarly, the EMM rate ratios for Round 1 LRVT (given in Table 3.12 and visualized in Figure 3.7) and Round 2 VT (given in Table 3.13 and visualized in Figure 3.8) give non-significant results for the model as a whole. These results are also consistent with the Wald test results (p-value = 0.1513 for Round 1 LRVT and p-value = 0.4535 for Round 2 VT from Table 3.6) and the lack of a significant overall interaction (p-value = 0.158

for Round 1 LRVT and $p\text{-value} = 0.461$ for Round 2 VT from Table 3.5).

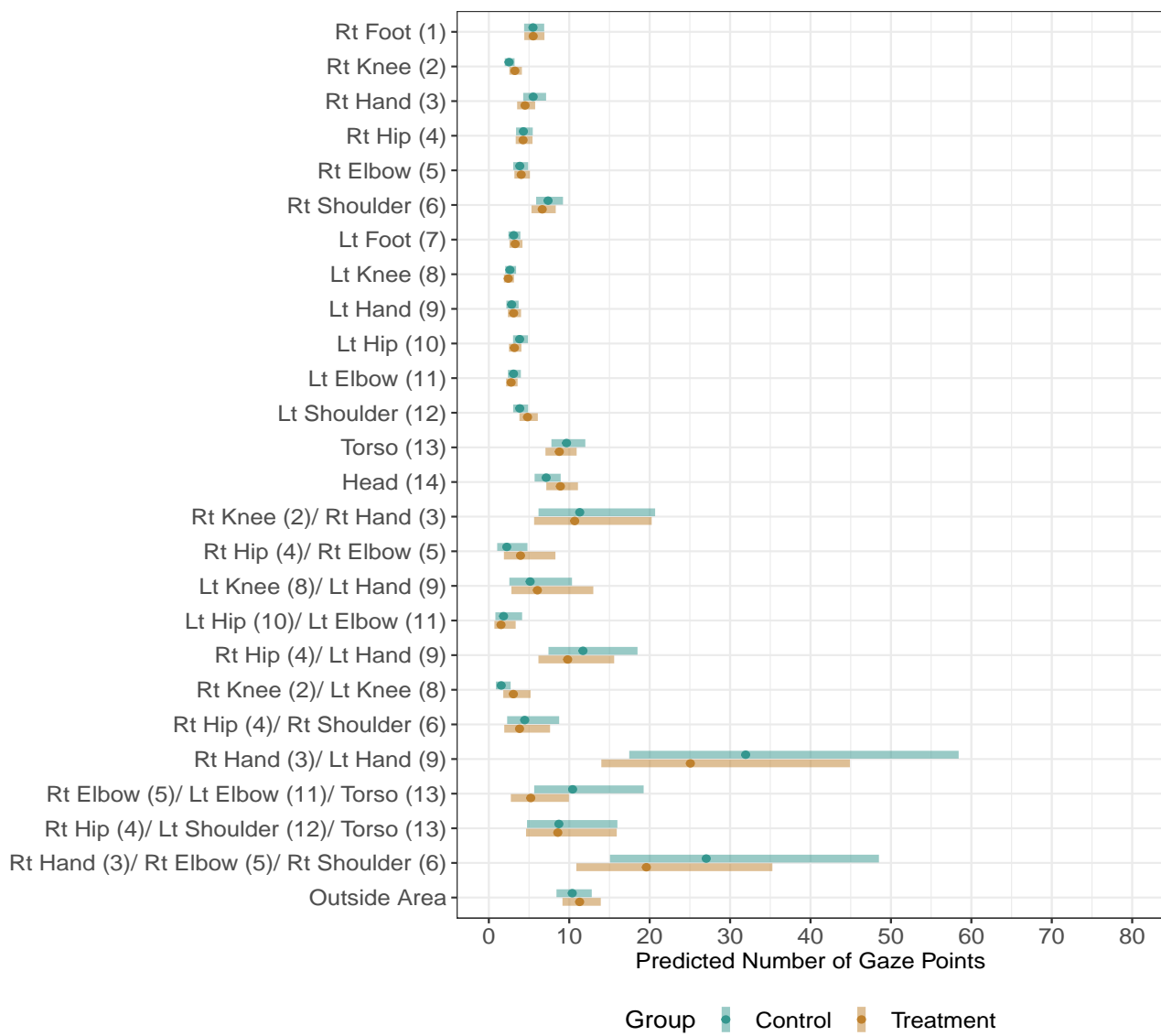


Fig. 3.7: Visual for EMM rate ratio pairwise comparison of predicted mean number of gaze points including 95% confidence intervals for Round 1 LRVT AOIs.

Table 3.13: Zero-Inflated Negative Binomial Multilevel regression estimated marginal mean gaze-point counts for each AOI by Group for Round 2 VT iteration

AOI Labels (Round 2)	Treatment (Trt)			Control (Ctl)			Trt vs. Ctl	
	Counts	CI (95%)		Counts	CI (95%)		RR	p-value
Rt Foot (1)	13.09	10.27	16.67	11.66	9.16	14.86	1.12	0.430
Rt Knee (2)	8.32	4.91	14.11	8.49	4.95	14.57	0.98	0.957
Rt Hand (3)	11.06	8.69	14.09	12.18	9.54	15.56	0.91	0.510
Lt Foot (7)	8.21	6.19	10.91	7.25	5.51	9.55	1.13	0.472
Lt Knee (8)	9.76	6.41	14.85	9.90	6.52	15.04	0.99	0.956
Lt Hand (9)	8.60	6.75	10.97	7.59	5.94	9.69	1.13	0.393
Torso (13)	17.26	13.72	21.71	18.94	15.06	23.81	0.91	0.497
Head (14)	28.25	20.93	38.11	30.24	22.28	41.04	0.93	0.708
Neck (15)	21.55	17.05	27.24	18.83	14.88	23.83	1.14	0.337
Sternum (16)	19.94	15.57	25.53	23.01	17.97	29.47	0.87	0.340
Middle of Feet (17)	8.65	6.77	11.05	8.42	6.61	10.74	1.03	0.858
Lt Hand (9)/ Torso (13)	13.75	8.82	21.43	13.19	8.41	20.70	1.04	0.887
Rt Shoulder (6)/ Neck (15)	22.03	13.72	35.39	17.12	10.72	27.35	1.29	0.396
Rt Hand (3)/ Lt Hand (9)/ Sternum (16)	31.77	20.32	49.69	46.78	30.04	72.85	0.68	0.166
Rt Elbow (5)/ Torso (13)	47.02	29.43	75.13	46.03	28.81	73.54	1.02	0.941
Lt Shoulder (12)/ Torso (13)	39.00	24.79	61.36	35.97	22.85	56.62	1.08	0.769
Rt Hand (3)/ Neck (15)	40.37	25.79	63.20	42.34	27.05	66.28	0.95	0.864

RR = Rate Ratio; *** $p < 0.001$; ** $p < 0.01$; * $p < 0.05$

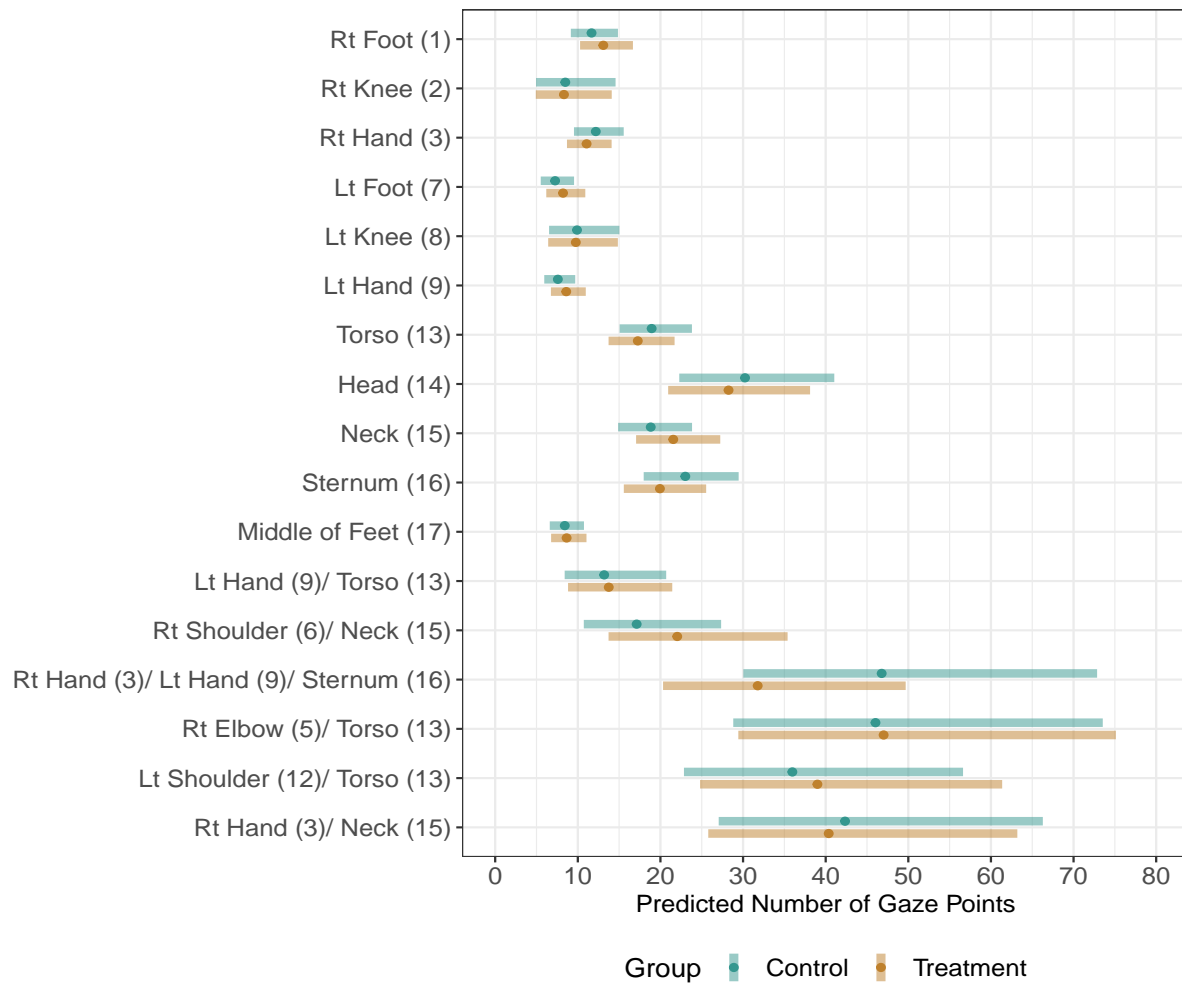


Fig. 3.8: Visual for EMM rate ratio pairwise comparison of predicted mean number of gaze points including 95% confidence intervals for Round 2 VT AOIs.

Table 3.14: Zero-Inflated Negative Binomial Multilevel regression estimated marginal mean gaze-point counts for each AOI by Group for Round 2 LRVT iteration

AOI Labels (Round 2)	Treatment (Trt)		Control (Ctl)		Trt vs. Ctl	
	Counts	CI (95%)	Counts	CI (95%)	RR	p-value
Rt Foot (1)	9.12	[7.17, 11.60]	8.57	[6.74, 10.91]	1.06	0.687
Rt Knee (2)	6.26	[3.56, 10.99]	6.25	[3.40, 11.50]	1.00	0.999
Rt Hand (3)	8.36	[6.52, 10.71]	11.08	[8.67, 14.17]	0.75	0.066
Lt Foot (7)	5.33	[3.96, 7.18]	4.85	[3.63, 6.48]	1.10	0.624
Lt Knee (8)	7.26	[4.71, 11.19]	7.36	[4.74, 11.43]	0.99	0.964
Lt Hand (9)	6.52	[5.06, 8.40]	5.73	[4.44, 7.39]	1.14	0.417
Torso (13)	10.88	[8.71, 13.61]	12.98	[10.40, 16.19]	0.84	0.207
Head (14)	17.39	[13.02, 23.23]	20.06	[14.96, 26.88]	0.87	0.443
Neck (15)	13.84	[11.05, 17.35]	13.22	[10.55, 16.58]	1.05	0.748
Sternum (16)	12.17	[9.56, 15.50]	16.03	[12.62, 20.36]	0.76	0.071
Middle of Feet (17)	6.68	[5.21, 8.57]	6.52	[5.10, 8.34]	1.02	0.877
Lt Hand (9)/ Torso (13)	13.66	[8.81, 21.18]	11.09	[7.03, 17.51]	1.23	0.483
Rt Shoulder (6)/ Neck (15)	14.36	[9.00, 22.92]	16.51	[10.25, 26.58]	0.87	0.653
Rt Hand (3)/ Lt Hand (9)/ Sternum (16)	24.53	[15.86, 37.94]	35.98	[23.40, 55.34]	0.68	0.175
Rt Elbow (5)/ Torso (13)	10.80	[6.79, 17.18]	12.14	[7.67, 19.21]	0.89	0.696
Lt Shoulder (12)/ Torso (13)	10.79	[6.87, 16.94]	10.22	[6.55, 15.94]	1.06	0.850
Rt Hand (3)/ Neck (15)	21.75	[13.99, 33.81]	33.14	[21.40, 51.31]	0.66	0.137
Outside Area	26.53	[21.59, 32.60]	22.38	[18.21, 27.50]	1.19	0.181

RR = Rate Ratio; *** $p < 0.001$; ** $p < 0.01$; * $p < 0.05$

The Round 2 LRVT findings, however, appear more contradictory. While the ZINB model Wald test indicates an overall significance for this model with a p-value of 0.0026 as seen in Table 3.6 and a significant AOI and Group interaction as shown in Table 3.5 with a p-value of 0.003, Table 3.14 shows a lack of significance for all pairwise AOI comparisons with no significant p-values supported by the overlapping confidence bands as shown in Figure 3.9. Table 3.14 shows that while two of the raw p-values approach significance for the Rt Hand (3) and Sternum (16) AOIs, none of the raw p-values are significant at the 0.05 level. While it appears that the Round 2 LRVT iteration shows that Group and AOI are significant in helping predict the gaze-point counts, this significance does not result in significant differences for specific AOIs for this iteration.

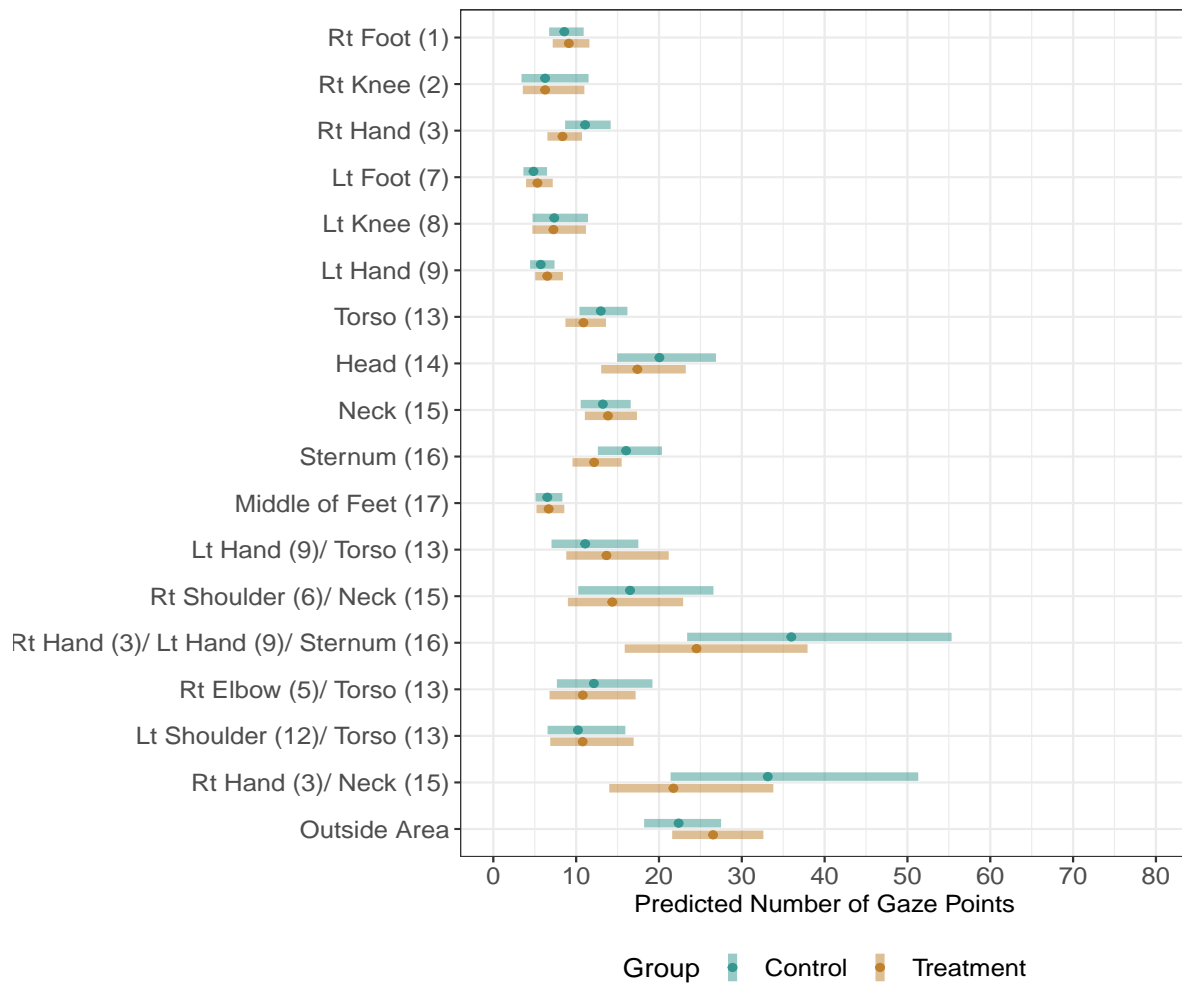


Fig. 3.9: Visual for EMM rate ratio pairwise comparison of predicted mean number of gaze points including 95% confidence intervals for Round 2 LRVT AOIs.

CHAPTER 4

Discussion

A goal of the USU Posture Study is to answer the question: “Does a person’s judgment of action capabilities of another person depend on personal knowledge and experience with human movement?” (Symanzik et al., 2018). This research looks specifically at the differences in gaze-point distribution from Treatment and Control participants in AOIs defined using a multilevel approach.

The Generalized Linear Mixed Effects Model (GLMM) framework handles multilevel data. Due to the count nature of the response variable (gaze points), we explored four generalizations: Poisson, Negative Binomial, Zero-Inflated Poisson, and Zero-Inflated Negative Binomial. Though Negative Binomial Regression is unable to converge, we are able to compare the model fits for the three remaining models and find that Zero-Inflated Negative Binomial Regression is the best fit for the data (see Table 3.1). The results for the Poisson and Zero-Inflated Poisson tests match the results from the single-level analyses. The p-values that describe the data as a whole for each iteration are highly significant with each iteration as seen in Table 3.6.

The results obtained from the Zero-Inflated Negative Binomial Regression model, however, do not match the results found in the other models. Here, the only significant AOI iteration is the Round 2 LRVT iteration with a p-value of 0.0026 and the p-values for the three other AOI iterations are non-significant as shown in Table 3.6. While the GLMM approach using the Zero-Inflated Negative Binomial Regression appears to be the most appropriate model to run on our data, we cannot definitely conclude that there is not enough evidence to suggest that the Group the participant belongs to (Treatment or Control) affects gaze-point counts. This conclusion cannot be drawn confidently because the level of significance is influenced by the way the gaze-point data is divided into areas of interest.

Looking at the inherent differences between the AOIs for each iteration of Posture ID 7 in Figure 2.18, it appears that the Round 2 LRVT iteration uses both smaller and fewer AOIs than the Round 1 VT and LRVT and Round 2 VT iterations. This can be

confirmed by comparing the Round 2 LRV T AOIs in Appendix B with the other AOI iteration visualizations. While it might be tempting to ignore the result from the Round 2 LRV T ZINB test and believe that there is not enough evidence to suggest that Treatment and Control participants look at these Posture IDs differently, the opposite might also be true. If the Round 2 LRV T eliminates a lot of the noise in the data and focuses on core points of a posture, this can result in a more meaningful focus on few specific AOIs than the results from the other three AOI iterations.

4.1 Conclusions

The variety of tests used are not definitive regarding the differences between how Treatment and Control participants judge the stability of a posture. It is inappropriate to confidently conclude that there is a generalizeable difference between Treatment and Control gaze-point distributions in the AOIs across the 22 Posture IDs. It is inappropriate to confidently conclude that the inverse is true. The findings appear to be largely dependent on two factors: how the AOIs are defined; and which regression generalization is applied. However, all the analyses agree that there are significant differences in gaze-point counts between AOIs regardless of participant group.

4.1.1 Defining AOIs

The significance values for the GLMM analyses show noticeable differences between the four AOI iterations. This suggests that results may vary based on how AOIs are defined. It is important to remember that the gaze-point locations do not change for any of these data iterations. The only thing that changes from one iteration to another is how the gaze points are classified or to which AOI each gaze point belong to. Seeing these differences between AOI iterations stresses the importance for researchers to select a proper method for defining their areas of interest.

The specific difference between the Round 2 LRV T AOI iteration and the others is noticeable in that there are very few AOIs and each AOI is also quite small. The Round 2 "Outside Area" AOIs typically contain 40 – 50% of the gaze points (see Appendix F). Noting this difference helps explain why the same gaze-point data categorized much differently than for the other three rounds can lead to a different result than for the other rounds.

4.1.2 Statistical Method Selection

The formal tests that provide meaningful results are the Poisson, Zero-Inflated Poisson (ZIP), and Zero-Inflated Negative Binomial (ZINB) GLMM approaches. While the ZINB model provides the best fit as shown by the low absolute values of the penalty criterion given in Table 3.1, the results for this analysis are not consistent across the four data iterations. While the majority of the data iterations do not provide significant p-values that would suggest that the Treatment and Control participants look at the stance of the stimulus subject differently, the fact that all other less-optimal tests and one AOI iteration from the ZINB model give highly significant p-values cannot be ignored. These drastic differences between these tests make coming to a definite conclusion about whether participants looked at the postures differently based on their prior yoga experience inappropriate.

One method that could be used in a future study to help with consistency of the results would be to use AOI labels more consistently. One complication in the analyses was the use of AOIs that combined two of the initial and main AOIs. The best way we found to handle these combined AOIs was not to arbitrarily divide the data into one of each original area, but to create a whole new area that was not connected across postures to either one or the other of the original areas. For example, the AOI Rt Knee (2)/ Rt Hand (3) is used in Posture ID 4 but does not appear in any other posture, and is not related to either the Rt Knee (2) or the Rt Hand (3) AOIs in the multilevel analyses. These combined AOIs also lead to the inconsistency of AOI appearances across the 22 postures as shown in Tables 3.3 and 3.4. If the AOIs that overlap are systematically selected as only the body part that is visible to the participant, this could lead to more consistent results.

Poisson, Negative Binomial, ZIP, and ZINB GLMMs

The Poisson, Negative Binomial, Zero-Inflated Poisson, and Zero-Inflated Negative Binomial GLMMs account for data in its natural multilevel framework and properly account for participant-to-participant differences and Posture ID-to-Posture ID differences as described in Section 2.3.3. The Negative Binomial model is unable to converge. The Poisson and ZIP models show an overall high level of significance ($p\text{-value} < 2e^{-16}$) for the Group, AOI, and Group \times AOI interaction fixed effects in determining the gaze-point counts for all AOI iterations as shown in Table 3.6. The application of the Zero-Inflated Negative Bino-

mial model shows that the effect of AOI (and not the Group \times AOI interaction) is highly significant.

Because the ZINB model shows the best overall fit, we run this model with and without the interaction for all AOI iteration,s and find that the interaction is only significant for the Round 2 LRVT iteration (see Table 3.5). The model without the interaction is used for interpretation when it is not significantly different from the model with the interaction. For Round 1 VT, Round 1 LRVT, and Round 2 VT iterations, we learn that while there is no significant gaze-point count differences from Treatment and Control Groups as a whole, there are highly statistically significant gaze-point count differences between the AOIs as shown in Table 3.6. This is consistent with the visual assessments of the proportional bar charts for each Posture ID given in Appendix F as Figures F.1 - F.44.

While the Round 2 LRVT data iteration shows significance for the model with the interaction term (see Table 3.5), this does not translate into any significant pairwise comparisons of gaze-point counts for Treatment and Control Groups within each AOI as seen in Table 3.14. Overall, it appears that while we do not have enough evidence to suggest that the Group main effect or the interaction of Group and AOI main effect are significant, all analyses point to a high level of significance for the AOI main effect. This means that there is evidence to suggest that the gaze-point differences between AOIs (from at least one AOI) are significant. Interpretation of which AOIs show significant differences can be drawn from the results in Tables 3.7 - 3.10. Notably, it appears that most participants give more attention (gaze points) to the Torso (13) when compared to the other AOIs that also appear in most Posture IDs for the Round 1 AOI iterations. The Round 1 iterations also show a particularly high mean gaze point for AOI Rt Hand (3)/ Lt Hand (9) (see Figures 3.6 and 3.7. This AOI only occurs in Posture ID 15 which when looking at Figure F.29 is positioned on top of the torso. The Round 2 iterations show that in addition to the torso, the head, neck and sternum AOIs give higher counts than the extremities (middle of feet and right or left foot, knee, and hand) as shown in Figures 3.8 and 3.9. This suggests that participants pay more attention (more gaze points) to the general center of mass than extremities when judging the stability of a posture.

4.2 Outlook

Taking an AOI approach to analyzing eye-tracking data is advantageous for data comparisons because it can not only tell if there are differences between subjects, but where those differences occur. A systematic approach to defining AOIs is especially important when the stimulus used is a continuous static stimulus (person) and the AOIs break up the continuous stimulus (parts of the body) as is the case with the USU Posture Study. The LRVT method for defining AOIs is unique in that it systematically creates the AOIs by drawing tessellations that represent midpoint lines between each of the AOI centers unless those tessellations fall outside of a given maximum radius in which case a circular area limits the extent of the AOI. While systematic, this approach gives the researcher the flexibility to define the AOI centers and define the maximum radius of each AOI.

The extreme the differences between the Round 2 VT method and Round 2 LRVT method (see Table 3.6) suggest that limiting the radius of an AOI makes a considerable difference in the classification of eye-tracking data. In terms of the particular methods chosen to define the AOIs, it is important to note that the LRVT method has an infinite number of possible AOI definitions for any set of AOI centers because the radius of the AOIs are selected by the researcher. We used the calibration data of the USU Posture Study to determine percentiles of gaze-point distances from a point center and selected the 90th percentile as the maximum radius for our LRVT AOIs as discussed in Section 2.2.4. Had we selected a larger radius such as the 95th or 99th percentile depicted in Figure 2.10, we suspect results would have more closely resembled the VT analyses. In the future, researchers should select a radius based on an understanding of the gaze-point variation that occurs when subjects are asked to look at a particular point on an image. If eye-tracking hardware records gaze points that have less variation around a defined point (if the eye-tracking hardware provides more precision), it would be appropriate to use smaller radii. As for the exact choice of a maximum radius in future studies, it is ultimately up to the researcher as long as there is an understanding of and use of margins of error provided from calibration data. The use of AOIs defined by the LRVT method reinforces the importance for eye-tracking studies to include a calibration component to understand the variance of the plotted gaze points. Future studies could use different percentiles to define the limited radius of LRVT AOIs and compare results.

The definition of AOIs in Rounds 1 and 2 should also be carefully considered in future

analyses. In this study, the Round 1 AOI centers were selected based on joints, the head, and the torso. Round 2 AOI centers were selected after understanding both the margin of error for gaze points and based off the combined gaze-point data for the Treatment and Control groups that were already collected. This approach for Round 2 not only further disconnected the AOIs being defined consistently across the 22 postures, it created a reversed approach to proper research methods. Future analyses may choose more than one approach to defining AOI centers, but all AOI centers should be defined before the data is collected and viewed.

Visualizing the difference in a defined area based off of the AOI iteration adds validity to the preference of the Limited Radius Voronoi Tessellation method over the Voronoi Tessellation method. Figure 2.18 shows AOIs 3 and 9 in all four AOI iterations for Posture ID 7. The LRVt iterations show that gaze points falling into any part of these areas can more intuitively be classified as belonging to the right and left hand than the VT counterparts. The LRVt method is the most appropriate systematic method for defining AOIs for continuous static stimuli if it is viewed as more important to reduce the noise at the expense of losing some of the gaze points that may belong to an area that falls outside the defined radius.

Future eye-tracking studies that hope to analyze differences between groups using the AOI approach on a static continuous image can define AOIs using both VT and LRVt methods. The VT method is useful if a researcher wants to ensure that no gaze points on the image of interest get classified as “Outside Points” as is seen to be the case for some LRVt gaze points in this study (see Figure 2.18) and the LRVt method is useful in limiting and specifying an area which eliminates a lot of noise. Eye-tracking studies that use the human body as a continuous image should consider implementing VT and LRVt methods to define AOIs. The possibilities of studies that use eye-tracking data to understand how a particular group of people look at a continuous image differently are endless and these methods give a great framework for classifying gaze points using areas of interest.

While we do not find meaningful pairwise differences between Treatment and Control participants in any given AOI for a given round of AOI defined centers, knowing that the AOI labels are not consistently included in all Posture IDs influences the interpretation of any significant findings. An AOI that appears in fewer Posture IDs may be more sensitive to differences in gaze-point proportions from participant Groups because the AOI occurrence

is rare. Future studies using a series of images should consider exclusively defining AOIs that appear in each image to reduce the chance of observing a falsely significant pairwise comparison. The decision to combine area labels for some AOIs complicates the analysis as well. Posture ID 8 includes an area labeled “Rt Hip (4)/ Lt Hand (9)” in the Round 1 AOI centers. The gaze points contributed in this area could not be analyzed in conjunction with the “Rt Hip (4)” or “Lt Hand (9)” AOIs individually even though this combined AOI is clearly related to those individual AOIs. Perhaps choosing the area most visible (“Lt Hand (9)” in this instance) would be a more appropriate method in future analyses (see the far right image in Figure 2.9).

Future posture studies could include different levels of exposure to knowledge and experience with human movement. Our guideline for dividing students into the Treatment and Control groups was that the Treatment participants reported having practiced yoga at least twice a week for at least the three months prior to the study. Those in the Control group were students that did not meet the criteria for the Treatment group. The distinction between participants with two months vs. four months of yoga experience seems nearly trivial however. Future researchers could create a greater distinction in the two groups if they required Treatment participants to have the same minimum experience, but the Control group to be students that had no experience with yoga. It would also be interesting to use more than two groups and include samples of participants with varying levels and types of experiences of human movement. For example, it would be interesting to take a sample of physical therapists, exercise instructors, swimmers, and kinesiologists in addition to those who practice yoga and a Control group to see which, if any, of these specialists judge the stability of a posture differently. This research could also be extended to dynamic stimuli. If participants were not asked to judge how long a posture could be held, it would be interesting to see how those with knowledge of human movement might study a video of a person engaging in different levels of human movement.

Another extension to this research could include using different stimulus subjects to see how body type, gender, and other factors affect how participants judge posture stability. Researchers could explore gaze-point differences within and between participant groups when judging stability of the same posture depicted by different stimulus subjects.

There are other USU Posture Study analyses pending related to the actual stability

of the participant. The participants stood on a force plate while studying the postures and rating the stability of the actor in the posture. The pending analyses using the USU Posture Study data will compare the participants' own stability with the rating of stability that the participant gives the stimulus subject in each Posture ID. The question of interest here will be "Does a person that is more stable judge others to be more (or less) stable?". A recent analysis used a modified Syrjala test to analyze the full gaze-point distribution for Treatment and Control participants (McKinney and Symanzik, 2019, 2021).

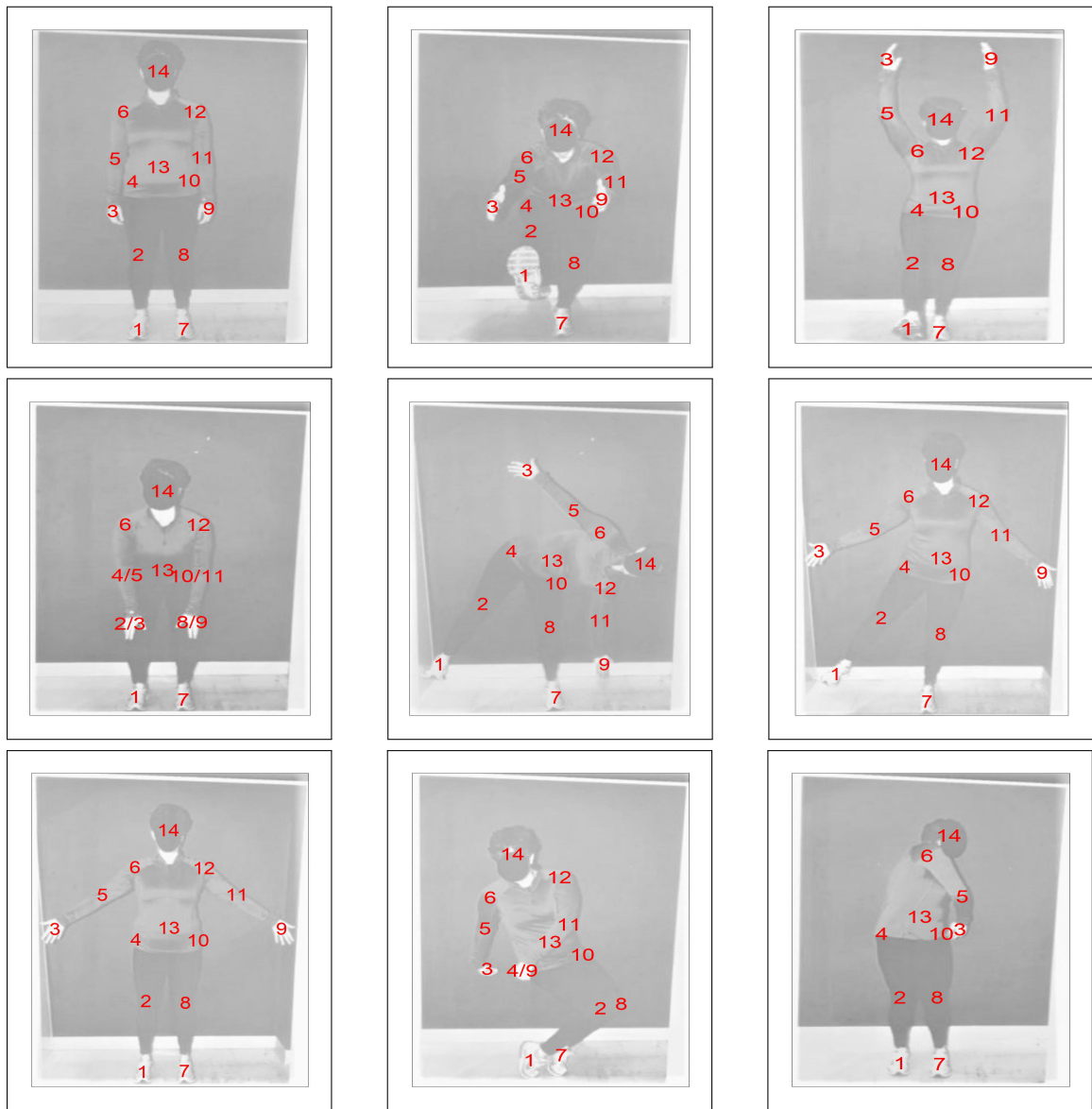
Overall, there are a variety of settings the methods used in this study could be applied to future eye-tracking studies. When using AOIs, it is important to use a systematic method that is appropriate for classifying AOIs for the observation stimulus. The VT and LRVT methods are great for continuous static images. Future analyses that use both would add to the knowledge of these AOI classification methods since the outcomes of our analyses are mixed. The VT method is better if a researcher wants to include all possible gaze points related to an AOI where the LRVT method is preferable if the goal is to eliminate as much noise in the data as possible and if the researcher is interested in the points that are most precisely located near the defined AOIs. Using these AOI classification methods side-by-side would be advantageous to gain more insight about the comparison of these classification methods. Future analyses can also study how radius selection for LRVT AOI affects results. Studies that use a series of images should consider defining areas that appear consistently in each image. Posture studies could be extended in the future by adding levels to the grouping factor for those with different types of experience with human movement. There are a variety of meaningful ways this research can be extended.

APPENDICES

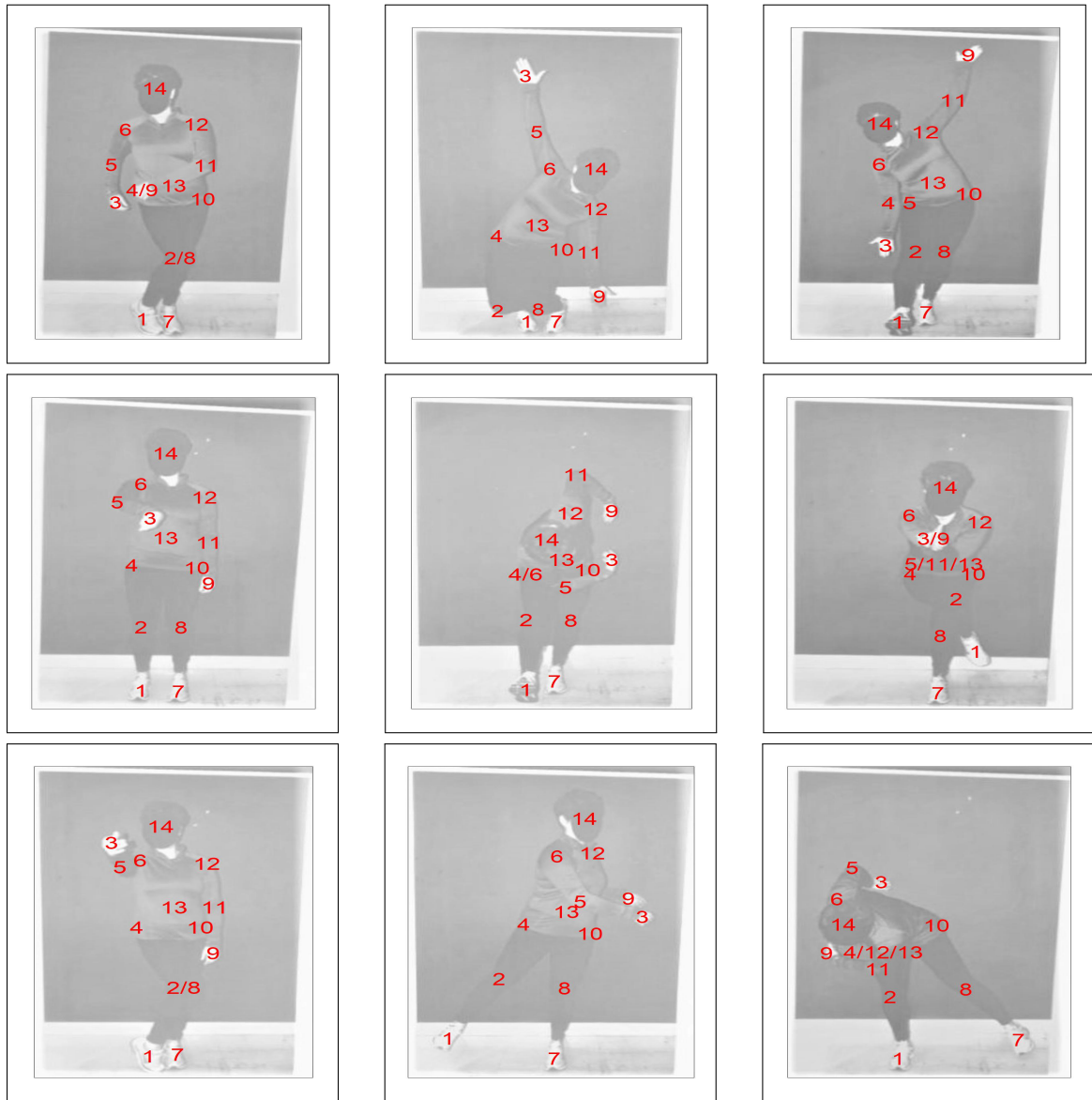
APPENDIX A

Visualizations for AOI Centers

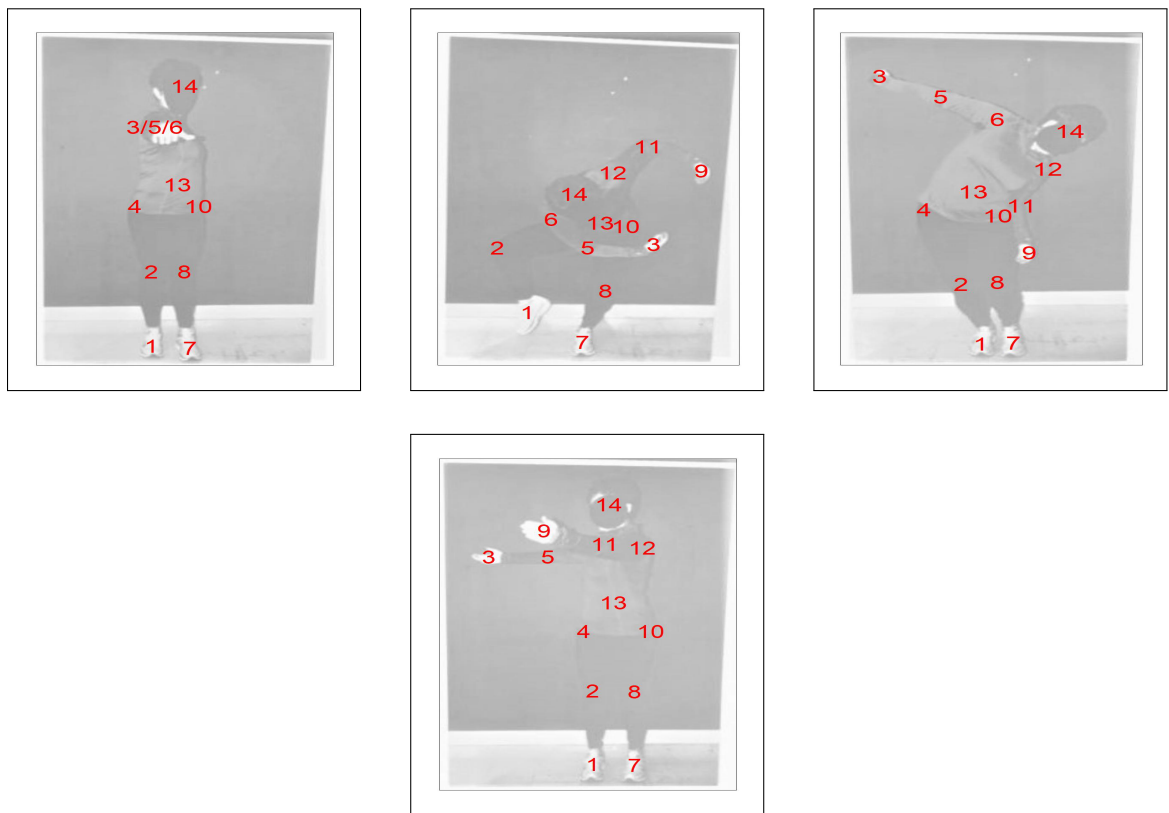
Figure A.1 shows the first round (Round 1) of AOI centers defined by our kinesiology expert for Posture IDs 1-22. The philosophy driving the defined centers for these postures is described in Section 2.2.1.



(a) Posture IDs 1-9 (from Lt to Rt: first row 1-3; second row 4-6; third row 7-9) with Round 1 AOI labels.



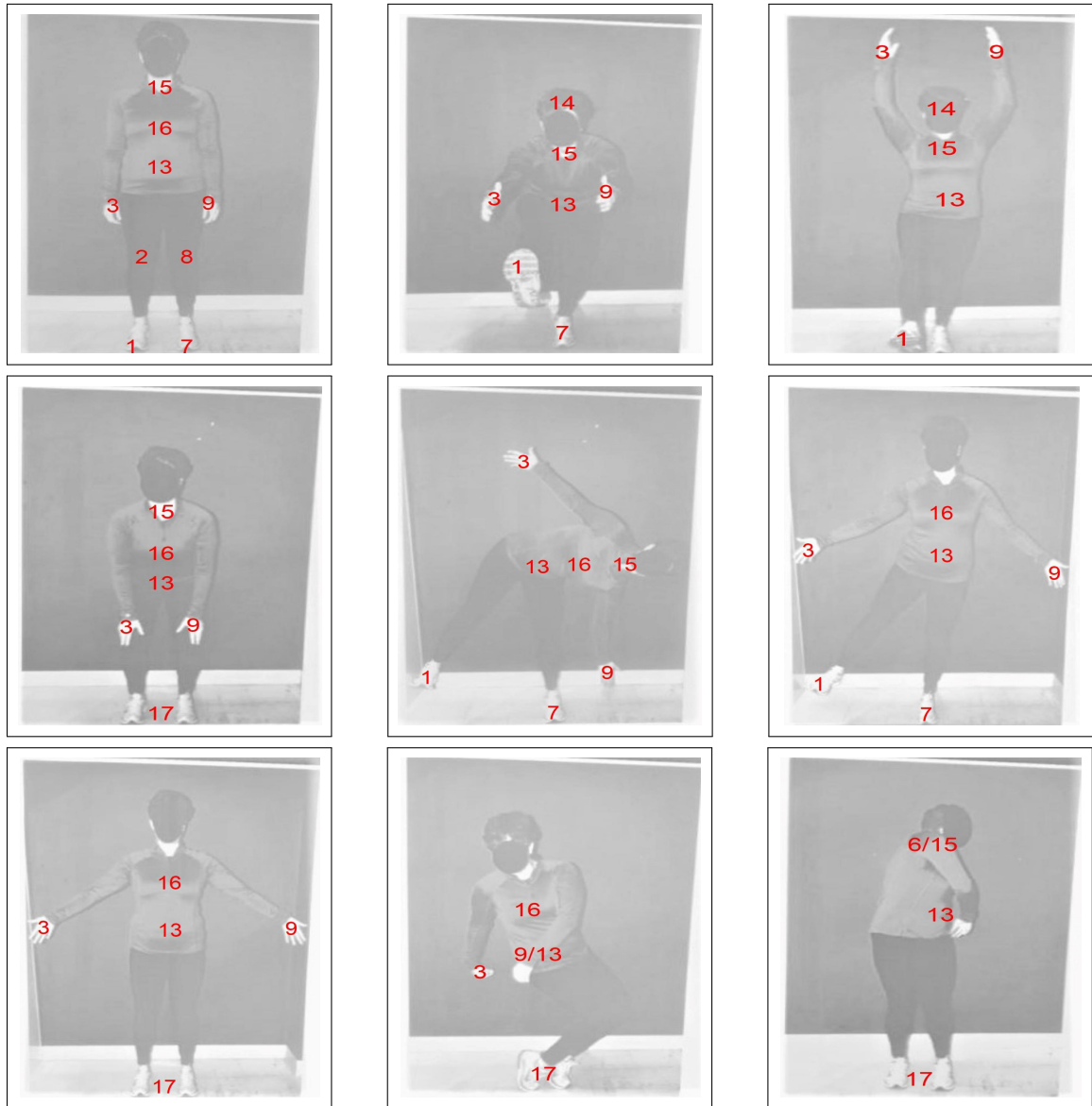
(b) Posture IDs 10-18 (from Lt to Rt: first row 10-12; second row 13-15; third row 16-18) with Round 1 AOI labels.



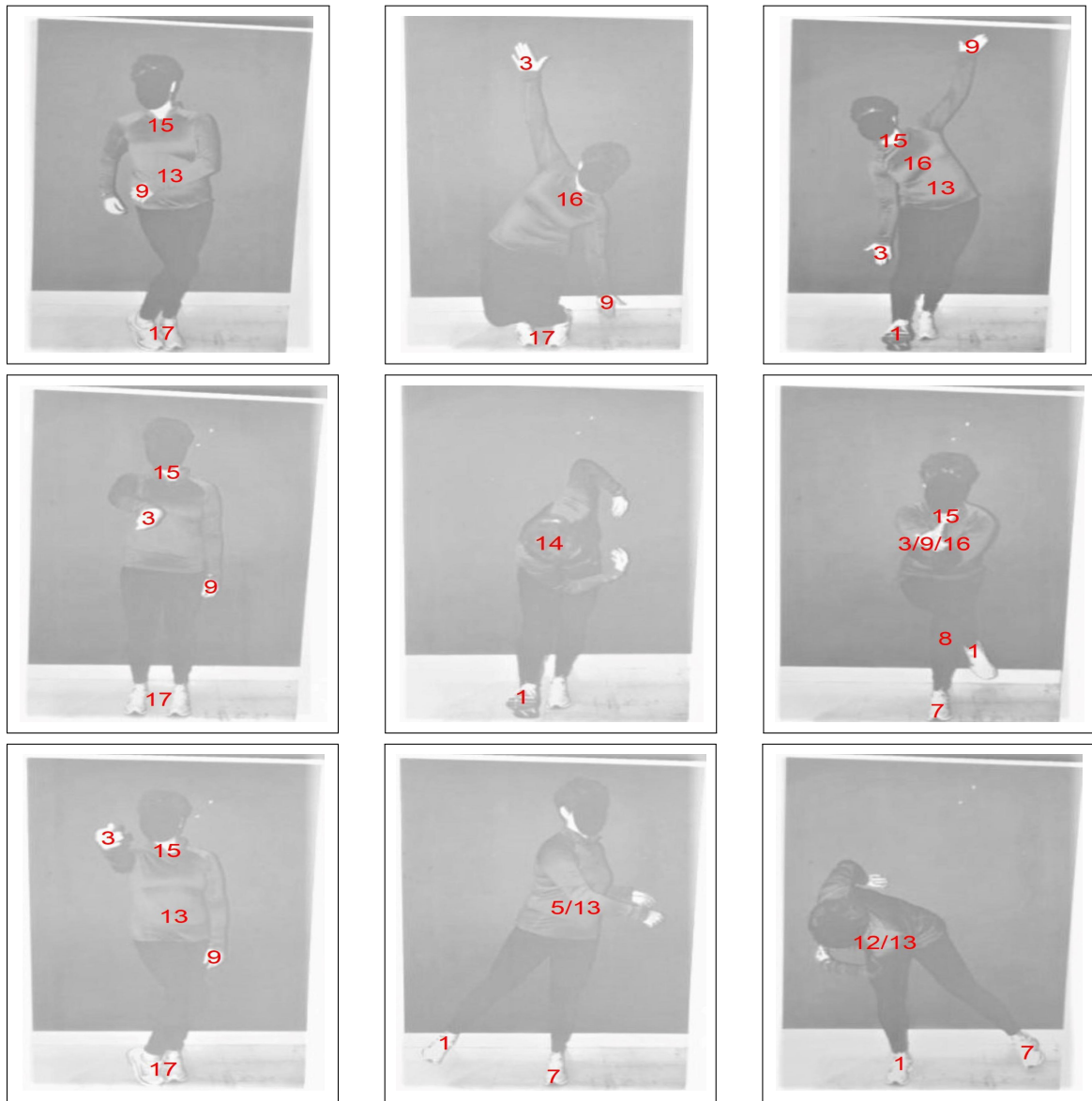
(c) Posture IDs 19-22 (from Lt to Rt: first row 19-21; second row 22) with Round 1 AOI labels.

Fig. A.1: Round 1 AOI labels.

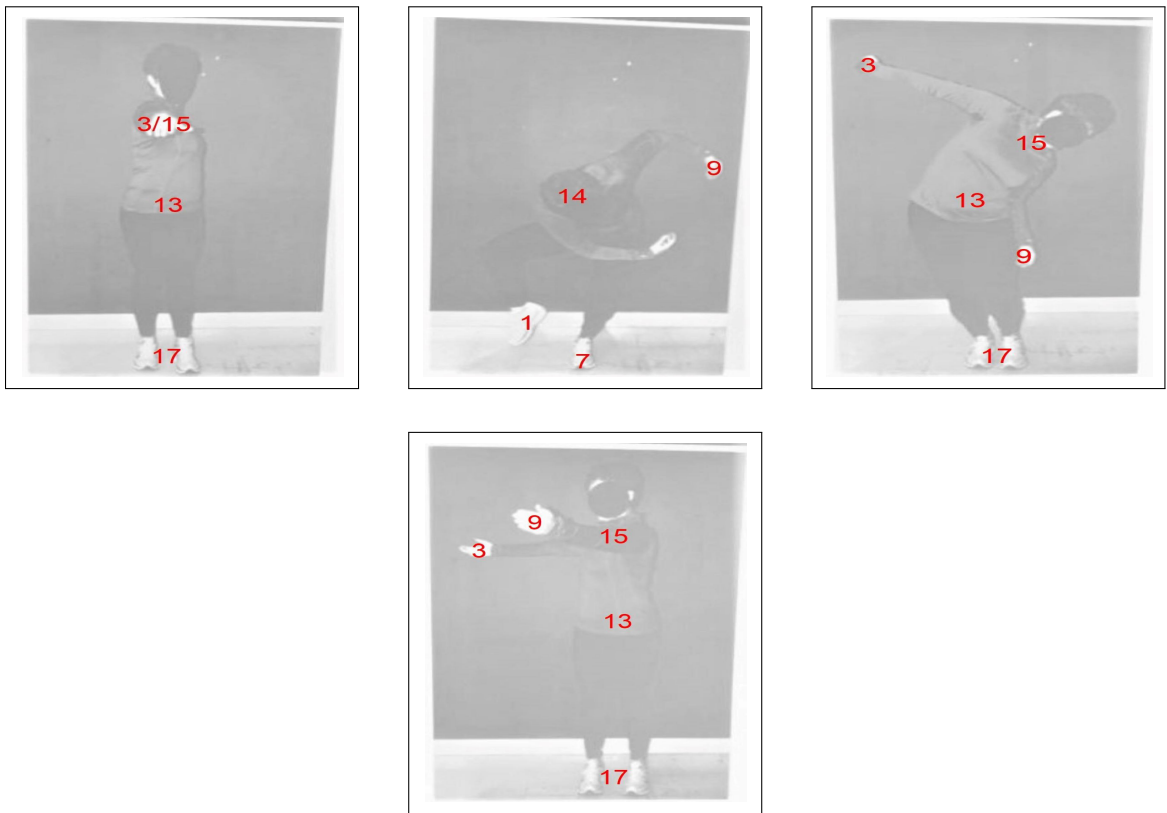
Figure A.2 shows the second round (Round 2) of AOI centers defined by our kinesiology expert for Posture IDs 1-22. The philosophy driving the defined centers for these postures is described in Section 2.2.2.



(a) Posture IDs 1-9 with Round 2 AOI labels. The ordering of the Posture IDs matches the ordering of the postures in Figure A.1.



(b) Posture IDs 10-18 with Round 2 AOI labels.



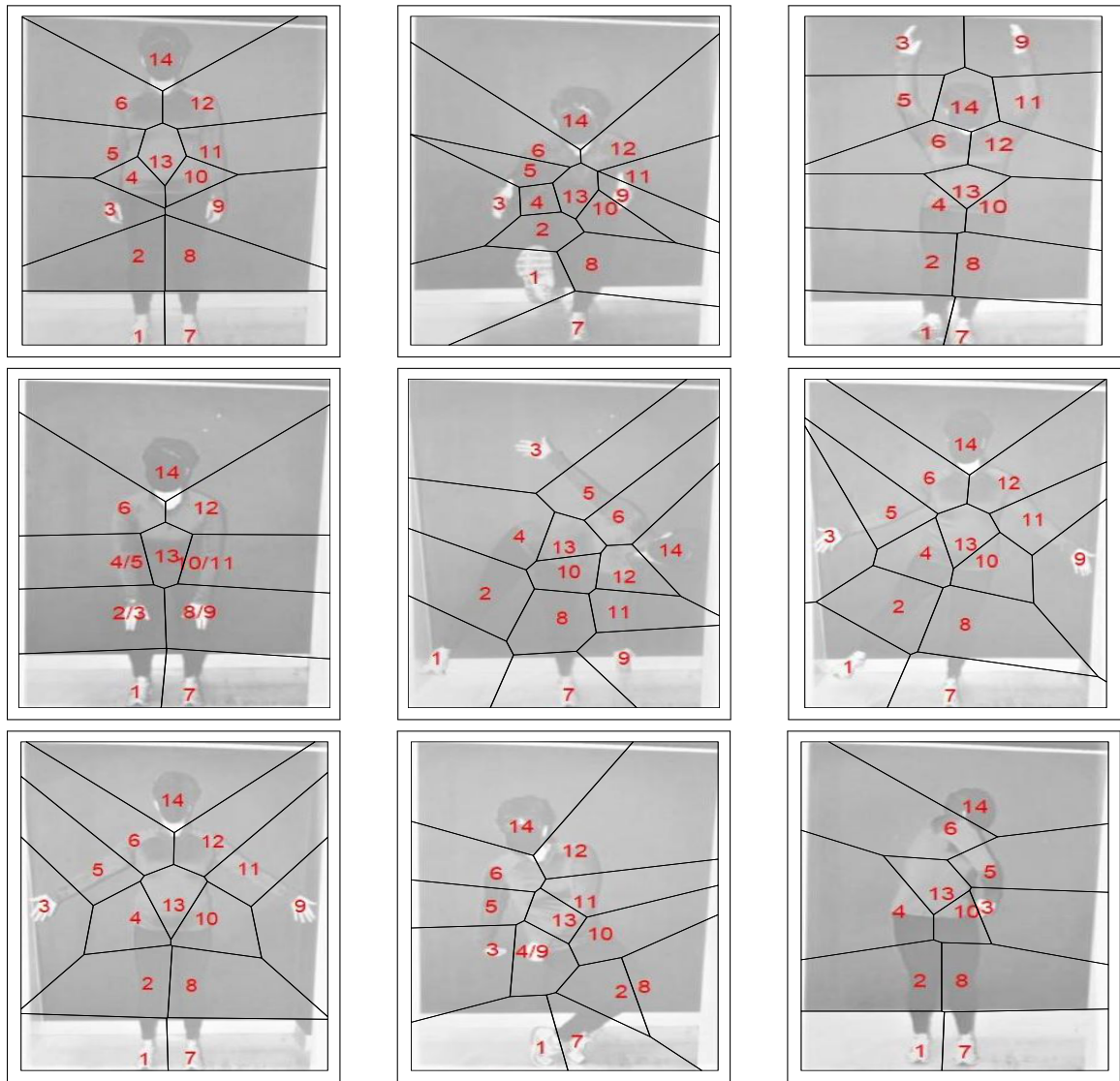
(c) Posture IDs 19-22 with Round 2 AOI labels.

Fig. A.2: Round 2 AOI labels.

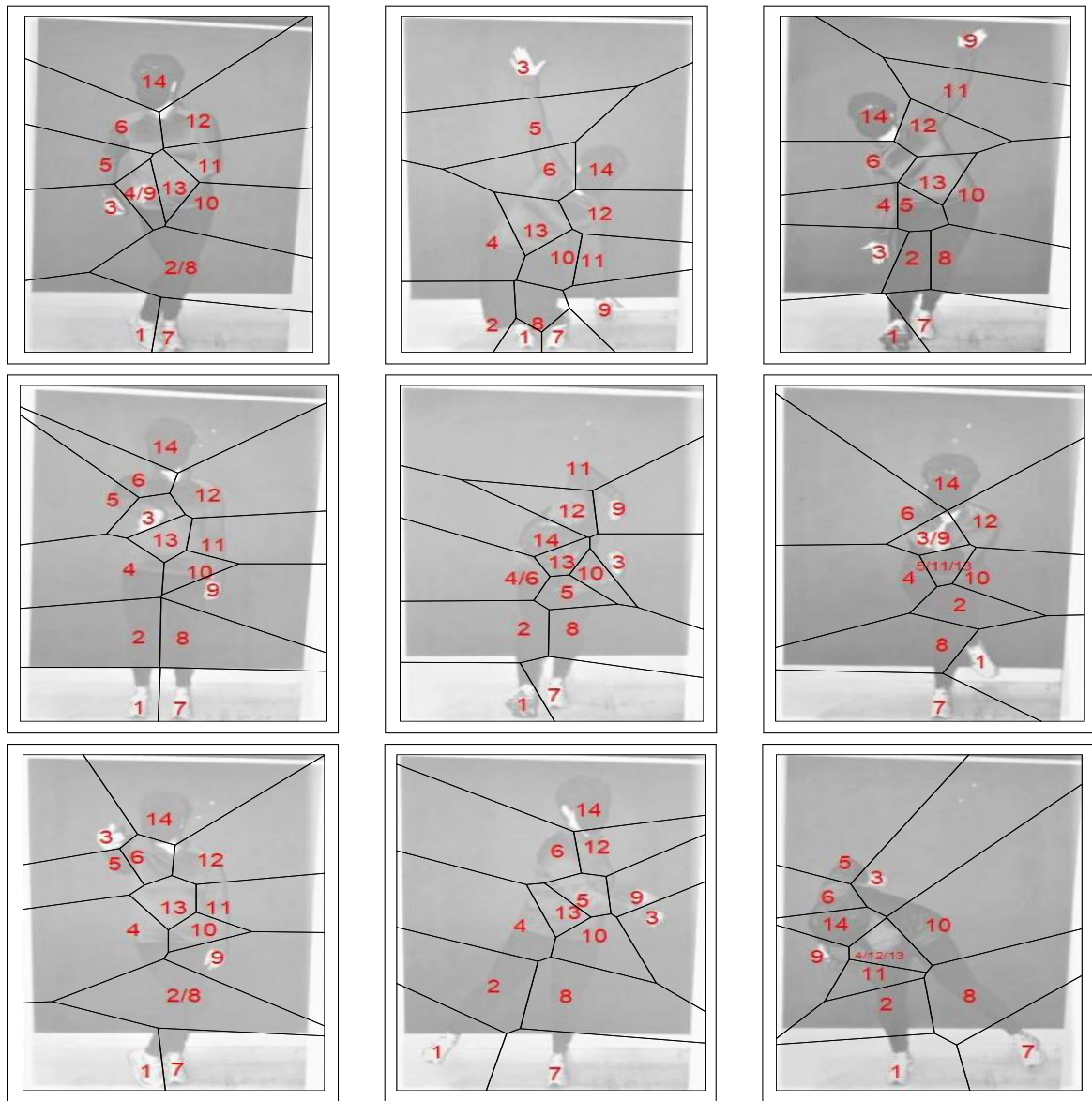
APPENDIX B

Visualizations of Round 1 VT, Round 1 LRVT, Round 2 VT, and Round 2 LRVT AOIs

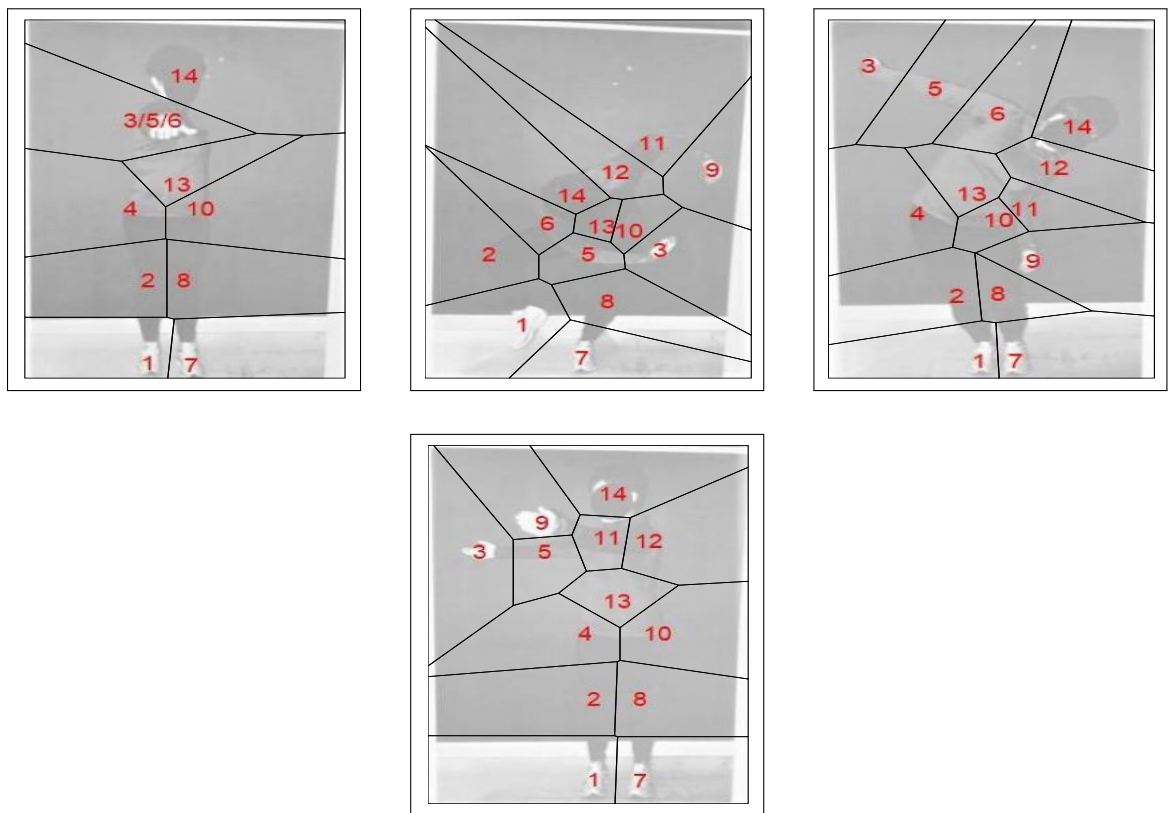
Figure B.1 shows Voronoi Tessellations applied to Round 1 AOI centers for Posture IDs 1-22. These are VT Round 1 AOIs. The explanation of the Voronoi Tessellation method is given in Section 1.2.1 and applied to these postures in Section 2.2.3. The order of the Posture IDs is the same as the postures in Appendix A.



(a) Posture IDs 1-9 with Round 1 VTs.



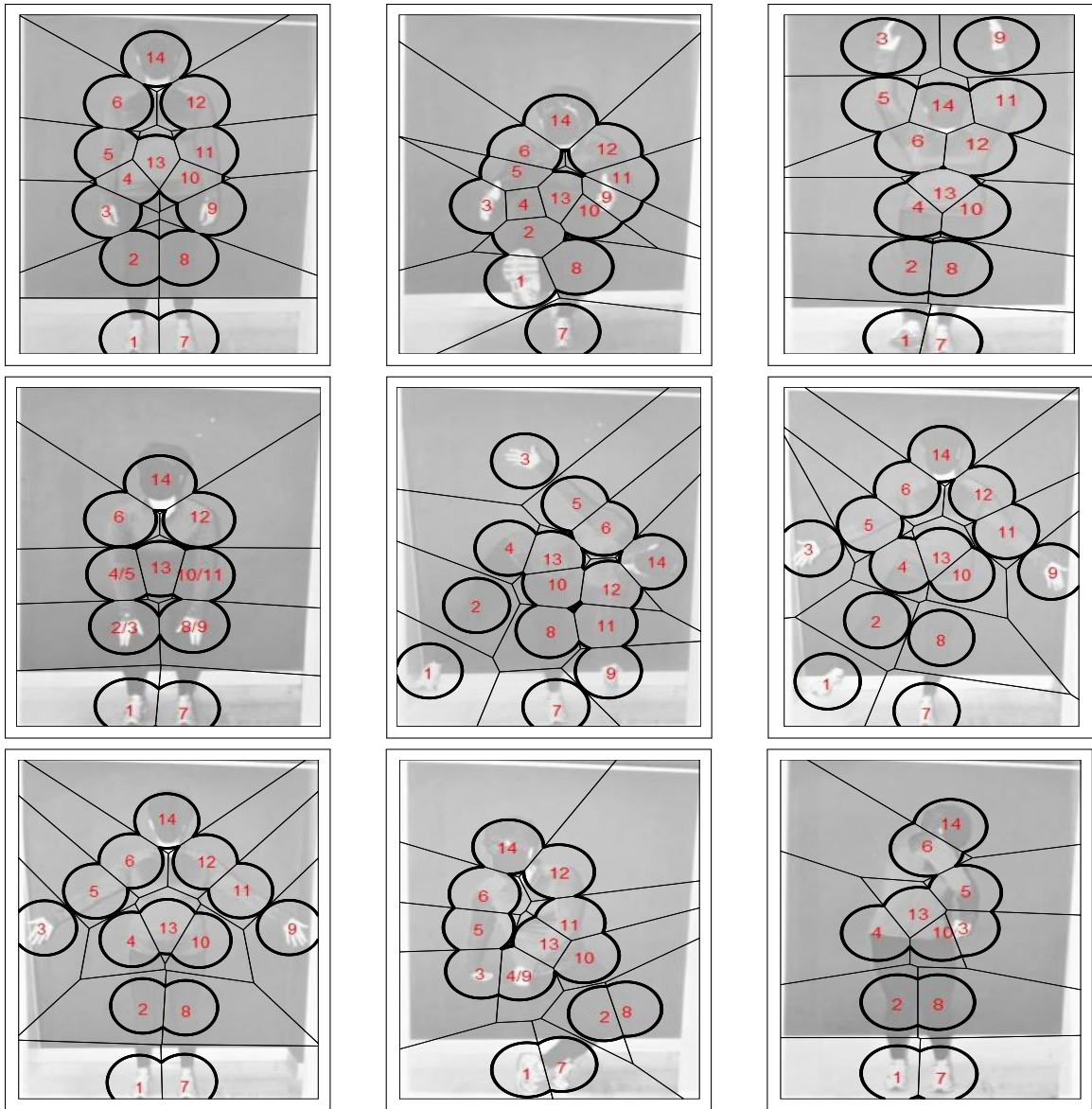
(b) Posture IDs 10-18 with Round 1 VTs.



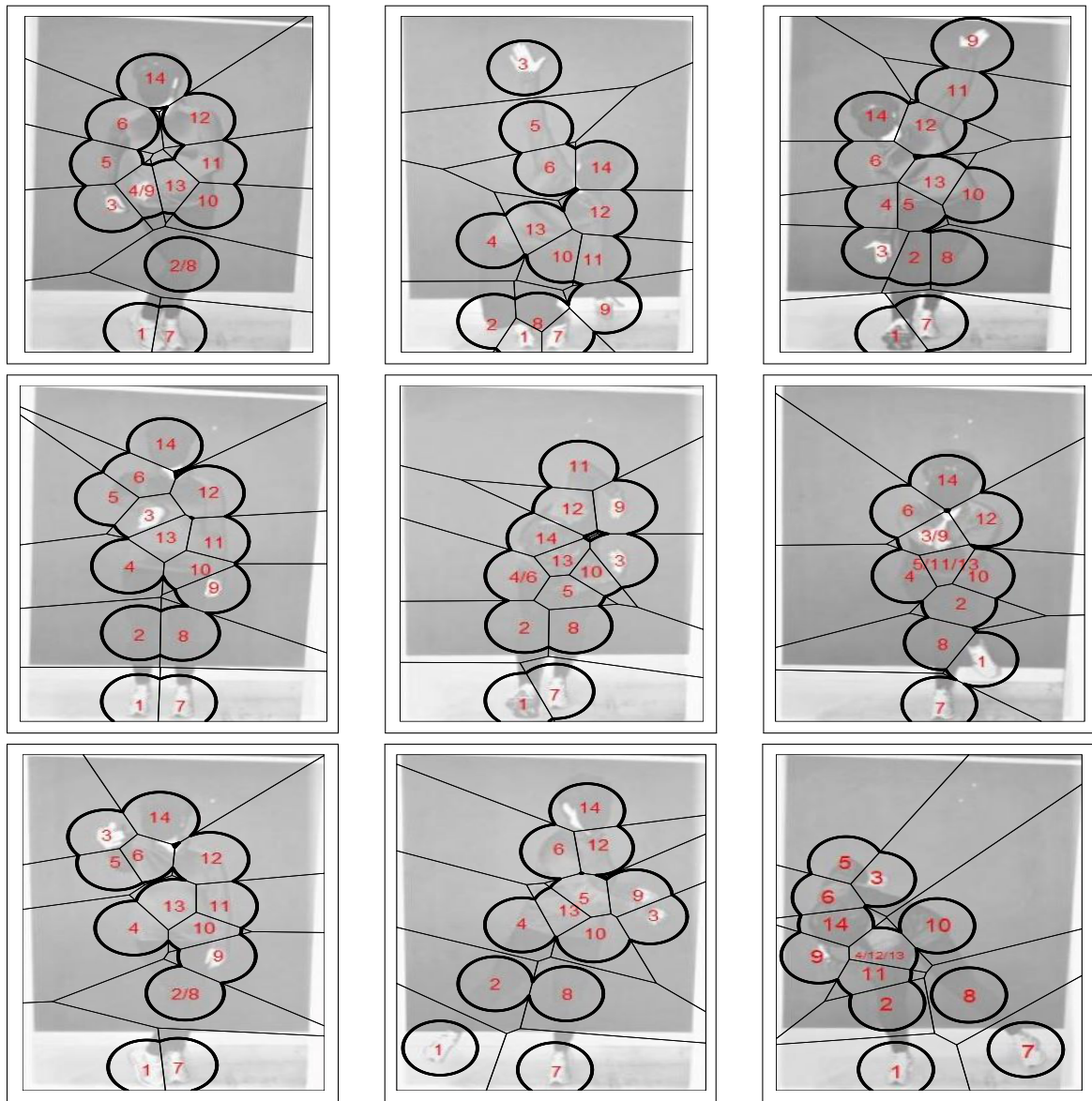
(c) Posture IDs 19-22 with Round 1 VTs.

Fig. B.1: Round 1 VT AOIs.

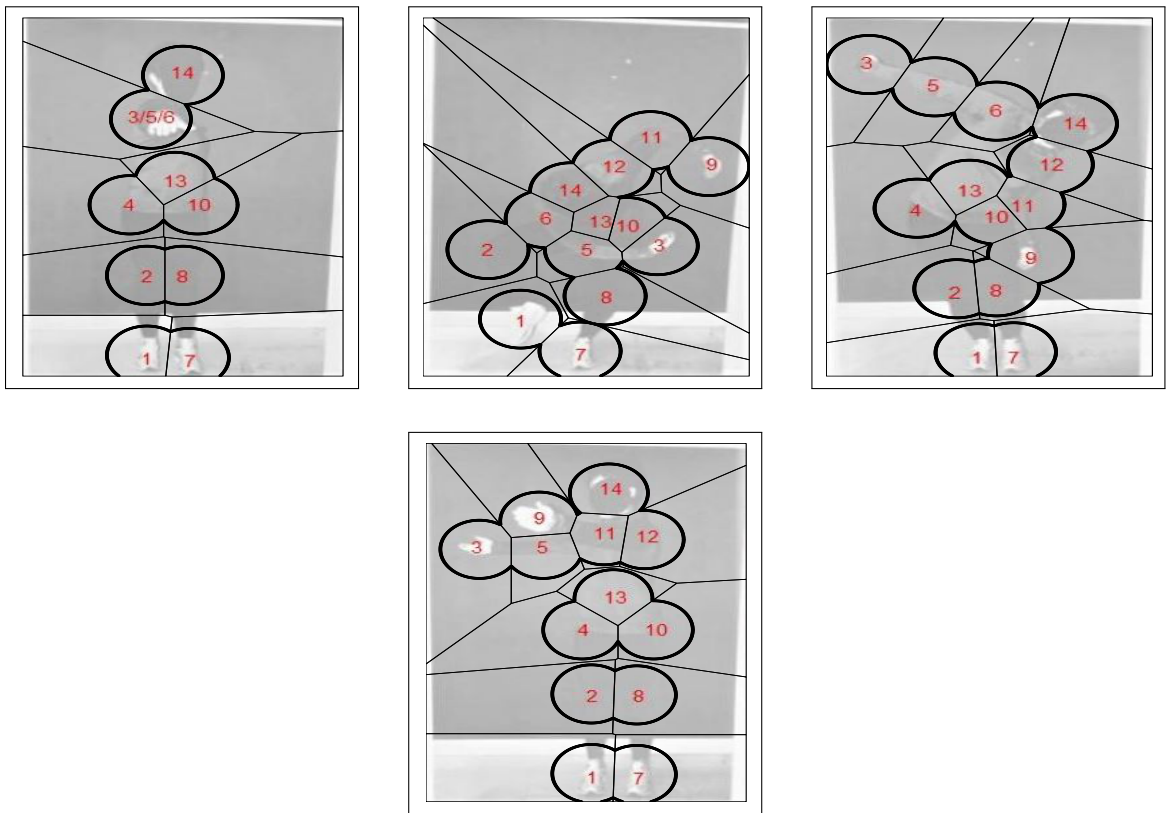
Figure B.2 shows Limited-Radius Voronoi Tessellations applied to Round 1 AOI centers for Posture IDs 1-22. These are LRVT Round 1 AOIs. The explanation of Limited-Radius Voronoi Tessellation method is given in Section 1.2.1 and applied to these postures in Section 2.2.4.



(a) Posture IDs 1-9 with Round 1 LRVTs.



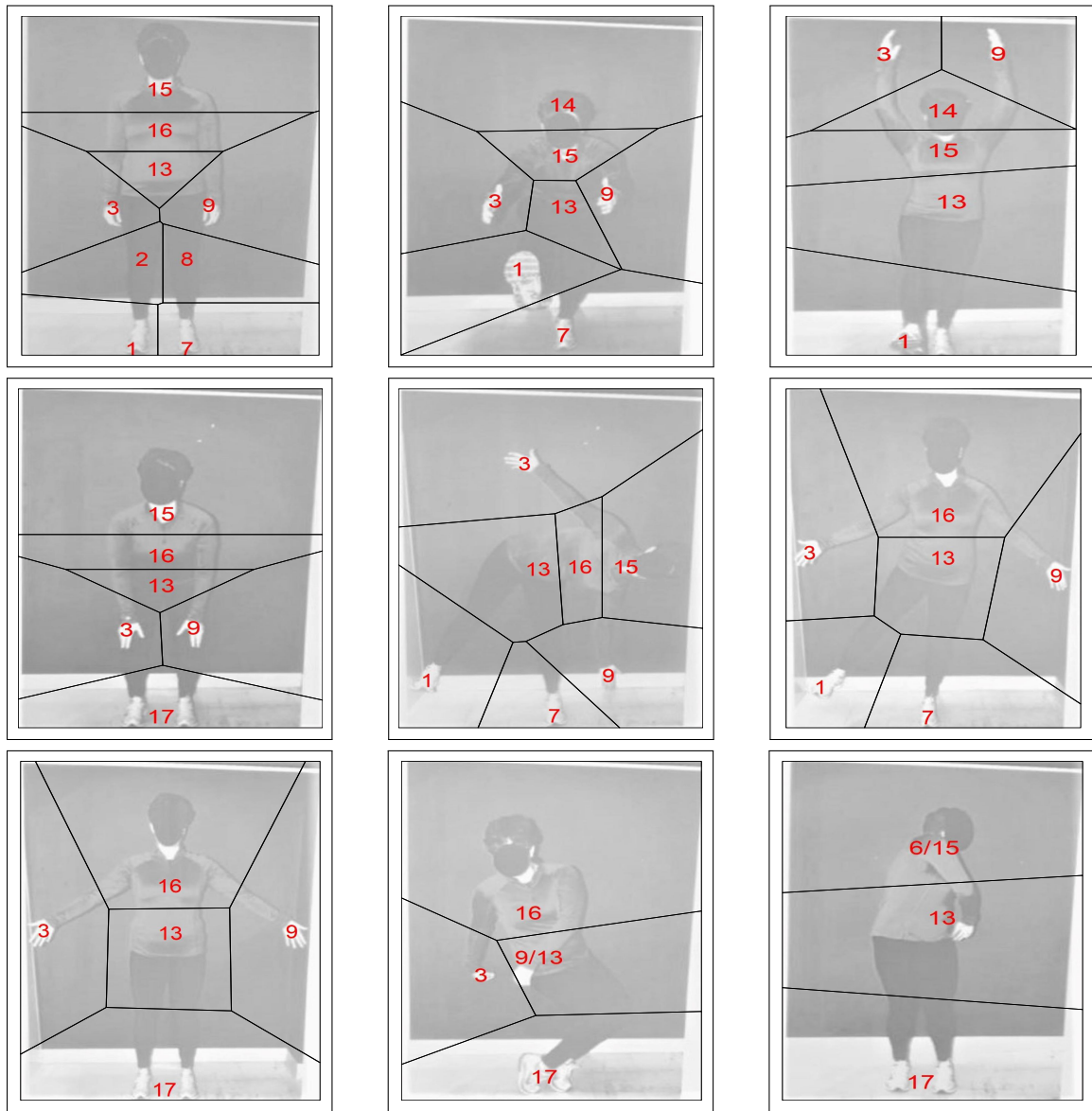
(b) Posture IDs 10-18 with Round 1 LRVTs.



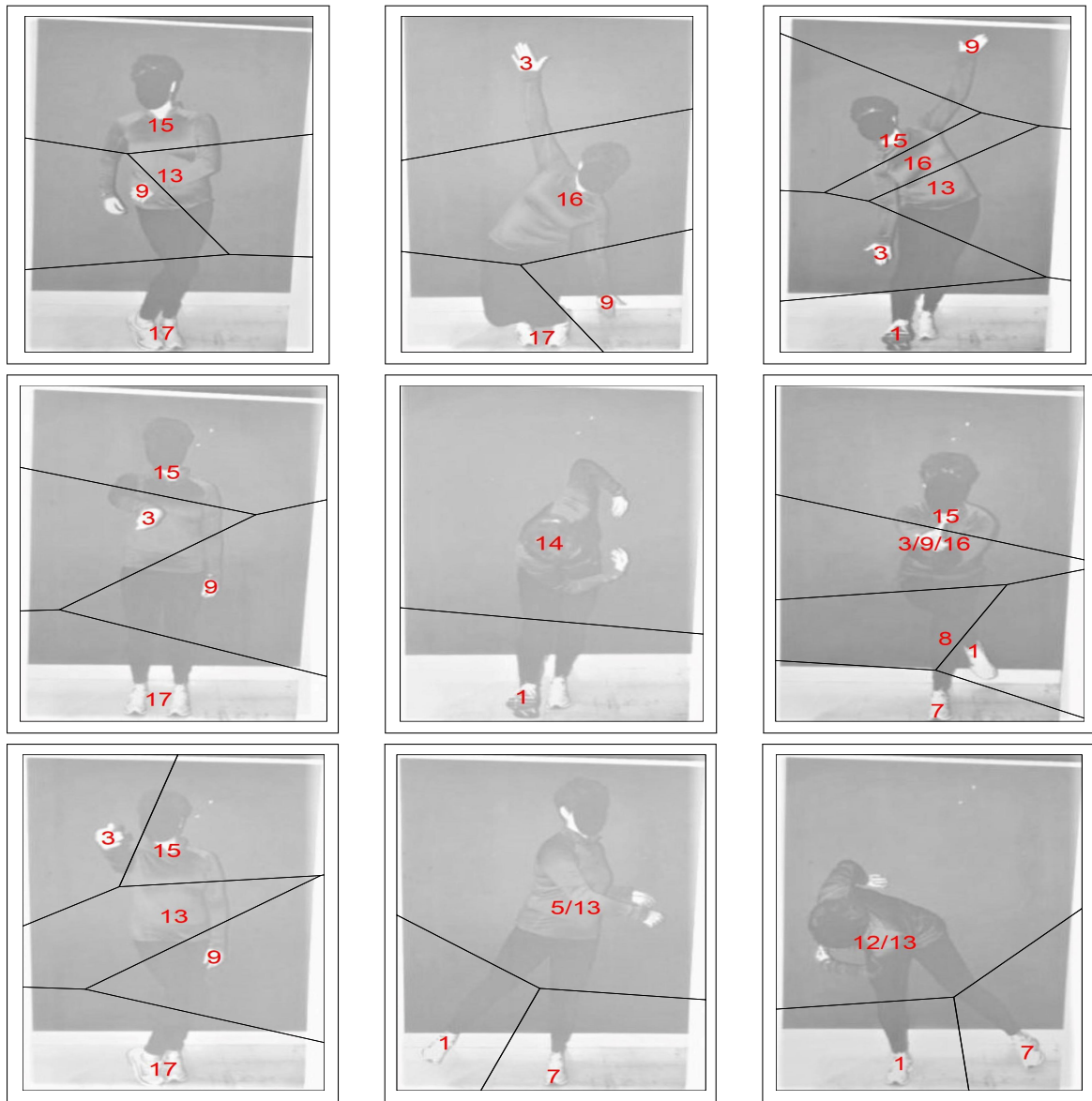
(c) Posture IDs 19-22 with Round 1 LRVTs.

Fig. B.2: Round 1 LRVT AOIs.

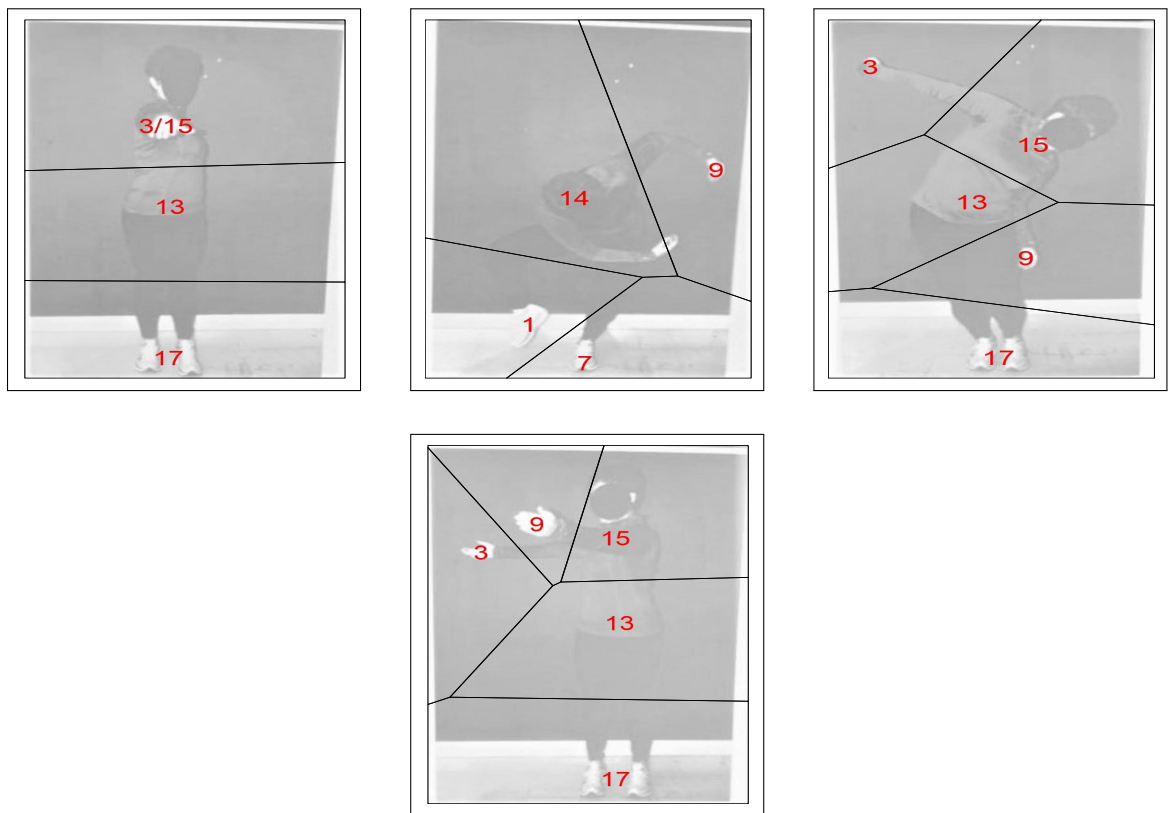
Figure B.3 shows Voronoi Tessellations applied to Round 2 AOI centers for Posture IDs 1-22. These are VT Round 2 AOIs. The explanation of Voronoi Tessellation method is given in Section 1.2.1 and applied to these postures in Section 2.2.3.



(a) Posture IDs 1-9 with Round 2 VTs.



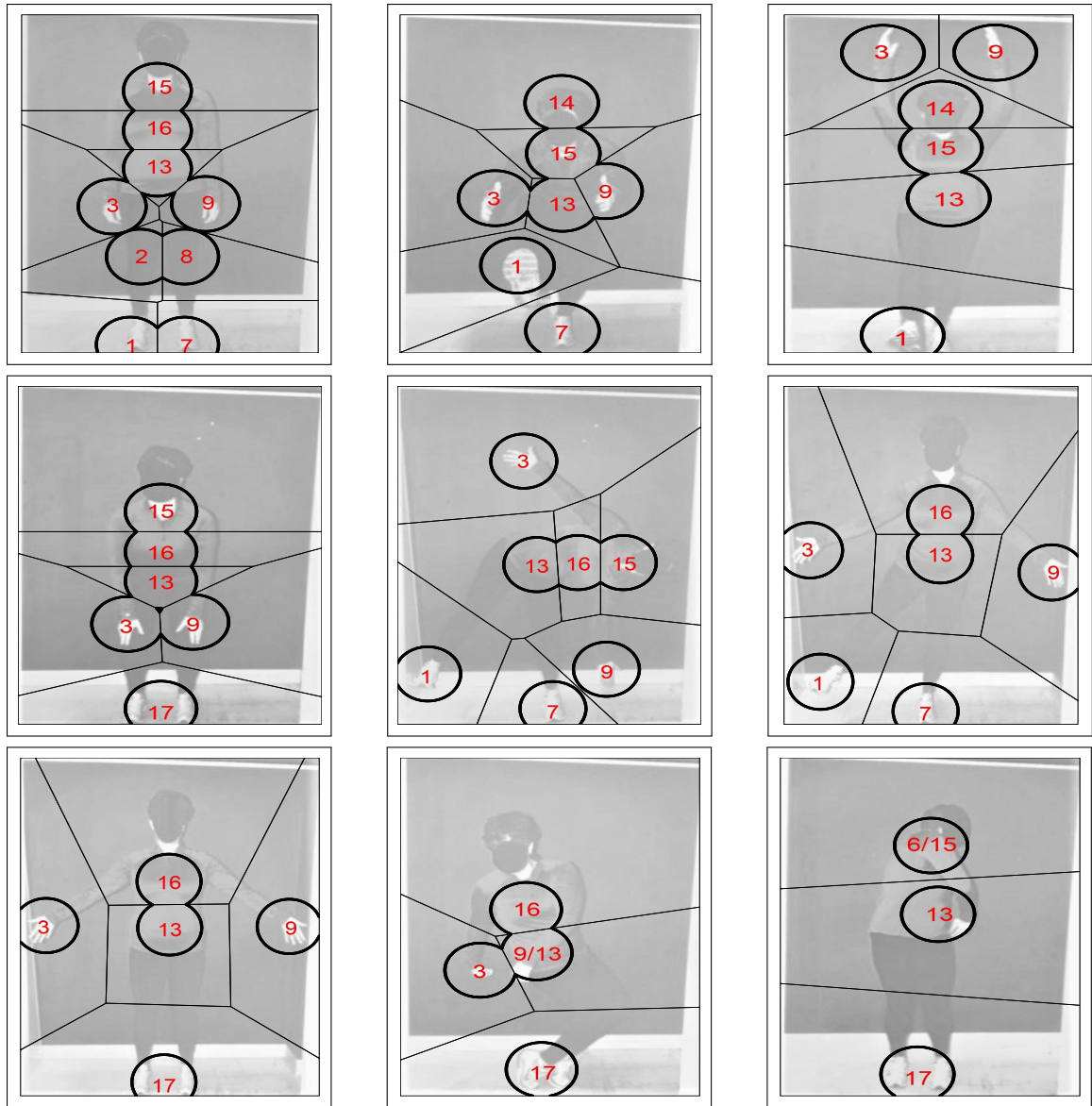
(b) Posture IDs 10-18 with Round 2 VTs.



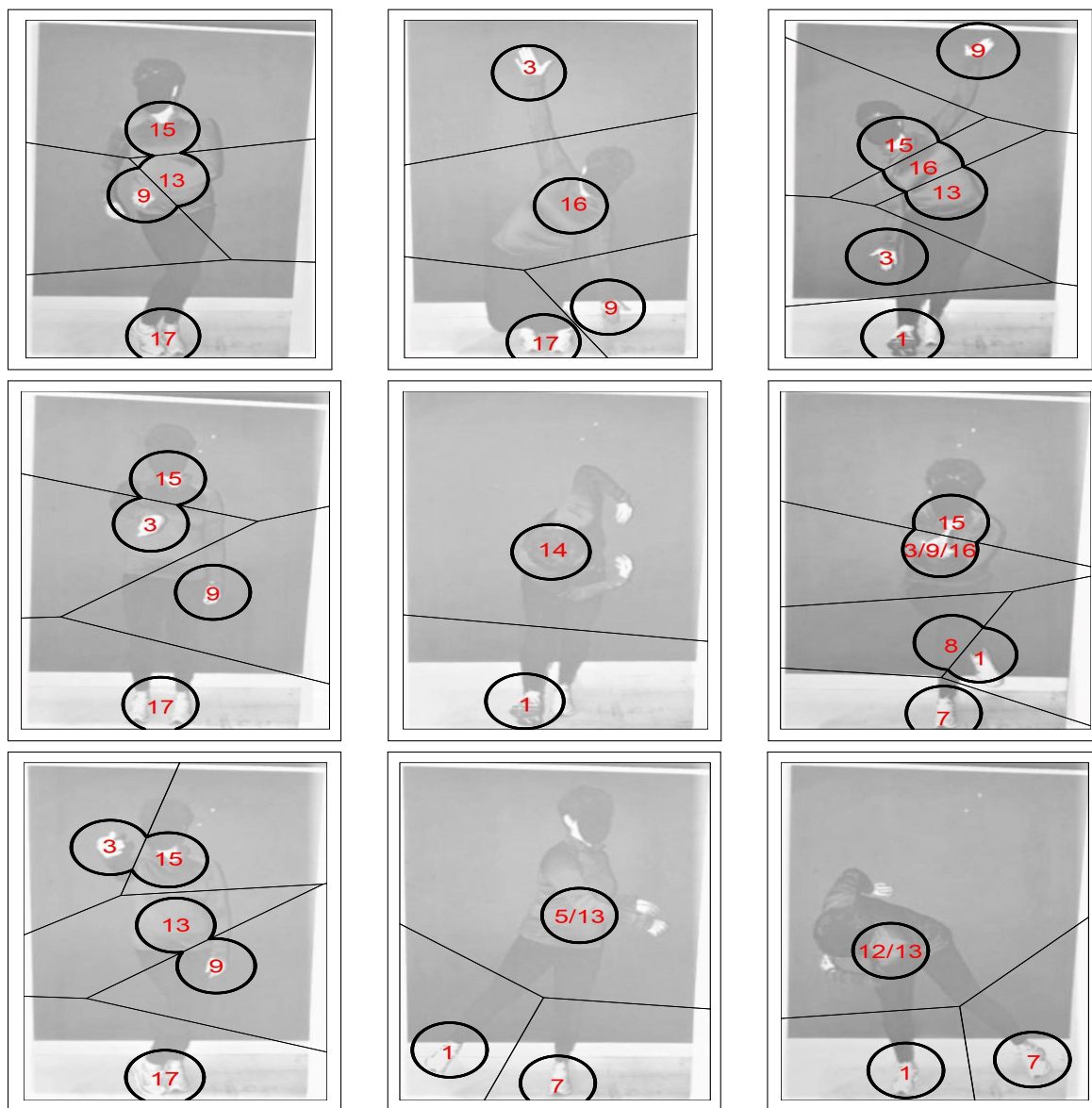
(c) Posture IDs 19-22 with Round 2 VTs.

Fig. B.3: Round 2 VT AOIs.

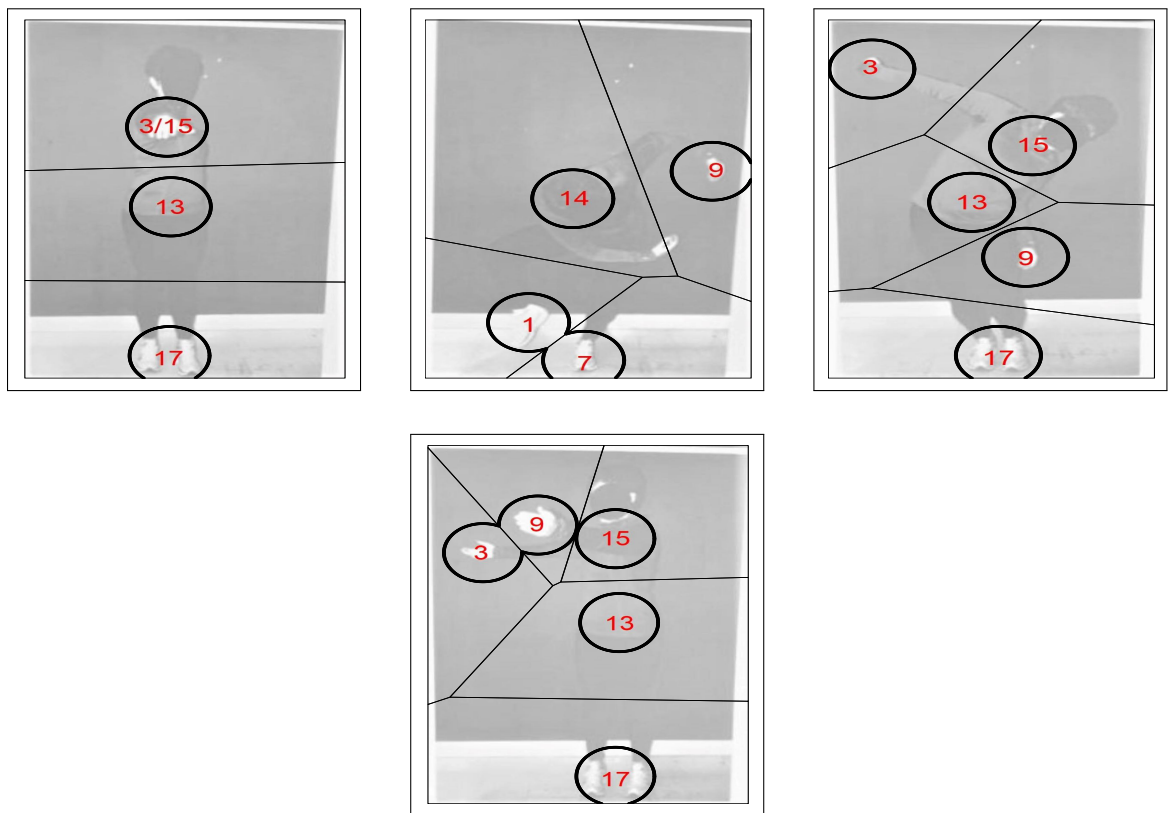
Figure B.4 shows Limited-Radius Voronoi Tessellations applied to Round 2 AOI centers for Posture IDs 1-22. These are LRVT Round 2 AOIs. The explanation of Limited-Radius Voronoi Tessellation method is given in Section 1.2.1 and applied to these postures in Section 2.2.4.



(a) Posture IDs 1-9 with Round 2 LRVTs.



(b) Posture IDs 10-18 with Round 2 LRVTs.



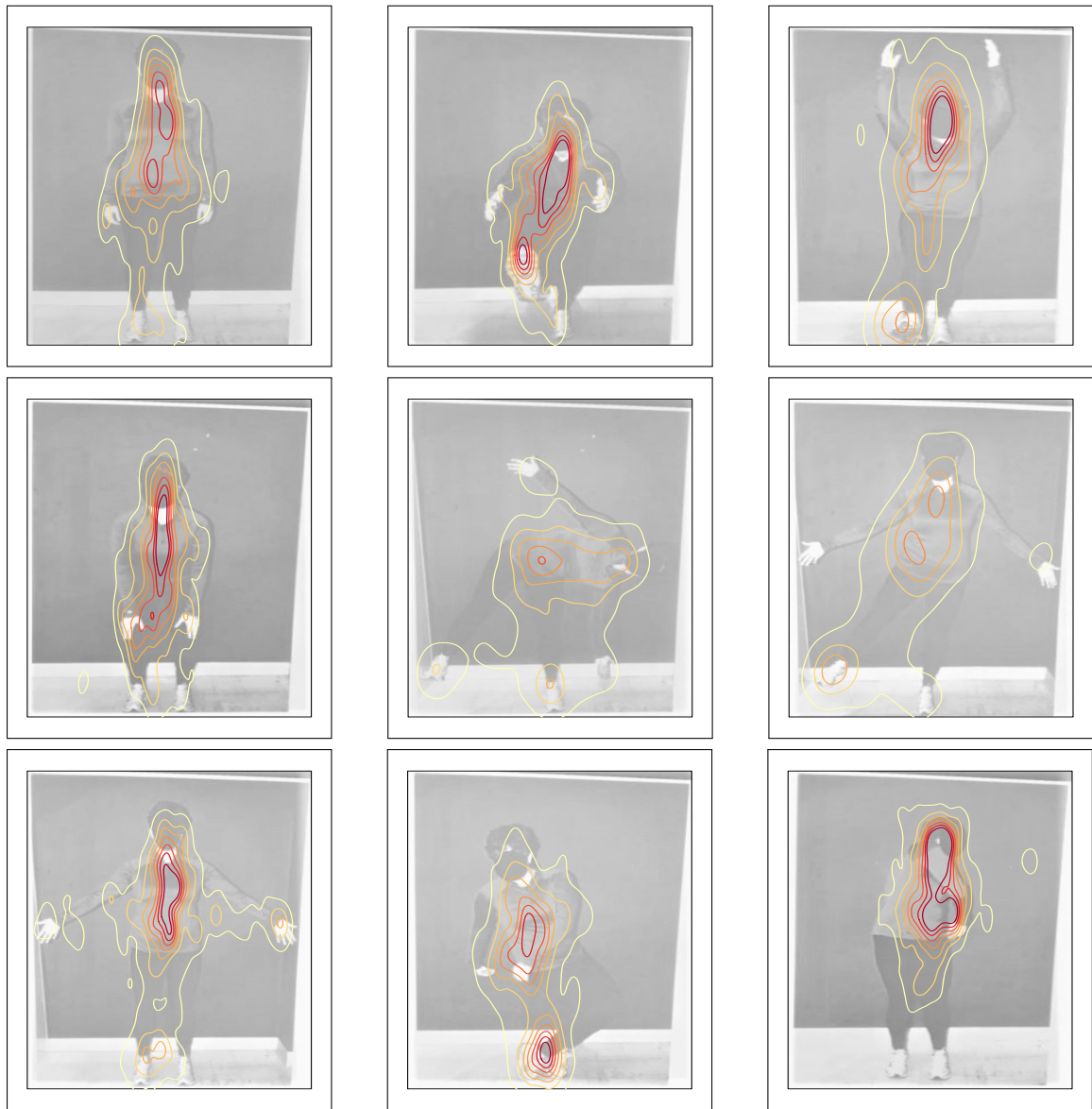
(c) Posture IDs 19-22 with Round 2 LRVTs.

Fig. B.4: Round 2 LRVT AOIs.

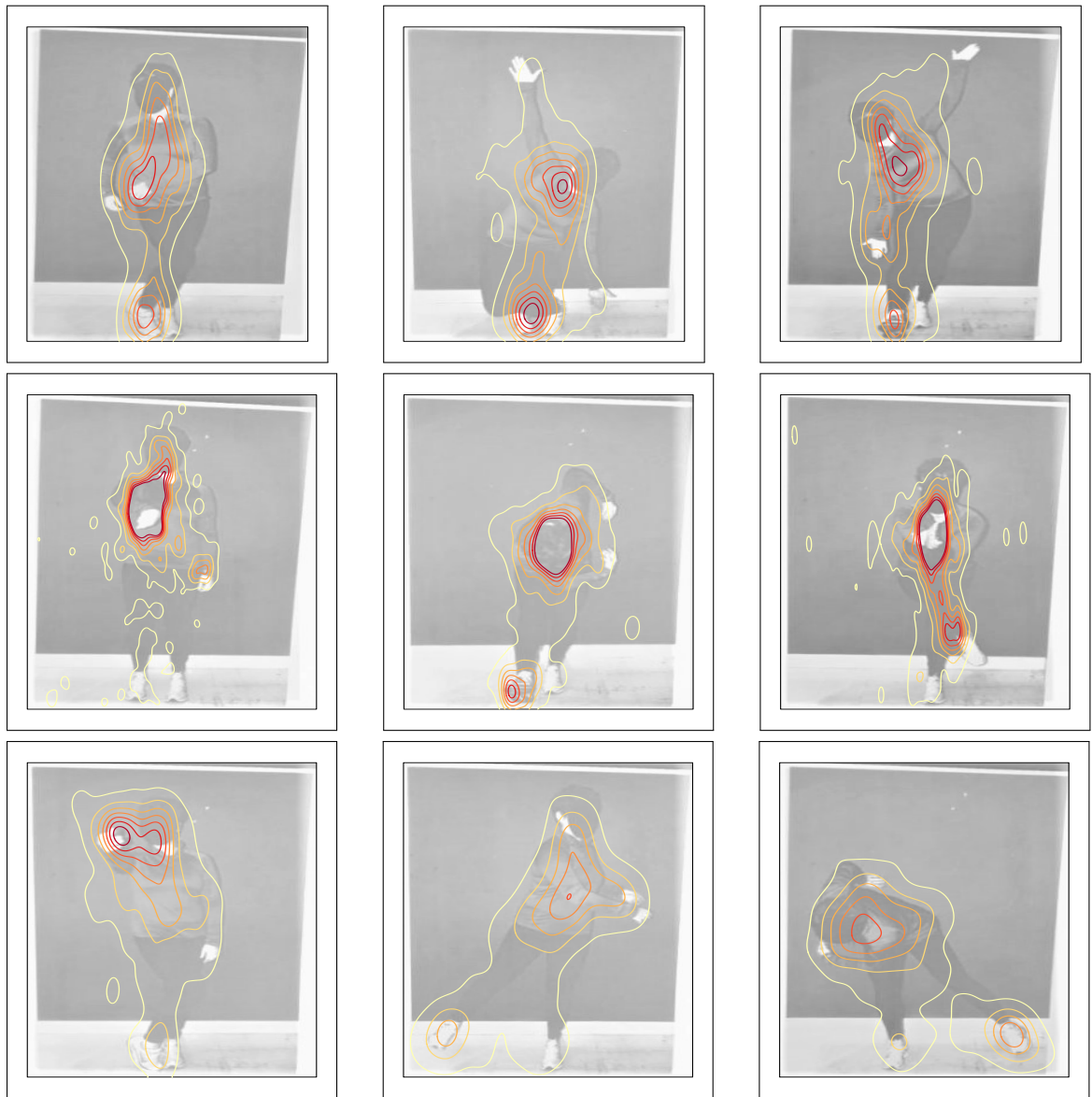
APPENDIX C

Contour Plots of Gaze-Point Data for All Participants

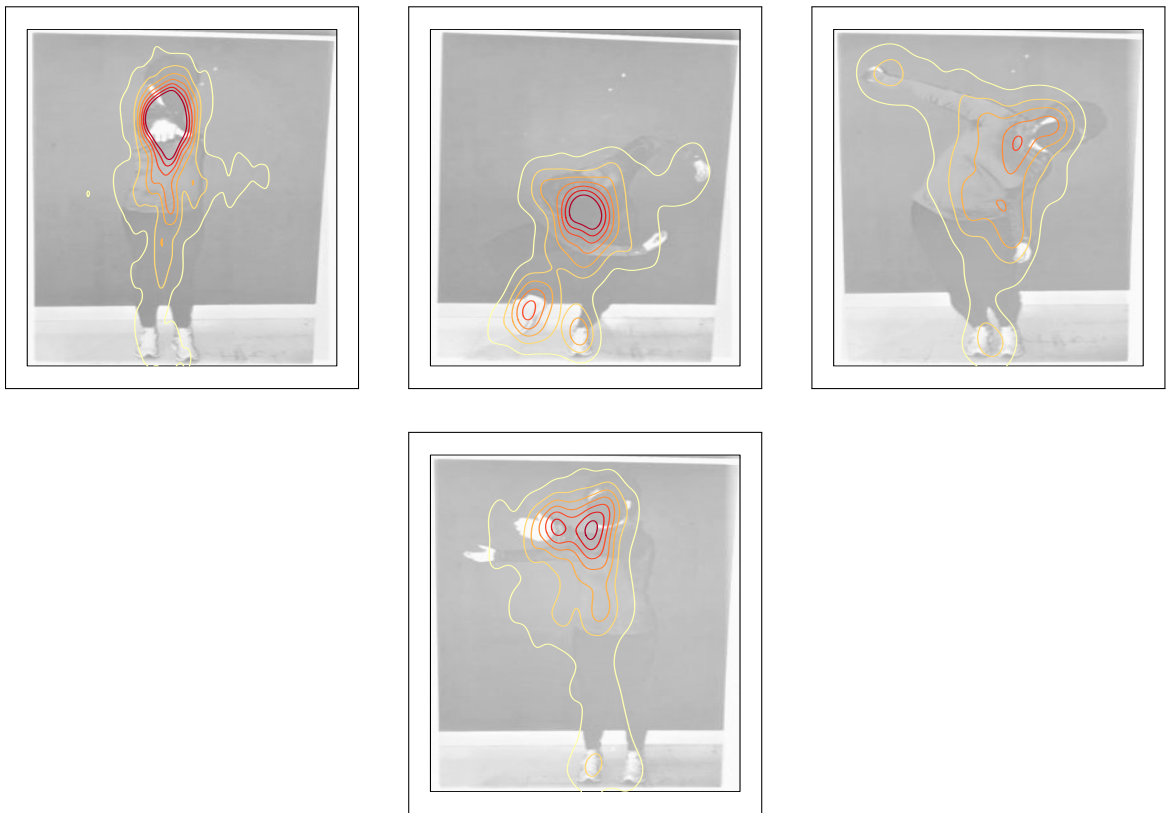
Figure C.1 shows contours of concentration of gaze points from all participants combined for Posture IDs 1-22. These plots were discussed in Section 1.2.2 and applied to these postures in Section 2.2.2. The order of the Posture IDs is the same as the postures in Appendix A and B.



(a) Posture IDs 1-9 showing contours of gaze-point data from all participants



(b) Posture IDs 10-18 showing contours of gaze-point data from all participants



(c) Posture IDs 19-22 showing contours of gaze-point data from all participants

Fig. C.1: Contours of gaze-point data from all participants

APPENDIX D

Extensive Tables of p-values for Statistical Analyses

Included in this appendix are the tables that list p-values and q-values for the statistical methods that rendered results. The tables are organized by statistical method and then for each iteration of the data. This appendix is divided into the following groups: Poisson GLMM EMM results (4 tables D.1 - D.4), Zero-Inflated Poisson GLMM EMM results (4 tables D.5-D.8), and Zero-Inflated Negative Binomial GLMM EMM results (4 tables D.9-D.12).

Poisson GLMM EMM Results

EMM rate ratio p-values for Round 1 VT Poisson GLMM

Table D.1: EMM rate ratio for Poisson GLMM showing raw p-values, Bonferroni adjusted p-values, and BH q-values for Round 1 VT data iteration (alternative = “two-sided”).

Round 1 VT AOI Labels	Raw p-values	Bonferroni p-values	BH q-values
Rt Foot (1)	0.3025	1.00	0.5042
Rt Knee (2)	0.0811	1.00	0.2028
Rt Hand (3)	0.7031	1.00	0.7990
Rt Hip (4)	0.9407	1.00	0.9407
Rt Elbow (5)	0.3640	1.00	0.5296
Rt Shoulder (6)	0.4215	1.00	0.5296
Lt Foot (7)	0.1598	1.00	0.3330
Lt Knee (8)	0.8993	1.00	0.9367
Lt Hand (9)	0.0544	1.00	0.1510
Lt Hip (10)	0.2338	1.00	0.4496
Lt Elbow (11)	0.3708	1.00	0.5296
Lt Shoulder (12)	0.2799	1.00	0.4999
Torso (13)	0.0306*	0.7641	0.1274
Head (14)	0.0255*	0.6382	0.1274
Rt Knee (2)/ Rt Hand (3)	0.4237	1.00	0.5296
Rt Hip (4)/ Rt Elbow (5)	0.0266*	0.6662	0.1274
Lt Knee (8)/ Lt Hand (9)	0.5258	1.00	0.6259
Lt Hip (10)/ Lt Elbow (11)	0.4088	1.00	0.5296
Rt Hip (4)/ Lt Hand (9)	0.0295*	0.7374	0.1274
Rt Knee (2)/ Lt Knee (8)	0.0086**	0.2153	0.1076
Rt Hip (4)/ Rt Shoulder (6)	0.1590	1.00	0.3330
Rt Hand (3)/ Lt Hand (9)	0.0531	1.00	0.1510
Rt Elbow (5)/ Lt Elbow (11)/ Torso (13)	0.0016**	0.0392*	0.0392*
Rt Hip (4)/ Lt Shoulder (12)/ Torso (13)	0.7575	1.00	0.8233
Rt Hand (3)/ Rt Elbow (5)/ Rt Shoulder (6)	0.0471*	1.00	0.1510

*** $p < 0.001$; ** $p < 0.01$; * $p < 0.05$

EMM rate ratio p-values for Round 1 LRVT Poisson GLMM

Table D.2: EMM rate ratio for Poisson GLMM showing raw p-values, Bonferroni adjusted p-values, and BH q-values for Round 1 LRVT data iteration (alternative = “two-sided”).

Round 1 LRVT AOI Labels	Raw p-values	Bonferroni p-values	BH q-values
Rt Foot (1)	0.2990	1.00	0.4859
Rt Knee (2)	0.0711	1.00	0.1849
Rt Hand (3)	0.3691	1.00	0.5398
Rt Hip (4)	0.8775	1.00	0.9362
Rt Elbow (5)	0.9259	1.00	0.9362
Rt Shoulder (6)	0.5310	1.00	0.6574
Lt Foot (7)	0.1263	1.00	0.2736
Lt Knee (8)	0.6558	1.00	0.7751
Lt Hand (9)	0.0706	1.00	0.1849
Lt Hip (10)	0.1415	1.00	0.2830
Lt Elbow (11)	0.2765	1.00	0.4793
Lt Shoulder (12)	0.1251	1.00	0.2736
Torso (13)	0.0448*	1.00	0.1849
Head (14)	0.0449*	1.00	0.1849
Rt Knee (2)/ Rt Hand (3)	0.1828	1.00	0.3395
Rt Hip (4)/ Rt Elbow (5)	0.0386*	1.00	0.1849
Lt Knee (8)/ Lt Hand (9)	0.9362	1.00	0.9362
Lt Hip (10)/ Lt Elbow (11)	0.5154	1.00	0.6574
Rt Hip (4)/ Lt Hand (9)	0.0574	1.00	0.1849
Rt Knee (2)/ Lt Knee (8)	0.0014**	0.0353*	0.0205*
Rt Hip (4)/ Rt Shoulder (6)	0.3737	1.00	0.5398
Rt Hand (3)/ Lt Hand (9)	0.0578	1.00	0.1849
Rt Elbow (5)/ Lt Elbow (11)/ Torso (13)	0.0016**	0.0409*	0.0205*
Rt Hip (4)/ Lt Shoulder (12)/ Torso (13)	0.8336	1.00	0.9362
Rt Hand (3)/ Rt Elbow (5)/ Rt Shoulder (6)	0.0608	1.00	0.1849
Outside Area	0.0706	1.00	0.1849

*** $p < 0.001$; ** $p < 0.01$; * $p < 0.05$

EMM rate ratio p-values for Round 2 VT Poisson GLMM

Table D.3: EMM rate ratio for Poisson GLMM showing raw p-values, Bonferroni adjusted p-values, and BH q-values for Round 2 VT data iteration (alternative = “two-sided”).

Round 2 VT AOI Labels	Raw p-values	Bonferroni p-values	BH q-values
Rt Foot (1)	0.1628	1.00	0.3955
Rt Knee (2)	0.8778	1.00	0.9063
Rt Hand (3)	0.6223	1.00	0.8816
Lt Foot (7)	0.0933	1.00	0.3955
Lt Knee (8)	0.0976	1.00	0.3955
Lt Hand (9)	0.1423	1.00	0.3955
Torso (13)	0.3350	1.00	0.6301
Head (14)	0.8967	1.00	0.9063
Neck (15)	0.1880	1.00	0.3994
Sternum (16)	0.1218	1.00	0.3955
Middle of Feet (17)	0.7663	1.00	0.9063
Lt Hand (9)/ Torso (13)	0.4794	1.00	0.7409
Rt Shoulder (6)/ Neck (15)	0.1557	1.00	0.3955
Rt Hand (3)/ Lt Hand (9)/ Sternum (16)	0.0010**	0.0178*	0.0178*
Rt Elbow (5)/ Torso (13)	0.9063	1.00	0.9063
Lt Shoulder (12)/ Torso (13)	0.3706	1.00	0.6301
Rt Hand (3)/ Neck (15)	0.8387	1.00	0.9063

*** $p < 0.001$; ** $p < 0.01$; * $p < 0.05$

EMM rate ratio p-values for Round 2 LRVT Poisson GLMM

Table D.4: EMM rate ratio for Poisson GLMM showing raw p-values, Bonferroni adjusted p-values, and BH q-values for Round 2 LRVT data iteration (alternative = “two-sided”).

Round 2 LRVT AOI Labels	Raw p-values	Bonferroni p-values	BH q-values
Rt Foot (1)	0.1512	1.00	0.2722
Rt Knee (2)	0.6059	1.00	0.6816
Rt Hand (3)	0.0382*	0.6882	0.1448
Lt Foot (7)	0.0402*	0.7241	0.1448
Lt Knee (8)	0.0870	1.00	0.1957
Lt Hand (9)	0.1067	1.00	0.2135
Torso (13)	0.0621	1.00	0.1597
Head (14)	0.3143	1.00	0.4715
Neck (15)	0.5656	1.00	0.6816
Sternum (16)	0.0015**	0.0266*	0.0133*
Middle of Feet (17)	0.6556	1.00	0.6881
Lt Hand (9)/ Torso (13)	0.6037	1.00	0.6816
Rt Shoulder (6)/ Neck (15)	0.5214	1.00	0.6816
Rt Hand (3)/ Lt Hand (9)/ Sternum (16)	0.0002***	0.0029**	0.0029**
Rt Elbow (5)/ Torso (13)	0.0490*	0.8826	0.1471
Lt Shoulder (12)/ Torso (13)	0.6881	1.00	0.6881
Rt Hand (3)/ Neck (15)	0.0154*	0.2767	0.0922
Outside Area	0.6059	1.00	0.6816

*** $p < 0.001$; ** $p < 0.01$; * $p < 0.05$

Zero-Inflated Poisson GLMM EMM Results

EMMRratio p-values for Round 1 VT Zero-Inflated Poisson GLMM

Table D.5: EMM rate ratio for ZIP GLMM showing raw p-values, Bonferroni adjusted p-values, and BH q-values for Round 1 VT data iteration (alternative = “two-sided”).

Round 1 VT AOI Labels	Raw p-values	Bonferroni p-values	BH q-values
Rt Foot (1)	0.1037	1.00	0.1729
Rt Knee (2)	0.0708	1.00	0.1608
Rt Hand (3)	0.0449*	1.00	0.1466
Rt Hip (4)	0.8321	1.00	0.9456
Rt Elbow (5)	0.2265	1.00	0.3540
Rt Shoulder (6)	0.4196	1.00	0.5739
Lt Foot (7)	0.0131*	0.3284	0.0657
Lt Knee (8)	0.9884	1.00	0.9884
Lt Hand (9)	0.1022	1.00	0.1729
Lt Hip (10)	0.0922	1.00	0.1729
Lt Elbow (11)	0.0586	1.00	0.1466
Lt Shoulder (12)	0.2716	1.00	0.3994
Torso (13)	0.0961	1.00	0.1729
Head (14)	0.0472*	1.00	0.1466
Rt Knee (2)/ Rt Hand (3)	0.4624	1.00	0.5780
Rt Hip (4)/ Rt Elbow (5)	0.0546	1.00	0.1466
Lt Knee (8)/ Lt Hand (9)	0.6954	1.00	0.8279
Lt Hip (10)/ Lt Elbow (11)	0.9359	1.00	0.9838
Rt Hip (4)/ Lt Hand (9)	0.0057**	0.1434	0.0478*
Rt Knee (2)/ Lt Knee (8)	0.0015**	0.0363*	0.0345*
Rt Hip (4)/ Rt Shoulder (6)	0.9444	1.00	0.9838
Rt Hand (3)/ Lt Hand (9)	0.0028**	0.0691	0.0345*
Rt Elbow (5)/ Lt Elbow (11)/ Torso (13)	0.0095**	0.2363	0.0591
Rt Hip (4)/ Lt Shoulder (12)/ Torso (13)	0.4362	1.00	0.5739
Rt Hand (3)/ Rt Elbow (5)/ Rt Shoulder (6)	0.0332*	0.8306	0.1384

*** $p < 0.001$; ** $p < 0.01$; * $p < 0.05$

EMM rate ratio p-values for Round 1 LRVT Zero-Inflated Poisson GLMM

Table D.6: EMM rate ratio for ZIP GLMM showing raw p-values, Bonferroni adjusted p-values, and BH q-values for Round 1 LRVT data iteration (alternative = “two-sided”).

Round 1 LRVT AOI Labels	Raw p-values	Bonferroni p-values	BH q-values
Rt Foot (1)	0.2675	1.00	0.3661
Rt Knee (2)	0.0507	1.00	0.1199
Rt Hand (3)	0.0158*	1.00	0.0686
Rt Hip (4)	0.6357	1.00	0.7186
Rt Elbow (5)	0.9361	1.00	0.9361
Rt Shoulder (6)	0.5845	1.00	0.7186
Lt Foot (7)	0.0091**	1.00	0.0596
Lt Knee (8)	0.8296	1.00	0.8627
Lt Hand (9)	0.1456	1.00	0.2783
Lt Hip (10)	0.1898	1.00	0.3084
Lt Elbow (11)	0.0119*	1.00	0.0620
Lt Shoulder (12)	0.2311	1.00	0.3338
Torso (13)	0.1498	1.00	0.2783
Head (14)	0.1608	1.00	0.2787
Rt Knee (2)/ Rt Hand (3)	0.7780	1.00	0.8428
Rt Hip (4)/ Rt Elbow (5)	0.0407*	1.00	0.1182
Lt Knee (8)/ Lt Hand (9)	0.0401*	1.00	0.1182
Lt Hip (10)/ Lt Elbow (11)	0.0409*	1.00	0.1182
Rt Hip (4)/ Lt Hand (9)	0.0745	1.00	0.1613
Rt Knee (2)/ Lt Knee (8)	0.0034**	0.0353*	0.0441*
Rt Hip (4)/ Rt Shoulder (6)	0.6102	1.00	0.7186
Rt Hand (3)/ Lt Hand (9)	0.0034**	1.00	0.0441*
Rt Elbow (5)/ Lt Elbow (11)/ Torso (13)	0.0092**	0.0409*	0.0596
Rt Hip (4)/ Lt Shoulder (12)/ Torso (13)	0.3465	1.00	0.4504
Rt Hand (3)/ Rt Elbow (5)/ Rt Shoulder (6)	0.0473*	1.00	0.1199
Outside Area	0.1498	1.00	0.2783

*** $p < 0.001$; ** $p < 0.01$; * $p < 0.05$

EMM rate ratio p-values for Round 2 VT Zero-Inflated Poisson GLMM

Table D.7: EMM rate ratio for ZIP GLMM showing raw p-values, Bonferroni adjusted p-values, and BH q-values for Round 2 VT data iteration (alternative = “two-sided”).

Round 2 VT AOI Labels	Raw p-values	Bonferroni p-values	BH q-values
Rt Foot (1)	0.1110	1.00	0.3378
Rt Knee (2)	0.4428	1.00	0.5377
Rt Hand (3)	0.2164	1.00	0.3969
Lt Foot (7)	0.0256*	0.4357	0.2179
Lt Knee (8)	0.1192	1.00	0.3378
Lt Hand (9)	0.1418	1.00	0.3444
Torso (13)	0.3588	1.00	0.5083
Head (14)	0.5587	1.00	0.6331
Neck (15)	0.2216	1.00	0.3969
Sternum (16)	0.1044	1.00	0.3378
Middle of Feet (17)	0.4294	1.00	0.5377
Lt Hand (9)/ Torso (13)	0.3145	1.00	0.4861
Rt Shoulder (6)/ Neck (15)	0.0407*	0.6922	0.2307
Rt Hand (3)/ Lt Hand (9)/ Sternum (16)	0.0007***	0.0112*	0.0112*
Rt Elbow (5)/ Torso (13)	0.9288	1.00	0.9748
Lt Shoulder (12)/ Torso (13)	0.2335	1.00	0.3969
Rt Hand (3)/ Neck (15)	0.9748	1.00	0.9748

*** $p < 0.001$; ** $p < 0.01$; * $p < 0.05$

EMM rate ratio p-values for Round 2 LRVT Zero-Inflated Poisson GLMM

Table D.8: EMM rate ratio for ZIP GLMM showing raw p-values, Bonferroni adjusted p-values, and BH q-values for Round 2 LRVT data iteration (alternative = “two-sided”).

Round 2 LRVT AOI Labels	Raw p-values	Bonferroni p-values	BH q-values
Rt Foot (1)	0.2715	1.00	0.4072
Rt Knee (2)	0.4994	1.00	0.5618
Rt Hand (3)	0.0064**	0.1148	0.0383*
Lt Foot (7)	0.0166*	0.2982	0.0596
Lt Knee (8)	0.1278	1.00	0.2271
Lt Hand (9)	0.1388	1.00	0.2271
Torso (13)	0.1067	1.00	0.2270
Head (14)	0.1135	1.00	0.2270
Neck (15)	0.7208	1.00	0.7632
Sternum (16)	0.0018**	0.0328*	0.0164*
Middle of Feet (17)	0.3510	1.00	0.4543
Lt Hand (9)/ Torso (13)	0.9091	1.00	0.9091
Rt Shoulder (6)/ Neck (15)	0.4000	1.00	0.4800
Rt Hand (3)/ Lt Hand (9)/ Sternum (16)	0.0001***	0.0012**	0.0012**
Rt Elbow (5)/ Torso (13)	0.0527	0.9489	0.1581
Lt Shoulder (12)/ Torso (13)	0.3534	1.00	0.4543
Rt Hand (3)/ Neck (15)	0.0127*	0.2281	0.0570
Outside Area	0.1135	1.00	0.2270

*** $p < 0.001$; ** $p < 0.01$; * $p < 0.05$

Zero-Inflated Negative Binomial GLMM EMM Results

EMM rate ratio p-values for Round 1 VT Zero-Inflated Negative Binomial GLMM

Table D.9: EMM rate ratio for ZINB GLMM showing raw p-values, Bonferroni adjusted p-values, and BH q-values for Round 1 VT data iteration (alternative = “two-sided”).

Round 1 VT AOI Labels	Raw p-values	Bonferroni p-values	BH q-values
Rt Foot (1)	0.7673	1.00	0.9445
Rt Knee (2)	0.1792	1.00	0.8255
Rt Hand (3)	0.3637	1.00	0.8255
Rt Hip (4)	0.9925	1.00	0.9925
Rt Elbow (5)	0.3175	1.00	0.8255
Rt Shoulder (6)	0.4226	1.00	0.8255
Lt Foot (7)	0.6667	1.00	0.9445
Lt Knee (8)	0.9678	1.00	0.9925
Lt Hand (9)	0.4808	1.00	0.8255
Lt Hip (10)	0.2710	1.00	0.8255
Lt Elbow (11)	0.5258	1.00	0.8255
Lt Shoulder (12)	0.2278	1.00	0.8255
Torso (13)	0.3871	1.00	0.8255
Head (14)	0.0881	1.00	0.8255
Rt Knee (2)/ Rt Hand (3)	0.8312	1.00	0.9445
Rt Hip (4)/ Rt Elbow (5)	0.2572	1.00	0.8255
Lt Knee (8)/ Lt Hand (9)	0.8230	1.00	0.9445
Lt Hip (10)/ Lt Elbow (11)	0.6914	1.00	0.9445
Rt Hip (4)/ Lt Hand (9)	0.4415	1.00	0.8255
Rt Knee (2)/ Lt Knee (8)	0.1722	1.00	0.8255
Rt Hip (4)/ Rt Shoulder (6)	0.7294	1.00	0.9445
Rt Hand (3)/ Lt Hand (9)	0.5283	1.00	0.8255
Rt Elbow (5)/ Lt Elbow (11)/ Torso (13)	0.1095	1.00	0.8255
Rt Hip (4)/ Lt Shoulder (12)/ Torso (13)	0.9825	1.00	0.9925
Rt Hand (3)/ Rt Elbow (5)/ Rt Shoulder (6)	0.3925	1.00	0.8255

*** $p < 0.001$; ** $p < 0.01$; * $p < 0.05$

EMM rate ratio p-values for Round 1 LRVT Zero-Inflated Negative Binomial GLMM

Table D.10: EMM rate ratio for ZINB GLMM showing raw p-values, Bonferroni adjusted p-values, and BH q-values for Round 1 LRVT data iteration (alternative = “two-sided”).

Round 1 LRVT AOI Labels	Raw p-values	Bonferroni p-values	BH q-values
Rt Foot (1)	0.9763	1.00	0.9763
Rt Knee (2)	0.1253	1.00	0.8702
Rt Hand (3)	0.2230	1.00	0.9220
Rt Hip (4)	0.9577	1.00	0.9763
Rt Elbow (5)	0.7802	1.00	0.9220
Rt Shoulder (6)	0.5057	1.00	0.9220
Lt Foot (7)	0.7213	1.00	0.9220
Lt Knee (8)	0.6276	1.00	0.9220
Lt Hand (9)	0.6463	1.00	0.9220
Lt Hip (10)	0.2551	1.00	0.9220
Lt Elbow (11)	0.5577	1.00	0.9220
Lt Shoulder (12)	0.1673	1.00	0.8702
Torso (13)	0.5189	1.00	0.9220
Head (14)	0.1480	1.00	0.8702
Rt Knee (2)/ Rt Hand (3)	0.8958	1.00	0.9763
Rt Hip (4)/ Rt Elbow (5)	0.2853	1.00	0.9220
Lt Knee (8)/ Lt Hand (9)	0.7537	1.00	0.9220
Lt Hip (10)/ Lt Elbow (11)	0.7379	1.00	0.9220
Rt Hip (4)/ Lt Hand (9)	0.5829	1.00	0.9220
Rt Knee (2)/ Lt Knee (8)	0.0781	1.00	0.8702
Rt Hip (4)/ Rt Shoulder (6)	0.7474	1.00	0.9220
Rt Hand (3)/ Lt Hand (9)	0.5585	1.00	0.9220
Rt Elbow (5)/ Lt Elbow (11)/ Torso (13)	0.1172	1.00	0.8702
Rt Hip (4)/ Lt Shoulder (12)/ Torso (13)	0.9718	1.00	0.9763
Rt Hand (3)/ Rt Elbow (5)/ Rt Shoulder (6)	0.4292	1.00	0.9220
Outside Area	0.2853	1.00	0.9220

*** $p < 0.001$; ** $p < 0.01$; * $p < 0.05$

EMM rate ratio p-values for Round 2 VT Zero-Inflated Negative Binomial GLMM

Table D.11: EMM rate ratio for ZINB GLMM showing raw p-values, Bonferroni adjusted p-values, and BH q-values for Round 2 VT data iteration (alternative = “two-sided”).

Round 2 VT AOI Labels	Raw p-values	Bonferroni p-values	BH q-values
Rt Foot (1)	0.4298	1.00	0.9580
Rt Knee (2)	0.9580	1.00	0.9580
Rt Hand (3)	0.5104	1.00	0.9580
Lt Foot (7)	0.4718	1.00	0.9580
Lt Knee (8)	0.9559	1.00	0.9580
Lt Hand (9)	0.3928	1.00	0.9580
Torso (13)	0.4970	1.00	0.9580
Head (14)	0.7081	1.00	0.9580
Neck (15)	0.3375	1.00	0.9580
Sternum (16)	0.3396	1.00	0.9580
Middle of Feet (17)	0.8583	1.00	0.9580
Lt Hand (9)/ Torso (13)	0.8867	1.00	0.9580
Rt Shoulder (6)/ Neck (15)	0.3957	1.00	0.9580
Rt Hand (3)/ Lt Hand (9)/ Sternum (16)	0.1660	1.00	0.9580
Rt Elbow (5)/ Torso (13)	0.9412	1.00	0.9580
Lt Shoulder (12)/ Torso (13)	0.7689	1.00	0.9580
Rt Hand (3)/ Neck (15)	0.8639	1.00	0.9580

*** $p < 0.001$; ** $p < 0.01$; * $p < 0.05$

EMM rate ratio p-values for Round 2 LRVT Zero-Inflated Negative Binomial GLMM

Table D.12: EMM rate ratio for ZINB GLMM showing raw p-values, Bonferroni adjusted p-values, and BH q-values for Round 2 LRVT data iteration (alternative = “two-sided”).

Round 2 LRVT AOI Labels	Raw p-values	Bonferroni p-values	BH q-values
Rt Foot (1)	0.6871	1.00	0.9611
Rt Knee (2)	0.9982	1.00	0.9982
Rt Hand (3)	0.0662	1.00	0.6209
Lt Foot (7)	0.6237	1.00	0.9611
Lt Knee (8)	0.9640	1.00	0.9982
Lt Hand (9)	0.4165	1.00	0.9611
Torso (13)	0.2070	1.00	0.6209
Head (14)	0.4431	1.00	0.9611
Neck (15)	0.7475	1.00	0.9611
Sternum (16)	0.0713	1.00	0.6209
Middle of Feet (17)	0.8768	1.00	0.9864
Lt Hand (9)/ Torso (13)	0.4829	1.00	0.9611
Rt Shoulder (6)/ Neck (15)	0.6530	1.00	0.9611
Rt Hand (3)/ Lt Hand (9)/ Sternum (16)	0.1749	1.00	0.6209
Rt Elbow (5)/ Torso (13)	0.6958	1.00	0.9611
Lt Shoulder (12)/ Torso (13)	0.8499	1.00	0.9864
Rt Hand (3)/ Neck (15)	0.1366	1.00	0.6209
Outside Area	0.0713	1.00	0.6209

*** $p < 0.001$; ** $p < 0.01$; * $p < 0.05$

APPENDIX E

Estimates Tables for Multilevel Analyses

Included in this appendix are the tables that list the δ estimates, standard errors, ratios, z-values, and p-values for the Poisson and Zero-Inflated Poisson interaction models. The tables are organized by statistical model where Poisson tables are given as Tables E.1 - E.4 and the Zero-Inflated Poisson tables are given as Tables E.5 - E.8. The tables that provide this information for the Zero-Inflated Negative Binomial model are included in Chapter 3 as Tables 3.7 - 3.10

Poisson Regression

Table E.1: Poisson multilevel regression estimates for Round 1 VT AOI iteration

	$\hat{\delta}$ label	$\hat{\delta}$ (SE)	RR	z-value	p-value
FIXED EFFECTS					
Intercept	$\hat{\delta}_{0,0,0}$	2.30 (0.09)	9.95	24.47	< 0.001***
Group, Treatment vs Control	$\hat{\delta}_{1,0,0}$	-0.27 (0.12)	0.76	-2.16	0.030*
AOI (Round 1)					
Rt Foot (1)	$\hat{\delta}_{0,0,1}$	-0.61 (0.03)	0.54	-23.77	< 0.001***
Rt Knee (2)	$\hat{\delta}_{0,0,2}$	-1.27 (0.03)	0.28	-36.83	< 0.001***
Rt Hand (3)	$\hat{\delta}_{0,0,3}$	-0.80 (0.03)	0.45	-27.76	< 0.001***
Rt Hip (4)	$\hat{\delta}_{0,0,4}$	-0.54 (0.03)	0.58	-16.55	< 0.001***
Rt Elbow (5)	$\hat{\delta}_{0,0,5}$	-1.07 (0.03)	0.34	-33.78	< 0.001***
Rt Shoulder (6)	$\hat{\delta}_{0,0,12}$	-0.27 (0.02)	0.76	-11.13	< 0.001***
Lt Foot (7)	$\hat{\delta}_{0,0,6}$	-1.20 (0.03)	0.30	-38.06	< 0.001***
Lt Knee (8)	$\hat{\delta}_{0,0,7}$	-1.40 (0.04)	0.25	-37.86	< 0.001***
Lt Hand (9)	$\hat{\delta}_{0,0,8}$	-1.37 (0.04)	0.25	-36.19	< 0.001***
Lt Hip (10)	$\hat{\delta}_{0,0,9}$	-1.04 (0.03)	0.35	-34.23	< 0.001***
Lt Elbow (11)	$\hat{\delta}_{0,0,10}$	-1.29 (0.04)	0.27	-35.84	< 0.001***
Lt Shoulder (12)	$\hat{\delta}_{0,0,11}$	-0.91 (0.03)	0.40	-30.29	< 0.001***
Head (14)	$\hat{\delta}_{0,0,13}$	-0.49 (0.02)	0.61	-19.59	< 0.001***
Rt Knee (2)/ Rt Hand (3)	$\hat{\delta}_{0,0,14}$	0.18 (0.07)	1.20	2.76	< 0.006**
Rt Hip (4)/ Rt Elbow (5)	$\hat{\delta}_{0,0,15}$	-1.82 (0.17)	0.16	-10.94	< 0.001***
Lt Knee (8)/ Lt Hand (9)	$\hat{\delta}_{0,0,16}$	-0.45 (0.09)	0.63	-4.83	< 0.001***
Lt Hip (10)/ Lt Elbow (11)	$\hat{\delta}_{0,0,17}$	-1.94 (0.18)	0.14	-11.00	< 0.001***
Rt Hip (4)/ Lt Hand (9)	$\hat{\delta}_{0,0,18}$	0.30 (0.05)	1.34	5.83	< 0.001***
Rt Knee (2)/ Lt Knee (8)	$\hat{\delta}_{0,0,19}$	-1.17 (0.09)	0.31	-12.89	< 0.001***
Rt Hip (4)/ Rt Shoulder (6)	$\hat{\delta}_{0,0,20}$	-0.99 (0.12)	0.37	-8.62	< 0.001***
Rt Hand (3)/ Lt Hand (9)	$\hat{\delta}_{0,0,21}$	1.23 (0.05)	3.43	23.67	< 0.001***
Rt Elbow (5)/ Lt Elbow (11)/ Torso (13)	$\hat{\delta}_{0,0,22}$	0.03 (0.08)	1.03	0.36	0.719
Rt Hip (4)/ Lt Shoulder (12)/ Torso (13)	$\hat{\delta}_{0,0,23}$	-0.14 (0.07)	0.87	-1.93	0.053
Rt Hand (3)/ Rt Elbow (5)/ Rt Shoulder (6)	$\hat{\delta}_{0,0,24}$	1.12 (0.05)	3.08	20.73	< 0.001***
Interaction: Group (Treatment) \times AOI					
Rt Foot (1)	$\hat{\delta}_{1,0,1}$	0.40 (0.04)	1.49	11.02	< 0.001***
Rt Knee (2)	$\hat{\delta}_{1,0,2}$	0.50 (0.05)	1.64	10.57	< 0.001***
Rt Hand (3)	$\hat{\delta}_{1,0,3}$	0.22 (0.04)	1.25	5.29	< 0.001***
Rt Hip (4)	$\hat{\delta}_{1,0,4}$	0.26 (0.04)	1.30	5.92	< 0.001***
Rt Elbow (5)	$\hat{\delta}_{1,0,5}$	0.39 (0.04)	1.47	8.79	< 0.001***
Rt Shoulder (6)	$\hat{\delta}_{1,0,12}$	0.17 (0.04)	1.18	4.78	< 0.001***
Lt Foot (7)	$\hat{\delta}_{1,0,6}$	0.45 (0.04)	1.57	10.34	< 0.001***
Lt Knee (8)	$\hat{\delta}_{1,0,7}$	0.29 (0.05)	1.33	5.51	< 0.001***
Lt Hand (9)	$\hat{\delta}_{1,0,8}$	0.52 (0.05)	1.68	10.23	< 0.001***
Lt Hip (10)	$\hat{\delta}_{1,0,9}$	0.12 (0.04)	1.12	2.65	0.008**
Lt Elbow (11)	$\hat{\delta}_{1,0,10}$	0.15 (0.05)	1.16	2.93	0.003**
Lt Shoulder (12)	$\hat{\delta}_{1,0,11}$	0.41 (0.04)	1.50	9.77	< 0.001***
Head (14)	$\hat{\delta}_{1,0,13}$	0.55 (0.03)	1.73	15.98	< 0.001***
Rt Knee (2)/ Rt Hand (3)	$\hat{\delta}_{1,0,14}$	0.15 (0.09)	1.16	1.67	0.096
Rt Hip (4)/ Rt Elbow (5)	$\hat{\delta}_{1,0,15}$	0.80 (0.21)	2.23	3.88	< 0.001***
Lt Knee (8)/ Lt Hand (9)	$\hat{\delta}_{1,0,16}$	0.16 (0.13)	1.17	1.25	0.212
Lt Hip (10)/ Lt Elbow (11)	$\hat{\delta}_{1,0,17}$	0.49 (0.23)	1.63	2.09	0.036*
Rt Hip (4)/ Lt Hand (9)	$\hat{\delta}_{1,0,18}$	-0.04 (0.07)	0.96	-0.50	0.619
Rt Knee (2)/ Lt Knee (8)	$\hat{\delta}_{1,0,19}$	0.71 (0.11)	2.03	6.16	< 0.001***
Rt Hip (4)/ Rt Shoulder (6)	$\hat{\delta}_{1,0,20}$	-0.02 (0.17)	0.98	-0.14	0.892
Rt Hand (3)/ Lt Hand (9)	$\hat{\delta}_{1,0,21}$	0.00 (0.07)	1.00	0.06	0.953
Rt Elbow (5)/ Lt Elbow (11)/ Torso (13)	$\hat{\delta}_{1,0,22}$	-0.28 (0.13)	0.76	-2.23	0.026*
Rt Hip (4)/ Lt Shoulder (12)/ Torso (13)	$\hat{\delta}_{1,0,23}$	0.32 (0.09)	1.37	3.42	< 0.001***
Rt Hand (3)/ Rt Elbow (5)/ Rt Shoulder (6)	$\hat{\delta}_{1,0,24}$	-0.01 (0.07)	0.99	-0.10	0.922
RANDOM EFFECTS					
	Notation	Var.	SD		
Participant Intercepts	\bar{u}_{i0}	0.1482	0.3850		
Posture Intercepts	\bar{u}_{0j}	0.0239	0.1547		

RR = Rate ratio; Reference AOI category: Torso (13); *** $p < 0.001$; ** $p < 0.01$; * $p < 0.05$

Table E.2: Poisson multilevel regression estimates for Round 1 LRV T AOI iteration

	$\hat{\delta}$ label	$\hat{\delta}$ (SE)	RR	z-value	p-value
FIXED EFFECTS					
Intercept	$\hat{\delta}_{0,0,0}$	2.16 (0.09)	8.69	22.94	< 0.001***
Group, Treatment vs Control	$\hat{\delta}_{1,0,0}$	-0.25 (0.13)	0.78	-2.01	0.045*
AOI (Round 1)					
Rt Foot (1)	$\hat{\delta}_{0,0,1}$	-0.73 (0.03)	0.48	-25.52	< 0.001***
Rt Knee (2)	$\hat{\delta}_{0,0,2}$	-1.47 (0.04)	0.23	-36.72	< 0.001***
Rt Hand (3)	$\hat{\delta}_{0,0,3}$	-0.75 (0.03)	0.47	-24.94	< 0.001***
Rt Hip (4)	$\hat{\delta}_{0,0,4}$	-0.92 (0.03)	0.40	-26.58	< 0.001***
Rt Elbow (5)	$\hat{\delta}_{0,0,5}$	-1.04 (0.03)	0.35	-31.15	< 0.001***
Rt Shoulder (6)	$\hat{\delta}_{0,0,6}$	-0.33 (0.03)	0.72	-12.59	< 0.001***
Lt Foot (7)	$\hat{\delta}_{0,0,7}$	-1.30 (0.04)	0.27	-37.12	< 0.001***
Lt Knee (8)	$\hat{\delta}_{0,0,8}$	-1.47 (0.04)	0.23	-36.10	< 0.001***
Lt Hand (9)	$\hat{\delta}_{0,0,9}$	-1.37 (0.04)	0.26	-33.84	< 0.001***
Lt Hip (10)	$\hat{\delta}_{0,0,10}$	-1.07 (0.03)	0.34	-32.64	< 0.001***
Lt Elbow (11)	$\hat{\delta}_{0,0,11}$	-1.32 (0.04)	0.27	-33.85	< 0.001***
Lt Shoulder (12)	$\hat{\delta}_{0,0,12}$	-1.08 (0.03)	0.34	-31.55	< 0.001***
Head (14)	$\hat{\delta}_{0,0,13}$	-0.46 (0.03)	0.63	-17.40	< 0.001***
Rt Knee (2)/ Rt Hand (3)	$\hat{\delta}_{0,0,14}$	0.19 (0.07)	1.20	2.64	0.008**
Rt Hip (4)/ Rt Elbow (5)	$\hat{\delta}_{0,0,15}$	-1.74 (0.17)	0.18	-10.12	< 0.001***
Lt Knee (8)/ Lt Hand (9)	$\hat{\delta}_{0,0,16}$	-0.78 (0.11)	0.46	-7.19	< 0.001***
Lt Hip (10)/ Lt Elbow (11)	$\hat{\delta}_{0,0,17}$	-1.89 (0.18)	0.15	-10.22	< 0.001***
Rt Hip (4)/ Lt Hand (9)	$\hat{\delta}_{0,0,18}$	0.27 (0.05)	1.31	5.04	< 0.001***
Rt Knee (2)/ Lt Knee (8)	$\hat{\delta}_{0,0,19}$	-1.93 (0.14)	0.14	-13.91	< 0.001***
Rt Hip (4)/ Rt Shoulder (6)	$\hat{\delta}_{0,0,20}$	-0.98 (0.12)	0.37	-7.94	< 0.001***
Rt Hand (3)/ Lt Hand (9)	$\hat{\delta}_{0,0,21}$	1.41 (0.05)	4.10	26.86	< 0.001***
Rt Elbow (5)/ Lt Elbow (11)/ Torso (13)	$\hat{\delta}_{0,0,22}$	0.21 (0.08)	1.24	2.60	0.009**
Rt Hip (4)/ Lt Shoulder (12)/ Torso (13)	$\hat{\delta}_{0,0,23}$	-0.08 (0.07)	0.93	-1.04	0.297
Rt Hand (3)/ Rt Elbow (5)/ Rt Shoulder (6)	$\hat{\delta}_{0,0,24}$	1.14 (0.06)	3.14	20.25	< 0.001***
Outside Area	$\hat{\delta}_{0,0,25}$	0.12 (0.02)	1.12	5.17	< 0.001***
Interaction: Group (Treatment) \times AOI					
Rt Foot (1)	$\hat{\delta}_{1,0,1}$	0.38 (0.04)	1.47	9.55	< 0.001***
Rt Knee (2)	$\hat{\delta}_{1,0,2}$	0.49 (0.05)	1.63	9.07	< 0.001***
Rt Hand (3)	$\hat{\delta}_{1,0,3}$	0.14 (0.04)	1.15	3.12	0.002**
Rt Hip (4)	$\hat{\delta}_{1,0,4}$	0.23 (0.05)	1.26	4.73	< 0.001***
Rt Elbow (5)	$\hat{\delta}_{1,0,5}$	0.26 (0.05)	1.30	5.56	< 0.001***
Rt Shoulder (6)	$\hat{\delta}_{1,0,6}$	0.17 (0.04)	1.19	4.49	< 0.001***
Lt Foot (7)	$\hat{\delta}_{1,0,7}$	0.45 (0.05)	1.57	9.34	< 0.001***
Lt Knee (8)	$\hat{\delta}_{1,0,8}$	0.19 (0.06)	1.21	3.30	< 0.001***
Lt Hand (9)	$\hat{\delta}_{1,0,9}$	0.49 (0.05)	1.63	8.99	< 0.001***
Lt Hip (10)	$\hat{\delta}_{1,0,10}$	0.06 (0.05)	1.06	1.26	0.207
Lt Elbow (11)	$\hat{\delta}_{1,0,11}$	0.11 (0.06)	1.11	1.89	0.058
Lt Shoulder (12)	$\hat{\delta}_{1,0,12}$	0.45 (0.05)	1.57	9.60	< 0.001***
Head (14)	$\hat{\delta}_{1,0,13}$	0.50 (0.04)	1.65	13.76	< 0.001***
Rt Knee (2)/ Rt Hand (3)	$\hat{\delta}_{1,0,14}$	0.04 (0.10)	1.05	0.45	0.654
Rt Hip (4)/ Rt Elbow (5)	$\hat{\delta}_{1,0,15}$	0.76 (0.21)	2.13	3.55	< 0.001***
Lt Knee (8)/ Lt Hand (9)	$\hat{\delta}_{1,0,16}$	0.27 (0.15)	1.31	1.80	0.072
Lt Hip (10)/ Lt Elbow (11)	$\hat{\delta}_{1,0,17}$	0.06 (0.27)	1.06	0.22	0.825
Rt Hip (4)/ Lt Hand (9)	$\hat{\delta}_{1,0,18}$	-0.02 (0.08)	0.98	-0.27	0.790
Rt Knee (2)/ Lt Knee (8)	$\hat{\delta}_{1,0,19}$	0.92 (0.17)	2.50	5.41	< 0.001***
Rt Hip (4)/ Rt Shoulder (6)	$\hat{\delta}_{1,0,20}$	0.06 (0.18)	1.06	0.34	0.736
Rt Hand (3)/ Lt Hand (9)	$\hat{\delta}_{1,0,21}$	-0.01 (0.07)	0.99	-0.15	0.881
Rt Elbow (5)/ Lt Elbow (11)/ Torso (13)	$\hat{\delta}_{1,0,22}$	-0.30 (0.13)	0.74	-2.37	0.018*
Rt Hip (4)/ Lt Shoulder (12)/ Torso (13)	$\hat{\delta}_{1,0,23}$	0.28 (0.10)	1.33	2.89	0.004**
Rt Hand (3)/ Rt Elbow (5)/ Rt Shoulder (6)	$\hat{\delta}_{1,0,24}$	-0.01 (0.07)	0.99	-0.19	0.849
Outside Area	$\hat{\delta}_{1,0,25}$	0.34 (0.03)	1.40	10.42	< 0.001***
RANDOM EFFECTS					
Participant Intercepts	Notation	Var.	SD		
	\bar{u}_{i0}	0.1503	0.3877		
Posture Intercepts	\bar{u}_{0j}	0.0235	0.1534		

RR = Rate ratio; Reference AOI category: Torso (13) *** p < 0.001; ** p < 0.01; * p < 0.05

Table E.3: Poisson multilevel regression estimates for Round 2 VT AOI iteration

	$\hat{\delta}$ label	$\hat{\delta}$ (<i>SE</i>)	RR	z-value	p-value
FIXED EFFECTS					
Intercept	$\hat{\delta}_{0,0,0}$	2.88 (0.11)	17.84	25.55	< 0.001***
Group, Treatment vs Control	$\hat{\delta}_{1,0,0}$	−0.12 (0.12)	0.89	−0.96	0.335
AOI (Round 2)					
Rt Foot (1)	$\hat{\delta}_{0,0,1}$	−0.61 (0.03)	0.54	−20.61	< 0.001***
Rt Knee (2)	$\hat{\delta}_{0,0,2}$	−0.79 (0.12)	0.45	−6.54	< 0.001***
Rt Hand (3)	$\hat{\delta}_{0,0,3}$	−0.59 (0.02)	0.56	−23.68	< 0.001***
Lt Foot (7)	$\hat{\delta}_{0,0,4}$	−1.17 (0.04)	0.31	−28.75	< 0.001***
Lt Knee (8)	$\hat{\delta}_{0,0,5}$	−0.81 (0.08)	0.44	−10.83	< 0.001***
Lt Hand (9)	$\hat{\delta}_{0,0,6}$	−1.08 (0.03)	0.34	−38.41	< 0.001***
Head (14)	$\hat{\delta}_{0,0,7}$	0.32 (0.03)	1.38	10.02	< 0.001***
Neck (15)	$\hat{\delta}_{0,0,8}$	−0.09 (0.02)	0.92	−3.83	< 0.001***
Sternum (16)	$\hat{\delta}_{0,0,9}$	0.25 (0.02)	1.29	10.41	< 0.001***
Middle of Feet (17)	$\hat{\delta}_{0,0,10}$	−0.84 (0.03)	0.43	−30.51	< 0.001***
Lt Hand (9)/ Torso (13)	$\hat{\delta}_{0,0,11}$	−0.21 (0.07)	0.81	−3.25	< 0.001***
Rt Shoulder (6)/ Neck (15)	$\hat{\delta}_{0,0,12}$	−0.16 (0.06)	0.86	−2.59	0.010**
Rt Hand (3)/ Lt Hand (9)/ Sternum (16)	$\hat{\delta}_{0,0,13}$	0.90 (0.05)	2.46	18.06	< 0.001***
Rt Elbow (5)/ Torso (13)	$\hat{\delta}_{0,0,14}$	0.84 (0.05)	2.31	15.52	< 0.001***
Lt Shoulder (12)/ Torso (13)	$\hat{\delta}_{0,0,15}$	0.69 (0.05)	1.99	13.45	< 0.001***
Rt Hand (3)/ Neck (15)	$\hat{\delta}_{0,0,16}$	0.89 (0.05)	2.43	16.73	< 0.001***
Interaction: Group (Treatment) × AOI					
Rt Foot (1)	$\hat{\delta}_{1,0,1}$	0.30 (0.04)	1.35	8.17	< 0.001***
Rt Knee (2)	$\hat{\delta}_{1,0,2}$	0.09 (0.17)	1.09	0.53	0.596
Rt Hand (3)	$\hat{\delta}_{1,0,3}$	0.06 (0.03)	1.06	1.69	0.091
Lt Foot (7)	$\hat{\delta}_{1,0,4}$	0.34 (0.05)	1.41	6.72	< 0.001***
Lt Knee (8)	$\hat{\delta}_{1,0,5}$	0.38 (0.10)	1.46	3.95	< 0.001***
Lt Hand (9)	$\hat{\delta}_{1,0,6}$	0.31 (0.04)	1.36	8.14	< 0.001***
Head (14)	$\hat{\delta}_{1,0,7}$	0.10 (0.04)	1.11	2.80	0.005**
Neck (15)	$\hat{\delta}_{1,0,8}$	0.29 (0.03)	1.33	9.37	< 0.001***
Sternum (16)	$\hat{\delta}_{1,0,9}$	−0.07 (0.03)	0.93	−2.24	0.025*
Middle of Feet (17)	$\hat{\delta}_{1,0,10}$	0.16 (0.04)	1.17	4.19	< 0.001***
Lt Hand (9)/ Torso (13)	$\hat{\delta}_{1,0,11}$	0.02 (0.09)	1.02	0.18	0.853
Rt Shoulder (6)/ Neck (15)	$\hat{\delta}_{1,0,12}$	0.32 (0.07)	1.38	4.50	< 0.001***
Rt Hand (3)/ Lt Hand (9)/ Sternum (16)	$\hat{\delta}_{1,0,13}$	−0.33 (0.06)	0.72	−5.26	< 0.001***
Rt Elbow (5)/ Torso (13)	$\hat{\delta}_{1,0,14}$	0.10 (0.05)	1.11	2.07	0.039*
Lt Shoulder (12)/ Torso (13)	$\hat{\delta}_{1,0,15}$	0.24 (0.05)	1.27	4.91	< 0.001***
Rt Hand (3)/ Neck (15)	$\hat{\delta}_{1,0,16}$	0.09 (0.06)	1.10	1.62	0.105
RANDOM EFFECTS					
	Notation	Var.	SD		
Participant Intercepts	\bar{u}_{i0}	0.1515	0.3893		
Posture Intercepts	\bar{u}_{0j}	0.1077	0.3282		
RR = Rate ratio; Reference AOI category: Torso (13) *** p < 0.001; ** p < 0.01; * p < 0.05					

Table E.4: Poisson multilevel regression estimates for Round 2 LRV T AOI iteration

	$\hat{\delta}$ label	$\hat{\delta}$ (SE)	RR	z-value	p-value
FIXED EFFECTS					
Intercept	$\hat{\delta}_{0,0,0}$	2.42 (0.11)	11.23	22.90	< 0.001***
Group, Treatment vs Control	$\hat{\delta}_{1,0,0}$	-0.24 (0.13)	0.79	-1.87	0.062
AOI (Round 2)					
Rt Foot (1)	$\hat{\delta}_{0,0,1}$	-0.68 (0.03)	0.51	-19.72	< 0.001***
Rt Knee (2)	$\hat{\delta}_{0,0,2}$	-0.85 (0.14)	0.43	-5.92	< 0.001***
Rt Hand (3)	$\hat{\delta}_{0,0,3}$	-0.39 (0.03)	0.67	-13.51	< 0.001***
Lt Foot (7)	$\hat{\delta}_{0,0,4}$	-1.30 (0.05)	0.27	-26.60	< 0.001***
Lt Knee (8)	$\hat{\delta}_{0,0,5}$	-0.83 (0.09)	0.44	-9.16	< 0.001***
Lt Hand (9)	$\hat{\delta}_{0,0,6}$	-1.16 (0.04)	0.31	-32.00	< 0.001***
Head (14)	$\hat{\delta}_{0,0,7}$	0.38 (0.04)	1.46	10.51	< 0.001***
Neck (15)	$\hat{\delta}_{0,0,8}$	0.00 (0.03)	1.00	-0.17	0.866
Sternum (16)	$\hat{\delta}_{0,0,9}$	0.28 (0.03)	1.33	9.75	< 0.001***
Middle of Feet (17)	$\hat{\delta}_{0,0,10}$	-0.82 (0.04)	0.44	-23.43	< 0.001***
Lt Hand (9)/ Torso (13)	$\hat{\delta}_{0,0,11}$	0.03 (0.08)	1.03	0.37	0.712
Rt Shoulder (6)/ Neck (15)	$\hat{\delta}_{0,0,12}$	0.34 (0.07)	1.40	5.18	< 0.001***
Rt Hand (3)/ Lt Hand (9)/ Sternum (16)	$\hat{\delta}_{0,0,13}$	1.16 (0.05)	3.19	22.44	< 0.001***
Rt Elbow (5)/ Torso (13)	$\hat{\delta}_{0,0,14}$	-0.05 (0.06)	0.95	-0.81	0.419
Lt Shoulder (12)/ Torso (13)	$\hat{\delta}_{0,0,15}$	-0.10 (0.06)	0.91	-1.56	0.118
Rt Hand (3)/ Neck (15)	$\hat{\delta}_{0,0,16}$	1.05 (0.05)	2.87	19.31	< 0.001***
Outside Area	$\hat{\delta}_{0,0,17}$	0.66 (0.02)	1.94	30.85	< 0.001***
Interaction: Group (Treatment) \times AOI					
Rt Foot (1)	$\hat{\delta}_{1,0,1}$	0.42 (0.05)	1.52	9.06	< 0.001***
Rt Knee (2)	$\hat{\delta}_{1,0,2}$	0.35 (0.19)	1.42	1.83	0.067
Rt Hand (3)	$\hat{\delta}_{1,0,3}$	-0.03 (0.04)	0.97	-0.67	0.502
Lt Foot (7)	$\hat{\delta}_{1,0,4}$	0.51 (0.06)	1.67	8.03	< 0.001***
Lt Knee (8)	$\hat{\delta}_{1,0,5}$	0.52 (0.12)	1.68	4.48	< 0.001***
Lt Hand (9)	$\hat{\delta}_{1,0,6}$	0.44 (0.05)	1.56	8.99	< 0.001***
Head (14)	$\hat{\delta}_{1,0,7}$	0.10 (0.05)	1.11	2.15	0.031*
Neck (15)	$\hat{\delta}_{1,0,8}$	0.31 (0.04)	1.36	7.98	< 0.001***
Sternum (16)	$\hat{\delta}_{1,0,9}$	-0.17 (0.04)	0.84	-3.94	< 0.001***
Middle of Feet (17)	$\hat{\delta}_{1,0,10}$	0.29 (0.05)	1.34	5.97	< 0.001***
Lt Hand (9)/ Torso (13)	$\hat{\delta}_{1,0,11}$	0.32 (0.10)	1.37	3.21	0.001**
Rt Shoulder (6)/ Neck (15)	$\hat{\delta}_{1,0,12}$	0.14 (0.09)	1.15	1.64	0.101
Rt Hand (3)/ Lt Hand (9)/ Sternum (16)	$\hat{\delta}_{1,0,13}$	-0.29 (0.07)	0.75	-4.08	< 0.001***
Rt Elbow (5)/ Torso (13)	$\hat{\delta}_{1,0,14}$	-0.06 (0.09)	0.94	-0.66	0.510
Lt Shoulder (12)/ Torso (13)	$\hat{\delta}_{1,0,15}$	0.29 (0.08)	1.34	3.71	< 0.001***
Rt Hand (3)/ Neck (15)	$\hat{\delta}_{1,0,16}$	-0.10 (0.07)	0.90	-1.44	0.149
Outside Area	$\hat{\delta}_{1,0,17}$	0.40 (0.03)	1.49	13.17	< 0.001***
RANDOM EFFECTS					
	Notation	Var.	SD		
Participant Intercepts	\bar{u}_{i0}	0.1511	0.3888		
Posture Intercepts	\bar{u}_{0j}	0.0711	0.2666		

RR = Rate ratio; Reference AOI category: Torso (13) *** $p < 0.001$; ** $p < 0.01$; * $p < 0.05$

Zero-Inflated Poisson Regression

Table E.5: Zero Inflated Poisson multilevel regression estimates for Round 1 VT AOI iteration

	$\hat{\delta}$ label	$\hat{\delta}$ (SE)	RR	z-value	p-value
FIXED EFFECTS					
Intercept	$\hat{\delta}_{0,0,0}$	2.42 (0.07)	11.28	34.07	< 0.001***
Group, Treatment vs Control	$\hat{\delta}_{1,0,0}$	-0.16 (0.09)	0.86	-1.66	0.096
AOI (Round 1)					
Rt Foot (1)	$\hat{\delta}_{0,0,1}$	-0.42 (0.03)	0.66	-16.33	< 0.001***
Rt Knee (2)	$\hat{\delta}_{0,0,2}$	-0.96 (0.04)	0.38	-27.27	< 0.001***
Rt Hand (3)	$\hat{\delta}_{0,0,3}$	-0.16 (0.03)	0.85	-5.70	< 0.001***
Rt Hip (4)	$\hat{\delta}_{0,0,4}$	-0.61 (0.03)	0.54	-19.56	< 0.001***
Rt Elbow (5)	$\hat{\delta}_{0,0,5}$	-0.69 (0.03)	0.50	-21.70	< 0.001***
Rt Shoulder (6)	$\hat{\delta}_{0,0,6}$	-0.16 (0.02)	0.85	-6.69	< 0.001***
Lt Foot (7)	$\hat{\delta}_{0,0,7}$	-0.64 (0.03)	0.53	-19.80	< 0.001***
Lt Knee (8)	$\hat{\delta}_{0,0,8}$	-0.77 (0.04)	0.46	-20.22	< 0.001***
Lt Hand (9)	$\hat{\delta}_{0,0,9}$	-0.56 (0.04)	0.57	-14.43	< 0.001***
Lt Hip (10)	$\hat{\delta}_{0,0,10}$	-0.47 (0.03)	0.63	-15.25	< 0.001***
Lt Elbow (11)	$\hat{\delta}_{0,0,11}$	-0.58 (0.04)	0.56	-15.89	< 0.001***
Lt Shoulder (12)	$\hat{\delta}_{0,0,12}$	-0.55 (0.03)	0.58	-18.13	< 0.001***
Head (14)	$\hat{\delta}_{0,0,13}$	-0.20 (0.02)	0.82	-8.06	< 0.001***
Rt Knee (2)/ Rt Hand (3)	$\hat{\delta}_{0,0,14}$	0.06 (0.07)	1.07	0.97	0.334
Rt Hip (4)/ Rt Elbow (5)	$\hat{\delta}_{0,0,15}$	-1.33 (0.18)	0.26	-7.39	< 0.001***
Lt Knee (8)/ Lt Hand (9)	$\hat{\delta}_{0,0,16}$	-0.28 (0.09)	0.75	-3.07	0.002**
Lt Hip (10)/ Lt Elbow (11)	$\hat{\delta}_{0,0,17}$	-1.26 (0.19)	0.28	-6.55	< 0.001***
Rt Hip (4)/ Lt Hand (9)	$\hat{\delta}_{0,0,18}$	0.30 (0.05)	1.35	5.85	< 0.001***
Rt Knee (2)/ Lt Knee (8)	$\hat{\delta}_{0,0,19}$	-0.90 (0.09)	0.41	-9.74	< 0.001***
Rt Hip (4)/ Rt Shoulder (6)	$\hat{\delta}_{0,0,20}$	-0.99 (0.12)	0.37	-8.56	< 0.001***
Rt Hand (3)/ Lt Hand (9)	$\hat{\delta}_{0,0,21}$	1.14 (0.05)	3.13	21.83	< 0.001***
Rt Elbow (5)/ Lt Elbow (11)/ Torso (13)	$\hat{\delta}_{0,0,22}$	-0.07 (0.08)	0.93	-0.90	0.366
Rt Hip (4)/ Lt Shoulder (12)/ Torso (13)	$\hat{\delta}_{0,0,23}$	-0.03 (0.07)	0.97	-0.39	0.699
Rt Hand (3)/ Rt Elbow (5)/ Rt Shoulder (6)	$\hat{\delta}_{0,0,24}$	0.99 (0.05)	2.69	18.22	< 0.001***
Interaction: Group (Treatment) \times AOI					
Rt Foot (1)	$\hat{\delta}_{1,0,1}$	0.31 (0.04)	1.36	8.50	< 0.001***
Rt Knee (2)	$\hat{\delta}_{1,0,2}$	0.34 (0.05)	1.40	7.03	< 0.001***
Rt Hand (3)	$\hat{\delta}_{1,0,3}$	-0.04 (0.04)	0.96	-0.92	0.355
Rt Hip (4)	$\hat{\delta}_{1,0,4}$	0.18 (0.04)	1.19	3.98	< 0.001***
Rt Elbow (5)	$\hat{\delta}_{1,0,5}$	0.27 (0.04)	1.32	6.17	< 0.001***
Rt Shoulder (6)	$\hat{\delta}_{1,0,6}$	0.08 (0.04)	1.08	2.24	0.025*
Lt Foot (7)	$\hat{\delta}_{1,0,7}$	0.40 (0.04)	1.49	9.03	< 0.001***
Lt Knee (8)	$\hat{\delta}_{1,0,8}$	0.15 (0.05)	1.17	2.88	0.004**
Lt Hand (9)	$\hat{\delta}_{1,0,9}$	0.32 (0.05)	1.38	6.22	< 0.001***
Lt Hip (10)	$\hat{\delta}_{1,0,10}$	-0.01 (0.04)	0.99	-0.22	0.828
Lt Elbow (11)	$\hat{\delta}_{1,0,11}$	-0.04 (0.05)	0.96	-0.71	0.477
Lt Shoulder (12)	$\hat{\delta}_{1,0,12}$	0.26 (0.04)	1.30	6.23	< 0.001***
Head (14)	$\hat{\delta}_{1,0,13}$	0.34 (0.03)	1.41	9.89	< 0.001***
Rt Knee (2)/ Rt Hand (3)	$\hat{\delta}_{1,0,14}$	0.06 (0.09)	1.07	0.70	0.482
Rt Hip (4)/ Rt Elbow (5)	$\hat{\delta}_{1,0,15}$	0.61 (0.22)	1.84	2.78	0.005**
Lt Knee (8)/ Lt Hand (9)	$\hat{\delta}_{1,0,16}$	0.09 (0.13)	1.10	0.74	0.457
Lt Hip (10)/ Lt Elbow (11)	$\hat{\delta}_{1,0,17}$	0.18 (0.25)	1.19	0.71	0.48
Rt Hip (4)/ Lt Hand (9)	$\hat{\delta}_{1,0,18}$	-0.16 (0.07)	0.85	-2.18	0.030*
Rt Knee (2)/ Lt Knee (8)	$\hat{\delta}_{1,0,19}$	0.62 (0.12)	1.86	5.32	< 0.001***
Rt Hip (4)/ Rt Shoulder (6)	$\hat{\delta}_{1,0,20}$	0.14 (0.17)	1.15	0.83	0.408
Rt Hand (3)/ Lt Hand (9)	$\hat{\delta}_{1,0,21}$	-0.17 (0.07)	0.84	-2.60	0.009**
Rt Elbow (5)/ Lt Elbow (11)/ Torso (13)	$\hat{\delta}_{1,0,22}$	-0.24 (0.13)	0.78	-1.92	0.054
Rt Hip (4)/ Lt Shoulder (12)/ Torso (13)	$\hat{\delta}_{1,0,23}$	0.25 (0.09)	1.29	2.75	0.006**
Rt Hand (3)/ Rt Elbow (5)/ Rt Shoulder (6)	$\hat{\delta}_{1,0,24}$	-0.08 (0.07)	0.92	-1.18	0.237
RANDOM EFFECTS					
	Notation	Var.	SD		
Participant Intercepts	\bar{u}_{i0}	0.0816	0.2857		
Posture Intercepts	\bar{u}_{0j}	0.0158	0.1259		

RR = Rate ratio; Reference AOI category: Torso (13); Zero-inflation parameter = -0.5043;

*** $p < 0.001$; ** $p < 0.01$; * $p < 0.05$

Table E.6: Zero-Inflated Poisson multilevel regression estimates for Round 1 LRVT AOI iteration

	$\hat{\delta}$ label	$\hat{\delta}$ (SE)	RR	z-value	p-value
FIXED EFFECTS					
Intercept	$\hat{\delta}_{0,0,0}$	2.30 (0.07)	9.98	32.23	< 0.001***
Group, Treatment vs Control	$\hat{\delta}_{1,0,0}$	-0.14 (0.09)	0.87	-1.44	0.150
AOI (Round 1)					
Rt Foot (1)	$\hat{\delta}_{0,0,1}$	-0.37 (0.03)	0.69	-12.78	< 0.001***
Rt Knee (2)	$\hat{\delta}_{0,0,2}$	-1.00 (0.04)	0.37	-23.86	< 0.001***
Rt Hand (3)	$\hat{\delta}_{0,0,3}$	-0.03 (0.03)	0.97	-0.86	0.392
Rt Hip (4)	$\hat{\delta}_{0,0,4}$	-0.66 (0.03)	0.52	-18.87	< 0.001***
Rt Elbow (5)	$\hat{\delta}_{0,0,5}$	-0.57 (0.03)	0.57	-16.75	< 0.001***
Rt Shoulder (6)	$\hat{\delta}_{0,0,6}$	-0.19 (0.03)	0.83	-7.07	< 0.001***
Lt Foot (7)	$\hat{\delta}_{0,0,7}$	-0.59 (0.04)	0.55	-16.40	< 0.001***
Lt Knee (8)	$\hat{\delta}_{0,0,8}$	-0.68 (0.04)	0.51	-16.02	< 0.001***
Lt Hand (9)	$\hat{\delta}_{0,0,9}$	-0.48 (0.04)	0.62	-11.67	< 0.001***
Lt Hip (10)	$\hat{\delta}_{0,0,10}$	-0.43 (0.03)	0.65	-12.95	< 0.001***
Lt Elbow (11)	$\hat{\delta}_{0,0,11}$	-0.47 (0.04)	0.62	-11.86	< 0.001***
Lt Shoulder (12)	$\hat{\delta}_{0,0,12}$	-0.61 (0.03)	0.54	-17.68	< 0.001***
Head (14)	$\hat{\delta}_{0,0,13}$	-0.13 (0.03)	0.88	-4.87	< 0.001***
Rt Knee (2)/ Rt Hand (3)	$\hat{\delta}_{0,0,14}$	0.03 (0.07)	1.03	0.47	0.637
Rt Hip (4)/ Rt Elbow (5)	$\hat{\delta}_{0,0,15}$	-1.28 (0.18)	0.28	-6.91	< 0.001***
Lt Knee (8)/ Lt Hand (9)	$\hat{\delta}_{0,0,16}$	-0.49 (0.11)	0.62	-4.46	< 0.001***
Lt Hip (10)/ Lt Elbow (11)	$\hat{\delta}_{0,0,17}$	-0.99 (0.20)	0.37	-4.96	< 0.001***
Rt Hip (4)/ Lt Hand (9)	$\hat{\delta}_{0,0,18}$	0.27 (0.05)	1.31	4.92	< 0.001***
Rt Knee (2)/ Lt Knee (8)	$\hat{\delta}_{0,0,19}$	-1.32 (0.16)	0.27	-8.46	< 0.001***
Rt Hip (4)/ Rt Shoulder (6)	$\hat{\delta}_{0,0,20}$	-0.81 (0.12)	0.44	-6.49	< 0.001***
Rt Hand (3)/ Lt Hand (9)	$\hat{\delta}_{0,0,21}$	1.31 (0.05)	3.71	24.84	< 0.001***
Rt Elbow (5)/ Lt Elbow (11)/ Torso (13)	$\hat{\delta}_{0,0,22}$	0.10 (0.08)	1.11	1.24	0.214
Rt Hip (4)/ Lt Shoulder (12)/ Torso (13)	$\hat{\delta}_{0,0,23}$	0.02 (0.07)	1.02	0.26	0.793
Rt Hand (3)/ Rt Elbow (5)/ Rt Shoulder (6)	$\hat{\delta}_{0,0,24}$	0.98 (0.06)	2.66	17.27	< 0.001***
Outside Area	$\hat{\delta}_{0,0,25}$	0.05 (0.02)	1.05	2.15	0.031*
Interaction: Group (Treatment) \times AOI					
Rt Foot (1)	$\hat{\delta}_{1,0,1}$	0.24 (0.04)	1.27	6.01	< 0.001***
Rt Knee (2)	$\hat{\delta}_{1,0,2}$	0.34 (0.06)	1.40	6.04	< 0.001***
Rt Hand (3)	$\hat{\delta}_{1,0,3}$	-0.10 (0.04)	0.90	-2.28	0.023*
Rt Hip (4)	$\hat{\delta}_{1,0,4}$	0.18 (0.05)	1.20	3.70	< 0.001***
Rt Elbow (5)	$\hat{\delta}_{1,0,5}$	0.13 (0.05)	1.14	2.67	0.008**
Rt Shoulder (6)	$\hat{\delta}_{1,0,6}$	0.08 (0.04)	1.09	2.17	0.030*
Lt Foot (7)	$\hat{\delta}_{1,0,7}$	0.40 (0.05)	1.49	8.10	< 0.001***
Lt Knee (8)	$\hat{\delta}_{1,0,8}$	0.16 (0.06)	1.17	2.63	0.009**
Lt Hand (9)	$\hat{\delta}_{1,0,9}$	0.29 (0.06)	1.33	5.17	< 0.001***
Lt Hip (10)	$\hat{\delta}_{1,0,10}$	0.00 (0.05)	1.00	0.09	0.928
Lt Elbow (11)	$\hat{\delta}_{1,0,11}$	-0.13 (0.06)	0.88	-2.21	0.027*
Lt Shoulder (12)	$\hat{\delta}_{1,0,12}$	0.25 (0.05)	1.29	5.38	< 0.001***
Head (14)	$\hat{\delta}_{1,0,13}$	0.27 (0.04)	1.31	7.31	< 0.001***
Rt Knee (2)/ Rt Hand (3)	$\hat{\delta}_{1,0,14}$	0.10 (0.10)	1.10	1.00	0.318
Rt Hip (4)/ Rt Elbow (5)	$\hat{\delta}_{1,0,15}$	0.63 (0.23)	1.88	2.79	0.005**
Lt Knee (8)/ Lt Hand (9)	$\hat{\delta}_{1,0,16}$	0.49 (0.15)	1.63	3.29	< 0.001***
Lt Hip (10)/ Lt Elbow (11)	$\hat{\delta}_{1,0,17}$	-0.50 (0.30)	0.61	-1.68	0.094
Rt Hip (4)/ Lt Hand (9)	$\hat{\delta}_{1,0,18}$	-0.07 (0.08)	0.93	-0.94	0.349
Rt Knee (2)/ Lt Knee (8)	$\hat{\delta}_{1,0,19}$	0.73 (0.18)	2.09	3.97	< 0.001***
Rt Hip (4)/ Rt Shoulder (6)	$\hat{\delta}_{1,0,20}$	0.03 (0.18)	1.03	0.19	0.852
Rt Hand (3)/ Lt Hand (9)	$\hat{\delta}_{1,0,21}$	-0.19 (0.07)	0.83	-2.78	0.005**
Rt Elbow (5)/ Lt Elbow (11)/ Torso (13)	$\hat{\delta}_{1,0,22}$	-0.27 (0.13)	0.77	-2.09	0.036*
Rt Hip (4)/ Lt Shoulder (12)/ Torso (13)	$\hat{\delta}_{1,0,23}$	0.26 (0.10)	1.30	2.64	0.008**
Rt Hand (3)/ Rt Elbow (5)/ Rt Shoulder (6)	$\hat{\delta}_{1,0,24}$	-0.09 (0.07)	0.91	-1.23	0.217
Outside Area	$\hat{\delta}_{1,0,25}$	0.25 (0.03)	1.29	7.76	< 0.001***
RANDOM EFFECTS					
Participant Intercepts	Notation	Var.	SD		
	\bar{u}_{i0}	0.0822	0.2867		
Posture Intercepts	\bar{u}_{0j}	0.0153	0.1237		

RR = Rate ratio; Reference AOI category: Torso (13); Zero-inflation parameter = -0.3555;

*** $p < 0.001$; ** $p < 0.01$; * $p < 0.05$

Table E.7: Zero-Inflated Poisson multilevel regression estimates for Round 2 VT AOI iteration

	$\hat{\delta}$ label	$\hat{\delta}$ (SE)	RR	z-value	p-value
FIXED EFFECTS					
Intercept	$\hat{\delta}_{0,0,0}$	2.91 (0.10)	18.36	29.47	< 0.001***
Group, Treatment vs Control	$\hat{\delta}_{1,0,0}$	-0.10 (0.11)	0.90	-0.92	0.359
AOI (Round 2)					
Rt Foot (1)	$\hat{\delta}_{0,0,1}$	-0.52 (0.03)	0.60	-17.37	< 0.001***
Rt Knee (2)	$\hat{\delta}_{0,0,2}$	-0.61 (0.12)	0.54	-4.94	< 0.001***
Rt Hand (3)	$\hat{\delta}_{0,0,3}$	-0.21 (0.03)	0.81	-8.33	< 0.001***
Lt Foot (7)	$\hat{\delta}_{0,0,4}$	-0.78 (0.04)	0.46	-19.17	< 0.001***
Lt Knee (8)	$\hat{\delta}_{0,0,5}$	-0.60 (0.08)	0.55	-7.84	< 0.001***
Lt Hand (9)	$\hat{\delta}_{0,0,6}$	-0.70 (0.03)	0.50	-24.65	< 0.001***
Head (14)	$\hat{\delta}_{0,0,7}$	0.45 (0.03)	1.56	13.44	< 0.001***
Neck (15)	$\hat{\delta}_{0,0,8}$	0.01 (0.02)	1.01	0.39	0.698
Sternum (16)	$\hat{\delta}_{0,0,9}$	0.24 (0.02)	1.27	9.77	< 0.001***
Middle of Feet (17)	$\hat{\delta}_{0,0,10}$	-0.70 (0.03)	0.50	-25.49	< 0.001***
Lt Hand (9)/ Torso (13)	$\hat{\delta}_{0,0,11}$	-0.10 (0.07)	0.90	-1.60	0.109
Rt Shoulder (6)/ Neck (15)	$\hat{\delta}_{0,0,12}$	-0.19 (0.06)	0.82	-3.25	< 0.001***
Rt Hand (3)/ Lt Hand (9)/ Sternum (16)	$\hat{\delta}_{0,0,13}$	0.80 (0.05)	2.22	15.88	< 0.001***
Rt Elbow (5)/ Torso (13)	$\hat{\delta}_{0,0,14}$	0.85 (0.05)	2.34	15.76	< 0.001***
Lt Shoulder (12)/ Torso (13)	$\hat{\delta}_{0,0,15}$	0.71 (0.05)	2.03	13.81	< 0.001***
Rt Hand (3)/ Neck (15)	$\hat{\delta}_{0,0,16}$	0.84 (0.05)	2.32	15.87	< 0.001***
Interaction: Group (Treatment) \times AOI					
Rt Foot (1)	$\hat{\delta}_{1,0,1}$	0.28 (0.04)	1.33	7.77	< 0.001***
Rt Knee (2)	$\hat{\delta}_{1,0,2}$	-0.05 (0.17)	0.95	-0.31	0.758
Rt Hand (3)	$\hat{\delta}_{1,0,3}$	-0.04 (0.03)	0.96	-1.08	0.282
Lt Foot (7)	$\hat{\delta}_{1,0,4}$	0.37 (0.05)	1.45	7.17	< 0.001***
Lt Knee (8)	$\hat{\delta}_{1,0,5}$	0.33 (0.10)	1.39	3.40	< 0.001***
Lt Hand (9)	$\hat{\delta}_{1,0,6}$	0.27 (0.04)	1.31	7.11	< 0.001***
Head (14)	$\hat{\delta}_{1,0,7}$	0.04 (0.04)	1.04	0.96	0.336
Neck (15)	$\hat{\delta}_{1,0,8}$	0.24 (0.03)	1.27	7.84	< 0.001***
Sternum (16)	$\hat{\delta}_{1,0,9}$	-0.08 (0.03)	0.92	-2.42	0.015*
Middle of Feet (17)	$\hat{\delta}_{1,0,10}$	0.19 (0.04)	1.21	5.09	< 0.001***
Lt Hand (9)/ Torso (13)	$\hat{\delta}_{1,0,11}$	-0.04 (0.09)	0.97	-0.42	0.677
Rt Shoulder (6)/ Neck (15)	$\hat{\delta}_{1,0,12}$	0.37 (0.07)	1.44	5.15	< 0.001***
Rt Hand (3)/ Lt Hand (9)/ Sternum (16)	$\hat{\delta}_{1,0,13}$	-0.32 (0.06)	0.73	-5.17	< 0.001***
Rt Elbow (5)/ Torso (13)	$\hat{\delta}_{1,0,14}$	0.11 (0.05)	1.12	2.22	0.026*
Lt Shoulder (12)/ Torso (13)	$\hat{\delta}_{1,0,15}$	0.24 (0.05)	1.27	5.02	< 0.001***
Rt Hand (3)/ Neck (15)	$\hat{\delta}_{1,0,16}$	0.10 (0.06)	1.10	1.71	0.087
RANDOM EFFECTS					
	Notation	Var.	SD		
Participant Intercepts	\bar{u}_{i0}	0.1198	0.3461		
Posture Intercepts	\bar{u}_{0j}	0.0774	0.2782		

RR = Rate ratio; Reference AOI category: Torso (13); Zero-inflation parameter = -1.471;

*** $p < 0.001$; ** $p < 0.01$; * $p < 0.05$

Table E.8: Zero-Inflated Poisson multilevel regression estimates for Round 2 LRVT AOI iteration

	$\hat{\delta}$ label	$\hat{\delta}$ (SE)	RR	z-value	p-value
FIXED EFFECTS					
Intercept	$\hat{\delta}_{0,0,0}$	2.54 (0.10)	12.71	26.72	< 0.001***
Group, Treatment vs Control	$\hat{\delta}_{1,0,0}$	-0.18 (0.11)	0.84	-1.61	0.107
AOI (Round 2)					
Rt Foot (1)	$\hat{\delta}_{0,0,1}$	-0.41 (0.03)	0.67	-11.76	< 0.001***
Rt Knee (2)	$\hat{\delta}_{0,0,2}$	-0.43 (0.15)	0.65	-2.92	0.004**
Rt Hand (3)	$\hat{\delta}_{0,0,3}$	0.13 (0.03)	1.14	4.33	< 0.001***
Lt Foot (7)	$\hat{\delta}_{0,0,4}$	-0.71 (0.05)	0.49	-14.20	< 0.001***
Lt Knee (8)	$\hat{\delta}_{0,0,5}$	-0.48 (0.09)	0.62	-5.10	< 0.001***
Lt Hand (9)	$\hat{\delta}_{0,0,6}$	-0.49 (0.04)	0.61	-13.30	< 0.001***
Head (14)	$\hat{\delta}_{0,0,7}$	0.45 (0.04)	1.56	12.16	< 0.001***
Neck (15)	$\hat{\delta}_{0,0,8}$	0.05 (0.03)	1.05	1.74	0.082
Sternum (16)	$\hat{\delta}_{0,0,9}$	0.21 (0.03)	1.24	7.29	< 0.001***
Middle of Feet (17)	$\hat{\delta}_{0,0,10}$	-0.53 (0.04)	0.59	-15.02	< 0.001***
Lt Hand (9)/ Torso (13)	$\hat{\delta}_{0,0,11}$	0.05 (0.08)	1.05	0.67	0.501
Rt Shoulder (6)/ Neck (15)	$\hat{\delta}_{0,0,12}$	0.29 (0.07)	1.34	4.44	< 0.001***
Rt Hand (3)/ Lt Hand (9)/ Sternum (16)	$\hat{\delta}_{0,0,13}$	1.04 (0.05)	2.83	19.98	< 0.001***
Rt Elbow (5)/ Torso (13)	$\hat{\delta}_{0,0,14}$	-0.17 (0.06)	0.84	-2.73	0.006**
Lt Shoulder (12)/ Torso (13)	$\hat{\delta}_{0,0,15}$	-0.23 (0.06)	0.80	-3.71	< 0.001***
Rt Hand (3)/ Neck (15)	$\hat{\delta}_{0,0,16}$	0.87 (0.05)	2.38	15.87	< 0.001***
Outside Area	$\hat{\delta}_{0,0,17}$	0.55 (0.02)	1.74	25.65	< 0.001***
Interaction: Group (Treatment) \times AOI					
Rt Foot (1)	$\hat{\delta}_{1,0,1}$	0.31 (0.05)	1.36	6.58	< 0.001***
Rt Knee (2)	$\hat{\delta}_{1,0,2}$	0.03 (0.20)	1.03	0.14	0.891
Rt Hand (3)	$\hat{\delta}_{1,0,3}$	-0.13 (0.04)	0.88	-2.99	0.003**
Lt Foot (7)	$\hat{\delta}_{1,0,4}$	0.48 (0.07)	1.61	7.27	< 0.001***
Lt Knee (8)	$\hat{\delta}_{1,0,5}$	0.42 (0.12)	1.52	3.54	< 0.001***
Lt Hand (9)	$\hat{\delta}_{1,0,6}$	0.35 (0.05)	1.42	7.04	< 0.001***
Head (14)	$\hat{\delta}_{1,0,7}$	0.00 (0.05)	1.00	-0.06	0.956
Neck (15)	$\hat{\delta}_{1,0,8}$	0.22 (0.04)	1.25	5.70	< 0.001***
Sternum (16)	$\hat{\delta}_{1,0,9}$	-0.17 (0.04)	0.84	-4.01	< 0.001***
Middle of Feet (17)	$\hat{\delta}_{1,0,10}$	0.29 (0.05)	1.33	5.83	< 0.001***
Lt Hand (9)/ Torso (13)	$\hat{\delta}_{1,0,11}$	0.20 (0.10)	1.22	2.00	0.046*
Rt Shoulder (6)/ Neck (15)	$\hat{\delta}_{1,0,12}$	0.07 (0.09)	1.07	0.77	0.441
Rt Hand (3)/ Lt Hand (9)/ Sternum (16)	$\hat{\delta}_{1,0,13}$	-0.32 (0.07)	0.72	-4.54	< 0.001***
Rt Elbow (5)/ Torso (13)	$\hat{\delta}_{1,0,14}$	-0.09 (0.09)	0.92	-0.97	0.334
Lt Shoulder (12)/ Torso (13)	$\hat{\delta}_{1,0,15}$	0.30 (0.08)	1.35	3.82	< 0.001***
Rt Hand (3)/ Neck (15)	$\hat{\delta}_{1,0,16}$	-0.14 (0.07)	0.87	-1.90	0.058
Outside Area	$\hat{\delta}_{1,0,17}$	0.37 (0.03)	1.45	12.07	< 0.001***
RANDOM EFFECTS					
	Notation	Var.	SD		
Participant Intercepts	\bar{u}_{i0}	0.1169	0.3419		
Posture Intercepts	\bar{u}_{0j}	0.0627	0.2504		

RR = Rate ratio; Reference AOI category: Torso (13); Zero-inflation parameter = -1.037;

*** $p < 0.001$; ** $p < 0.01$; * $p < 0.05$

APPENDIX F

Gaze-Point Visualizations by Posture ID

Included in Appendix F are scatterplots depicting treatment and control gaze points on each Posture ID as divided by VT and LRVt AOIs and defined by centers from Round 1 and Round 2 (the four iterations of the data). Also included in this appendix are the associated bar charts showing the proportional distribution of gaze points from treatment and control subjects based on these iterations. This appendix organizes the visualizations by Posture ID. There are two figures for each Posture ID. The figures associated with Posture ID 1, for example, are Figures F.1 - F.2 and the figures associated with Posture ID 2 are Figures F.3 - F.4. This pattern continues for all remaining 20 Posture IDs.

It should be noted that the scatterplots of the data are not the best way to view the distribution of the treatment and control gaze points for two main reasons. The first reason discussed in Section 1.2.2 is that there is a considerable amount of overplotting. The second reason is that the scatterplots were created by plotting the control gaze points first and overlaying the treatment gaze points thereafter. This makes it appear as though there is a much greater amount of treatment gaze points because the treatment gaze points are plotted over the control points. If the treatment gaze points were plotted first, it would appear as though there was a much greater amount of control gaze points. The reason the scatterplots were used in spite of these major shortcomings is because it was the best way to give a general idea of the gaze-point distribution while also showing the method and round used to define the AOIs. To overcome these shortcomings, a bar chart of the proportional distribution of gaze points separated by treatment and control participants was provided to give the more specific detail in relation to the comparison per AOI.

Posture ID 1 Round 1 Visualizations

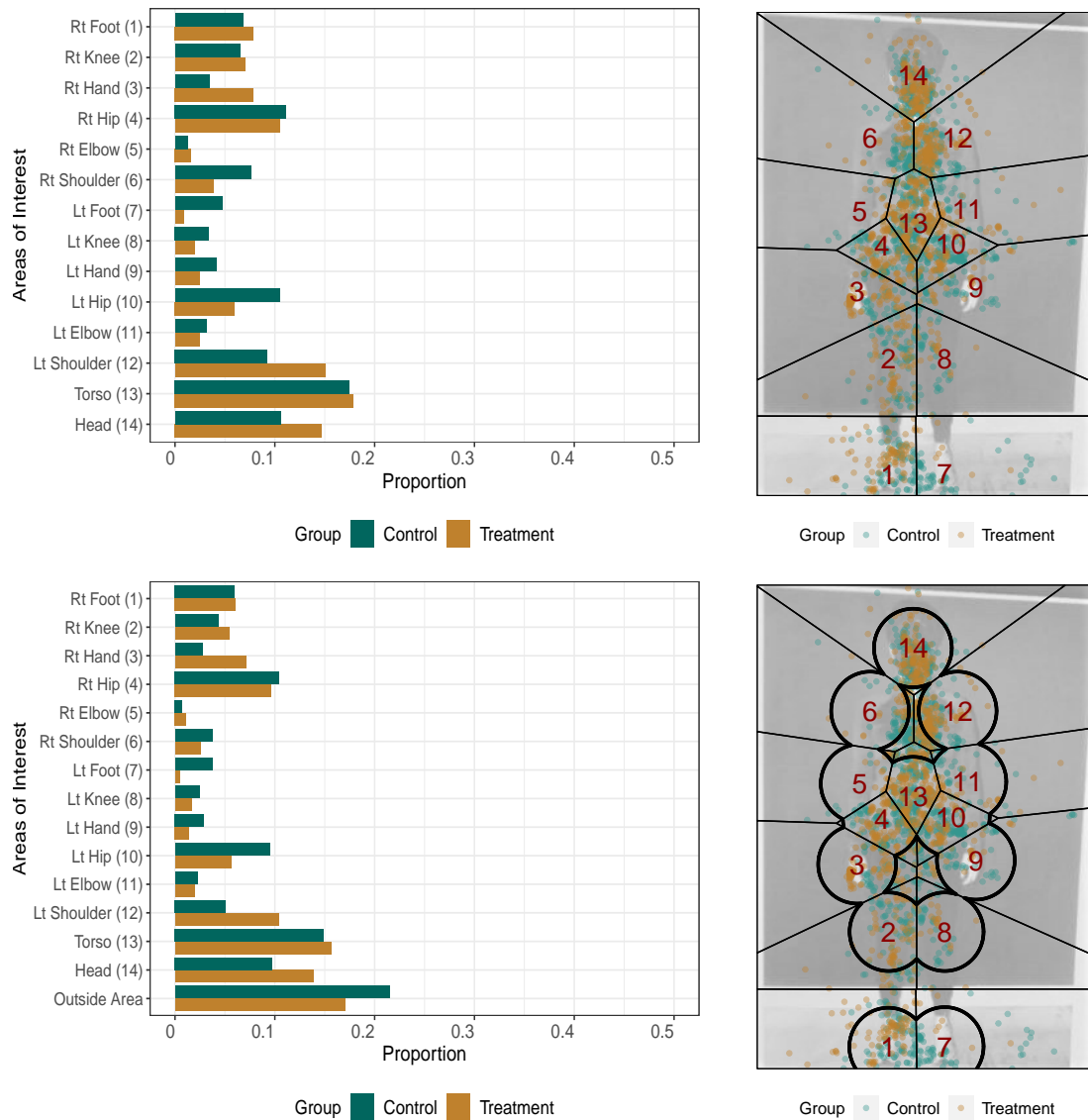


Fig. F.1: Posture ID 1 gaze-point bar chart (left) and scatterplot (right) for Round 1 VT (top) and Round 1 LRVT (bottom) AOIs.

Posture ID 1 Round 2 Visualizations

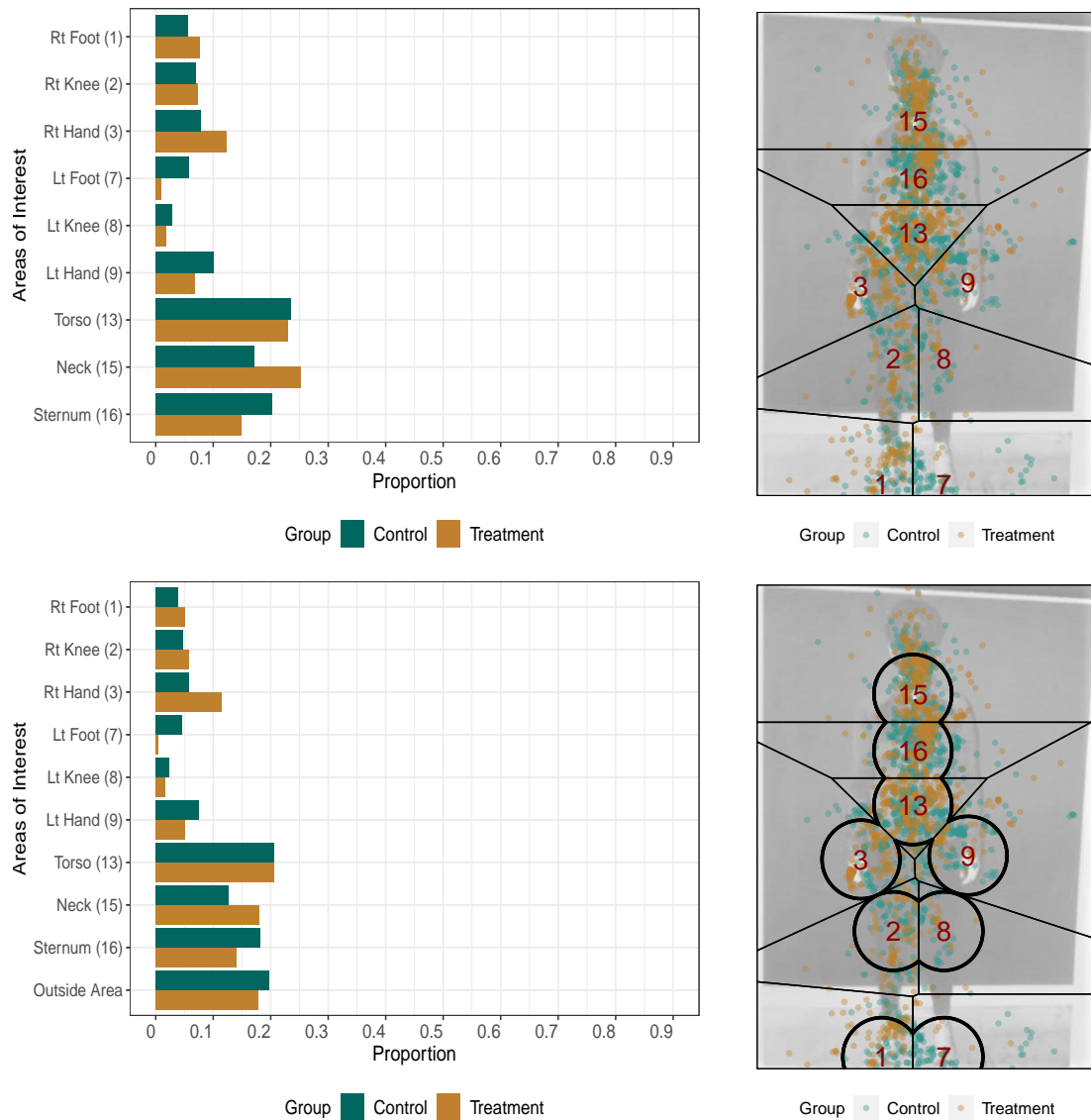


Fig. F.2: Posture ID 1 gaze-point bar chart (left) and scatterplot (right) for Round 2 VT (top) and Round 2 LRVT (bottom) AOIs.

Posture ID 2 Round 1 Visualizations

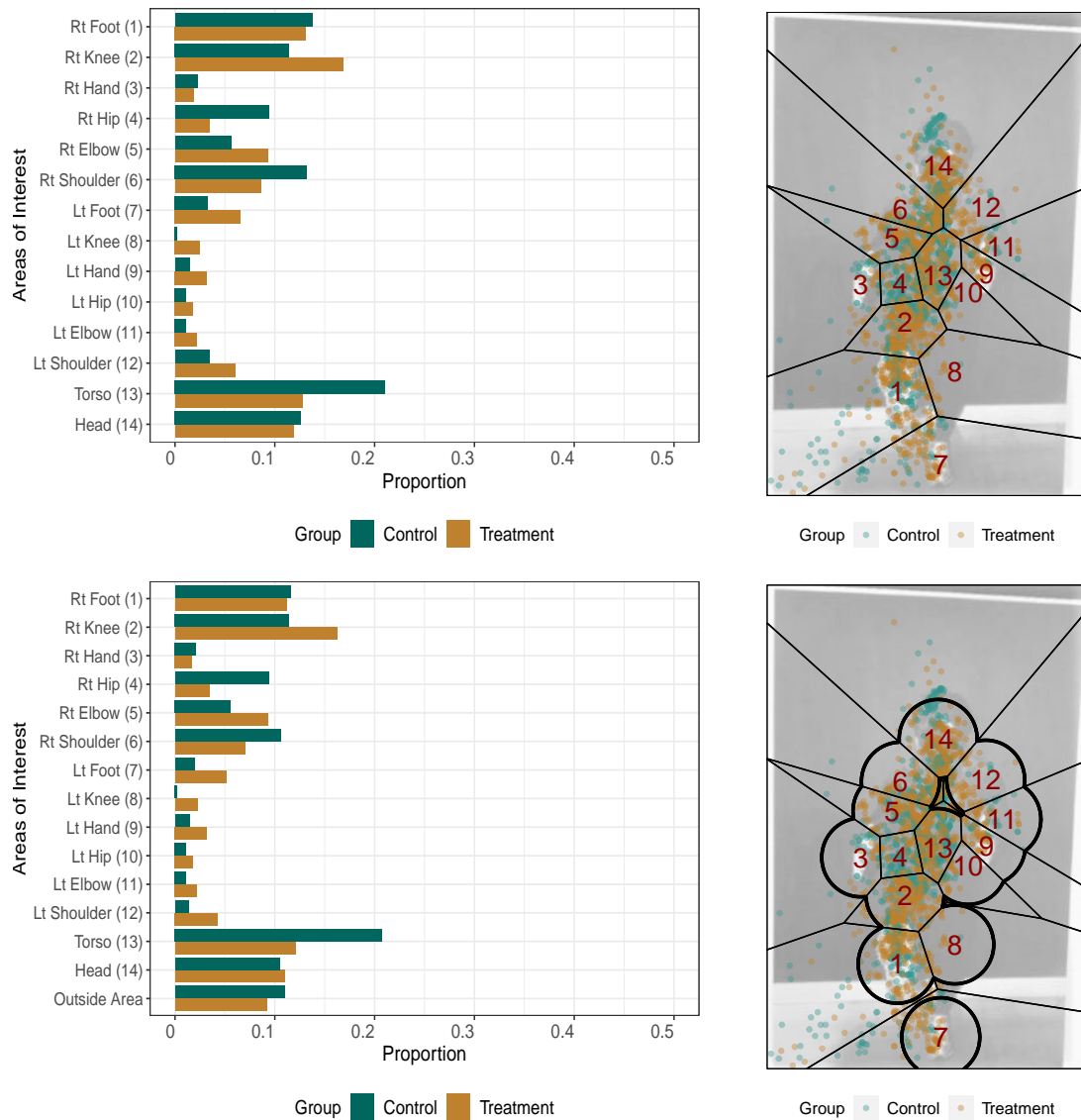


Fig. F.3: Posture ID 2 gaze-point bar chart (left) and scatterplot (right) for Round 1 VT (top) and Round 1 LRVT (bottom) AOIs.

Posture ID 2 Round 2 Visualizations

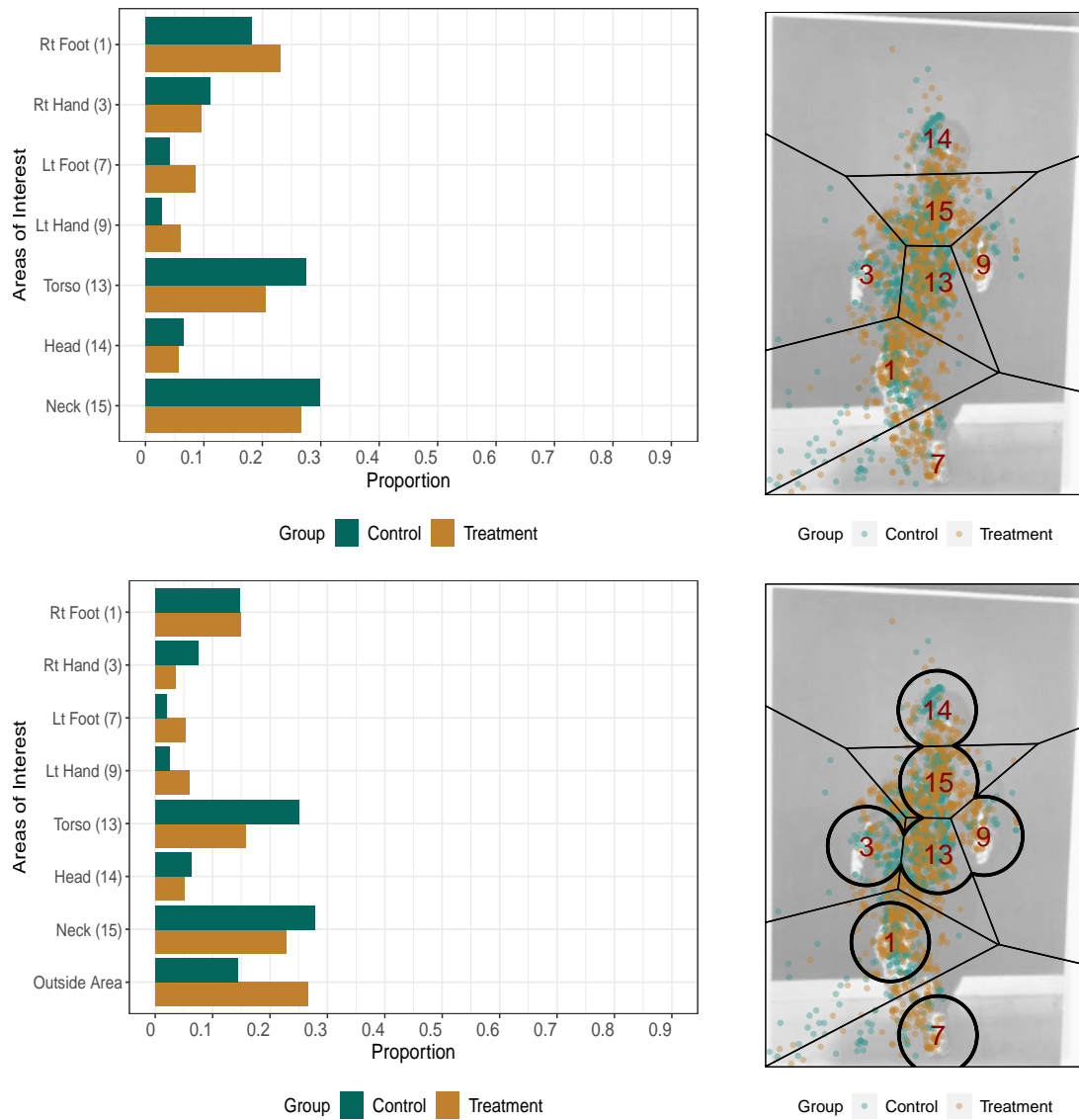


Fig. F.4: Posture ID 2 gaze-point bar chart (left) and scatterplot (right) for Round 2 VT (top) and Round 2 LRVT (bottom) AOIs.

Posture ID 3 Round 1 Visualizations

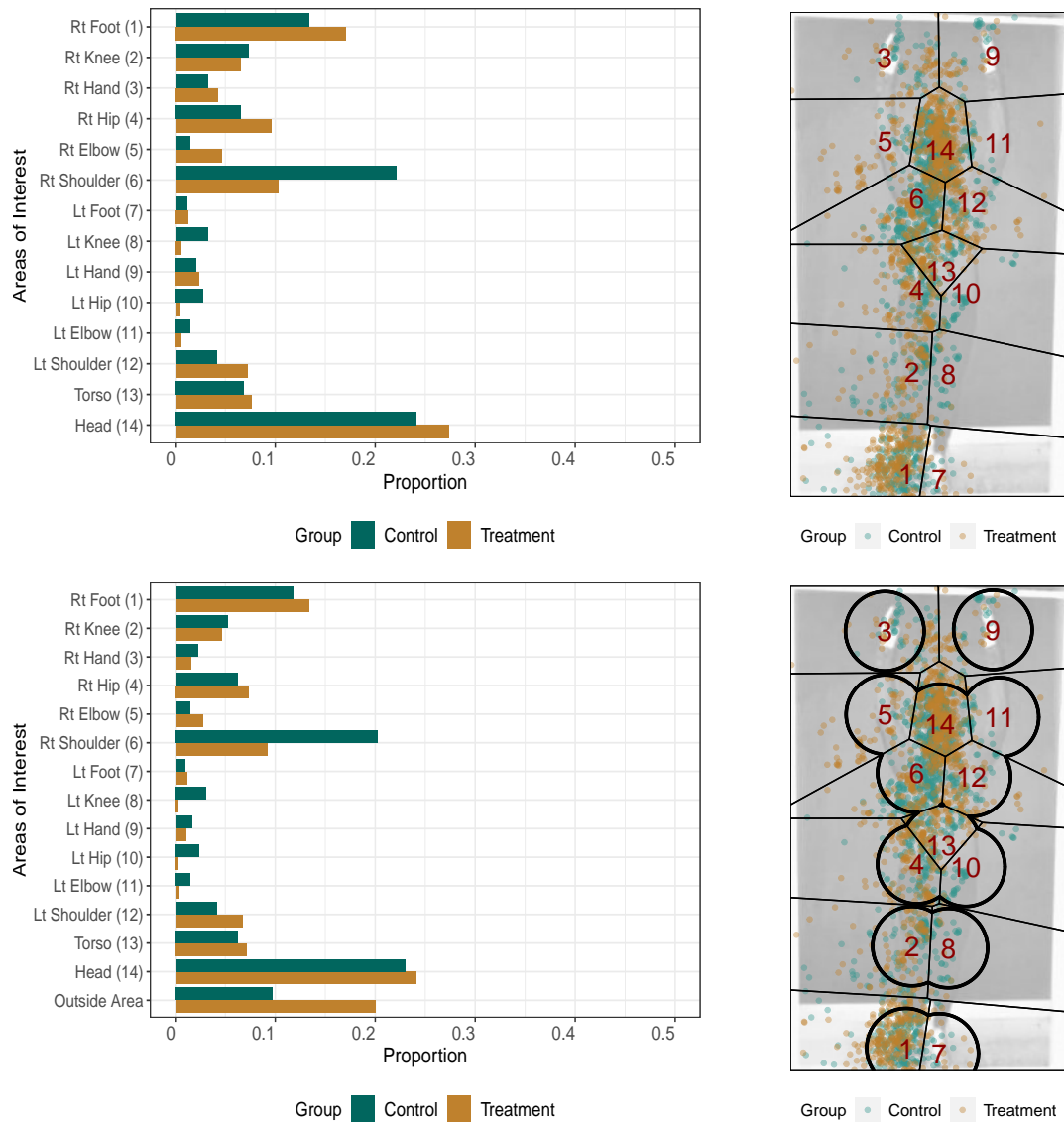


Fig. F.5: Posture ID 3 gaze-point bar chart (left) and scatterplot (right) for Round 1 VT (top) and Round 1 LRVT (bottom) AOIs.

Posture ID 3 Round 2 Visualizations

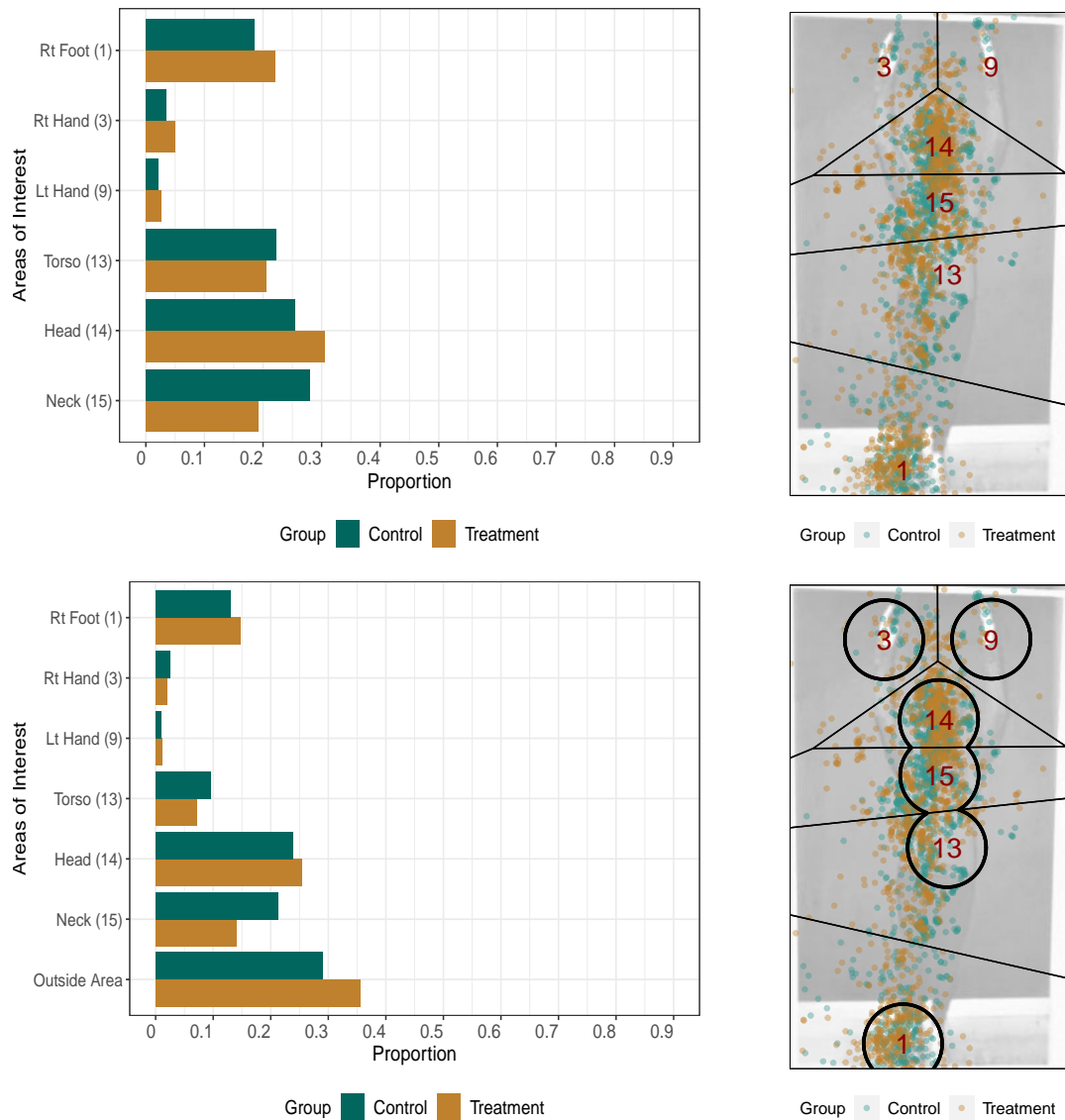


Fig. F.6: Posture ID 3 gaze-point bar chart (left) and scatterplot (right) for Round 2 VT (top) and Round 2 LRV (bottom) AOIs.

Posture ID 4 Round 1 Visualizations

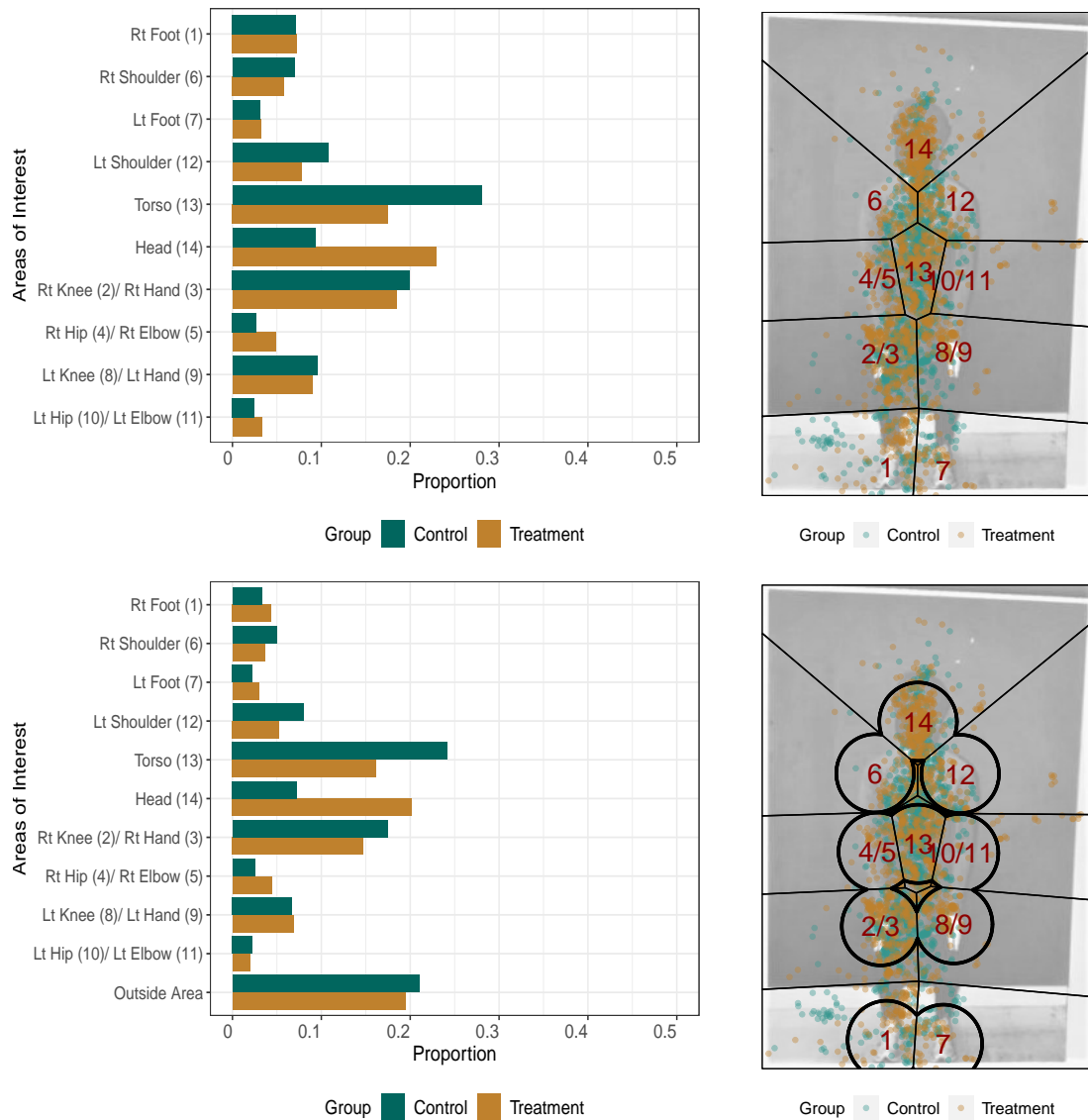


Fig. F.7: Posture ID 4 gaze-point bar chart (left) and scatterplot (right) for Round 1 VT (top) and Round 1 LRVT (bottom) AOIs.

Posture ID 4 Round 2 Visualizations

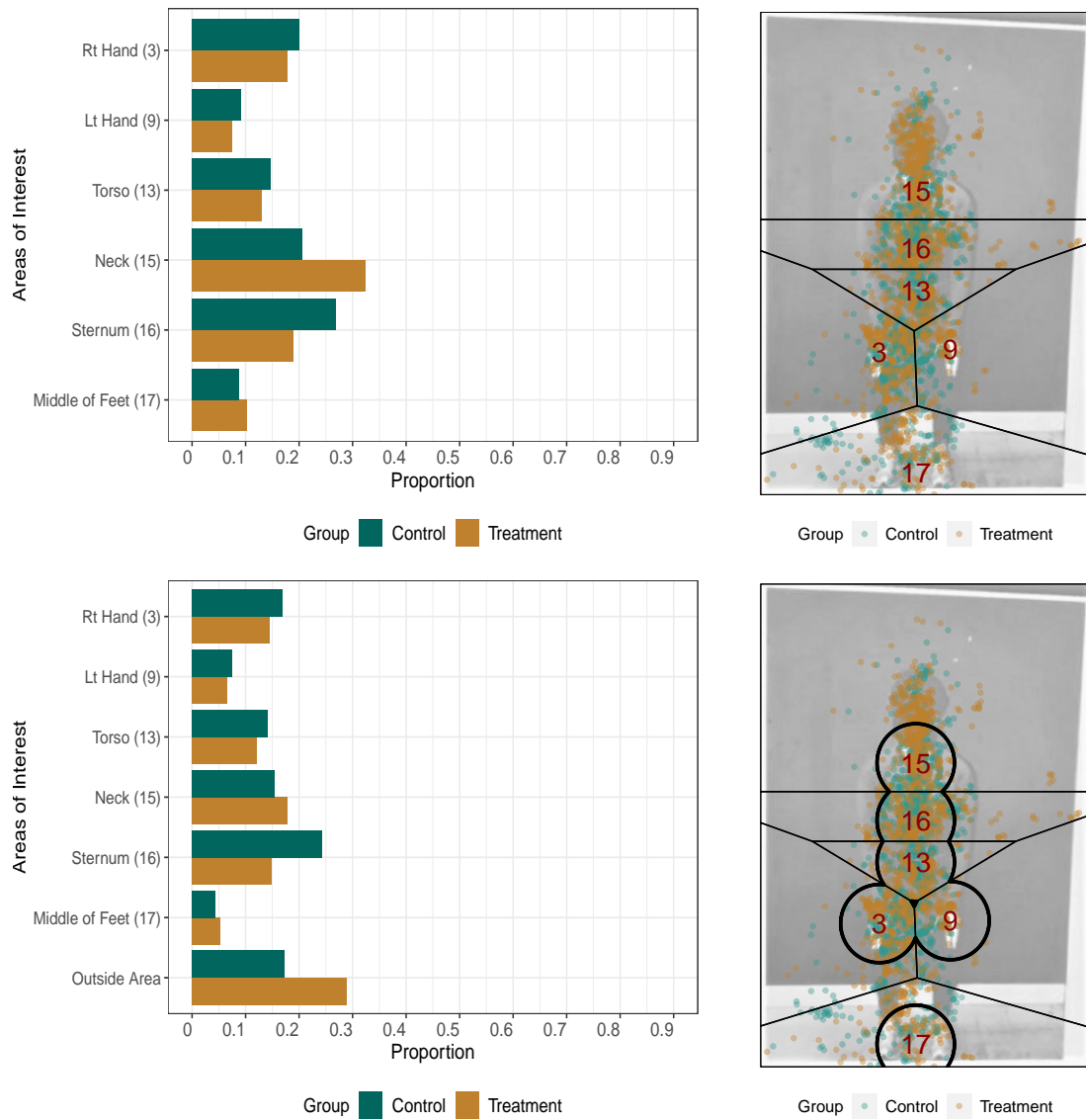


Fig. F.8: Posture ID 4 gaze-point bar chart (left) and scatterplot (right) for Round 2 VT (top) and Round 2 LRV (bottom) AOIs.

Posture ID 5 Round 1 Visualizations

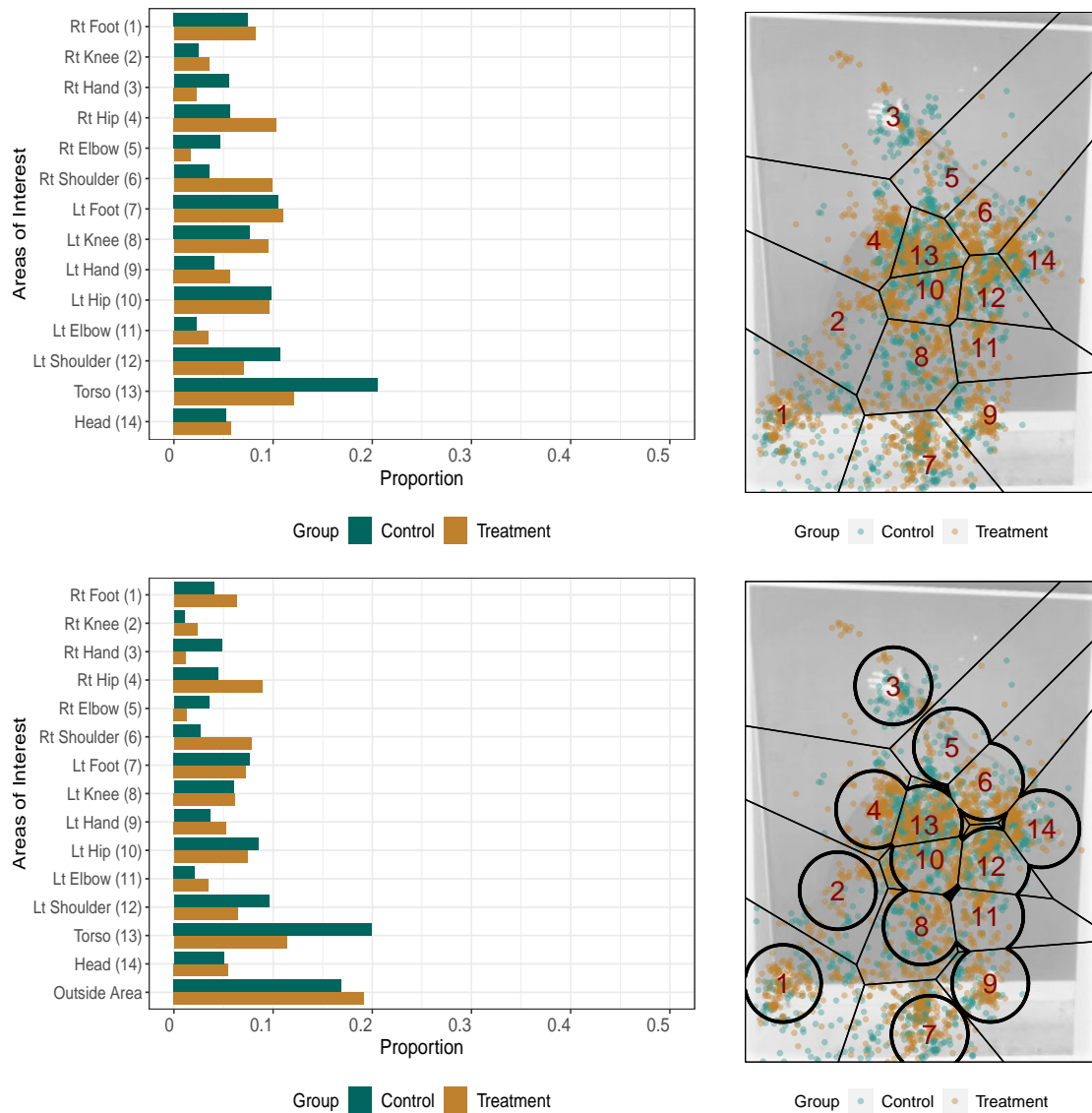


Fig. F.9: Posture ID 5 gaze-point bar chart (left) and scatterplot (right) for Round 1 VT (top) and Round 1 LRVT (bottom) AOIs.

Posture ID 5 Round 2 Visualizations

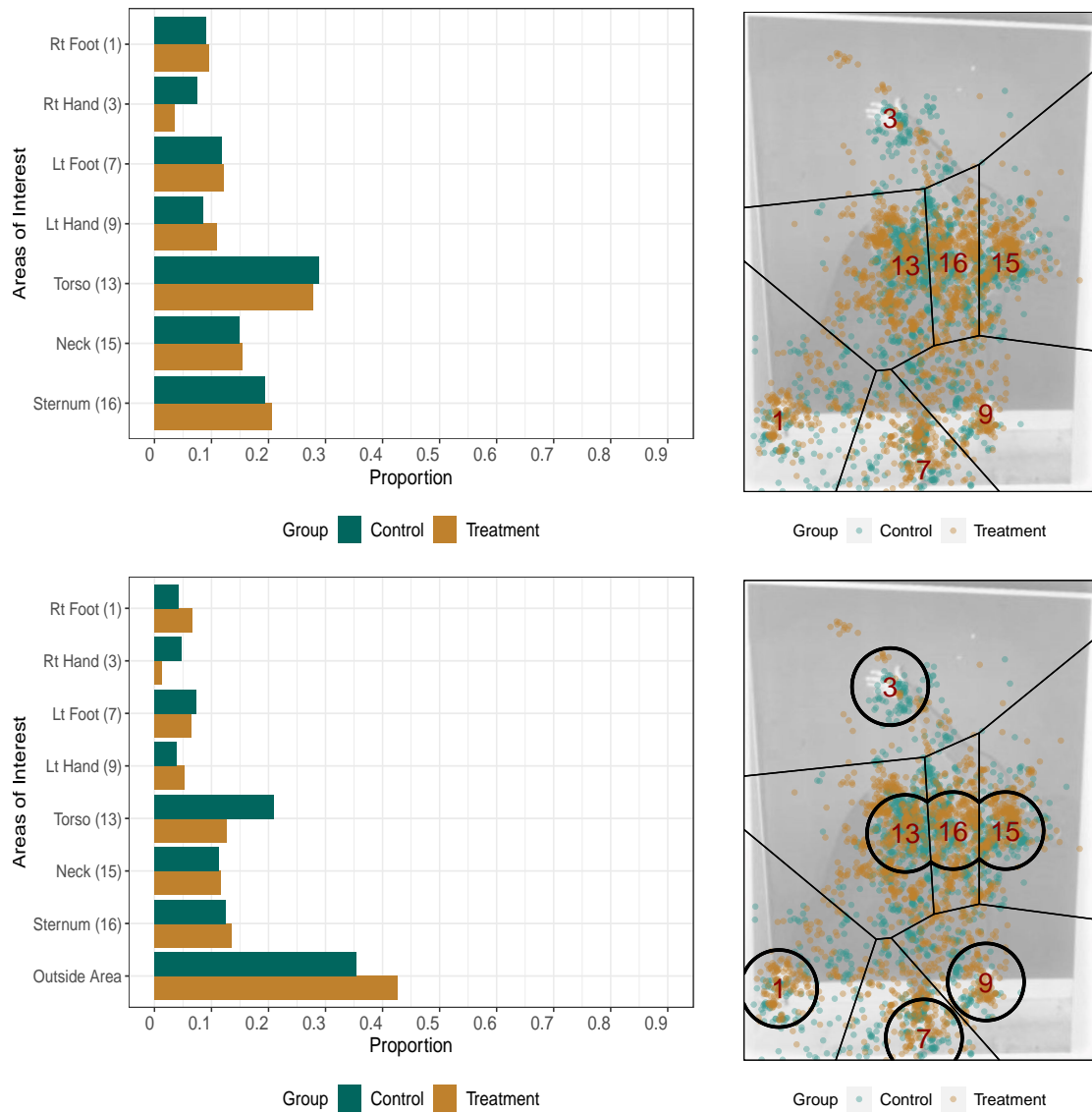


Fig. F.10: Posture ID 5 gaze-point bar chart (left) and scatterplot (right) for Round 2 VT (top) and Round 2 LRV (bottom) AOIs.

Posture ID 6 Round 1 Visualizations

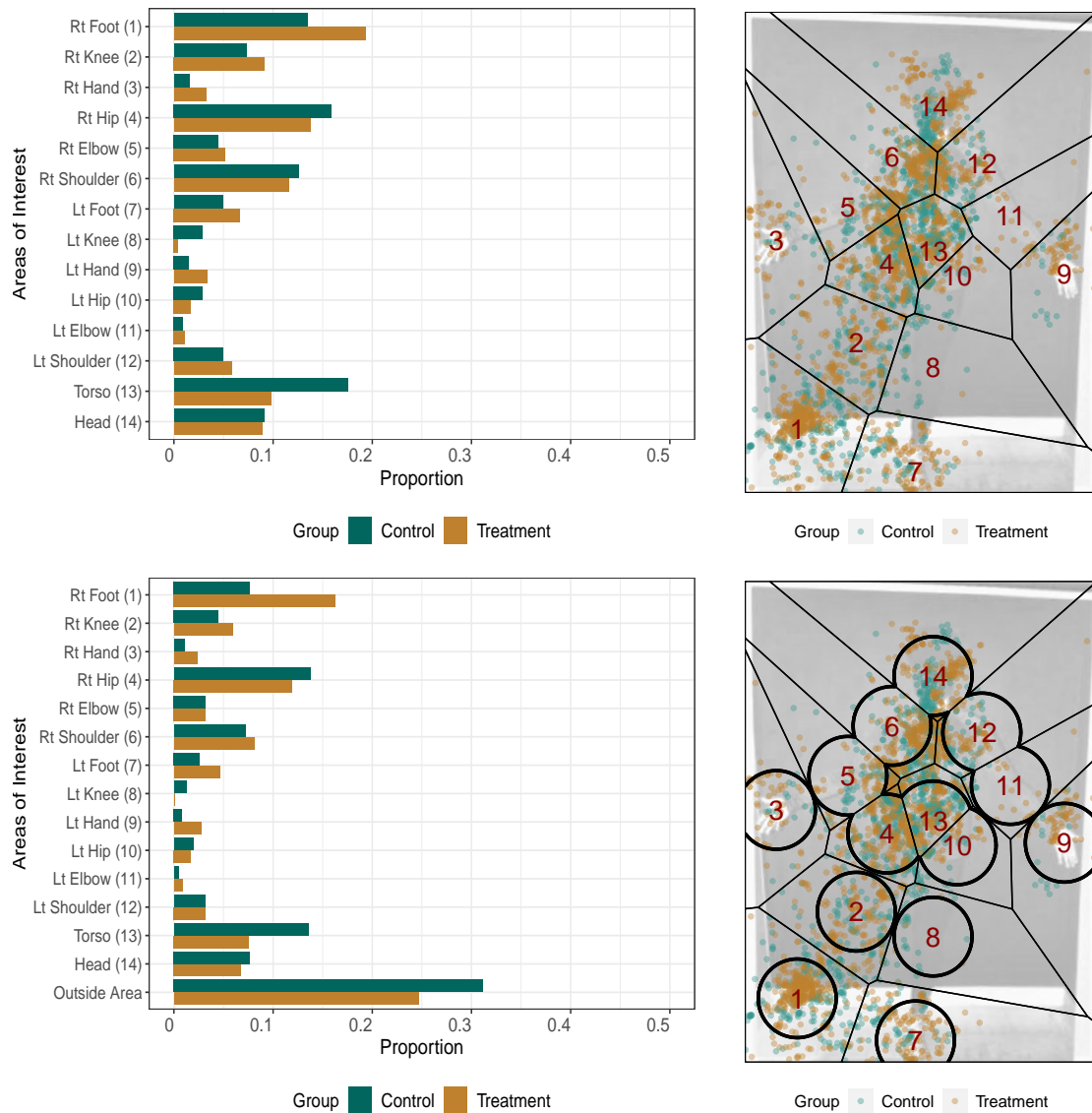


Fig. F.11: Posture ID 6 gaze-point bar chart (left) and scatterplot (right) for Round 1 VT (top) and Round 1 LRVT (bottom) AOIs.

Posture ID 6 Round 2 Visualizations

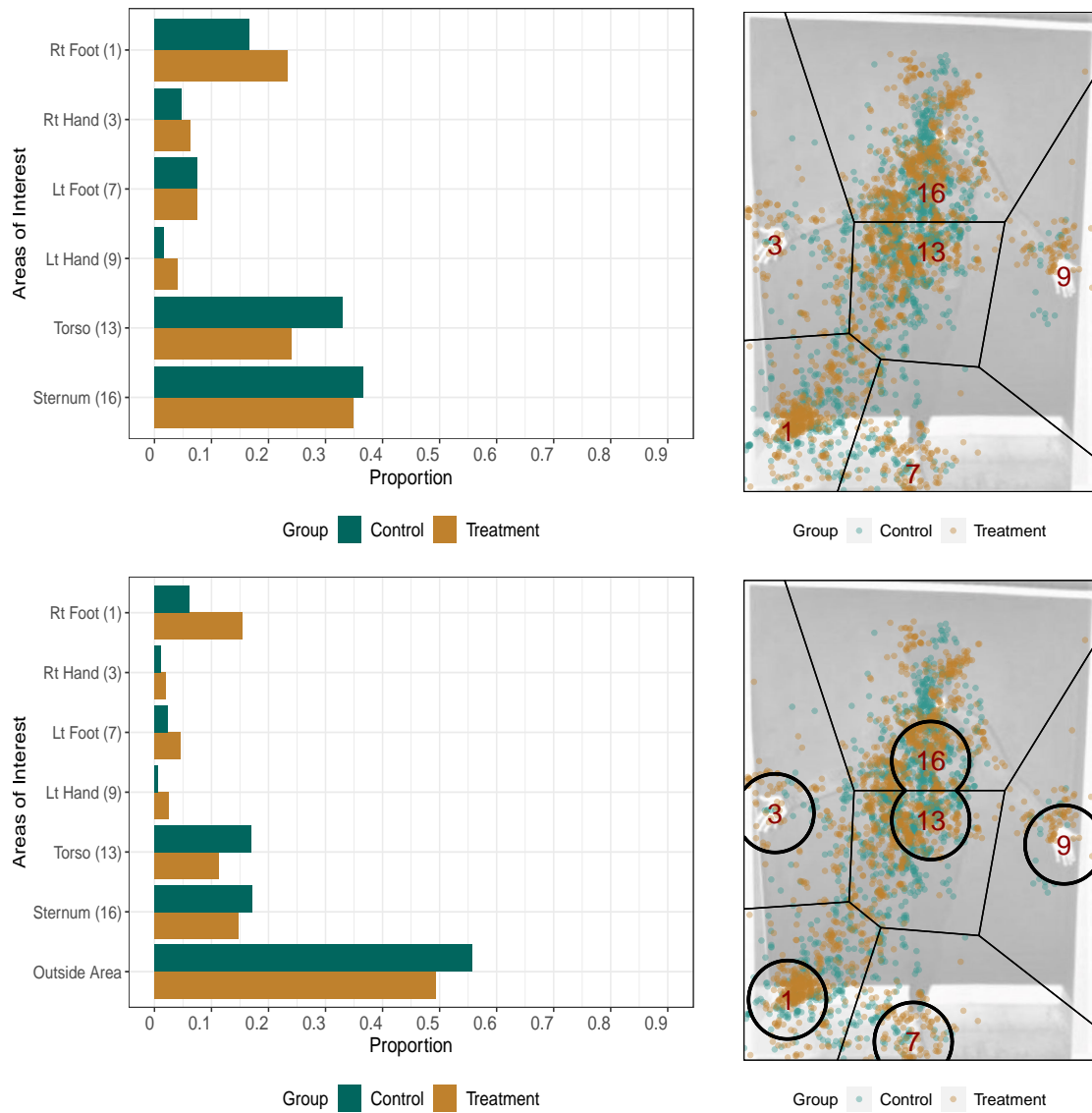


Fig. F.12: Posture ID 6 gaze-point bar chart (left) and scatterplot (right) for Round 2 VT (top) and Round 2 LRV (bottom) AOIs.

Posture ID 7 Round 1 Visualizations

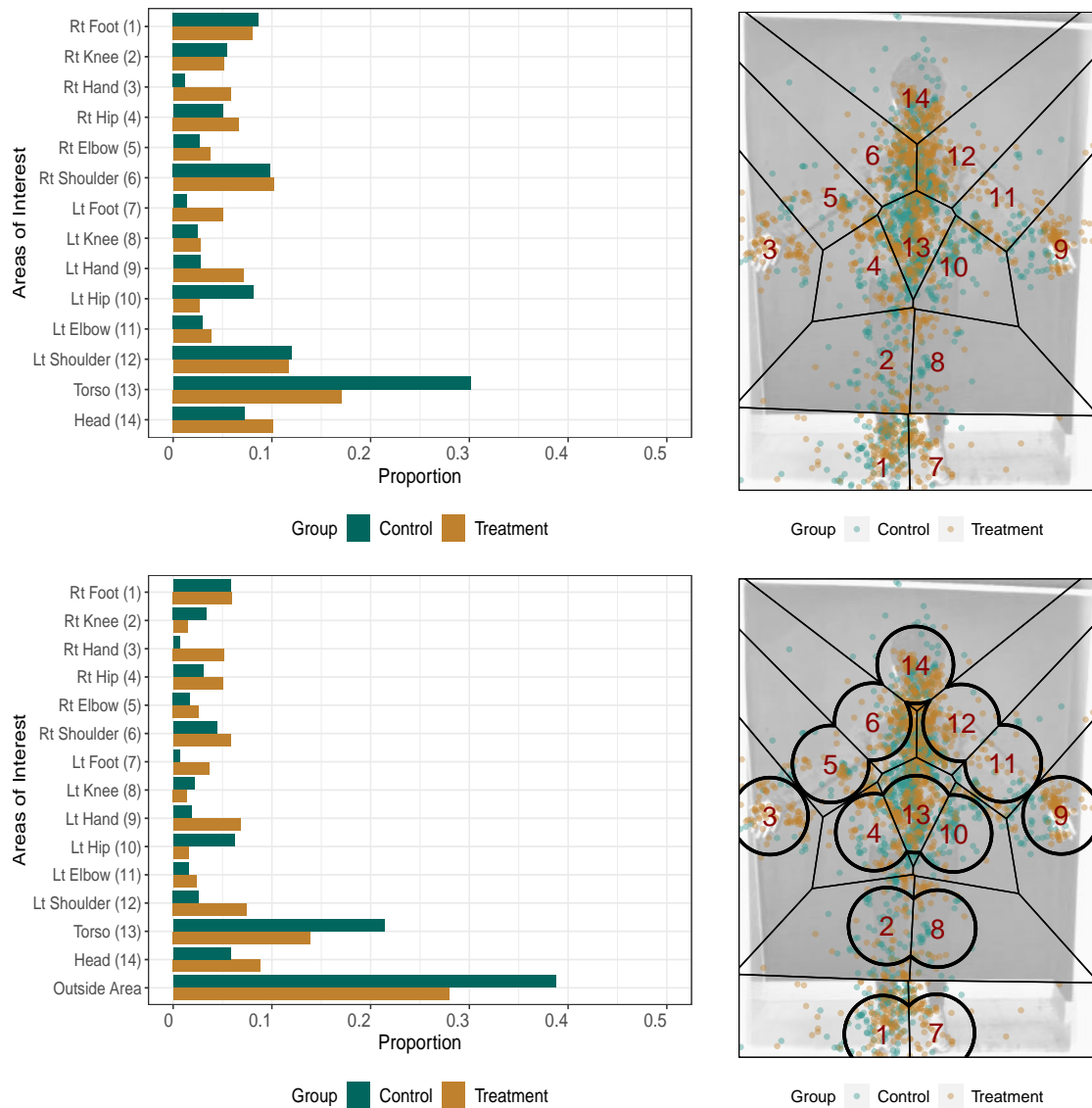


Fig. F.13: Posture ID 7 gaze-point bar chart (left) and scatterplot (right) for Round 1 VT (top) and Round 1 LRVT (bottom) AOIs.

Posture ID 7 Round 2 Visualizations

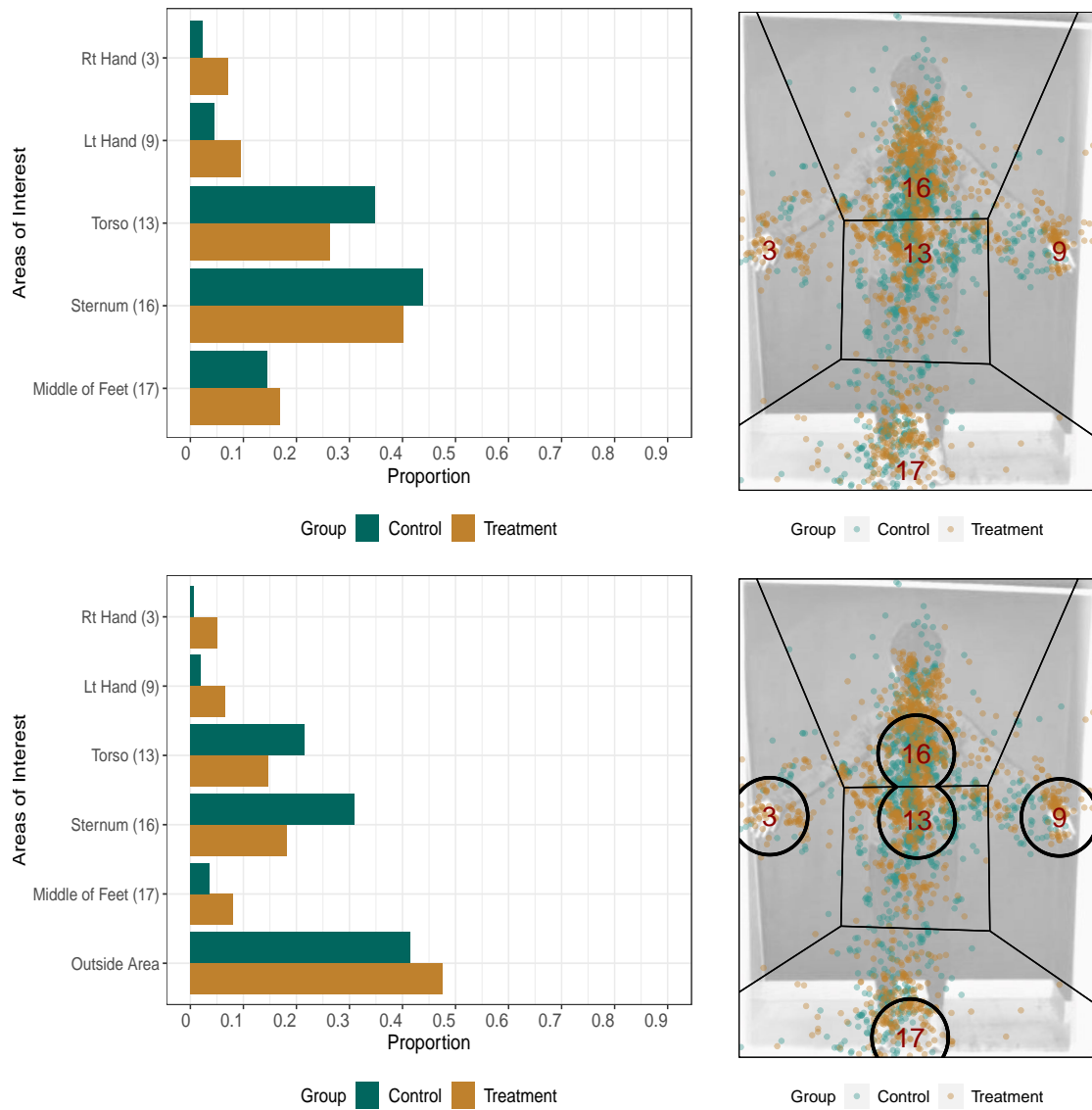


Fig. F.14: Posture ID 7 gaze-point bar chart (left) and scatterplot (right) for Round 2 VT (top) and Round 2 LRV (bottom) AOIs.

Posture ID 8 Round 1 Visualizations

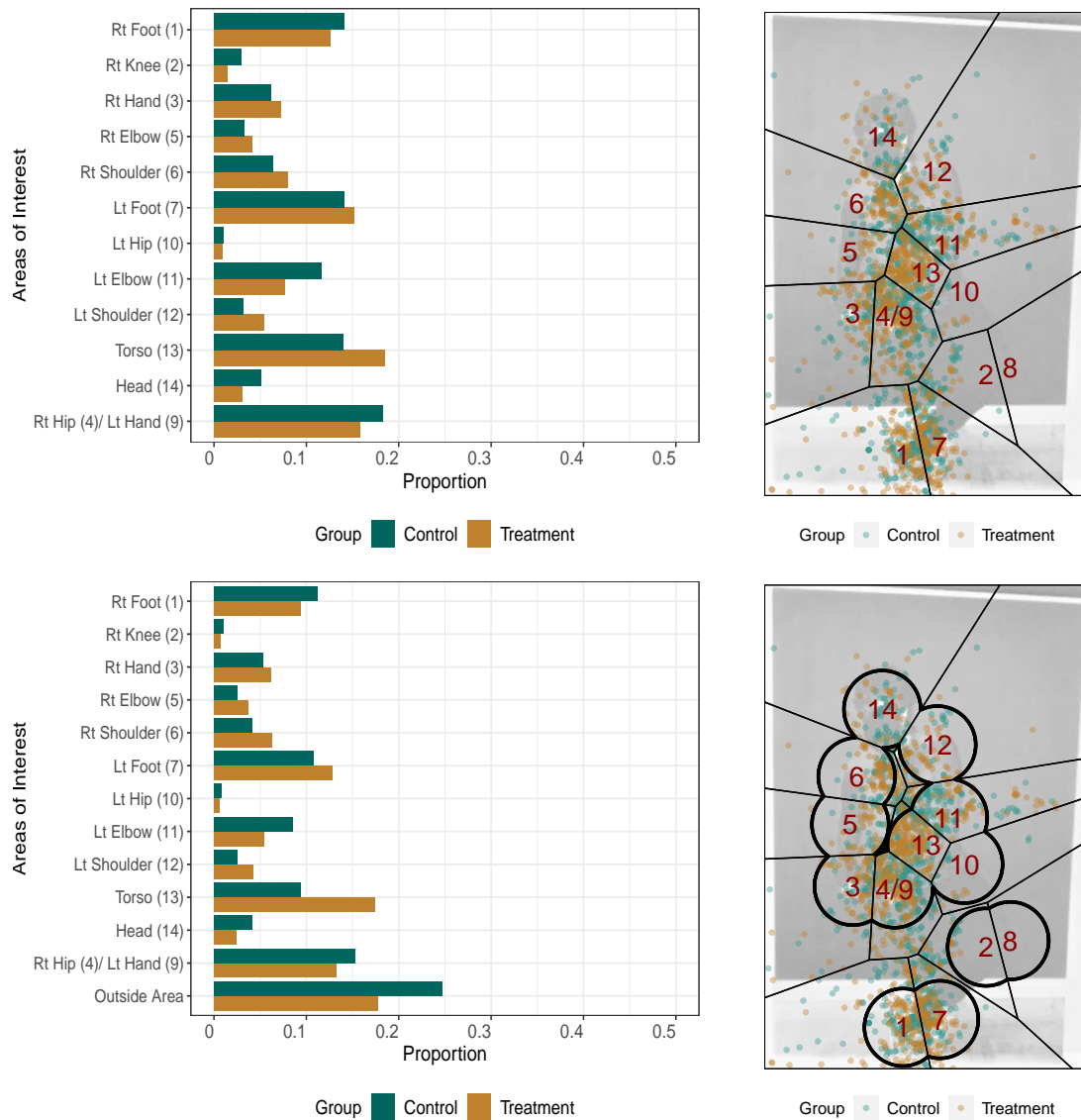


Fig. F.15: Posture ID 8 gaze-point bar chart (left) and scatterplot (right) for Round 1 VT (top) and Round 1 LRVT (bottom) AOIs.

Posture ID 8 Round 2 Visualizations

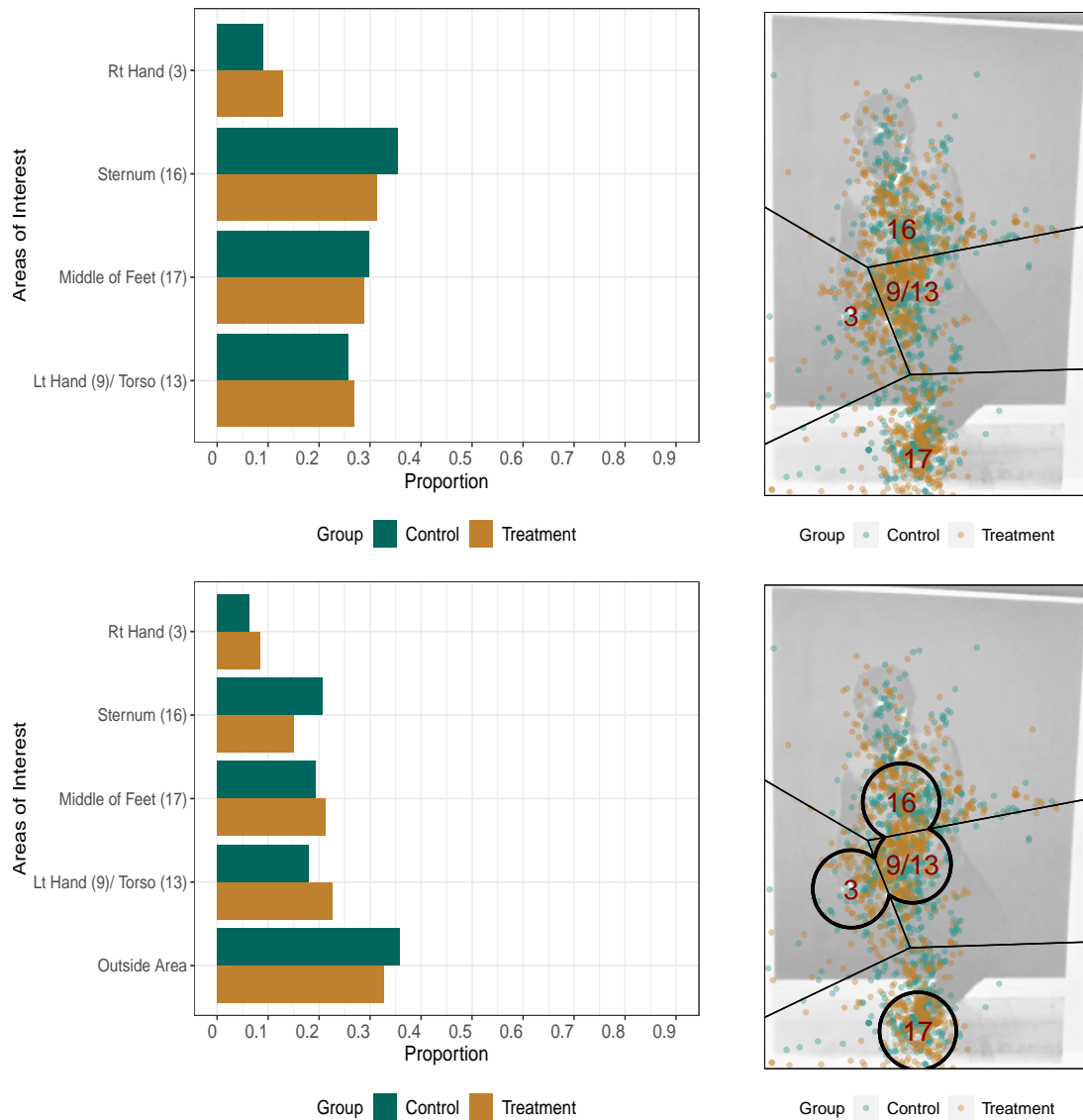


Fig. F.16: Posture ID 8 gaze-point bar chart (left) and scatterplot (right) for Round 2 VT (top) and Round 2 LRV (bottom) AOIs.

Posture ID 9 Round 1 Visualizations

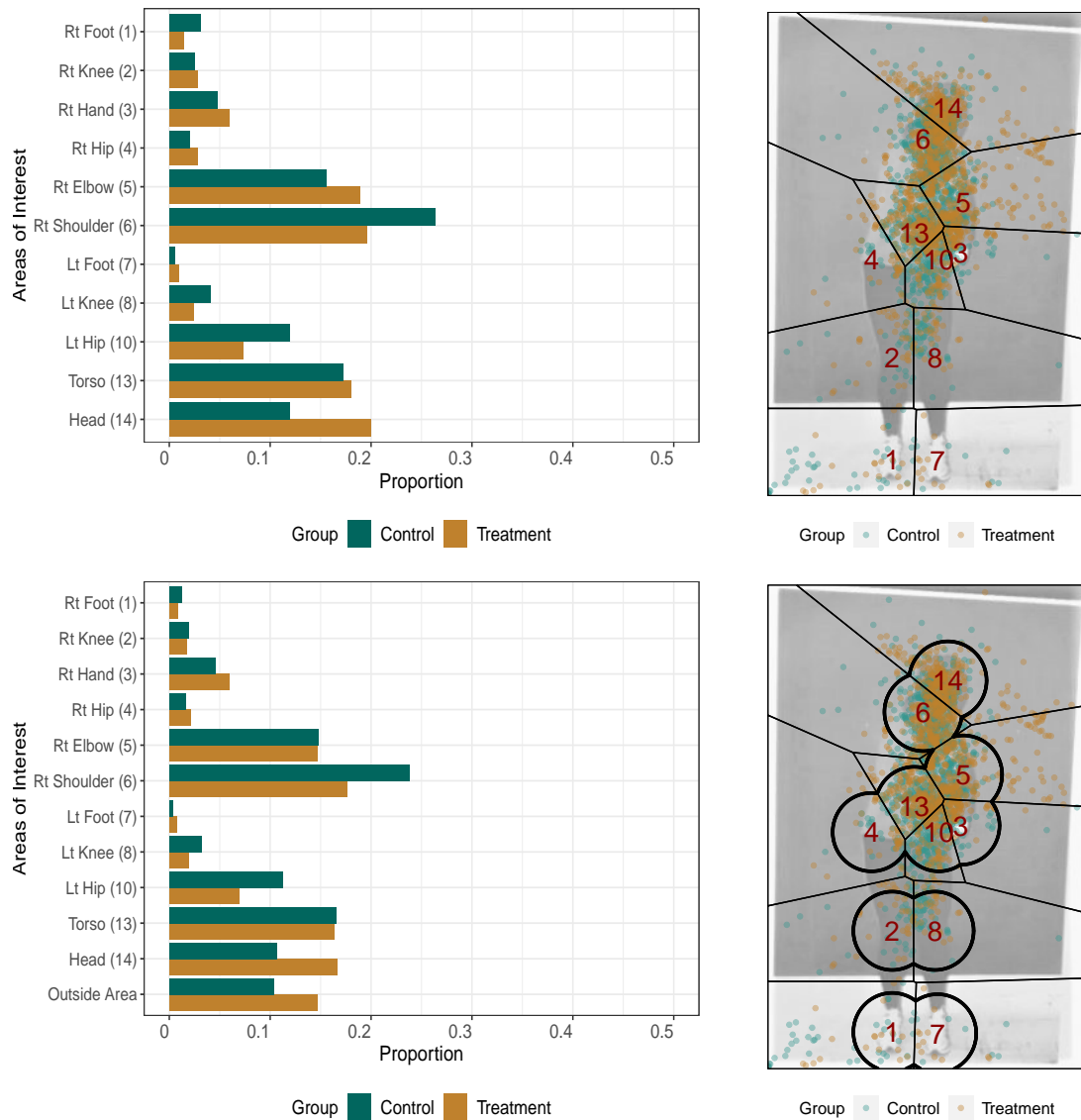


Fig. F.17: Posture ID 9 gaze-point bar chart (left) and scatterplot (right) for Round 1 VT (top) and Round 1 LRVT (bottom) AOIs.

Posture ID 9 Round 2 Visualizations

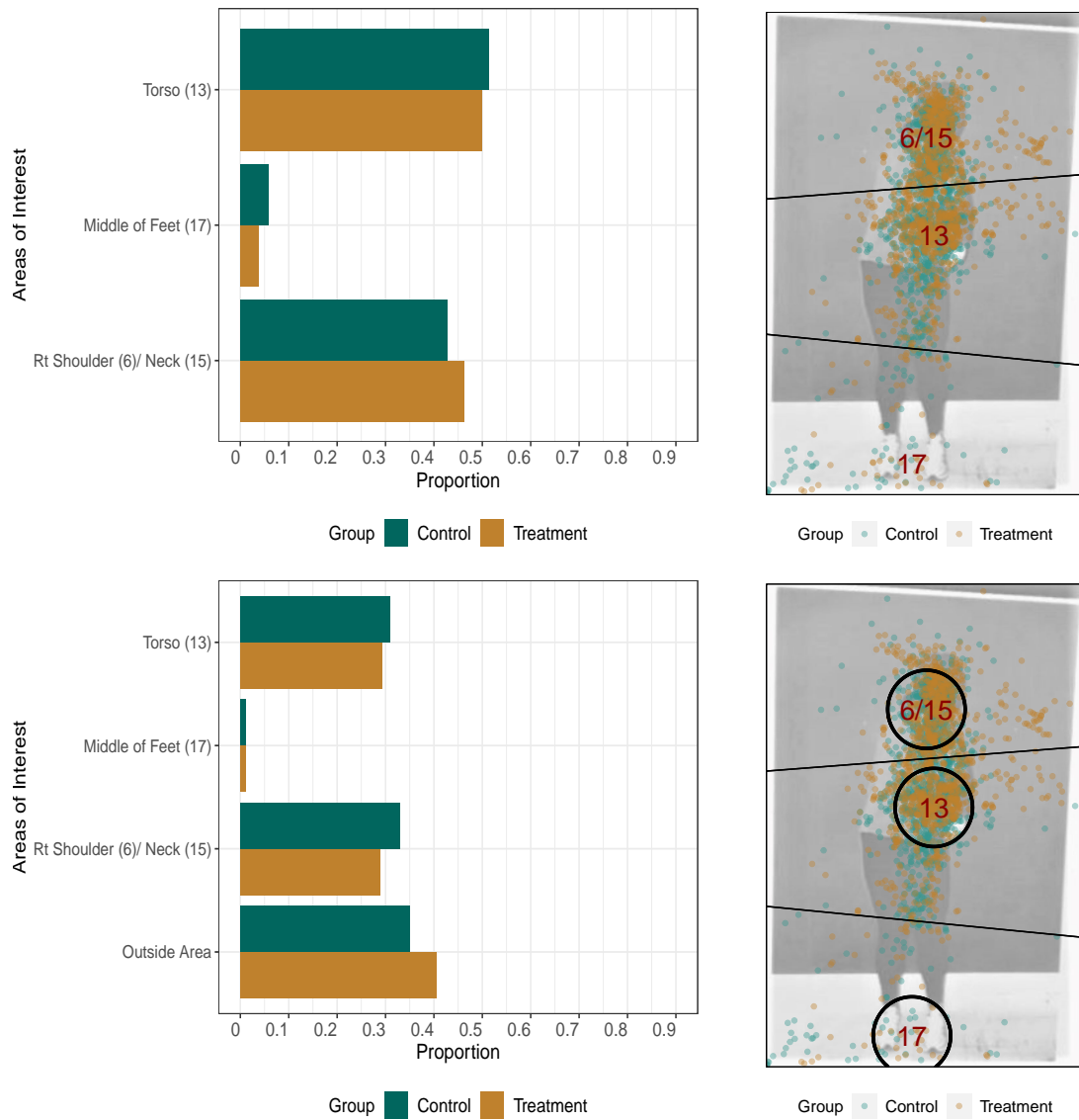


Fig. F.18: Posture ID 9 gaze-point bar chart (left) and scatterplot (right) for Round 2 VT (top) and Round 2 LRV (bottom) AOIs.

Posture ID 10 Round 1 Visualizations

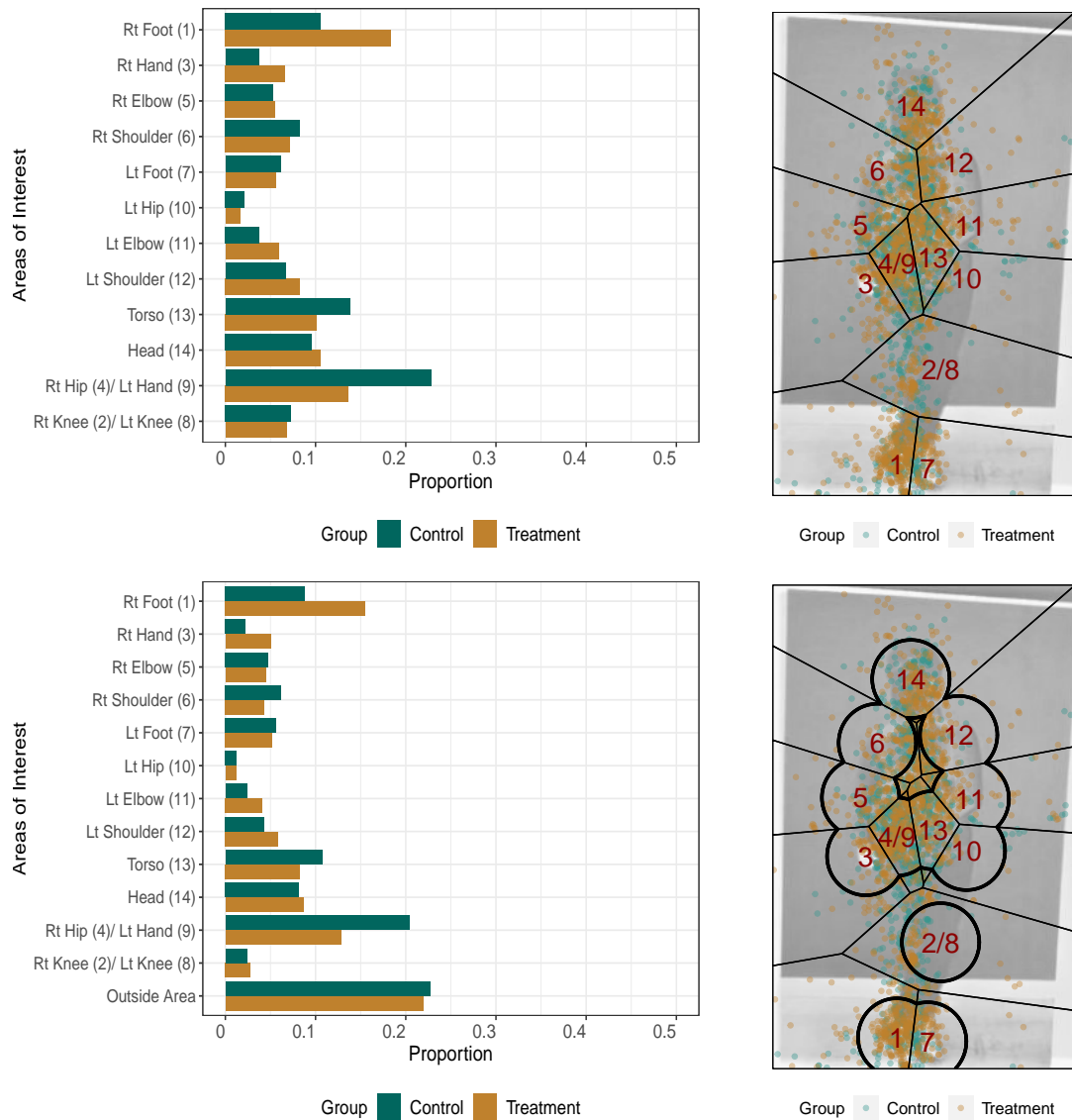


Fig. F.19: Posture ID 10 gaze-point bar chart (left) and scatterplot (right) for Round 1 VT (top) and Round 1 LRVT (bottom) AOIs.

Posture ID 10 Round 2 Visualizations

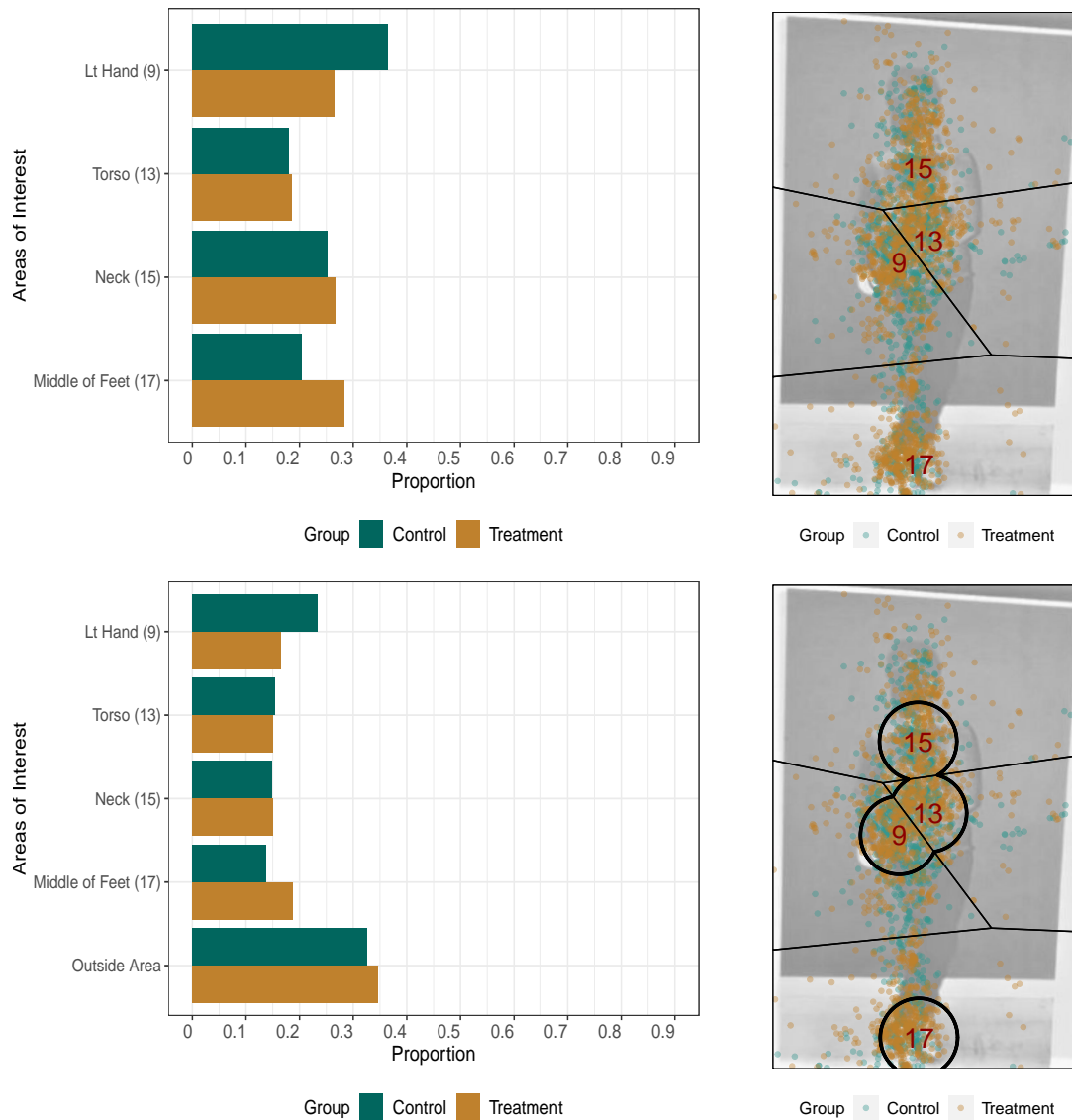


Fig. F.20: Posture ID 10 gaze-point bar chart (left) and scatterplot (right) for Round 2 VT (top) and Round 2 LRV (bottom) AOIs.

Posture ID 11 Round 1 Visualizations

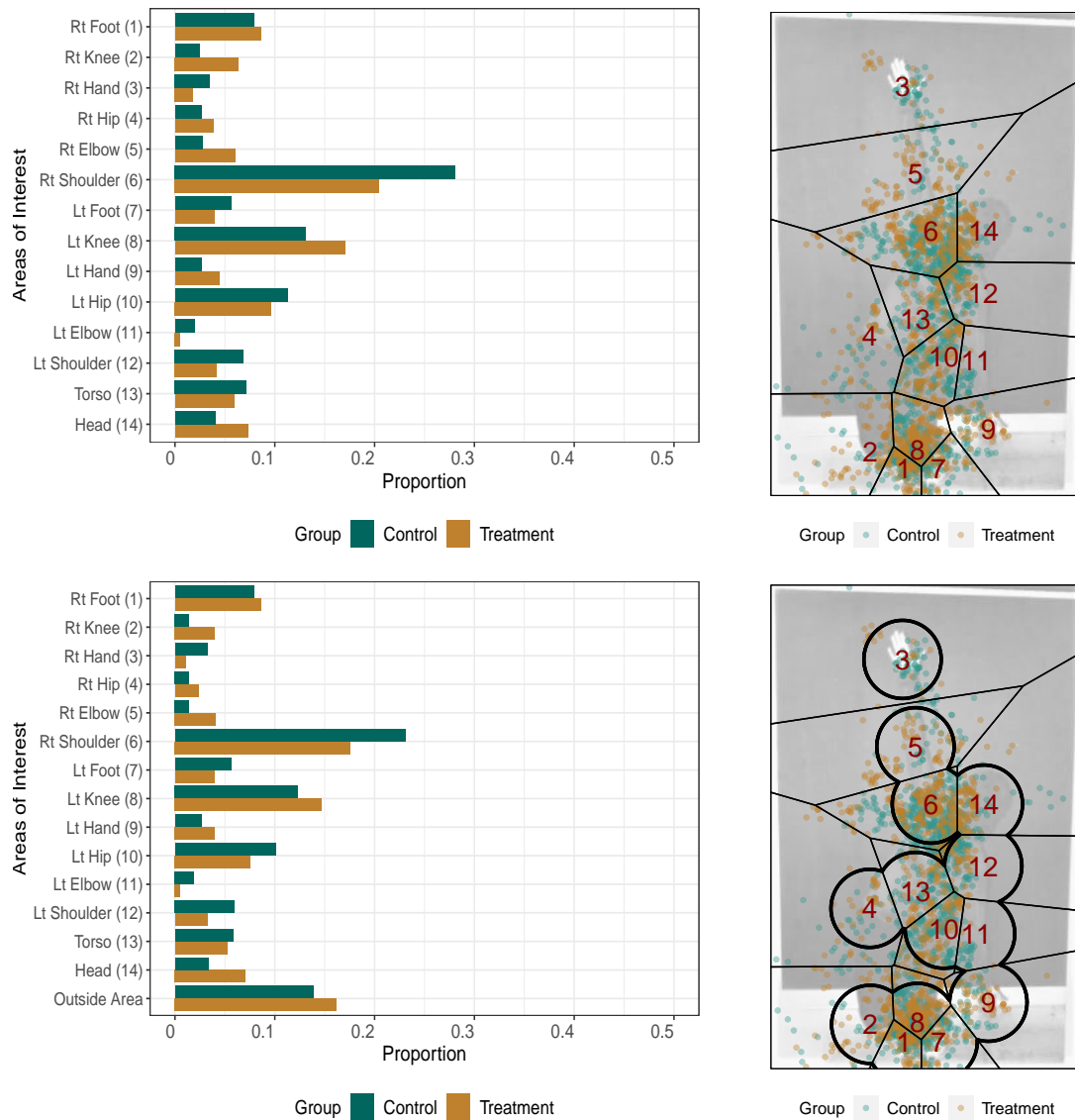


Fig. F.21: Posture ID 11 gaze-point bar chart (left) and scatterplot (right) for Round 1 VT (top) and Round 1 LRVT (bottom) AOIs.

Posture ID 11 Round 2 Visualizations

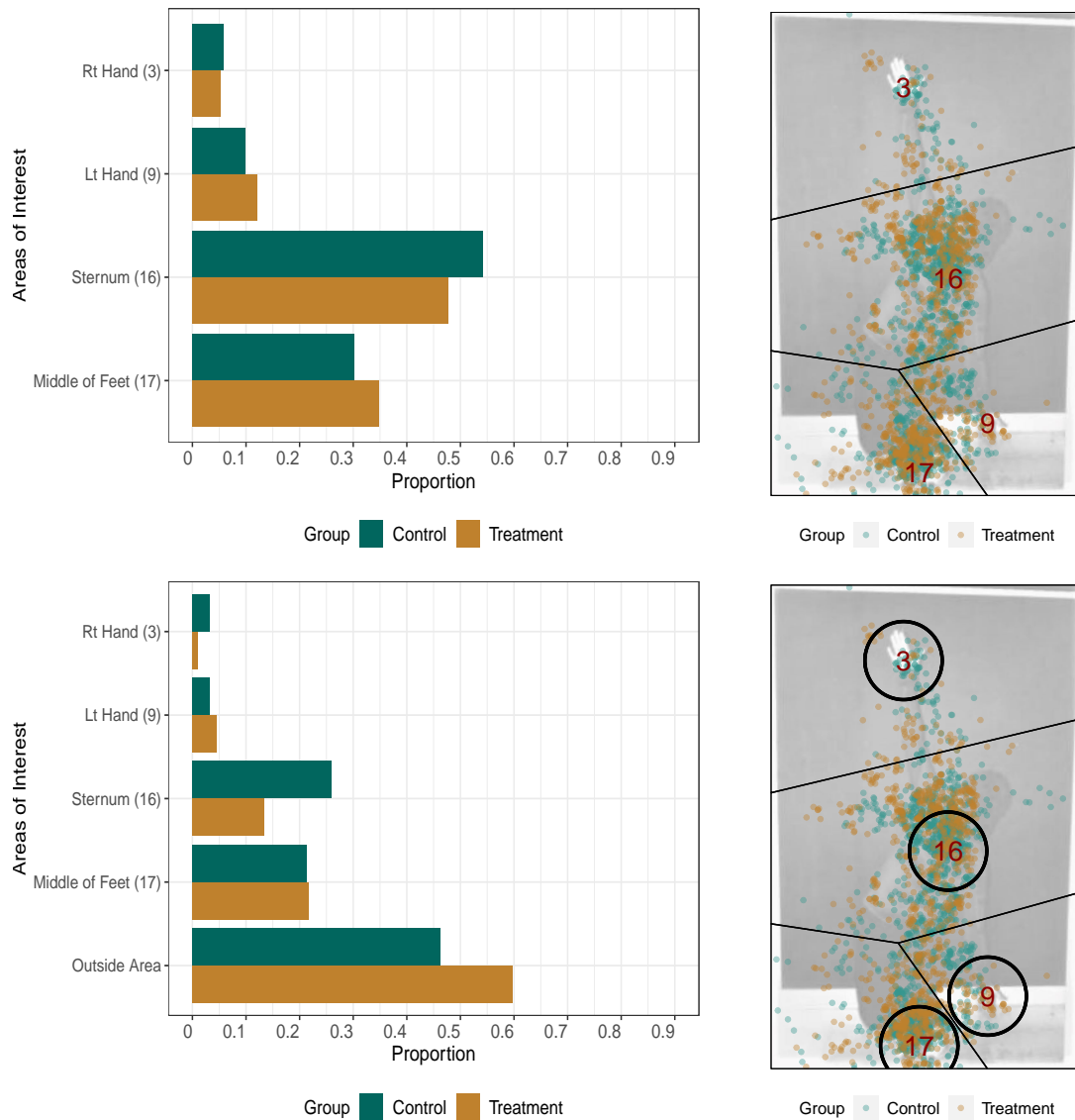


Fig. F.22: Posture ID 11 gaze-point bar chart (left) and scatterplot (right) for Round 2 VT (top) and Round 2 LRV (bottom) AOIs.

Posture ID 12 Round 1 Visualizations

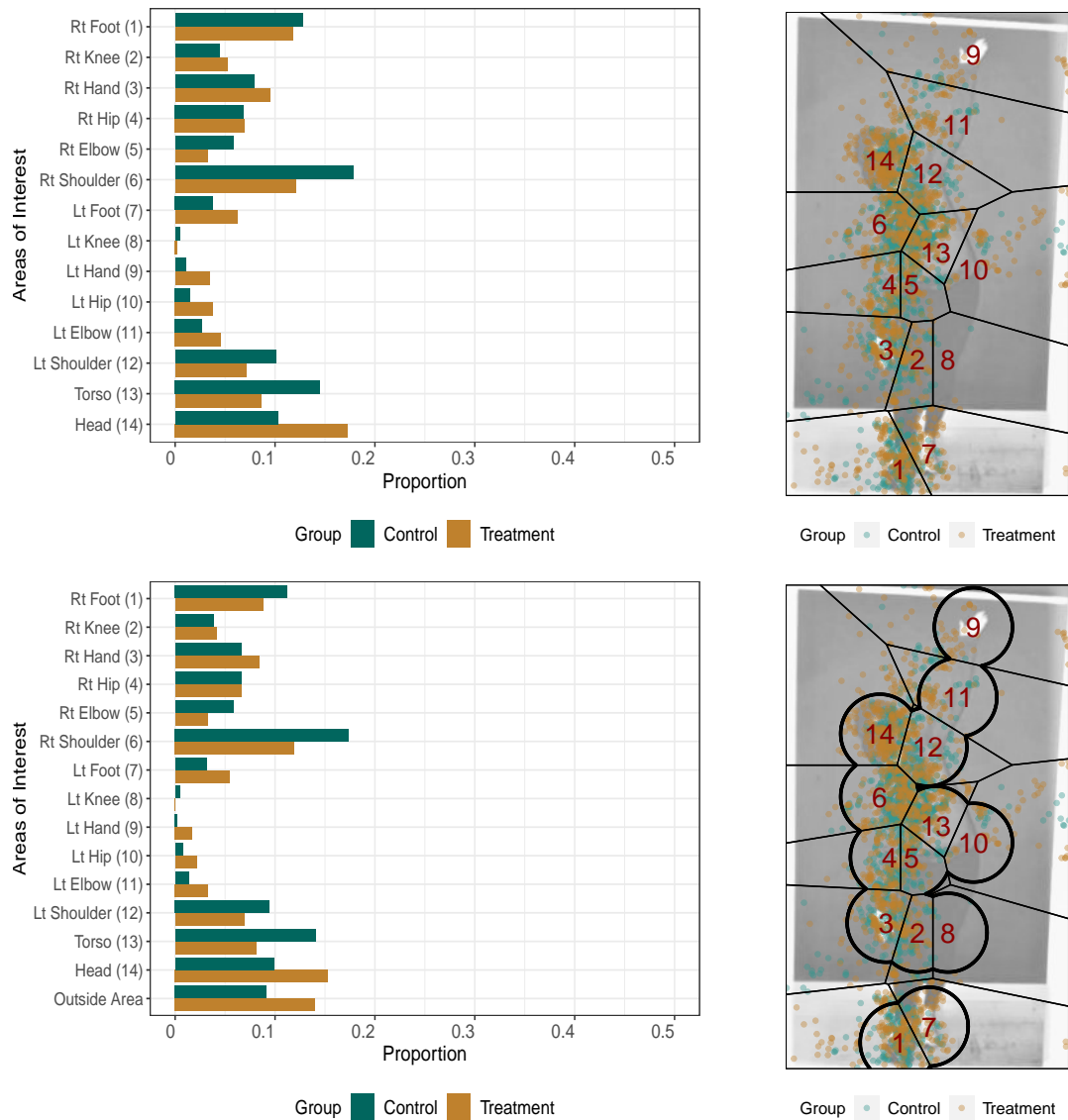


Fig. F.23: Posture ID 12 gaze-point bar chart (left) and scatterplot (right) for Round 1 VT (top) and Round 1 LRVT (bottom) AOIs.

Posture ID 12 Round 2 Visualizations

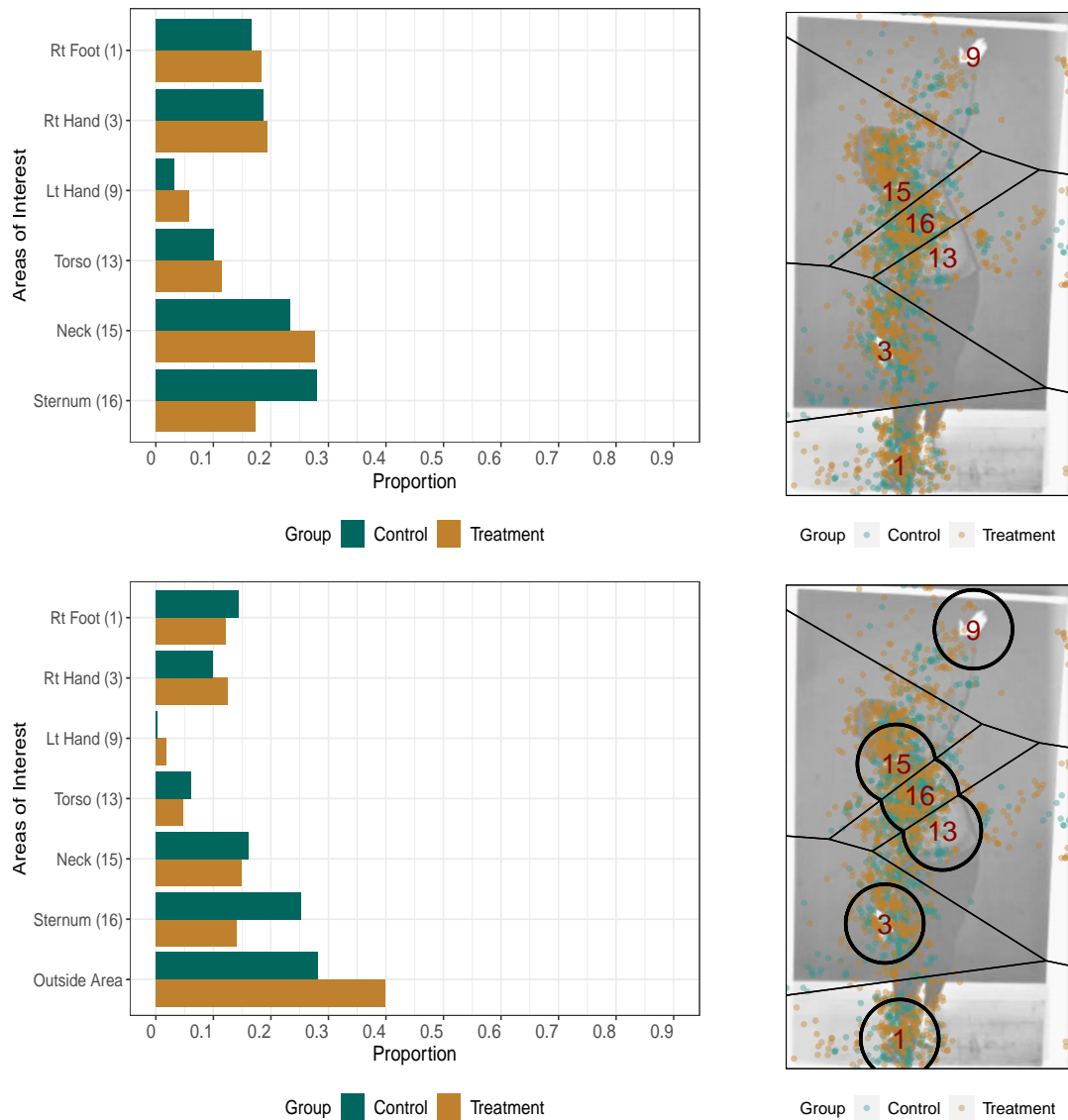


Fig. F.24: Posture ID 12 gaze-point bar chart (left) and scatterplot (right) for Round 2 VT (top) and Round 2 LRV (bottom) AOIs.

Posture ID 13 Round 1 Visualizations

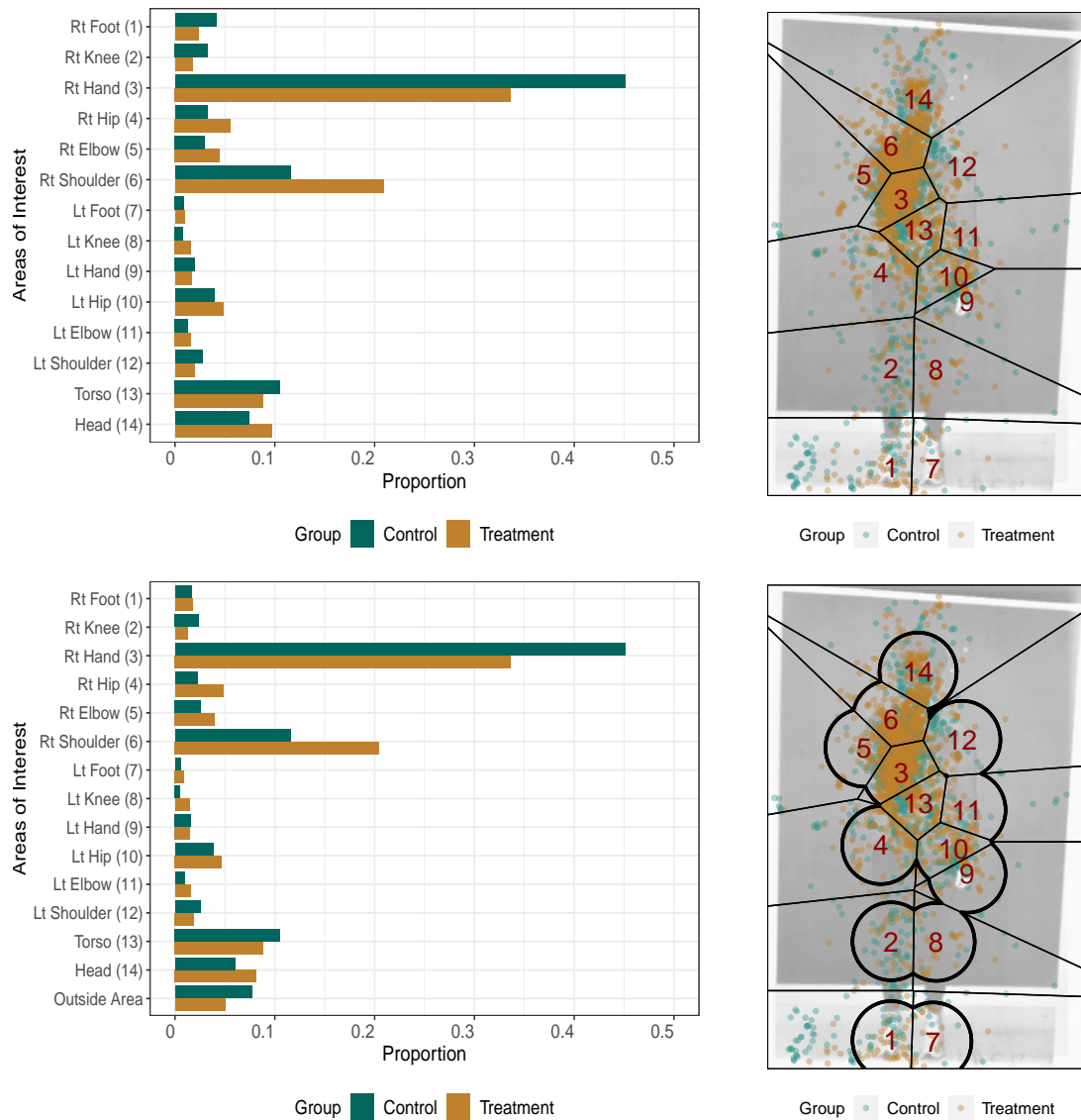


Fig. F.25: Posture ID 13 gaze-point bar chart (left) and scatterplot (right) for Round 1 VT (top) and Round 1 LRVT (bottom) AOIs.

Posture ID 13 Round 2 Visualizations

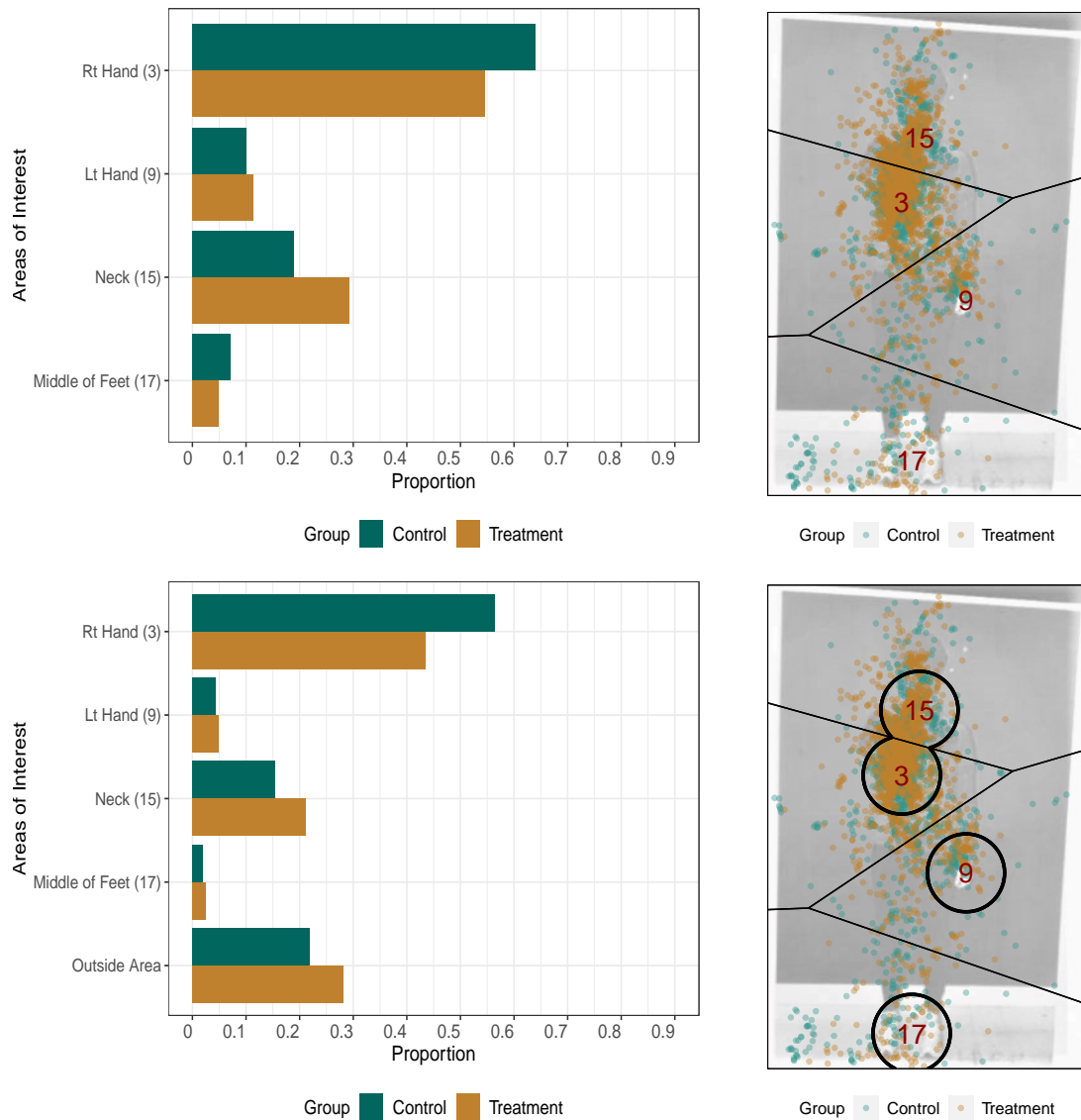


Fig. F.26: Posture ID 13 gaze-point bar chart (left) and scatterplot (right) for Round 2 VT (top) and Round 2 LRV (bottom) AOIs.

Posture ID 14 Round 1 Visualizations

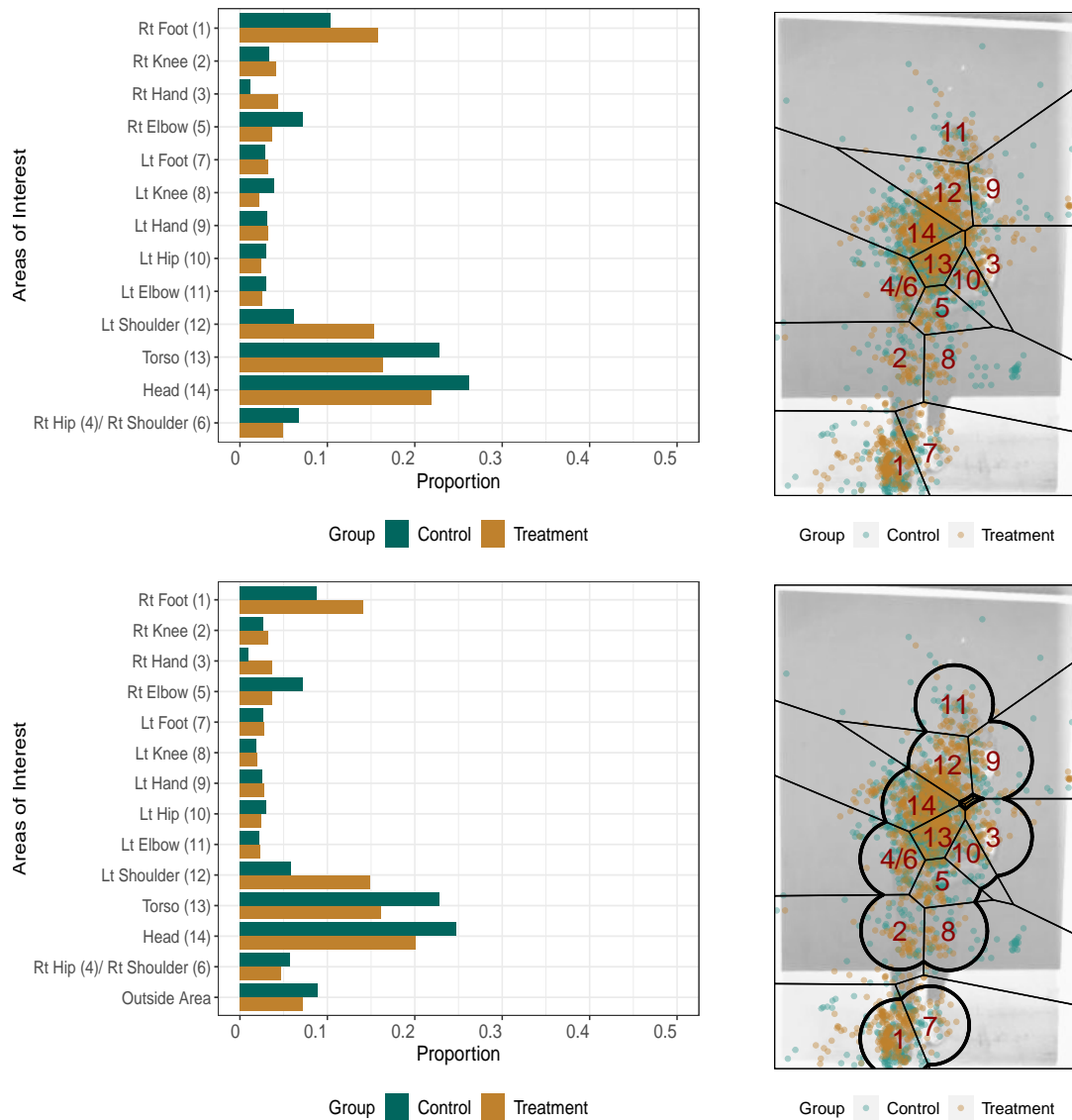


Fig. F.27: Posture ID 14 gaze-point bar chart (left) and scatterplot (right) for Round 1 VT (top) and Round 1 LRVT (bottom) AOIs.

Posture ID 14 Round 2 Visualizations

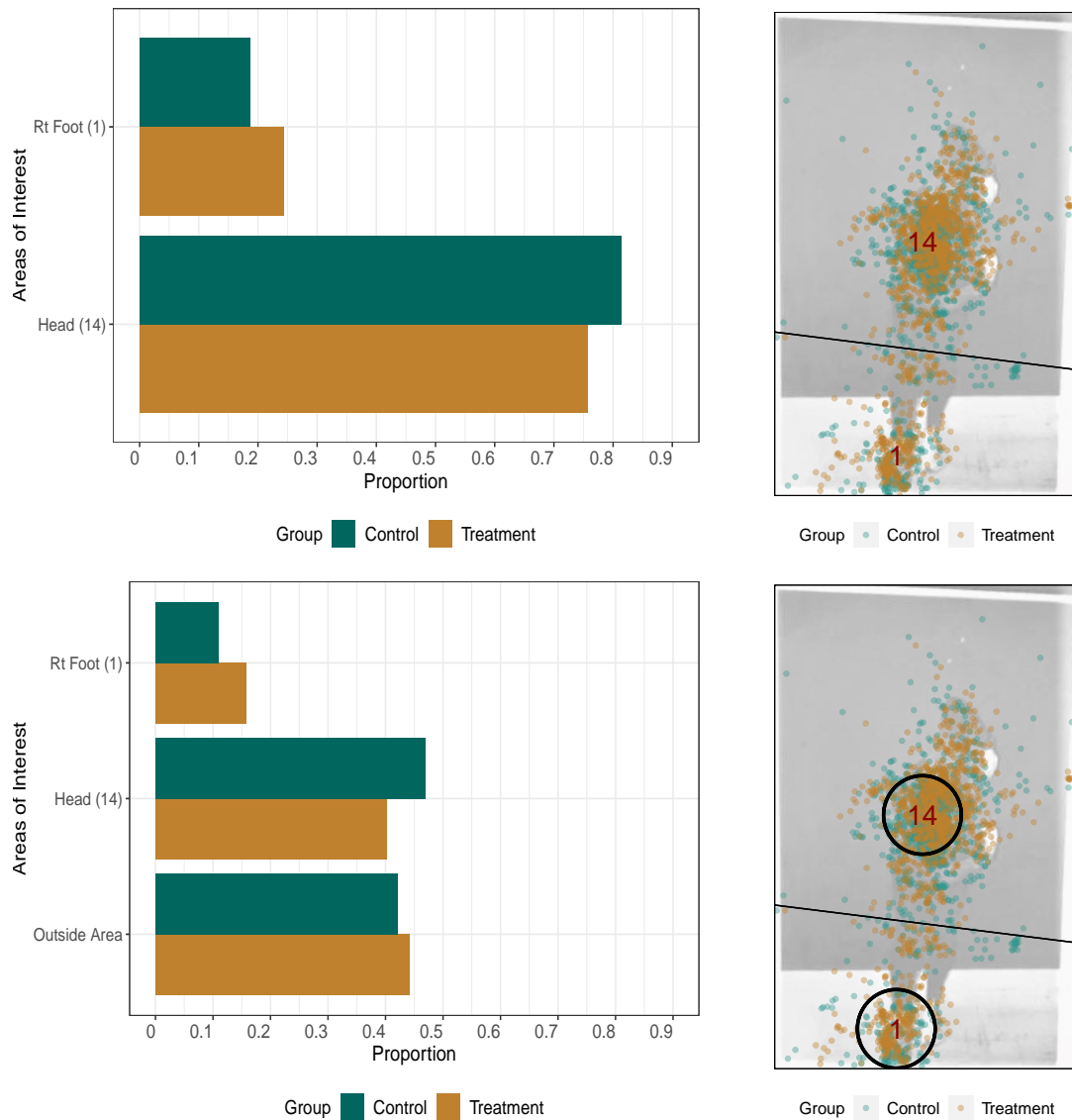


Fig. F.28: Posture ID 14 gaze-point bar chart (left) and scatterplot (right) for Round 2 VT (top) and Round 2 LRV (bottom) AOIs.

Posture ID 15 Round 1 Visualizations

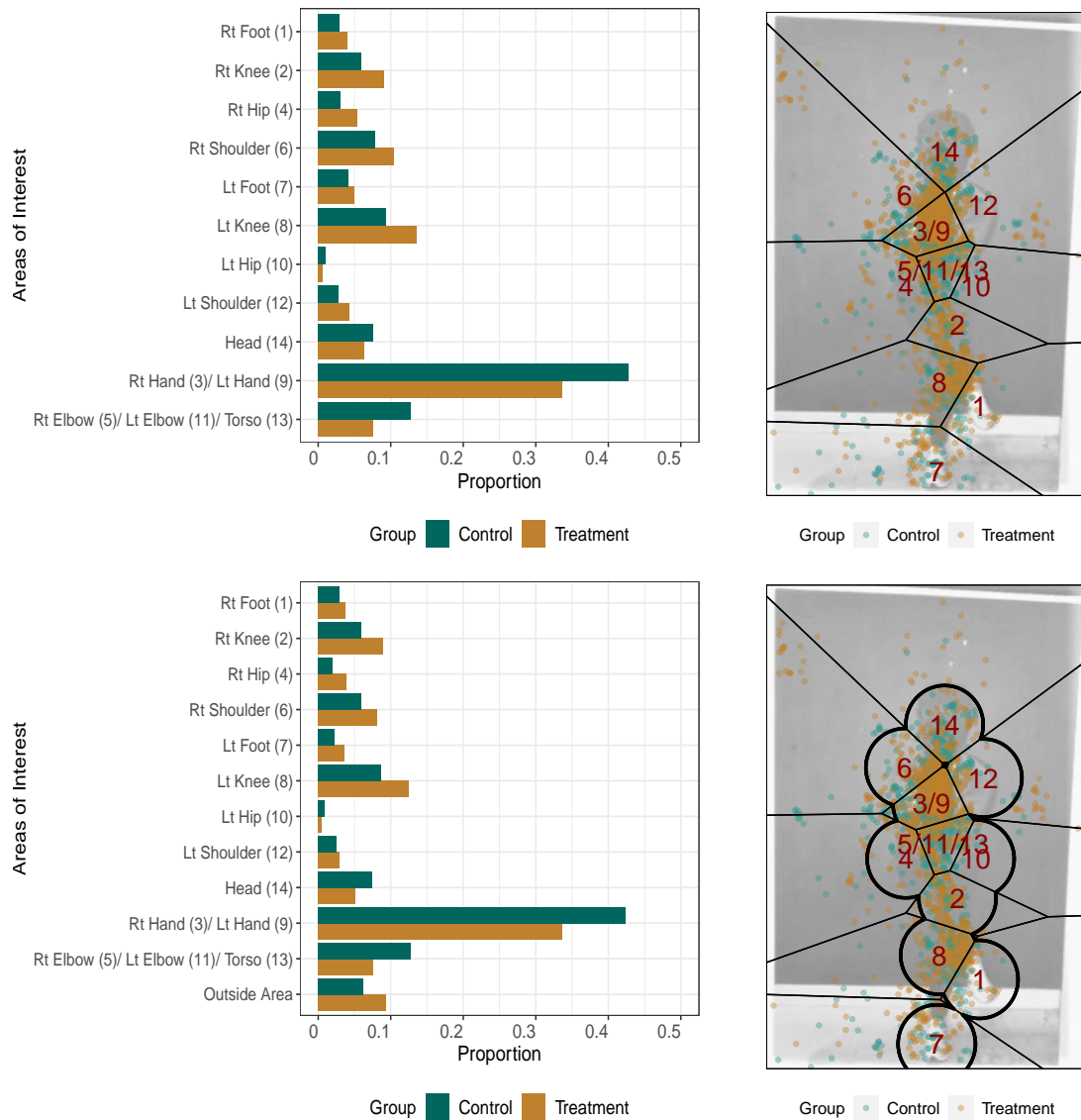


Fig. F.29: Posture ID 15 gaze-point bar chart (left) and scatterplot (right) for Round 1 VT (top) and Round 1 LRVT (bottom) AOIs.

Posture ID 15 Round 2 Visualizations

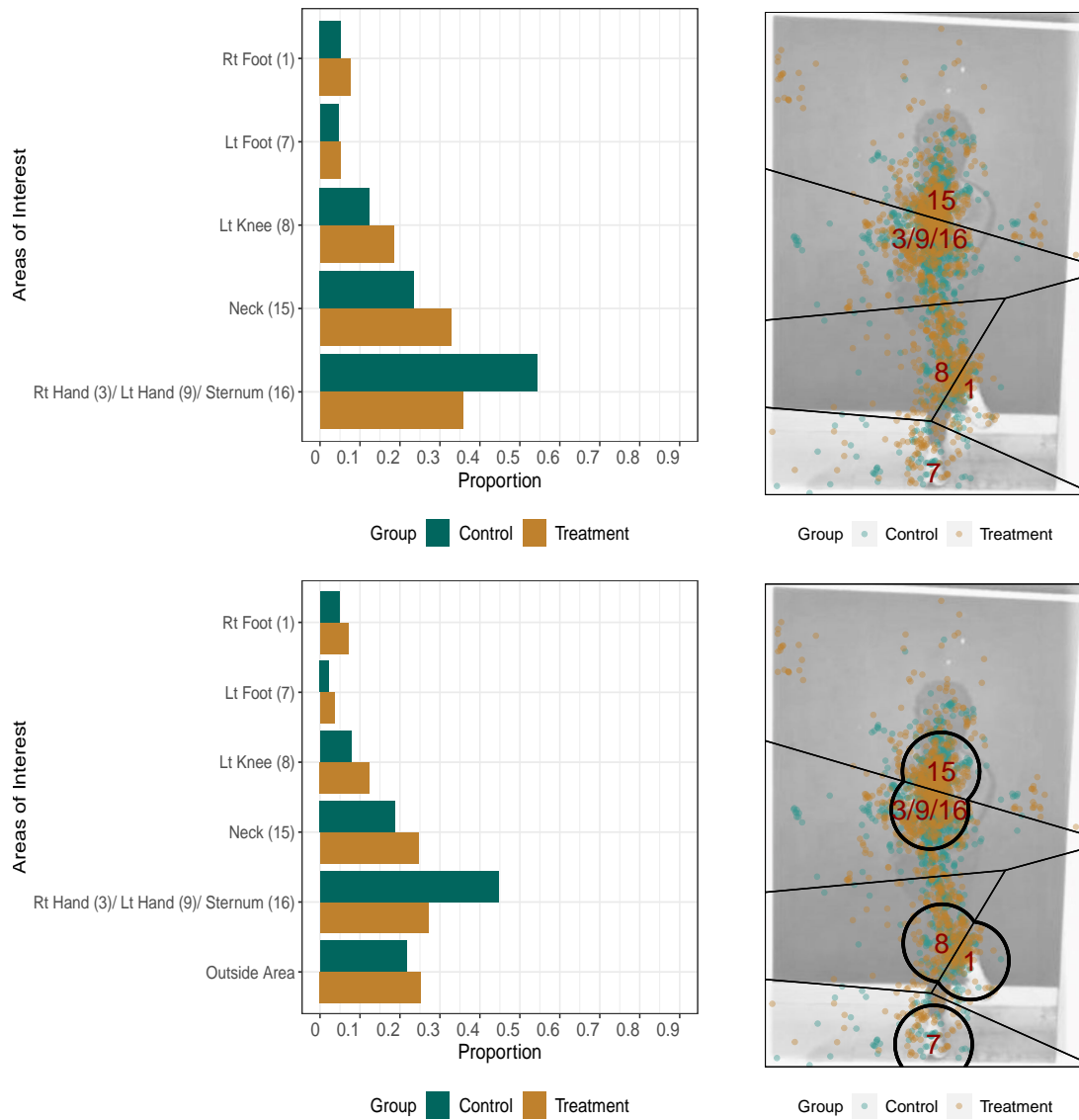


Fig. F.30: Posture ID 15 gaze-point bar chart (left) and scatterplot (right) for Round 2 VT (top) and Round 2 LRVG (bottom) AOIs.

Posture ID 16 Round 1 Visualizations

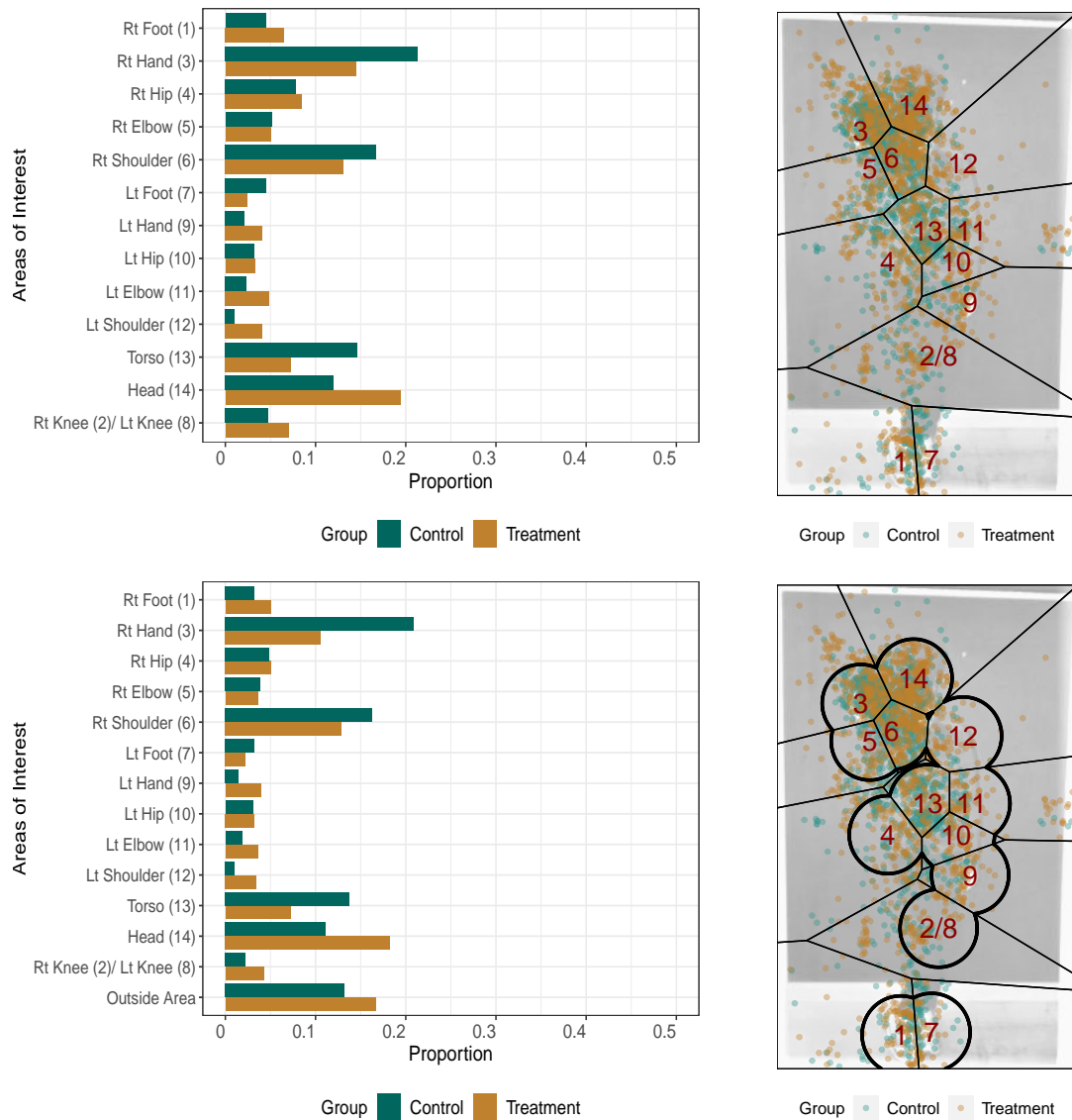


Fig. F.31: Posture ID 16 gaze-point bar chart (left) and scatterplot (right) for Round 1 VT (top) and Round 1 LRVT (bottom) AOIs.

Posture ID 16 Round 2 Visualizations

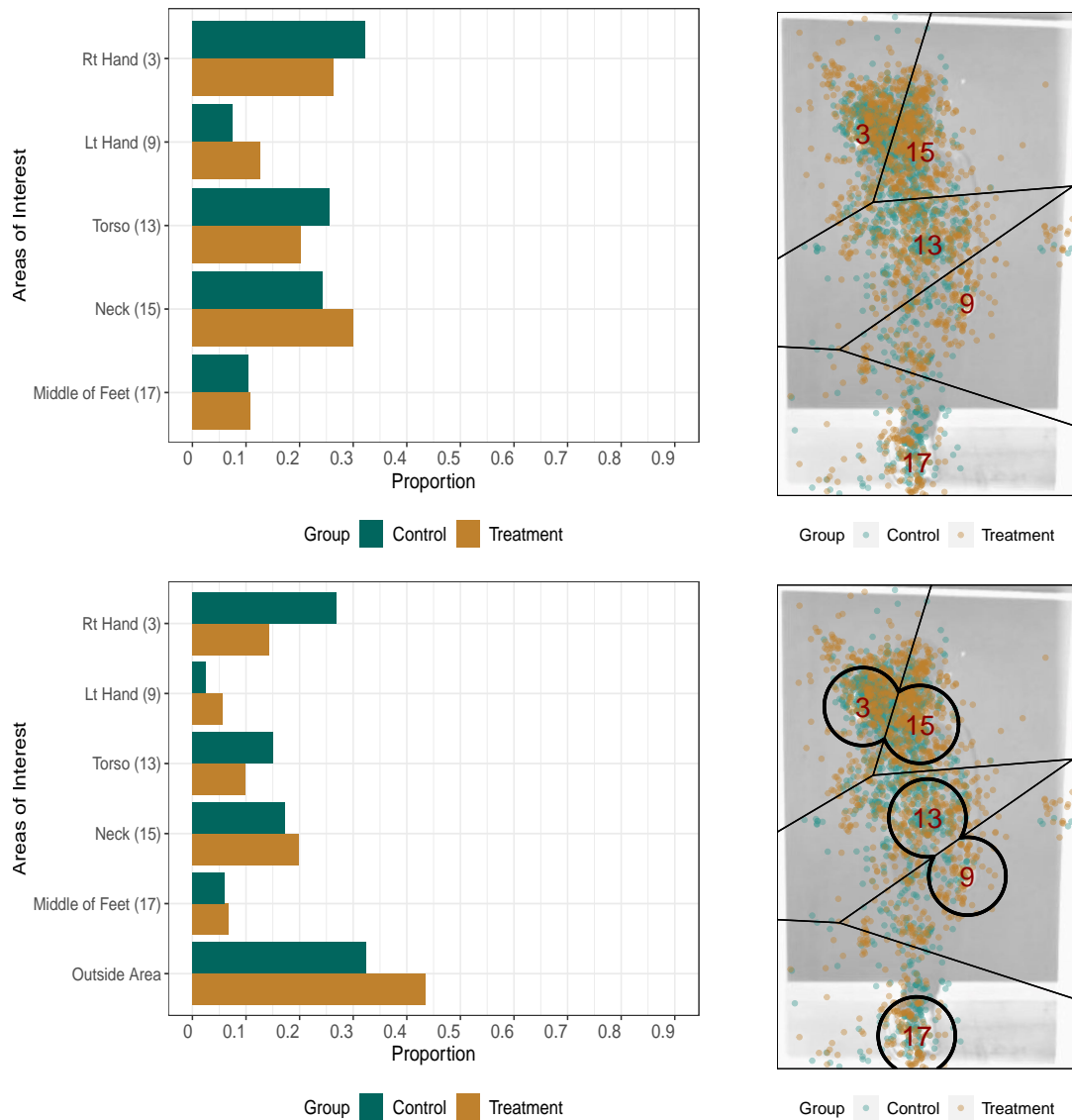


Fig. F.32: Posture ID 16 gaze-point bar chart (left) and scatterplot (right) for Round 2 VT (top) and Round 2 LRV (bottom) AOIs.

Posture ID 17 Round 1 Visualizations

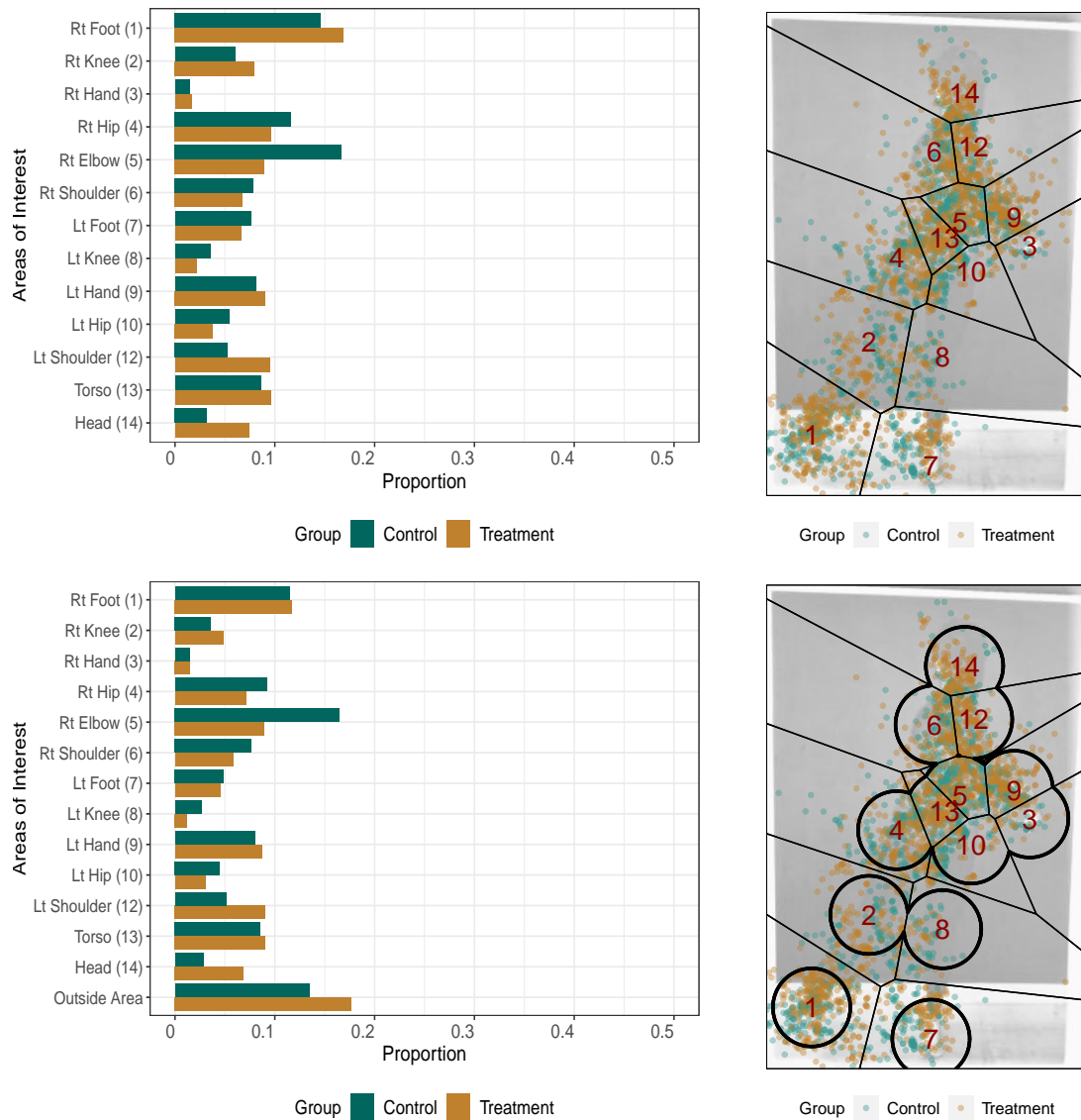


Fig. F.33: Posture ID 17 gaze-point bar chart (left) and scatterplot (right) for Round 1 VT (top) and Round 1 LRVT (bottom) AOIs.

Posture ID 17 Round 2 Visualizations

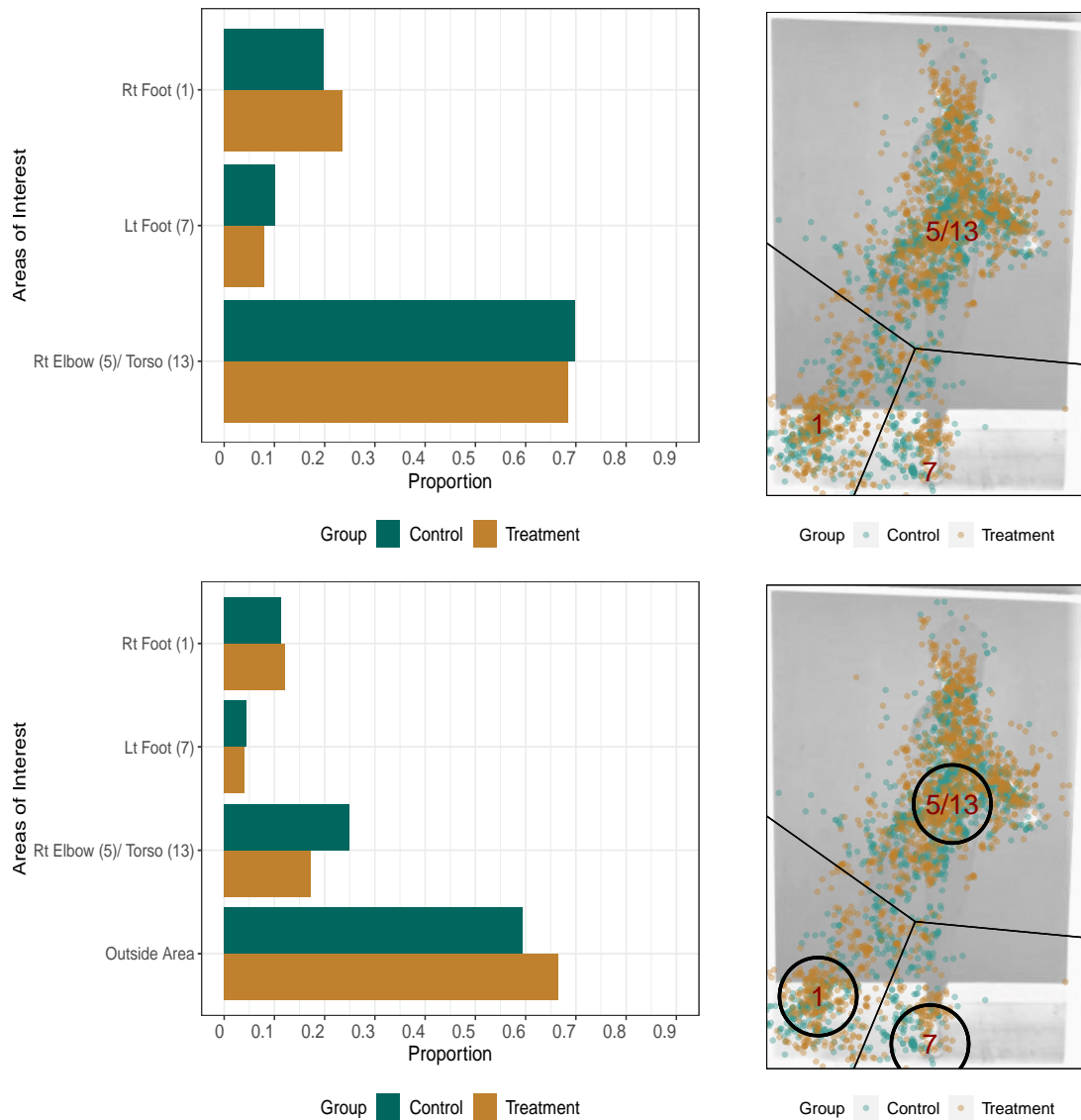


Fig. F.34: Posture ID 17 gaze-point bar chart (left) and scatterplot (right) for Round 2 VT (top) and Round 2 LRVT (bottom) AOIs.

Posture ID 18 Round 1 Visualizations

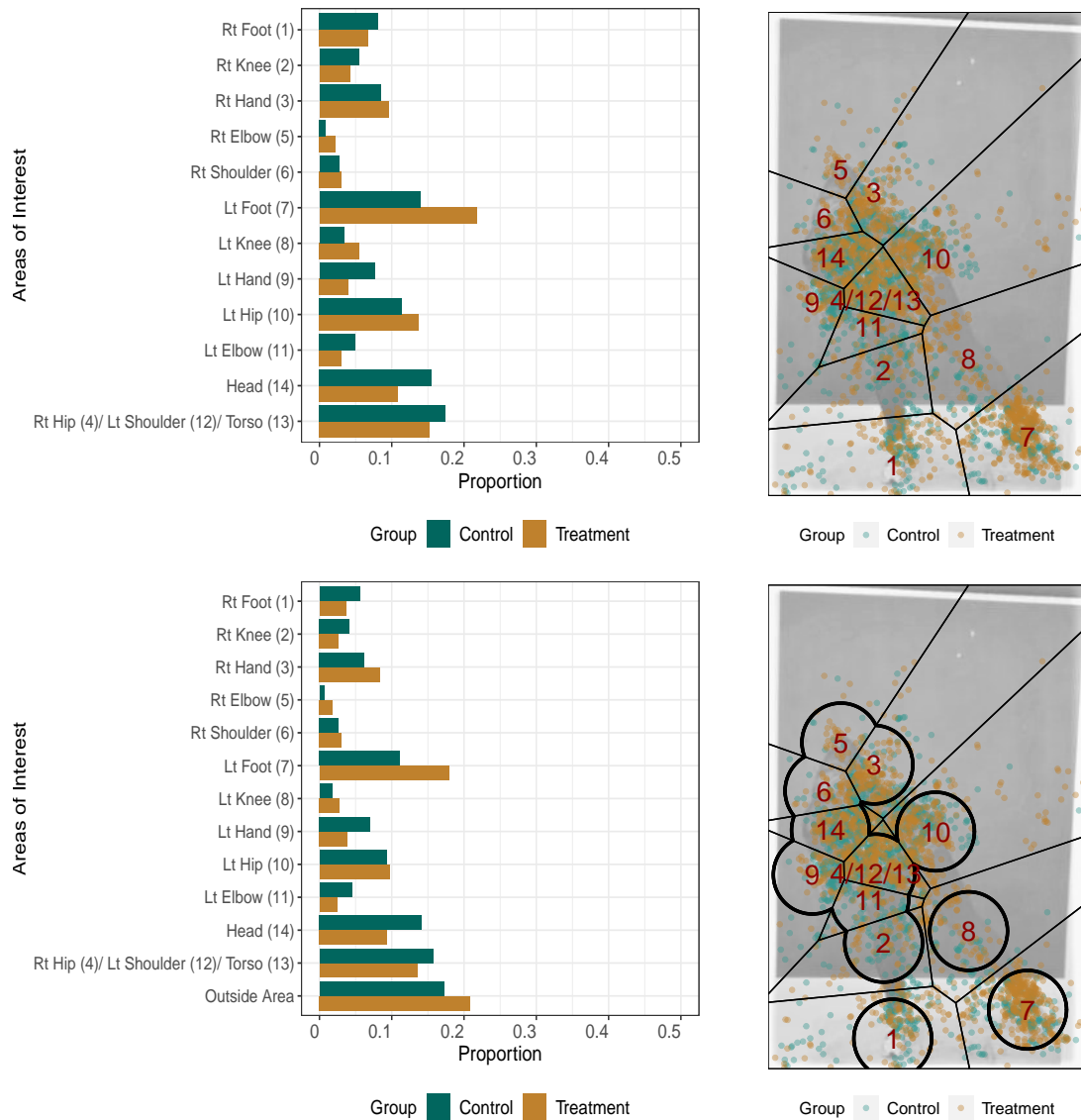


Fig. F.35: Posture ID 18 gaze-point bar chart (left) and scatterplot (right) for Round 1 VT (top) and Round 1 LRVT (bottom) AOIs.

Posture ID 18 Round 2 Visualizations

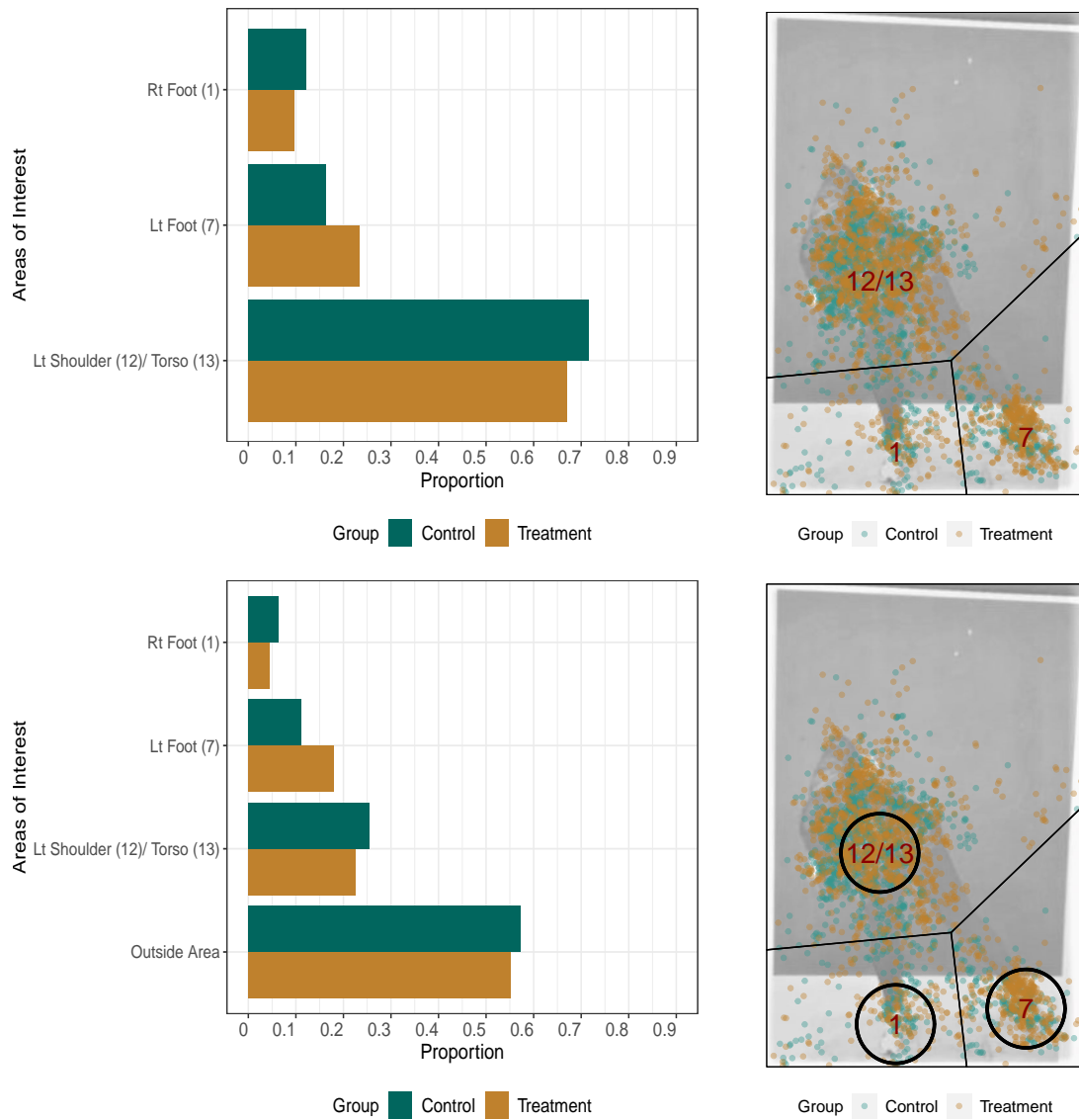


Fig. F.36: Posture ID 18 gaze-point bar chart (left) and scatterplot (right) for Round 2 VT (top) and Round 2 LRV (bottom) AOIs.

Posture ID 19 Round 1 Visualizations

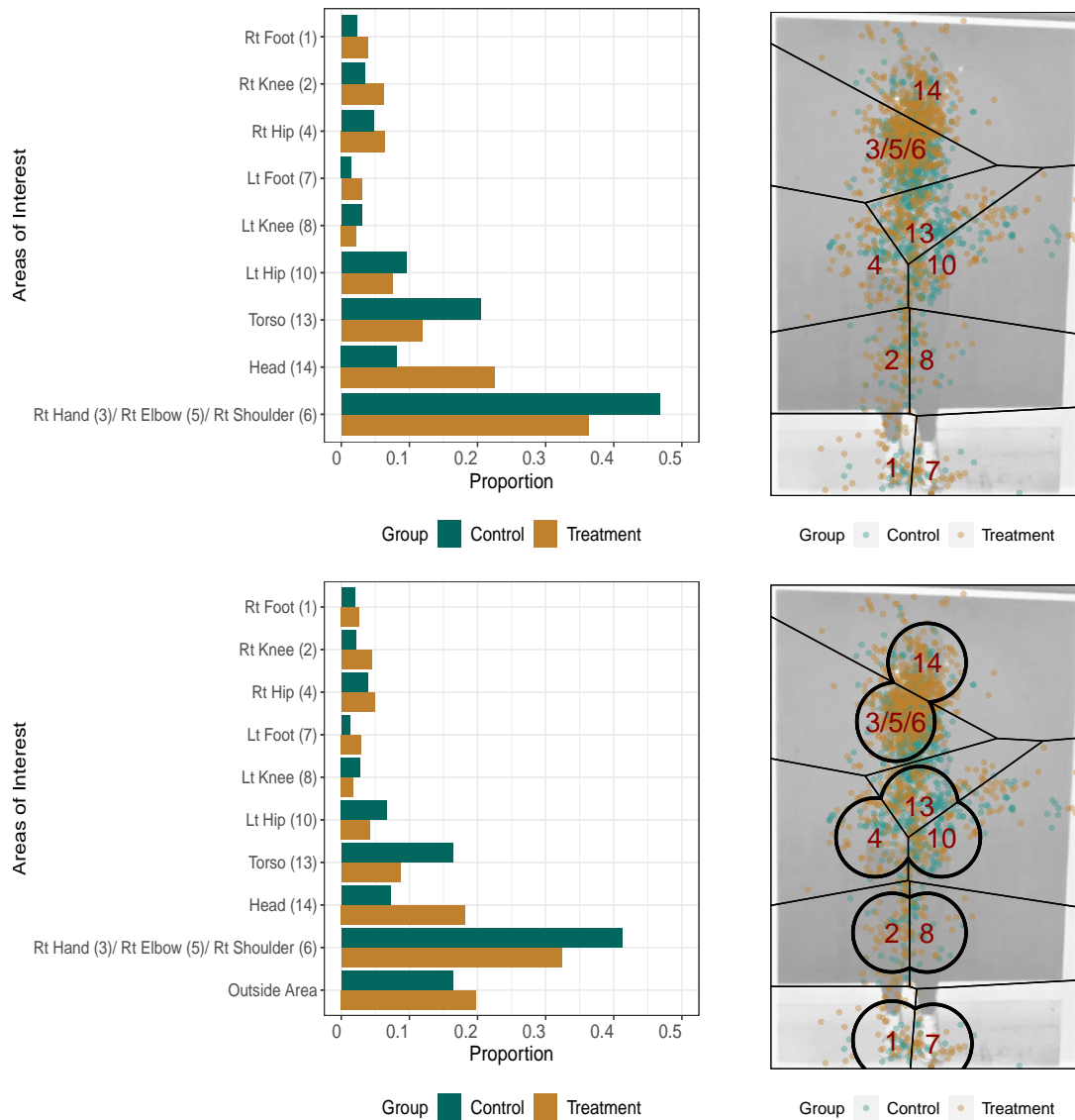


Fig. F.37: Posture ID 19 gaze-point bar chart (left) and scatterplot (right) for Round 1 VT (top) and Round 1 LRVT (bottom) AOIs.

Posture ID 19 Round 2 Visualizations

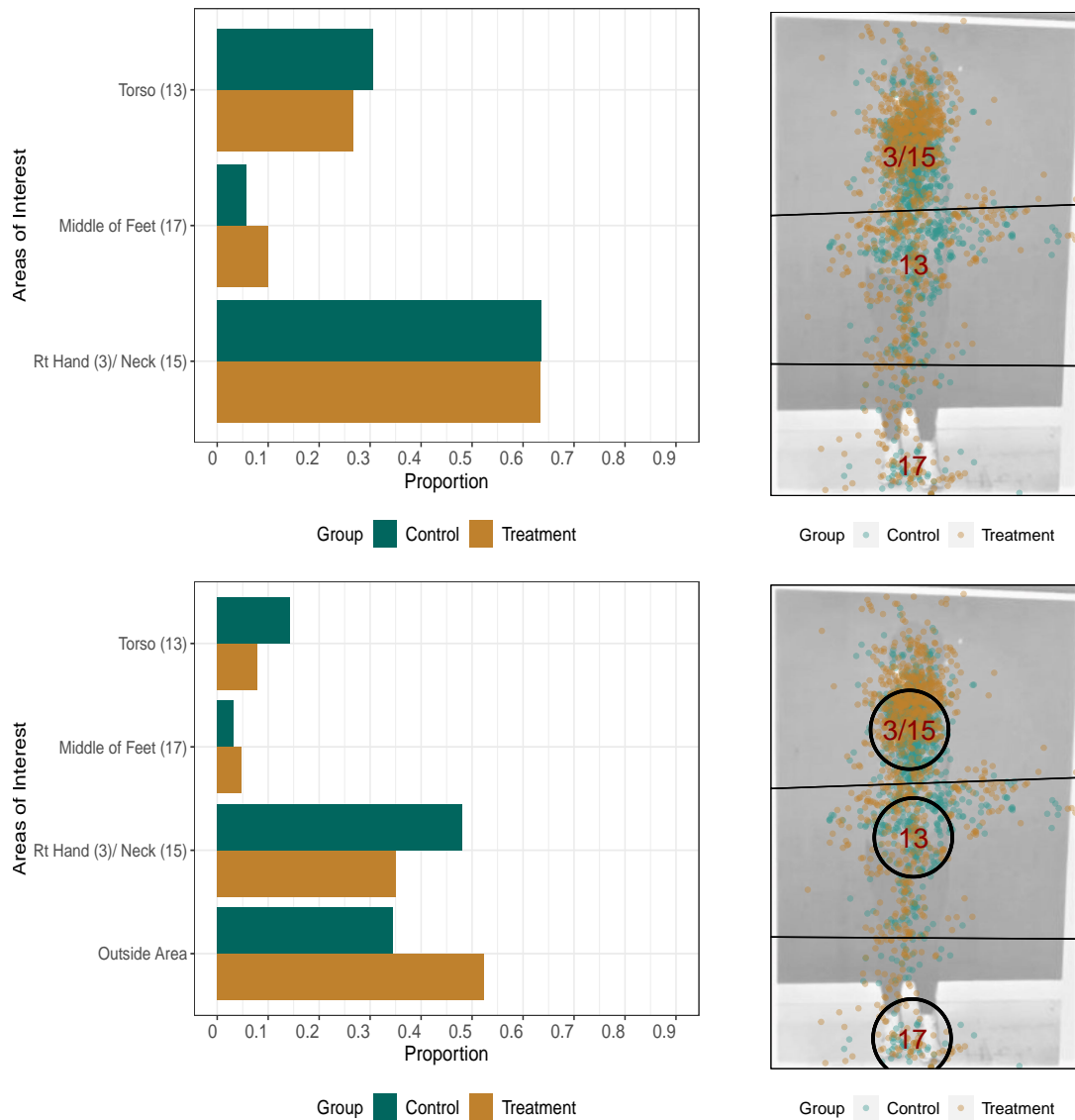


Fig. F.38: Posture ID 19 gaze-point bar chart (left) and scatterplot (right) for Round 2 VT (top) and Round 2 LRV (bottom) AOIs.

Posture ID 20 Round 1 Visualizations

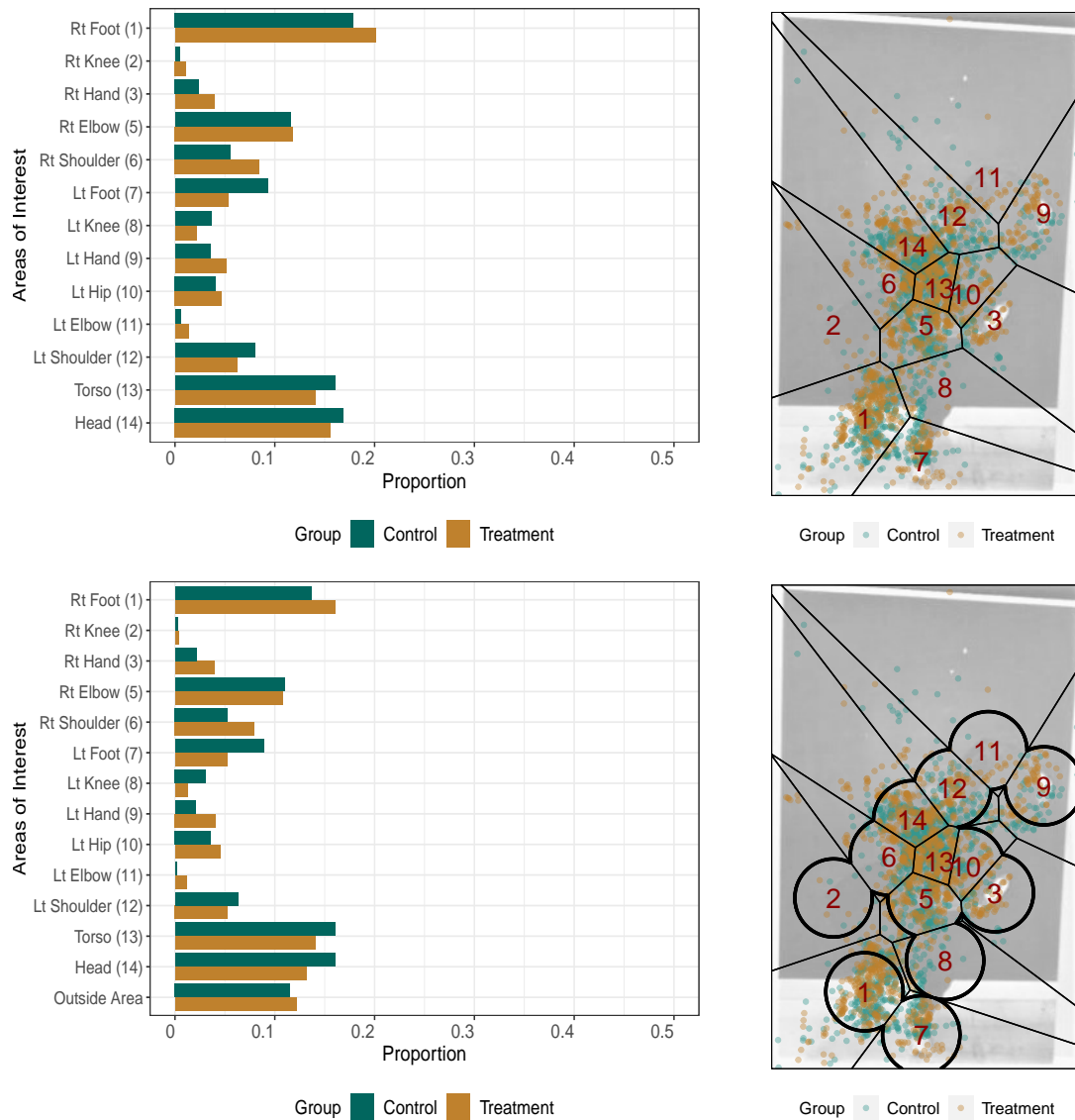


Fig. F.39: Posture ID 20 gaze-point bar chart (left) and scatterplot (right) for Round 1 VT (top) and Round 1 LRVT (bottom) AOIs.

Posture ID 20 Round 2 Visualizations

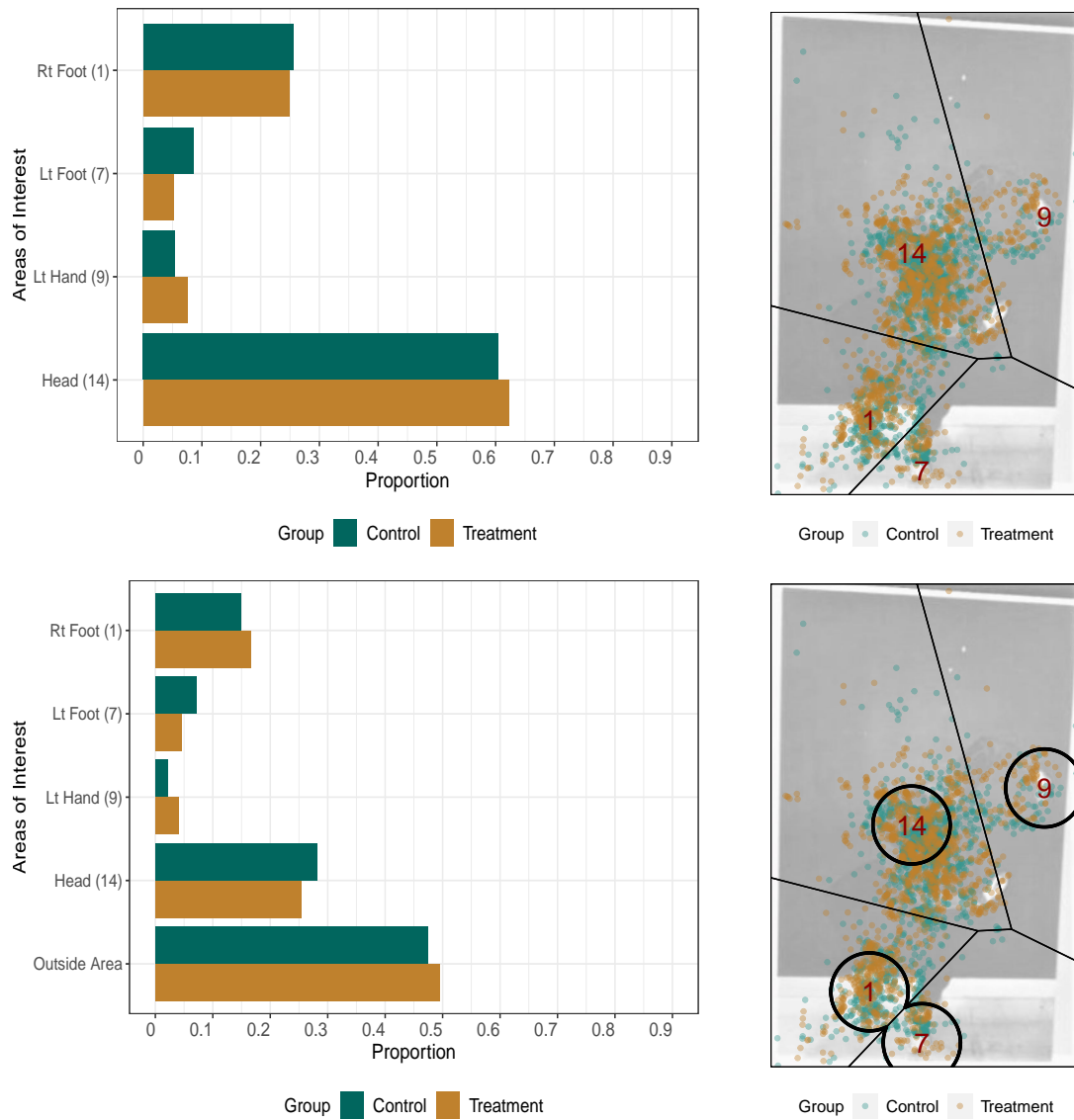


Fig. F.40: Posture ID 20 gaze-point bar chart (left) and scatterplot (right) for Round 2 VT (top) and Round 2 LRV (bottom) AOIs.

Posture ID 21 Round 1 Visualizations

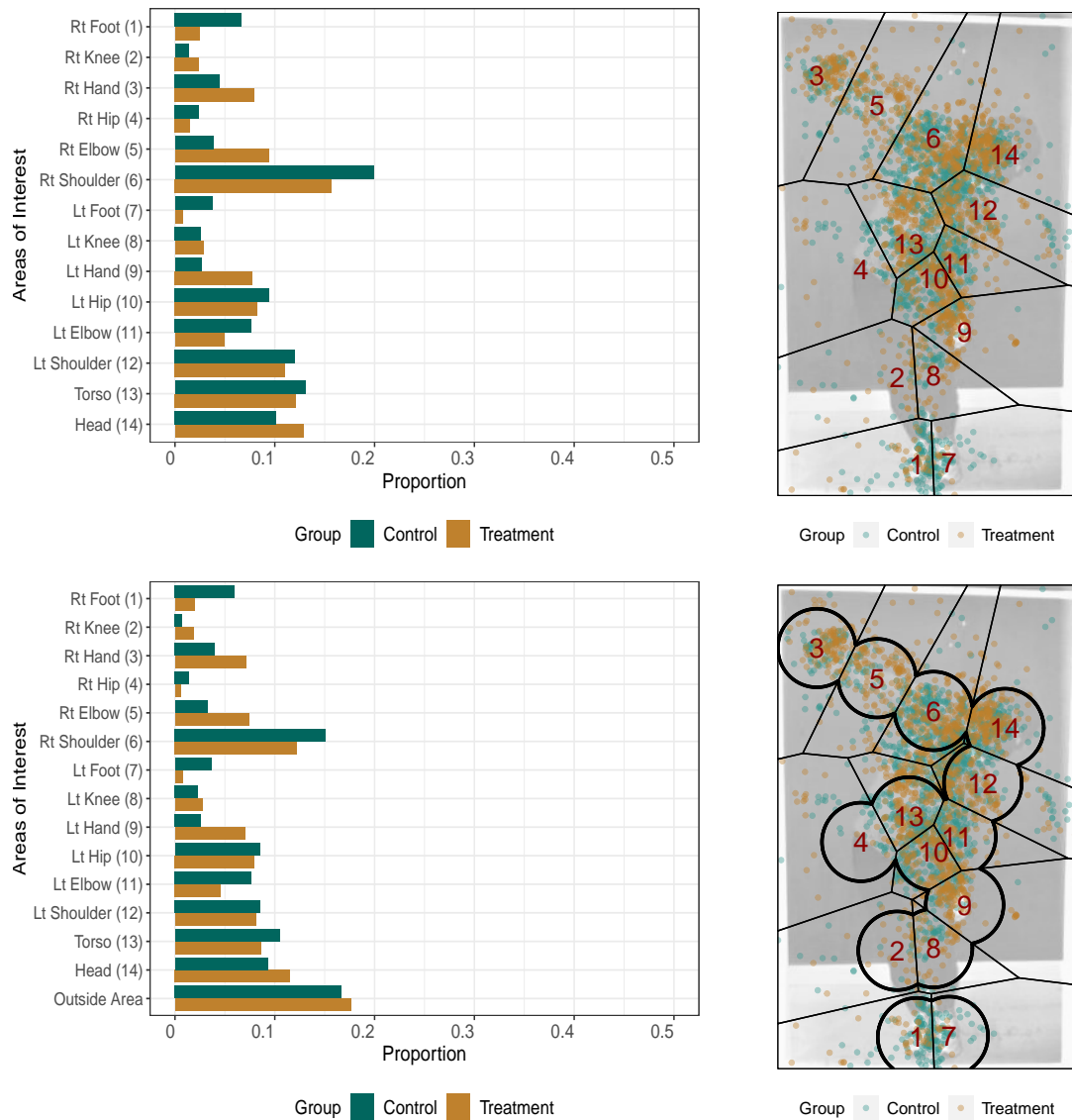


Fig. F.41: Posture ID 21 gaze-point bar chart (left) and scatterplot (right) for Round 1 VT (top) and Round 1 LRVT (bottom) AOIs.

Posture ID 21 Round 2 Visualizations

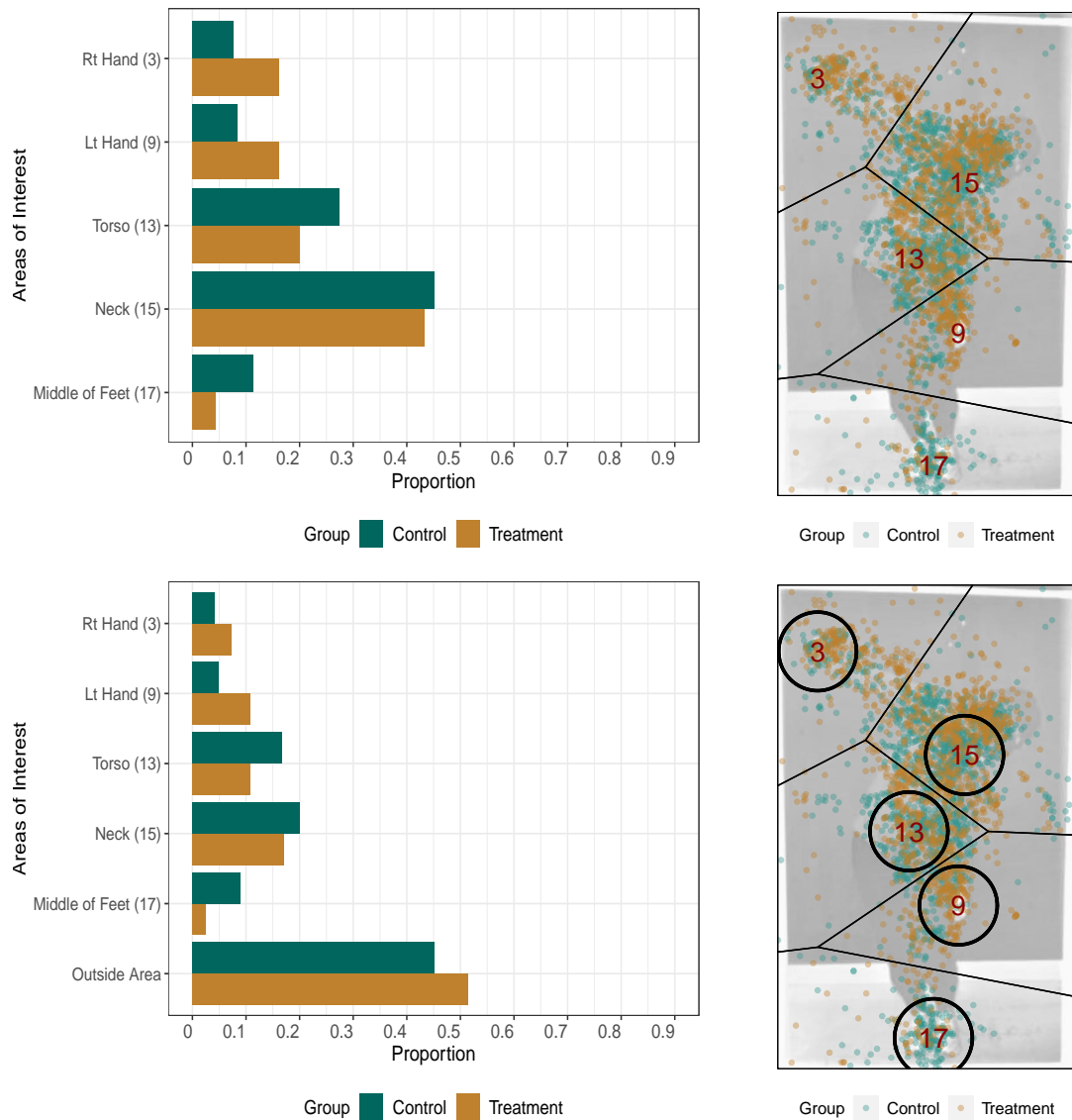


Fig. F.42: Posture ID 21 gaze-point bar chart (left) and scatterplot (right) for Round 2 VT (top) and Round 2 LRV (bottom) AOIs.

Posture ID 22 Round 1 Visualizations

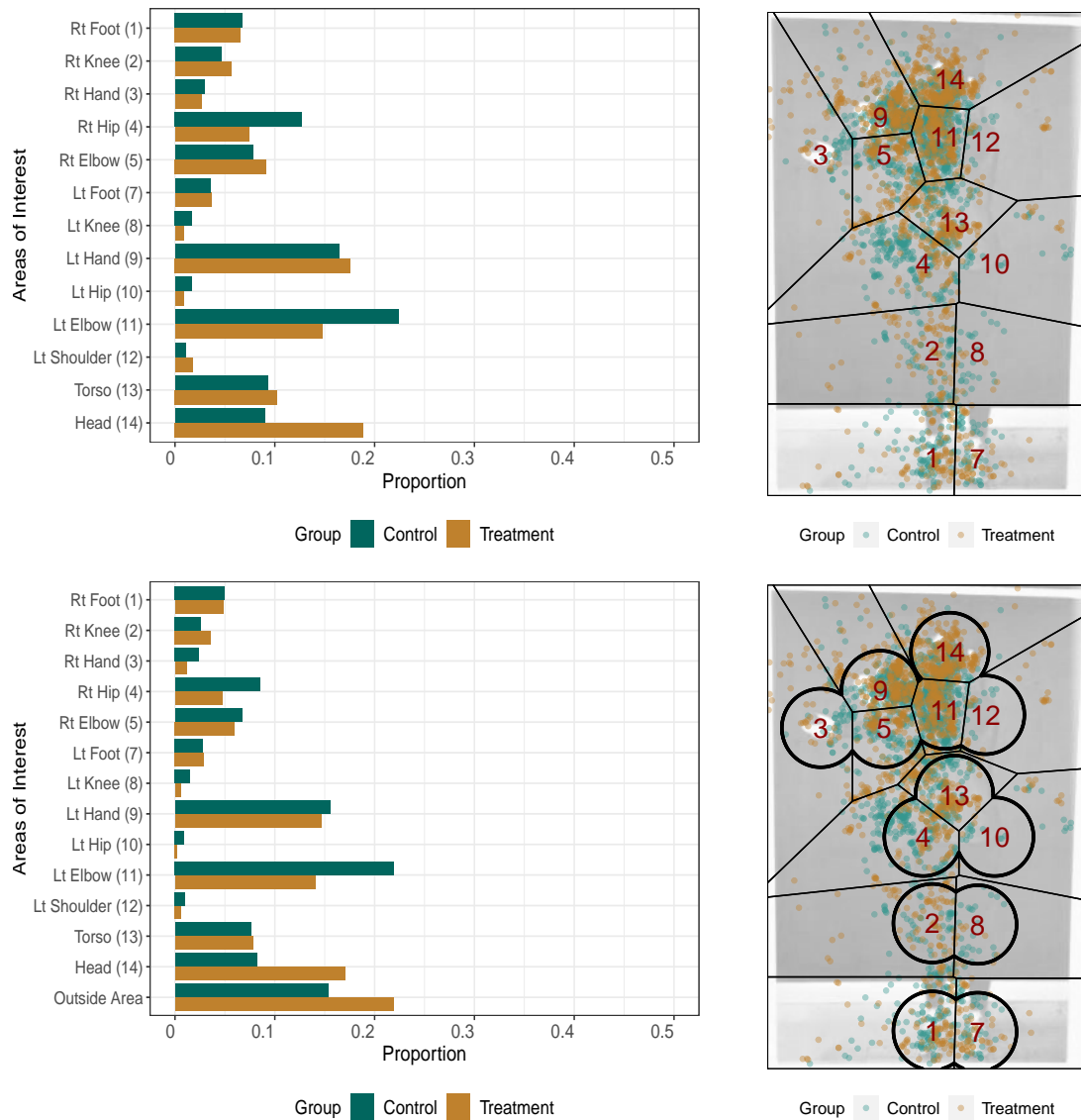


Fig. F.43: Posture ID 22 gaze-point bar chart (left) and scatterplot (right) for Round 1 VT (top) and Round 1 LRVT (bottom) AOIs.

Posture ID 22 Round 2 Visualizations

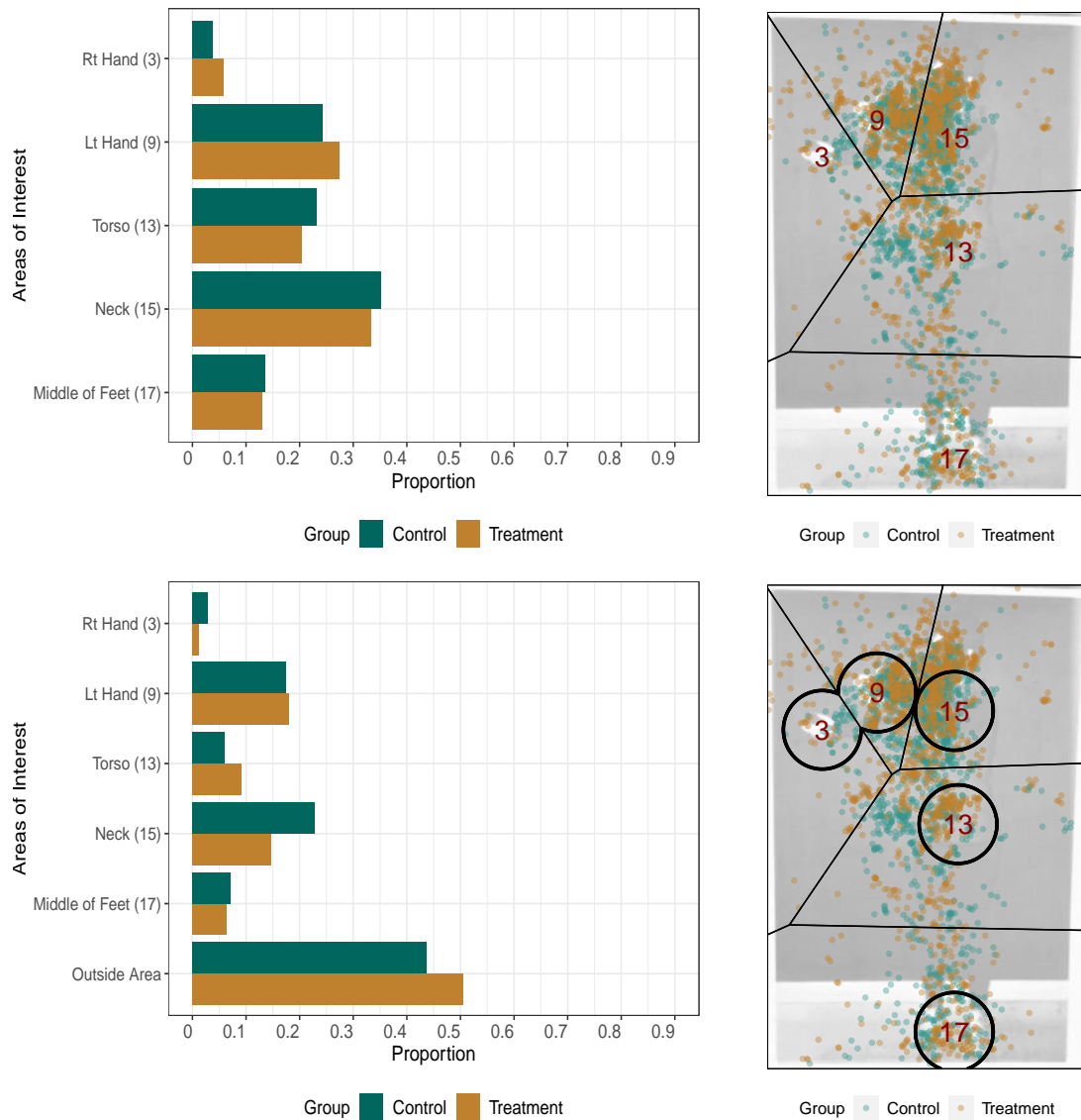


Fig. F.44: Posture ID 22 gaze-point bar chart (left) and scatterplot (right) for Round 2 VT (top) and Round 2 LRV (bottom) AOIs.

Bibliography

- Agresti, A., 1990. *Categorical Data Analysis*. Wiley, New York, NY.
- Almourad, M. B., Bataineh, E., Stocker, J., Marir, F., 2018. Analyzing the Behavior of Autistic and Normal Developing Children Using Eye Tracking Data. In: *International Conference on Kansei Engineering & Emotion Research*. Springer, New York, NY, pp. 340–349.
- Ares, G., Giménez, A., Bruzzone, F., Vidal, L., Antúnez, L., Maiche, A., 2013. Consumer Visual Processing of Food Labels: Results from an Eye-Tracking Study. *Journal of Sensory Studies* 28 (2), 138–153.
- Arundina, D. R., Tantular, B., Pontoh, R. S., 2017. Multilevel Poisson Regression Modelling for Determining Factors of Dengue Fever Cases in Bandung. In: *AIP Conference Proceedings*. Vol. 1827. AIP Publishing LLC, pp. 020043–1—020043–6.
- Baldi, P., Brunak, S., Chauvin, Y., Andersen, C. A., Nielsen, H., 2000. Assessing the Accuracy of Prediction Algorithms for Classification: An Overview. *Bioinformatics* 16 (5), 412–424.
- Bates, D., Mächler, M., Bolker, B., Walker, S., 2015. Fitting Linear Mixed-Effects Models Using lme4. *Journal of Statistical Software* 67 (1), 1–48.
- Benjamini, Y., Hochberg, Y., 1995. Controlling the False Discovery Rate: A Practical and Powerful Approach to Multiple Testing. *Journal of the Royal Statistical Society: Series B (Methodological)* 57 (1), 289–300.
- Blascheck, T., Kurzhals, K., Raschke, M., Burch, M., Weiskopf, D., Ertl, T., 2017. Visualization of Eye Tracking Data: A Taxonomy and Survey. In: *Computer Graphics Forum*. Vol. 36. Wiley Online Library, Hoboken, NJ, pp. 260–284.
- Breslow, N., 1970. A Generalized Kruskal-Wallis Test for Comparing K Samples Subject to Unequal Patterns of Censorship. *Biometrika* 57 (3), 579–594.

- Brooks, M. E., Kristensen, K., van Benthem, K. J., Magnusson, A., Berg, C. W., Nielsen, A., Skaug, H. J., Maechler, M., Bolker, B. M., 2017. glmmTMB Balances Speed and Flexibility Among Packages for Zero-Inflated Generalized Linear Mixed Modeling. *The R Journal* 9 (2), 378–400, <https://journal.r-project.org/archive/2017/RJ-2017-066/index.html>.
- Burnham, K. P., Anderson, D. R., 2004. Multimodel Inference: Understanding AIC and BIC in Model Selection. *Sociological Methods & Research* 33 (2), 261–304.
- Cai, W., 2014. Making Comparisons Fair: How LS-Means Unify the Analysis of Linear Models. In: *SAS Glob. Forum. Vol. 142.* pp. 1–22, <https://support.sas.com/resources/papers/proceedings14/SAS060-2014.pdf>.
- Cantoni, V., Porta, M., De Maio, L., Distasi, R., Nappi, M., 2012. Towards a Novel Technique for Identification Based on Eye Tracking. In: *Workshop on Biometric Measurements and Systems for Security and Medical Applications Proceedings. IEEE, Salerno, Italy*, pp. 1–4.
- Cheung, Y. B., 2002. Zero-Inflated Models for Regression Analysis of Count Data: A Study of Growth and Development. *Statistics in Medicine* 21 (10), 1461–1469.
- Coltrin, J., McKinney, E., Studenka, B., Symanzik, J., 2020. Defining Areas of Interest for Eye-Tracking Data: Implementing a Systematic Approach. In: *2020 JSM Proceedings. American Statistical Association, Alexandria, VA*, pp. 1144–1153.
- Coxe, S., West, S. G., Aiken, L. S., 2009. The Analysis of Count Data: A Gentle Introduction to Poisson Regression and Its Alternatives. *Journal of Personality Assessment* 91 (2), 121–136.
- Cureton, E. E., 1967. The Normal Approximation to the Signed-Rank Sampling Distribution when Zero Differences are Present. *Journal of the American Statistical Association* 62 (319), 1068–1069.
- Damacharla, P., Javaid, A. Y., Devabhaktuni, V. K., 2018. Human Error Prediction Using Eye Tracking to Improve Team Cohesion in Human-Machine Teams. In: *International*

- Conference on Applied Human Factors and Ergonomics. Springer, New York, NY, pp. 47–57.
- Damji, O., Lee-Nobbee, P., Borkenhagen, D., Cheng, A., 2019. Analysis of Eye-Tracking Behaviours in a Pediatric Trauma Simulation. *Canadian Journal of Emergency Medicine* 21 (1), 138–140.
- Darbro, D., 2020. multilevelmodelv1pta. <https://www.youtube.com/watch?v=jHQLBNee41A>.
- Delabarre, E. B., 1898. A Method of Recording Eye-Movements. *The American Journal of Psychology* 9 (4), 572–574.
- Duchowski, A. T., 2007. *Eye Tracking Methodology: Theory and Practice*. Springer, New York, NY.
- Dunn, O. J., 1964. Multiple Comparisons Using Rank Sums. *Technometrics* 6 (3), 241–252.
- Fichtel, E., Lau, N., Park, J., Parker, S. H., Ponnala, S., Fitzgibbons, S., Safford, S. D., 2019. Eye Tracking in Surgical Education: Gaze-Based Dynamic Area of Interest Can Discriminate Adverse Events and Expertise. *Surgical Endoscopy* 33 (7), 2249–2256.
- Figueiredo, G. R., Campos, D., Ripka, W. L., Ulbricht, L., 2018. Attentional Bias for Faces in Relation to Severity of Depressive Symptoms: An Eye-Tracking Study. In: Costa-Felix, R., Machado, J. C., Alvarenga, A. V. (Eds.), XXVI Brazilian Congress on Biomedical Engineering: CBEB 2018, Armação de Buzios, RJ, Brazil, 21-25 October 2018. Vol. 1. Springer, New York, NY, pp. 415–419.
- Fitzmaurice, G. M., Laird, N. M., Ware, J. H., 2012. *Applied Longitudinal Analysis*. John Wiley & Sons, Hoboken, NJ.
- Fox, J., 1997. *Applied Regression Analysis, Linear Models, and Related Methods*. Sage Publications, Inc, Newbury Park, CA.
- Fox, J., Weisberg, S., 2019. *An R Companion to Applied Regression*, 3rd Edition. Sage Publications, Thousand Oaks, CA.

- Gao, X., 2011. Multiple Testing Corrections for Imputed SNPs. *Genetic Epidemiology* 35 (3), 154–158.
- Garrett, R. C., Nar, A., Fisher, T. J., 2019. ggvoronoi: Voronoi Diagrams and Heatmaps with 'ggplot2'. R package version 0.8.3, <https://CRAN.R-project.org/package=ggvoronoi>.
- Goldberg, J. H., Helfman, J. I., 2010. Comparing Information Graphics: A Critical Look at Eye Tracking. In: *Proceedings of the 3rd BELIV'10 Workshop: Beyond Time and Errors: Novel Evaluation Methods for Information Visualization*. Association for Computing Machinery, New York, NY, pp. 71–78.
- Goodnight, J. H., Harvey, W. R., 1978. *Least Squares Means in the Fixed Effects General Linear Model*. SAS Institute, Cary, NC.
- Harvey, W. R., 1960. *Least-Squares Analysis of Data with Unequal Subclass Numbers*. Vol. 20. Agricultural Research Service, United States Department of Agriculture, Washington, DC.
- Hershman, R., Henik, A., Cohen, N., 2018. A Novel Blink Detection Method Based on Pupillometry Noise. *Behavior Research Methods* 50 (1), 107–114.
- Hessels, R. S., Benjamins, J. S., Cornelissen, T. H., Hooge, I. T., 2018. A Validation of Automatically-Generated Areas-of-Interest in Videos of a Face for Eye-Tracking Research. *Frontiers in Psychology* 9, 1367.
- Hessels, R. S., Kemner, C., Van Den Boomen, C., Hooge, I. T., 2016. The Area-Of-Interest Problem in Eyetracking Research: A Noise-Robust Solution for Face and Sparse Stimuli. *Behavior Research Methods* 48 (4), 1694–1712.
- Holmqvist, K., Nyström, M., Andersson, R., Dewhurst, R., Jarodzka, H., Van de Weijer, J., 2011. *Eye Tracking: A Comprehensive Guide to Methods and Measures*. Oxford University Press, Oxford, United Kingdom.
- Hox, J. J., Moerbeek, M., Van de Schoot, R., 2017. *Multilevel Analysis: Techniques and Applications*. Routledge, England, UK.

- Huey, E. B., 1898. Preliminary Experiments in the Physiology and Psychology of Reading. *The American Journal of Psychology* 9 (4), 575–586.
- Hur, K., Hedeker, D., Henderson, W., Khuri, S., Daley, J., 2002. Modeling Clustered Count Data with Excess Zeros in Health Care Outcomes Research. *Health Services and Outcomes Research Methodology* 3 (1), 5–20.
- Kodde, D. A., Palm, F. C., 1986. Wald Criteria for Jointly Testing Equality and Inequality Restrictions. *Econometrica: Journal of the Econometric Society* 54 (5), 1243–1248.
- Krafka, K., Khosla, A., Kellnhofer, P., Kannan, H., Bhandarkar, S., Matusik, W., Torralba, A., June 2016. Eye Tracking for Everyone. In: *Proceedings of the IEEE Conference on Computer Vision and Pattern Recognition*. No. 1063-6919. IEEE Computer Society, Los Alamitos, CA, USA, pp. 2176–2184, <https://doi.ieeecomputersociety.org/10.1109/CVPR.2016.239>.
- Lambert, D., 1992. Zero-Inflated Poisson Regression, with an Application to Defects in Manufacturing. *Technometrics* 34 (1), 1–14.
- Land, K. C., McCall, P. L., Nagin, D. S., 1996. A Comparison of Poisson, Negative Binomial, and Semiparametric Mixed Poisson Regression Models: With Empirical Applications to Criminal Careers Data. *Sociological Methods & Research* 24 (4), 387–442.
- Lazic, S. E., 2010. The Problem of Pseudoreplication in Neuroscientific Studies: Is It Affecting Your Analysis? *BMC Neuroscience* 11 (1), 1–17.
- Lee, A. H., Wang, K., Scott, J. A., Yau, K. K., McLachlan, G. J., 2006. Multi-Level Zero-Inflated Poisson Regression Modelling of Correlated Count Data with Excess Zeros. *Statistical Methods in Medical Research* 15 (1), 47–61.
- Lenth, R. V., 2021. emmeans: Estimated Marginal Means, aka Least-Squares Means. R package version 1.6.2-1, <https://CRAN.R-project.org/package=emmeans>.
- Li, C., 2017. Extracting and Visualizing Data from Mobile and Static Eye Trackers in R and Matlab. Ph.D. thesis, Department of Mathematics and Statistics, Utah State University, <https://digitalcommons.usu.edu/etd/6880/>.

- Li, S., Singh, C. V., Talreja, R., 2009. A Representative Volume Element Based on Translational Symmetries for FE Analysis of Cracked Laminates with Two Arrays of Cracks. *International Journal of Solids and Structures* 46 (7-8), 1793–1804.
- Liao, J., Yu, S., Yang, F., Yang, M., Hu, Y., Zhang, J., 2016. Short-Term Effects of Climatic Variables on Hand, Foot, and Mouth Disease in Mainland China, 2008–2013: A Multi-level Spatial Poisson Regression Model Accounting for Overdispersion. *PLoS One* 11 (1), e0147054.
- McKinney, E., Symanzik, J., 2019. Modifications of the Syrjala Test for Testing Spatial Distribution Differences Between Two Populations. In: 2019 JSM Proceedings. American Statistical Association, Alexandria, VA, pp. 2518–2530.
- McKinney, E., Symanzik, J., 2021. Extensions to the Syrjala Test with Eye-Tracking Analysis Applications. In: 2021 JSM Proceedings. American Statistical Association, Alexandria, VA, pp. 853–889.
- Michelon, P., Zacks, J. M., 2006. Two Kinds of Visual Perspective Taking. *Perception & Psychophysics* 68 (2), 327–337.
- Moghimbeigi, A., Eshraghian, M. R., Mohammad, K., Mcardle, B., 2008. Multilevel Zero-Inflated Negative Binomial Regression Modeling for Over-Dispersed Count Data with Extra Zeros. *Journal of Applied Statistics* 35 (10), 1193–1202.
- Napierala, M. A., 2012. What is the Bonferroni Correction? *American Academy of Orthopaedic Surgeons Now* 6 (4), 40.
- R Core Team, 2020. R: A Language and Environment for Statistical Computing. R Foundation for Statistical Computing, Vienna, Austria, <https://www.R-project.org/>.
- Ridout, M., Hinde, J., Demétrio, C. G., 2001. A Score Test for Testing a Zero-Inflated Poisson Regression Model Against Zero-Inflated Negative Binomial Alternatives. *Biometrics* 57 (1), 219–223.
- Rochat, P., 1995. Perceived Reachability for Self and for Others by 3-to 5-Year-Old Children and Adults. *Journal of Experimental Child Psychology* 59 (2), 317–333.

- Saha, A., Dong, D., 1997. Estimating Nested Count Data Models. *Oxford Bulletin of Economics and Statistics* 59 (3), 423–430.
- Schlager, S., 2017. Morpho and Rvcg – Shape Analysis in R. In: Zheng, G., Li, S., Szekely, G. (Eds.), *Statistical Shape and Deformation Analysis*. Academic Press, Cambridge, MA, pp. 217–256.
- Searle, S. R., Speed, F. M., Milliken, G. A., 1980. Population Marginal Means in the Linear Model: An Alternative to Least Squares Means. *The American Statistician* 34 (4), 216–221.
- Symanzik, J., Li, C., Zhang, B., Studenka, B., McKinney, E., 2017. Eye-Tracking in Practice: A First Analysis of a Study on Human Postures. In: *2017 JSM Proceedings*. American Statistical Association, Alexandria, VA, pp. 2212–2226.
- Symanzik, J., McKinney, E., Studenka, B., Bean, B., Athens, M., Hansen, M., 2018. Eye-Tracking in Practice: Results from a Study on Human Postures. *2018 JSM Proceedings*. American Statistical Association, Alexandria, VA, 2696–2706.
- Thissen, D., Steinberg, L., Kuang, D., 2002. Quick and Easy Implementation of the Benjamini-Hochberg Procedure for Controlling the False Positive Rate in Multiple Comparisons. *Journal of Educational and Behavioral Statistics* 27 (1), 77–83.
- Vaeyens, R., Lenoir, M., Williams, A. M., Philippaerts, R. M., 2007. Mechanisms Underpinning Successful Decision Making in Skilled Youth Soccer Players: An Analysis of Visual Search Behaviors. *Journal of Motor Behavior* 39 (5), 395–408.
- Van der Lans, R., Wedel, M., Pieters, R., 2011. Defining Eye-Fixation Sequences Across Individuals and Tasks: The Binocular-Individual Threshold (BIT) Algorithm. *Behavior Research Methods* 43 (1), 239–257.
- Voronoi, G., 1909. Nouvelles Applications des Paramètres Continus à Théorie des Formes Quadratiques. Deuxième Mémoire. Recherches sur les Paralléloèdres Primitifs. *Journal für die Reine und Angewandte Mathematik (Crelles Journal)* 1909 (136), 67–182.

- Wästlund, E., Shams, P., Otterbring, T., 2018. Unsold is Unseen ... Or Is It? Examining the Role of Peripheral Vision in the Consumer Choice Process Using Eye-Tracking Methodology. *Appetite* 120, 49–56.
- Wilcoxon, F., 1992. Individual Comparisons by Ranking Methods. In: Kotz, S., Johnson, L. (Eds.), *Breakthroughs in Statistics*. Springer, New York, NY, pp. 196–202.
- Woolson, R., 2007. Wilcoxon Signed-Rank Test. *Wiley Encyclopedia of Clinical Trials*, 1–3.
- Xie, H., Tao, J., McHugo, G. J., Drake, R. E., 2013. Comparing Statistical Methods for Analyzing Skewed Longitudinal Count Data with Many Zeros: An Example of Smoking Cessation. *Journal of Substance Abuse Treatment* 45 (1), 99–108.
- Zandkarimi, E., Moghimbeigi, A., Mahjub, H., Majdzadeh, R., 2019. Robust Inference in the Multilevel Zero-Inflated Negative Binomial Model. *Journal of Applied Statistics* 47 (2), 287–305.